Arctic Report Card 2025

Twenty years of tracking rapid Arctic warming and change

DOI: 10.25923/nrzf-j897

M.L. Druckenmiller, R.L. Thoman,
and T.A. Moon, Eds.

December 2025

Matthew L. Druckenmiller, Richard L. Thoman, Twila A. Moon; Editors
Mary Beth Armstrong, Cynthia Garcia; NOAA Coordinating Editors
Sandy Lucas; NOAA Federal Advisor

arctic.noaa.gov/report-card

How to Cite Arctic Report Card 2025
Citing the complete report or Executive Summary:
Druckenmiller, M. L., R. L. Thoman, and T. A. Moon, Eds., 2025: *Arctic Report Card 2025*. M. B. Armstrong and C. Garcia, Coordinating Eds., https://doi.org/10.25923/nrzf-j897.

Citing an essay (example):
Mudryk, L. R., A. Elias Chereque, C. Derksen, K. Luojus, and B. Decharme, 2025: Terrestrial snow cover. *Arctic Report Card 2025*, M. L. Druckenmiller, R. L. Thoman, and T. A. Moon, Eds., M. B. Armstrong and C. Garcia, Coordinating Eds., https://doi.org/10.25923/cfhv-c239.

(Note: Each essay has a unique DOI assigned)

Front Cover Photo Credits
Left: *Two men examine a large sea-ice crack in Eclipse Sound, Nunavut, Canada.* Credit: Vincent Denarié
Top Right: *Aerial view of a camping site at Salmon Creek, Nunavut, Canada.* Credit: Vincent Denarié
Bottom Right: *Back deck of the USCGC Healy in the Beaufort Sea*. Credit: Kaleigh Ballantine

Funding Acknowledgments for the Arctic Report Card
Financial support for Arctic Report Card 2025 was provided by NOAA's Global Ocean Monitoring and Observing (GOMO) Arctic Research Program, including content editing funded through the Cooperative Institute for Earth System Research and Data Science (CIESRDS) via NOAA Cooperative Agreement NA22OAR4320151 (Druckenmiller and Moon) and by the Cooperative Institute for Climate, Ocean, and Ecosystem Studies (CICOES) under NOAA Cooperative Agreement NA20OAR4320271 (Thoman). The editors thank the Arctic Monitoring and Assessment Programme (AMAP) Secretariat for organizing the independent peer review and all the reviewers. The editors also recognize the contribution of coordinating editors Mary Beth Armstrong and Cynthia Garcia from the Arctic Research Program in NOAA's GOMO, who coordinated and managed the various elements of the ARC's production process, and the entire ARC production team for the professionalism, dedication, and enthusiasm in producing each year's Report.

Table of Contents

2025 Headlines

Twenty years of tracking rapid Arctic warming and change

Now in its 20th year, the Arctic Report Card (ARC) 2025 provides a clear view of a region warming far faster than the rest of the planet. Along with reports on the state of the Arctic's atmosphere, oceans, cryosphere, and tundra, this year's report highlights major transformations underway—atlantification bringing warmer, saltier waters northward, boreal species expanding northward into Arctic ecosystems, and "rivers rusting" as thawing permafrost mobilizes iron and other metals. Across these changing landscapes, sustained observations and strong research partnerships, including those led by communities and Indigenous organizations, remain essential for understanding and adaptation.

Headlines

In the air

- Surface air temperatures across the Arctic from October 2024 through September 2025 were the warmest recorded since 1900.
- Autumn 2024 and winter 2025 were especially warm across the Arctic with temperatures ranking 1st and 2nd warmest, respectively.
- The last 10 years are the 10 warmest on record in the Arctic.
- Since 2006, Arctic annual temperature has increased at more than double the global rate of temperature changes.
- Precipitation from October 2024 to September 2025 set a new record high.
- Arctic precipitation totals for winter, spring, and autumn were each among the top five since 1950.

In the ocean

- In March 2025, Arctic winter sea ice reached the lowest annual maximum extent in the 47-year satellite record.
- September 2025 saw the 10th lowest minimum sea ice extent. All of the 19 lowest September minimum ice extents have occurred in the last 19 years.
- In August 2025, the marginal seas of the Arctic Ocean's Atlantic sector saw average sea surface temperatures ~13°F (~7°C) warmer than the 1991-2020 August average.
- The oldest, thickest Arctic sea ice (> 4 years) has declined by more than 95% since the 1980s. Multi-year sea ice is now largely confined to the area north of Greenland and the Canadian Archipelago.
- Arctic Ocean regions that are ice-free in August have warmed by 2.3°F since 1982.
- From 2003 to 2025, phytoplankton productivity spiked by 80% in the Eurasian Arctic, 34% in the Barents Sea, and 27% in Hudson Bay.
- Plankton productivity in 2025 was higher than the 2003-22 average in eight of nine regions assessed across the Arctic.
- Atlantification—an influx of water properties from lower latitudes—has reached the central Arctic Ocean, hundreds of miles from the former edge of the Atlantic Ocean.

- Atlantification weakens the Arctic Ocean's layering of waters of different densities, therefore enhancing heat transfer, melting sea ice, and threatening ocean circulation patterns that exert a long-term influence on the weather.
- Warming bottom waters, declining sea ice, and rising chlorophyll in the Chukchi and northern Bering Seas are driving shifts in mid-water and bottom-dwelling species, reshaping fisheries, affecting Arctic food security and Indigenous subsistence practices.

On land

- Glaciers in Arctic Scandinavia and Svalbard experienced the largest annual net loss of ice on record between 2023 and 2024.
- The Greenland Ice Sheet lost an estimated 129 billion tons of ice in 2025, less than the annual average of 219 billion tons between 2003 and 2024, but continuing the long-term trend of net loss.
- Alaskan glaciers have lost an average of 125 vertical feet (38 meters) of ice since the mid-20th century, dramatically lowering ice surfaces statewide.
- Ongoing glacier loss contributes to steadily rising global sea levels, threatening Arctic communities' water supplies, driving destructive floods and increasing landslide and tsunami hazards that endanger people, infrastructure, and coastline.
- Throughout the Arctic, snowpack was higher than normal during the 2024/25 snow season and remained high through May. Despite this, by June snow cover extent dropped below normal, consistent with levels the past 15 years.
- June snow cover extent over the Arctic today is half of what it was six decades ago.
- In over 200 Arctic Alaska watersheds, iron, and other elements released by thawing permafrost have turned pristine rivers and streams orange over the past decade.
- In "rusting rivers", the increased acidity and elevated levels of toxic metals degrade water quality, compromising aquatic habitat and eroding biodiversity.
- Scientists are studying the causes of rusting rivers and impacts to rural drinking water supplies and subsistence fisheries.
- First detected in the late 1990s, the "greening of the Arctic" has far-reaching impacts to Arctic habitats, permafrost conditions, and the livelihood of Arctic people, with implications for global climate and the carbon cycle.
- In 2025, maximum Arctic tundra greenness was the third highest in the 26-year satellite record, continuing a sequence of record or near-record high values since 2020.
- For more than 20 years, the Indigenous Sentinels Network has supported Arctic communities by strengthening Indigenous-led observations of weather, wildlife, and environmental change.
- On St. Paul Island, Alaska, the BRAIDED Food Security Project and the new Bering Sea Research Center delivered food safety information directly to the community in 2025, recording observations of harvested traditional foods with analysis of contaminants like mercury.

20 Years of Partnerships with the Arctic Report Card

- The Arctic Report Card is sustained by a wide network of partnerships—spanning Indigenous communities, local and regional organizations, national institutions, and international science networks—that together strengthen our understanding of a rapidly changing Arctic.

- The Arctic Report Card's long-standing partnership with the Arctic Monitoring and Assessment Programme brings together rigorous peer review and timely reporting to strengthen internationally coordinated assessments of Arctic change.
- Indigenous knowledge and leadership are critically important to understanding the changing Arctic. The Arctic Report Card has been strengthened by partnerships with Indigenous communities.
- Despite a robust Arctic observing network, gaps in coverage hinder scientists' ability to monitor key environmental changes, affecting critical assessments of water availability, resource management, and food security.

Executive Summary

https://doi.org/10.25923/nrzf-j897

M. L. Druckenmiller[1], R. L. Thoman[2,3], and T. A. Moon[1]

[1]National Snow and Ice Data Center, Cooperative Institute for Research in Environmental Sciences, University of Colorado Boulder, Boulder, CO, USA
[2]Alaska Center for Climate Assessment and Preparedness, University of Alaska Fairbanks, Fairbanks, AK, USA
[3]International Arctic Research Center, University of Alaska Fairbanks, Fairbanks, AK, USA

To observe the Arctic is to take the pulse of the planet. The Arctic is warming several times faster than Earth as a whole, reshaping the northern landscapes, ecosystems, and livelihoods of Arctic peoples. Also transforming are the roles the Arctic plays in the global climate, economic, and societal systems. Arctic Report Card (ARC) 2025 marks the 20th annual installment of this report as a timely account of the state of the Arctic environment. Since its first publication in 2006, motivated by notable Arctic warming and change already underway, the Report Card has served as a peer-reviewed record of diverse environmental observations that together document an extraordinary, ongoing transformation. Its essays reveal the increasing pace, scale, and consequences of rapid environmental change across the Arctic's Vital Signs (Fig. 1)—annually reported critical indicators of marine, terrestrial, and atmospheric processes—and other consequential parts of the Arctic system. This 20th anniversary edition reflects the Arctic's trajectory, highlighting the persistence of long-term trends and the emergence of new and complex feedbacks and interactions (Figs. 2 and 3).

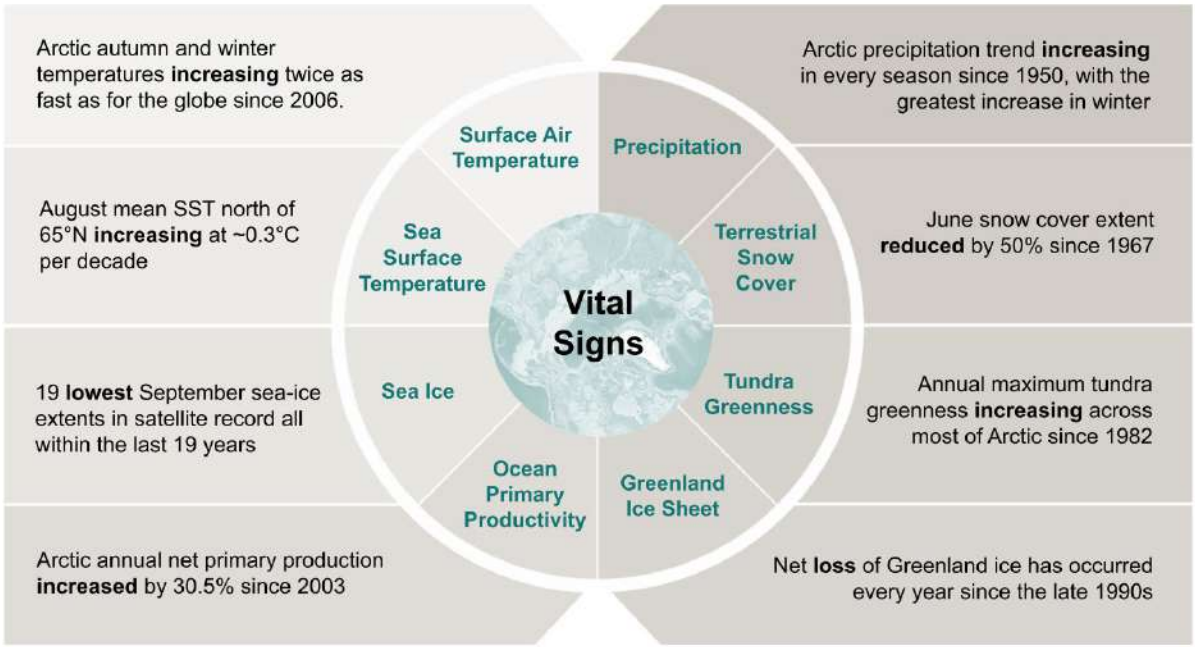

Fig. 1. Arctic Report Card Vital Signs with selected noteworthy trends and observations. The ARC annually reports on eight Vital Sign topics. Vital Sign data records vary in length based on dataset availability and considerations to methodological continuity. The historical record periods are used when computing ranked observations. When reporting anomalies, Vital Signs currently use 1991-2020 as the 30-year reference period, except for Tundra Greenness (2000-24) and Ocean Primary Productivity (2003-24).

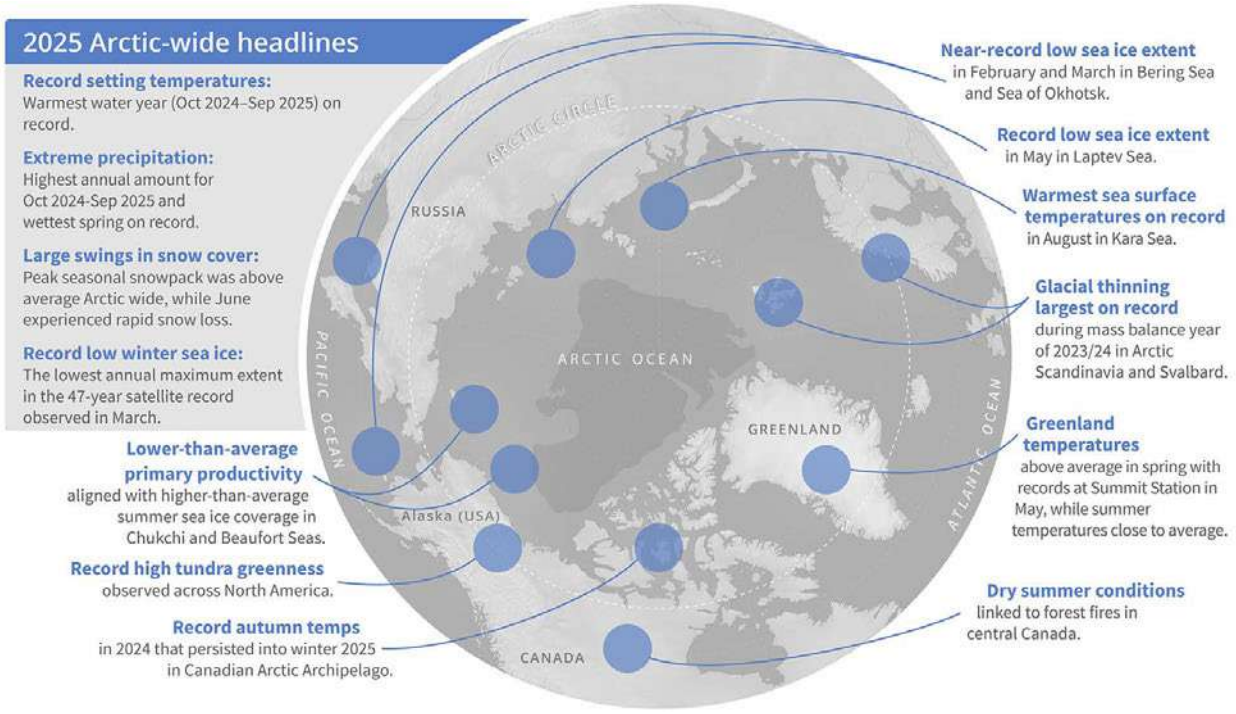

Fig. 2. A sample of notable events and important topics from across the Arctic.

Fig. 3. General geographic references for many locations mentioned in ARC 2025.

Arctic surface air temperatures during the past year (October 2024-September 2025; the annual period that aligns with the natural water cycle) were the highest on record since at least 1900. This included the Arctic experiencing its warmest autumn, second-warmest winter, and third-warmest summer since 1900, reinforcing the now well-established pattern of amplified regional warming. Over the past 20 years, Arctic autumn and winter air temperatures have each increased by more than twice the corresponding increases in global air temperatures.

An intensifying hydrologic cycle, driven by increased evaporation, precipitation, and meltwater production, continues to emerge as a central expression of persistent Arctic heating. The 2024/25 water year saw record-high precipitation averaged for the entire year and for spring, and ranked among the top five wettest years for all other seasons since 1950. These patterns are consistent with a more moisture-laden atmosphere and an increasing frequency of extreme precipitation events, including atmospheric rivers that can deliver heavy amounts of rain or snow to large regions. For example, an atmospheric river was responsible for heavy precipitation in the Aleutians and across Alaska in January 2025, contributing to an overall Arctic winter with more extreme precipitation events than any other season.

Snow cover on land is directly influenced by the observed increases in Arctic precipitation, while at the same time the reduction in snow cover duration amplifies Arctic warming. The year 2025 was a clear example of this, consistent with conditions over the last 15 years. While the winter snowpack was above average across much of the Arctic, rapid melting in late spring caused June snow extent to drop below normal, continuing a six-decade decline. June snow cover extent is now 50% of what it was in the 1960s, altering river discharge, vegetation processes, animal behavior, and fire risk. The loss of reflective snow surfaces in June, when incoming solar energy reaches its annual maximum, results in more heat absorbed at the surface, contributing to further Arctic warming trends.

The Arctic's highly reflective surfaces are also diminishing in the ocean as sea ice cover shrinks. The annual maximum sea ice extent in March 2025 was the lowest in the 47-year satellite record, while the minimum ice extent in September was the 10th lowest. Compared with 2005—the year discussed in the first Arctic Report Card—the end-of-summer sea ice extent in 2025 was 28% smaller and considerably thinner and younger. Multi-year sea ice is now largely confined to the area north of Greenland and the Canadian Archipelago, and the thickest, oldest (> 4 years) ice has declined by more than 95% since the 1980s.

Loss of ice is also apparent on land. The Greenland Ice Sheet continued to lose mass in 2025, though the annual loss was less than the 2003-24 mean due to enhanced snowfall and below-average melt. However, the long-term trend remains consistent; Greenland continues to be a major contributor to global sea-level rise and a driver of freshwater and nutrient inputs that influence North Atlantic ocean circulation and marine productivity. Similarly, Arctic glaciers and ice caps outside of Greenland have rapidly thinned since the 1950s, also contributing steadily to rising global sea levels.

The warming of ocean waters is also extremely consequential to the Arctic region. August mean sea surface temperatures (SSTs) show warming trends during 1982-2025 in almost all Arctic Ocean regions that are ice-free in August, with increases of ~0.3°C (~0.54°F) per decade in the region north of 65° N. This warming alters ecosystems and is a prime driver of sea ice loss. In 2025, August SSTs in most Arctic regions ranked among the warmest on record. Yet, stark regional differences were observed. While the Atlantic sector of the Arctic Ocean was anomalously warm, with SSTs as high as 7°C (12.6°F) above the

1991-2020 average, the Beaufort and northern Chukchi Seas in the Pacific sector were 1-2°C (1.8-3.6°F) cooler than average.

Yet waters in the Pacific sector's Bering Sea were well above normal throughout summer, and these warm conditions continued into early October 2025. This contributed to the devastating strength of Ex-Typhoon Halong that traveled northward over these waters before inundating Alaska's southwestern coast, delivering hurricane-force winds, storm surge, and catastrophic flooding. More than 1,500 residents from across the region had to be evacuated, and some villages, notably Kipnuk and Kwigillingok, were almost entirely destroyed. At the time of ARC 2025's release, communities across the region are still assessing damage and whether many will ever be able to return to their communities. This storm, following Ex-Typhoon Merbok in 2022 that caused extensive damage in western Alaska, provides a somber account of the risks that many coastal communities face in a warming Arctic and without climate-resilient infrastructure and adequate disaster response capabilities (ANTHC 2024).

The long-term warming of the Arctic Ocean is also influenced by ocean currents bringing oceanic heat northward from lower latitudes. Continued *atlantification*—a northward influx of warmer, saltier Atlantic water—has transformed large areas of the Eurasian Basin, weakening the stratification that has historically insulated sea ice from underlying warm water. Atlantification, which links Arctic Ocean and North Atlantic processes, illustrates how regional and global system changes are closely intertwined. ARC 2025 describes how atlantification has diminished winter sea-ice formation over the past decade, while also lifting nutrient rich waters to be available for increased ocean primary productivity, which is the rate at which marine algae produces organic material. These changes are not confined to the Arctic's Atlantic sector; atlantification has already been detected at the North Pole and is advancing toward Alaska, where warming and Pacific-origin waters are also causing change.

While higher primary productivity may benefit food webs in some cases, ecosystem health is often threatened. Misalignments between when food is available and when those species that depend on it are able to feed (i.e., trophic mismatches) hinder the movement of carbon through the food chain. Harmful algal blooms also present health risks to subsistence-based coastal communities. During 2003-25, primary productivity across the Arctic continued to exhibit positive trends in eight of the nine analyzed regions, with increases as large as 80% in the Eurasian Arctic.

The ARC 2025 essay on *Warming Waters and Borealization* further explores ecological shifts underway in the marine environment, detailing how warming waters, declining sea ice, and shifting productivity in the northern Bering Sea and Chukchi Sea are driving the northward expansion of southern species. As boreal species increase over time, Arctic species in the northern Bering and Chukchi Seas have declined by two-thirds and one-half, respectively.

Borealization is also happening on land as large swaths of Arctic tundra become more like the boreal forest due to warming temperatures. Tundra greening refers to the long-term increase in tundra vegetation productivity and abundance that began to be observed in the 1990s. In 2025, circumpolar mean maximum tundra greenness was the third highest in the 26-year modern satellite record, with the five highest values all reported in the last six years.

While greening has dominated across the Arctic throughout recent decades, tundra vegetation dynamics are complex as some causes of browning (i.e., declines in vegetation productivity) have also increased due to extreme events and disturbances, such as wildfires (York et. al 2020). While wildfires are not featured in ARC 2025, summer 2025 marked the fourth consecutive year in which northern North

America experienced an area burned that was above the median based on analysis since 1988, with over 1 million acres burned in both Alaska and the Northwest Territories (Thoman 2025).

Across Arctic watersheds, biogeochemical changes are also becoming more visible, influenced by multidecadal permafrost warming. In 2024, permafrost monitoring sites in North America and Svalbard saw their highest temperatures on record (Smith et al. 2025). One impact is the *rusting rivers* phenomenon—rivers appearing visibly orange as oxidized iron from thawing permafrost enters the water. This year's Report Card documents satellite observations from more than 200 discolored streams and rivers across the Arctic, finding that these rusting rivers degrade water quality and habitat, with increased acidity and toxic trace metal concentrations. Mounting evidence illuminates the need for ongoing research to better understand influences on water quality, especially as related to rural community drinking water and subsistence fisheries.

Given the pervasive, high-impact environmental changes, maintaining Arctic observing and data-sharing infrastructure, along with specialized scientific expertise, is critical to ensure that necessary information is available to support decision-making at local to global scales. ARC 2025 includes an assessment of the Arctic Observing Network's ability to support Arctic scientific assessments, like the Report Card itself, and discusses some of the vulnerabilities and risks facing nationally and internationally coordinated observing programs, especially amid risks of diminishing U.S. investments in climate and environmental observations.

At the same time, Arctic communities are increasingly establishing and leading monitoring programs to serve local information needs, shaping a more resilient and responsive Arctic observing system. ARC 2025 includes an essay from the Indigenous Sentinels Network (ISN), based on St. Paul Island in Alaska's Bering Sea. Founded and led by the Aleut Community of St. Paul Island (ACSPI) Tribal Government, ISN empowers local observers to systematically record environmental conditions—from mercury contamination in harvested subsistence foods to coastal erosion and fish river habitat—using custom software tools and mobile apps, a community-owned database, and observing protocols designed for community relevance and scientific rigor. ISN has established lab space for local sample testing, information products for the community, and capacity building and mentoring programs that grow Indigenous leadership in Arctic observing.

Taken together, the findings of Arctic Report Card 2025 underscore that components of the Arctic system are both rapidly changing and closely connected—permafrost thaw influencing river chemistry, northward ocean heat transport reshaping Arctic marine ecosystems, and widespread warming leading to borealization of Arctic waters and landscapes. After twenty years of continuous reporting (e.g., Table 1), the Report Card stands as a chronicle of change and a caution for what the future will bring. Transformations over the next twenty years will reshape Arctic environments and ecosystems, impact the wellbeing of Arctic residents, and influence the trajectory of the global climate system itself, which we all depend on. Sustained, long-term observations and research and monitoring partnerships that remain nimble to emerging phenomena are essential foundations upon which understanding and adaptation depend.

Table 1. Selected ecological events chronicled across the 20 editions of the Arctic Report Card since 2006. The full inventory of past ARC essays is available at https://arctic.noaa.gov/Report-Card/Report-Card-Archive/.

	Year	Topic
Two decades of highlighting ecological change	2006	Arctic as large contributor to warmest year on record for the planet in 2005
	2007	Bering Sea ecological structure questioned after 6 years of sustained warming
	2008	Declining caribou populations
	2009	Bering Sea ecosystems influenced more by climate variability than long-term change
	2010	Threatened Arctic char present conservation challenge
	2011	Amplified ocean acidification
	2012	Widespread shorebird population decline reported
	2013	Sub-Arctic fish species reported in Arctic waters
	2014	Polar bear reproductive rates linked to sea ice cover duration
	2015	Sea-ice loss seen as greatest threat to walrus populations
	2016	Northern permafrost soils contain twice the carbon as in atmosphere
	2017	High latitude wildfires burning more area as climate rapidly warms
	2018	Impact of increasing harmful algal blooms warrants new monitoring
	2019	Bering Sea Elders share perspectives on rapid regional warming
	2020	Bowhead whales resilient despite ecological and human impacts
	2021	Changing marine soundscape amid increasing sea ice loss, storms, and shipping
	2022	Arctic geese populations at or above historic levels
	2023	Record-low Chinook and Chum Salmon contrasted with record-high Sockeye in Western Alaska
	2024	Arctic tundra transitions to being a carbon source
	2025	Rusting rivers degrading water quality and fish habitat

References

ANTHC [Alaska Native Tribal Health Consortium], 2024: Unmet needs of environmentally threatened Alaska native villages: Assessment and recommendations. Available at: https://anthc.org/resource/unmet-needs-report/.

Smith, S. L., V. E. Romanovsky, K. Isaksen, K. E. Nyland, N. I. Shiklomanov, D. A. Streletskiy, and H. H. Christiansen, 2025: Permafrost [in "State of the Climate in 2024"]. *Bull. Amer. Meteor. Soc.*, **106**(8), S338-S341, https://doi.org/10.1175/BAMS-D-25-0104.1.

Thoman, R., 2025: Summer 2025 northern North America wildfire: Above median, but less than 2022-2024. Alaska and Arctic Climate Newsletter, https://alaskaclimate.substack.com/p/summer-2025-northern-north-america.

York, A., U. S. Bhatt, E. Gargulinski, Z. Grabinski, P. Jain, A. Soja, R. L. Thoman, and R. Ziel, 2020: Wildland fire in high northern latitudes. *Arctic Report Card 2020*, R. L. Thoman, J. Richter-Menge, and M. L. Druckenmiller, Eds., https://doi.org/10.25923/2gef-3964.

December 23, 2025

Surface Air Temperature

https://doi.org/10.25923/cj60-9s07

T. J. Ballinger[1], A. Crawford[2], M. C. Serreze[3], S. Bigalke[4], J. E. Walsh[1], B. Brettschneider[5], R. L. Thoman[1,6], U. S. Bhatt[7], E. Hanna[8], H. Motrøen Gjelten[9], S. -J. Kim[10], J. E. Overland[11], and M. Wang[11,12]

[1]International Arctic Research Center, University of Alaska Fairbanks, Fairbanks, AK, USA
[2]Department of Environment and Geography, University of Manitoba, Winnipeg, MB, Canada
[3]National Snow and Ice Data Center, Cooperative Institute for Research in Environmental Sciences, University of Colorado Boulder, Boulder, CO, USA
[4]Department of Geography, Portland State University, Portland, OR, USA
[5]National Weather Service Alaska Region, NOAA, Anchorage, AK, USA
[6]Alaska Center for Climate Assessment and Preparedness, University of Alaska Fairbanks, Fairbanks, AK, USA
[7]Geophysical Institute, University of Alaska Fairbanks, Fairbanks, AK, USA
[8]Department of Geography and Lincoln Climate Research Group, University of Lincoln, Lincoln, UK
[9]Norwegian Meteorological Institute, Oslo, Norway
[10]Korea Polar Research Institute, Incheon, Republic of Korea
[11]Pacific Marine Environmental Laboratory, NOAA, Seattle, WA, USA
[12]Cooperative Institute for Climate, Ocean, and Ecosystem Studies, University of Washington, Seattle, WA, USA

Headlines

- Dating back to 1900, the Arctic experienced the warmest water year (October 2024-September 2025) and autumn (2024) on record.
- Since 2006, Arctic autumn and winter air temperatures have each increased by more than twice the corresponding increases in global air temperatures.
- Amplified Arctic warming has cascading impacts on the Arctic system, including glacial melt, sea ice decline, greening landscapes, and various ecological changes.

Overview

Pan-Arctic (60° N-90° N) surface air temperatures continue to increase faster than those for the planet as a whole (90° S-90° N), especially during winter (Ballinger et al. 2025). Since 1980, the Arctic annual air temperatures have warmed nearly three times faster than the global mean due to global anthropogenic greenhouse gas emissions (Sweeney et al. 2023; Zhou et al. 2024). This amplified Arctic warming has been linked with a plethora of ongoing and emerging physical and ecological changes that profoundly affect transportation, infrastructure, and subsistence livelihoods for many people across the Arctic with impacts extending to societies in lower latitudes (Moon et al. 2019; Walsh et al. 2020). Some widespread responses to this warming include increased annual precipitation (see essay *Precipitation*), increased greening of Arctic landscapes (see essay *Tundra Greenness*), and sustained mass loss of the Greenland Ice Sheet (see essay *Greenland Ice Sheet*) and Arctic glaciers and ice caps (see essay *Glaciers and Ice Caps outside Greenland*). Increased winter temperatures affect the development and thickening

of sea ice across the Arctic marginal seas (see essay *Sea Ice*), while increasing summer temperatures are associated with more frequent and devastating high-latitude wildland fires across much of Alaska (York et al. 2020) and northern Canada (Jain et al. 2024). Surface air temperature observations from weather stations often provide localized, long-term records, which are augmented by atmospheric reanalyses to provide a more complete spatial representation of multidecadal Arctic change.

Consistent with previous Arctic Report Cards, the sections that follow examine this past year's Arctic surface air temperatures in an historical context. For this year's 20th anniversary issue of the Arctic Report Card, we also compare recent Arctic air temperature changes since 2006 against global rates of change. We subsequently highlight seasonal surface air temperature anomaly patterns and extremes and discuss associated large-scale atmospheric circulation patterns.

Annual and seasonal air temperatures in context

Annual air temperatures are averaged for the water year (i.e., October 2024-September 2025 represents 2025), while three-month seasons are referenced as follows: autumn 2024 (October-December [OND]), winter (January-March [JFM]), spring (April-June [AMJ]), and summer 2025 (July-September [JAS]).

Annual Arctic and global surface air temperature anomalies (i.e., differences from average temperature; see *Methods and data*) are shown in Fig. 1a. This past year was the warmest on record since 1900 with anomalies of 1.60°C above the 1991-2020 mean. Arctic temperature anomalies continue to be larger than those measured at the global scale. This is the 12th consecutive year where pan-Arctic temperature departures were above the global average. The years 2016-25 have been the Arctic's warmest ten individual years on record, punctuated by several new annual and seasonal records (Fig. 2).

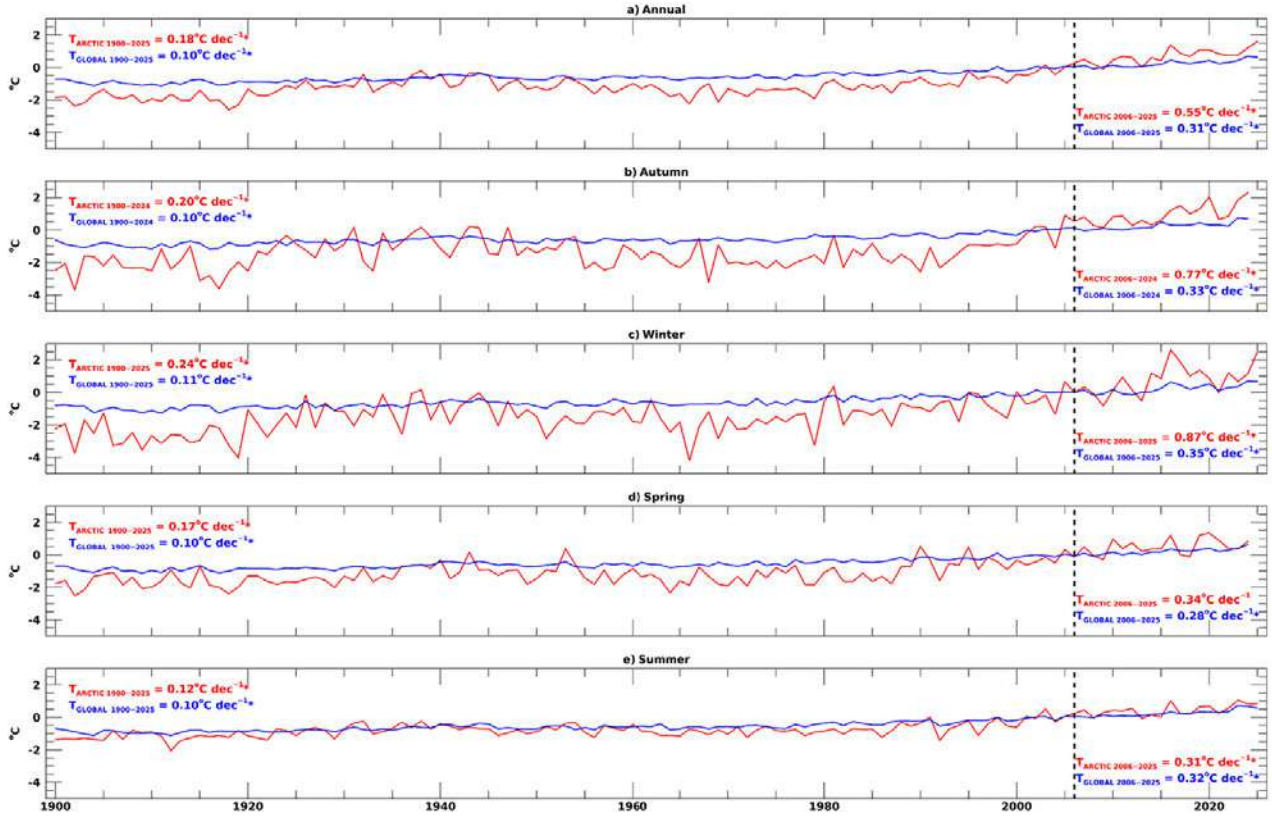

Fig. 1. Long-term time series of (a) annual, (b) autumn, (c) winter, (d) spring, and (e) summer surface air

temperature anomalies (in °C) averaged across Arctic (60-90° N) and Global (90° S-90° N) land and ocean areas. The Arctic (T_{ARCTIC}) and global (T_{GLOBAL}) air temperature change per decade (°C dec^{-1}) during the full period of record and since 2006 (indicated by dashed line) are shown in each panel. Statistically significant ($p \leq 0.05$) linear trends are marked by an asterisk. Source: NASA GISTEMP v4 data are obtained from the NASA Goddard Institute for Space Studies.

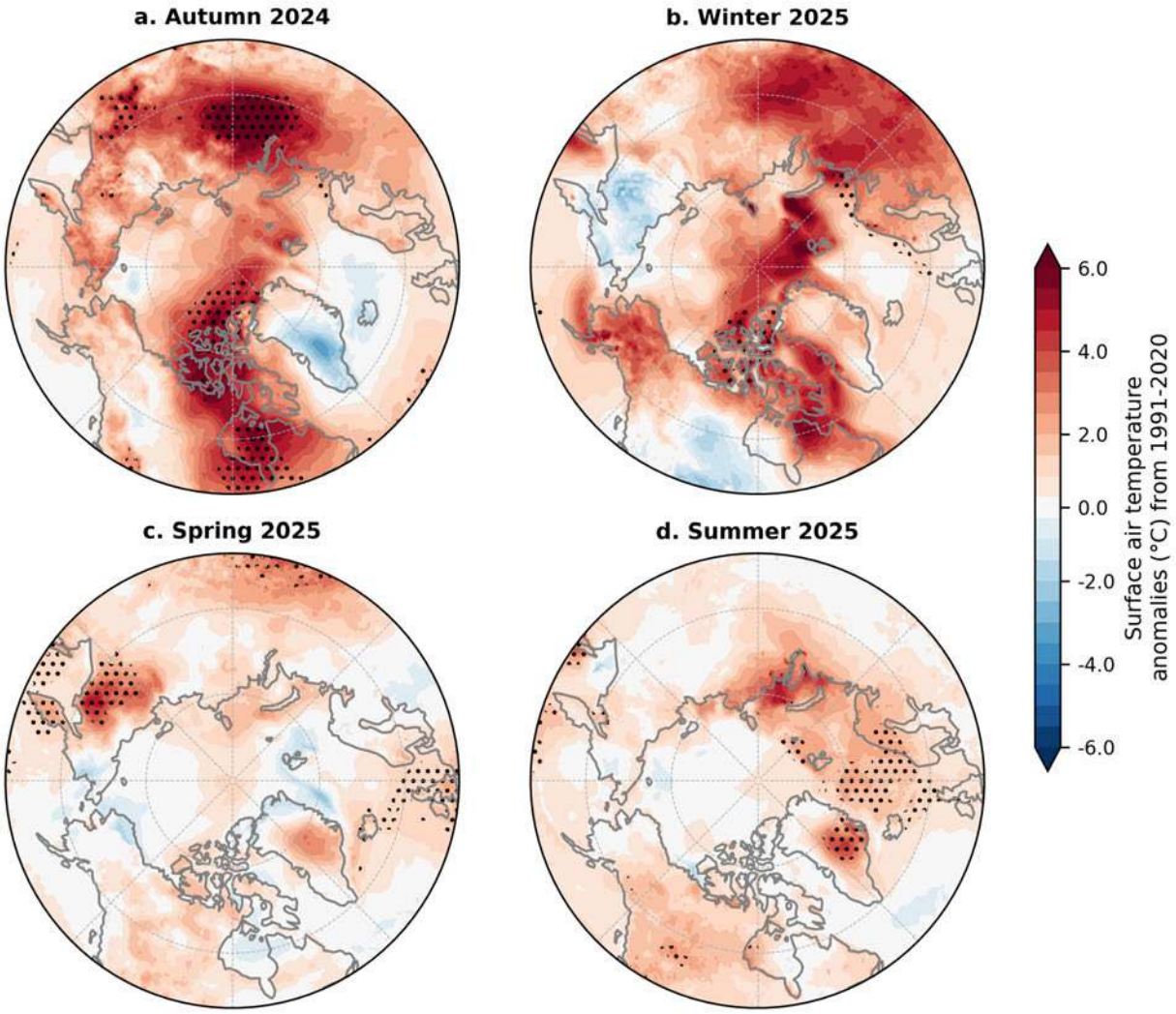

Fig. 2. Seasonal surface air temperature anomalies (in °C) for (a) autumn 2024, (b) winter 2025, (c) spring 2025, and (d) summer 2025. Temperature anomalies are shown relative to their 1991-2020 means. Hatching indicates the warmest seasonal temperatures since 1940. Source: ERA5 reanalysis air temperature data are obtained from the Copernicus Climate Change Service.

Arctic seasonal temperature anomalies during the past year were strikingly high (Fig. 1b-e). Autumn 2024 was the warmest on record since 1900 at 2.28°C above the 1991-2020 mean, while the winter and summer 2025 temperatures were the second and third warmest on record at 2.41°C and 0.83°C, respectively, above the 30-year average. Spring air temperatures were also elevated and ranked eighth warmest at 0.57°C above the 1991-2020 mean. Since the inception of the Arctic Report Card, the rates of annual and seasonal Arctic warming continue to exceed those of global warming. Most notably, from 2006 onward, autumn (0.77°C/decade versus 0.33°C/decade) and winter temperatures (0.87°C/decade versus 0.35°C/decade) have increased at rates more than double the corresponding global rates.

Several mechanisms and feedbacks underlie the ongoing Arctic warming pattern and explain why it has outpaced the global warming trend. For example, the water vapor feedback, whereby more water vapor from enhanced evaporation leads to higher longwave radiation at the surface, and northward heat and moisture transport from weather patterns contribute to year-round warm extremes (Cohen et al. 2020). In autumn and winter, when Arctic Amplification is strongest, Arctic Ocean heat accumulated from increased solar energy absorption amid summer sea-ice losses (see essay *Sea Ice*) and poleward advection of warm sub-Arctic water masses (see essay *Atlantification*) is released to the overlying atmosphere, driving warmer air temperatures. Patterns of seasonal air temperature anomalies, summarized below, align with some of these processes that drive Arctic climate change.

Seasonal air temperature anomaly patterns

Seasonal air temperature anomaly patterns are illustrated in Fig. 2. Autumn 2024 was characterized by positive temperature anomalies over most high latitude land and ocean areas except for the Chukchi Sea, Greenland Sea, Norwegian Sea, and Greenland (Fig. 2a). Record-high seasonal temperatures since 1940 (with anomalies of 4-6°C above the mean) were found around Hudson Bay, the Canadian Arctic Archipelago, Lincoln Sea, central Arctic Ocean, and in central Siberia. The extreme Hudson Bay temperatures during autumn 2024 were largely the result of record early sea ice retreat in eastern Hudson Bay that allowed for exceptional ocean heat uptake and supported a season-long marine heatwave (Soriot et al. 2025). Sea-level pressure (SLP) was anomalously high over Greenland and Iceland, yet anomalously low over the Barents Sea and Kara Sea (Fig. 3a), which supported the wet and cold versus dry and warm dipole in the North Atlantic Arctic (see essay *Precipitation*). Of note, the high SLP over Greenland and Iceland corresponded with a record-high September to November average value (1.78) of the Greenland Blocking Index, a measure of mid-tropospheric air pressure, since 1948 (Hanna et al. 2016, updated data). This high-pressure pattern supported warm air advection over areas of record warmth in the Canadian Arctic Archipelago and Lincoln Sea.

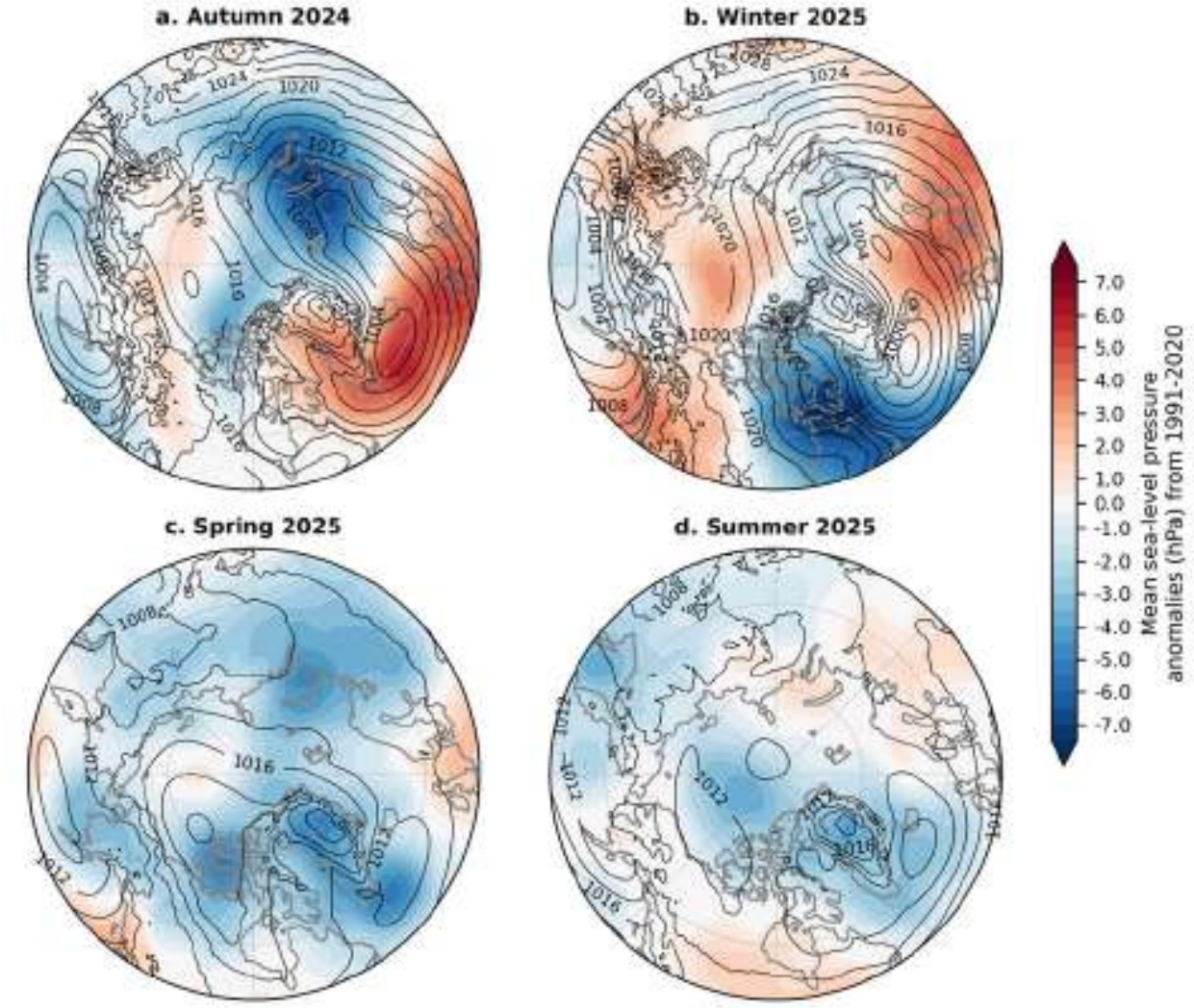

Fig. 3. Seasonal sea-level pressure (SLP) anomalies (shading) and raw values (isobars) (both in hPa) for (a) autumn 2024, (b) winter 2025, (c) spring 2025, and (d) summer 2025. SLP anomalies are shown relative to their 1991-2020 means. Source: ERA5 reanalysis SLP data are obtained from the Copernicus Climate Change Service.

There were some similarities between air temperature patterns in autumn 2024 (Fig. 2a) and winter 2025 (Fig. 2b). Most notably, Canadian Arctic Archipelago record-high temperatures persisted into winter, while the Lincoln Sea, adjacent central Arctic Ocean, and central and eastern Eurasia remained warmer than average. The southern Barents Sea also saw record-high winter temperatures in 2025. During February, Svalbard was 6-8°C above the 1991-2020 climatology, which was the archipelago's second warmest February since measurements began in the mid-1970s (Grinde et al. 2025). Much of the North Atlantic, from Baffin Bay to the Barents Sea, was anomalously warm, as was the southern Bering Sea and Alaska. The only areas of below-average temperatures were over the eastern Siberia and north central Canada. Much lower-than-average surface pressure indicative of an active storm track was found over eastern Canada (6-7 hPa), in contrast to above-average surface pressure south of Alaska and over northern Europe that supported southerly warm advection over those areas (Fig. 3b).

Spring 2025 was characterized by near-average air temperature patterns across the Arctic (Fig. 2c). Three regional exceptions were eastern Siberia and the Sea of Okhotsk, central Russia, and the

Norwegian Sea, which saw record spring warmth. Central Greenland also saw above-average air temperatures during this time. Much of the Arctic saw below-average to near-average SLP conditions in spring (Fig. 3c).

Summer 2025 was characterized by average to above-average air temperatures over most Arctic lands, especially in the north central Siberian littoral zones (Fig. 2d). Record warmth characterized much of the North Atlantic high latitudes including central and eastern Greenland, the Norwegian Sea, northern Scandinavia, and areas northeast of Svalbard. Lower-than-normal SLP around Greenland and Iceland suggest an invigorated storm track may have contributed to the record warm North Atlantic Arctic summer (Fig. 3d).

Methods and data

The NASA Goddard Institute for Space Studies surface temperature analysis version 4 (GISTEMP v4) is used to describe long-term Arctic and Global surface (i.e., two-meter) air temperatures since 1900 (Fig. 1). GISTEMP v4 air temperatures over lands are obtained from the NOAA Global Historical Climatology Network version 4 (GHCN v4) dataset and ocean surface temperatures are taken from the NOAA Extended Reconstructed Sea Surface Temperature version 5 (ERSST v5) dataset. The GISTEMP product is described in Hansen et al. (2010) and Lenssen et al. (2019).

We use ERA5 two-meter (i.e., near-surface) air temperature and sea-level pressure fields in Figs. 2 and 3, respectively, to provide spatial context to recent Arctic temporal variability shown in Fig. 1. ERA5 provides consistency with other sections of the Arctic Report Card, including Precipitation. Details of ERA5 reanalysis are provided in Hersbach et al. (2020). All values and fields are presented as anomalies with respect to the 1991-2020 mean. Temperature changes, spanning the subscripted periods in each Fig. 1 panel, represent linear least squares trends per decade.

References

Ballinger, T. J., and Coauthors, 2025: Surface air temperature. [in “State of the Climate in 2024”]. *Bull. Amer. Meteor. Soc.*, **106**(8), S311-S313, https://doi.org/10.1175/BAMS-D-25-0104.1.

Cohen, J., and Coauthors, 2020: Divergent consensuses on Arctic amplification influence on midlatitude severe winter weather. *Nat. Climate Change*, **10**, 20-29, https://doi.org/10.1038/s41558-019-0662-y.

Grinde, L., J. Mamen, K. Tunheim, and S. Aaboe, 2025: Været i Norge – Klimatologisk månedsoversikt februar 2025 [The weather in Norway – Climatological monthly overview February 2025]. MET info, 02-2025, Norwegian Meteorological Institute, https://www.met.no/publikasjoner/met-info.

Hanna, E., T. E. Cropper, R. J. Hall, and J. Cappelen, 2016: Greenland Blocking Index 1851-2015: a regional climate change signal. *Int. J. Climatol.*, **36**(15), 4847-4861. https://doi.org/10.1002/joc.4673.

Hansen, J., R. Ruedy, M. Sato, and K. Lo, 2010: Global surface temperature change. *Rev. Geophys.*, **48**, RG4004, https://doi.org/10.1029/2010RG000345.

Hersbach, H., and Coauthors, 2020: The ERA5 global reanalysis. *Quart. J. Roy. Meteor. Soc.*, **146**, 1999-2049, https://doi.org/10.1002/qj.3803.

Jain, P., and Coauthors, 2024: Drivers and impacts of the record-breaking 2023 wildfire season in Canada. *Nat. Commun.*, **15**, 6764, https://doi.org/10.1038/s41467-024-51154-7.

Lenssen, N. J. L., G. A. Schmidt, J. E. Hansen, M. J. Menne, A. Persin, R. Ruedy, and D. Zyss, 2019: Improvements in the GISTEMP uncertainty model. *J. Geophys. Res.-Atmos.*, **124**, 6307-6326, https://doi.org/10.1029/2018JD029522.

Moon, T. A., and Coauthors, 2019: The expanding footprint of rapid Arctic change. *Earth's Future*, **7**(3), 212-218, https://doi.org/10.1029/2018EF001088.

Soriot, C., J. Stroeve, and A. Crawford, 2025: Record early sea ice loss in southeastern Hudson Bay in Spring 2024. *Geophys. Res. Lett.*, **52**(4), e2024GL112584, https://doi.org/10.1029/2024GL112584.

Sweeney, A. J., Q. Fu, S. Po-Chedley, H. Wang, and M. Wang, 2023: Internal variability increased Arctic amplification during 1980-2022. *Geophys. Res. Lett.*, **50**, e2023GL106060, https://doi.org/10.1029/2023GL106060.

Thoman, R., 2025: Arctic summer 2025 climate summary. https://alaskaclimate.substack.com/p/arctic-summer-2025-climate-summary.

Walsh, J. E., T. J. Ballinger, E. S. Euskirchen, E. Hanna, J. Mård, J. E. Overland, H. Tangen, and T. Vihma, 2020: Extreme weather and climate events in northern areas: A review. *Earth Sci. Rev.*, **209**, 103324, https://doi.org/10.1016/j.earscirev.2020.103324.

York, A., U. S. Bhatt, E. Gargulinski, Z. Grabinski, P. Jain, A. Soja, R. L. Thoman, and R. Ziel, 2020: Wildland fire in high northern latitudes. *Arctic Report Card 2020*, R. L. Thoman, J. Richter-Menge, and M. L. Druckenmiller, Eds., https://doi.org/10.25923/2gef-3964.

Zhou, W., L. R. Leung, and J. Lu, 2024: Steady threefold Arctic amplification of externally forced warming masked by natural variability. *Nat. Geosci.*, **17**, 508-515, https://doi.org/10.1038/s41561-024-01441-1.

November 18, 2025

Precipitation

https://doi.org/ 10.25923/11nn-hn03

M. C. Serreze[1], S. Bigalke[2], R. Lader[3], A. Crawford[4], and T. J. Ballinger[3]

[1]National Snow and Ice Data Center, Cooperative Institute for Research in Environmental Sciences, University of Colorado Boulder, Boulder, CO, USA
[2]Department of Geography, Portland State University, Portland, OR, USA
[3]International Arctic Research Center, University of Alaska Fairbanks, Fairbanks, AK, USA
[4]Department of Environment and Geography, University of Manitoba, Winnipeg, MB, Canada

Headlines

- Precipitation averaged across the Arctic for water year 2024/25 (October 2024-September 2025) was at a record high, and precipitation totals for the winter, spring, and autumn seasons were each in the top five highest, reinforcing positive trends in Arctic precipitation over the 1950-2025 period.
- Summer was unusually dry, notably over parts of Eurasia and Canada.
- An intensifying water cycle with more extreme precipitation events threatens to further disrupt Arctic ecosystems, infrastructure, and communities.

Introduction

Annual precipitation over the Arctic region, taken here as poleward of 60° N, is characterized by high totals over the Atlantic sector due to open water and the frequent passage of storm systems, locally exceeding 2000 mm, and generally dry conditions elsewhere. Polar desert, with annual precipitation of 250 mm or less, characterizes much of the Canadian Arctic Archipelago and central Arctic Ocean, reflecting cold conditions and distance from moisture sources. However, within these patterns, there is strong seasonality and local to regional variability related largely to the passage of storms and forced uplift of air masses by orography (orographic precipitation). Convective precipitation (thunderstorms), caused by strong surface heating, is found over land areas in summer. However, convective precipitation also occurs over the ice-free ocean in some circumstances.

For the Arctic as a whole, annual precipitation for the October 2024-September 2025 water year was the highest on record. This has reinforced upward trends in precipitation as observed over the period 1950-2025. The year 2025 also saw the widespread occurrence of extreme precipitation events in winter, as well as summer dryness. As the water cycle intensifies and extreme precipitation events become more common (Yu and Zhong 2021; Dou et al. 2022), disruption to ecosystems (e.g., Christensen et al. 2021; Serreze et al. 2021) and human infrastructure (e.g., Hansen et al. 2014; Fox et al. 2023) will further impact Arctic communities.

As with other essays in Arctic Report Card 2025, water-year seasons are defined as autumn (October-December), winter (January-March), spring (April-June), and summer (July- September). Anomalies are relative to the 1991-2020 average. The results presented here use both precipitation gauges and atmospheric reanalysis data, which are derived by assimilating observations with output from numerical

weather prediction models. Atmospheric reanalysis data are helpful for filling in the many gaps in the sparse precipitation gauge network in the Arctic, especially over the Arctic Ocean, though in general in situ precipitation measurements are not assimilated.

Precipitation at a glance

The 2024/25 water year included several prominent features. Record-high precipitation for spring, and high ranks for autumn (4th highest) and winter (4th highest) stand in contrast to an unusually dry summer (35th highest). However, despite summer dryness, the water year, as a whole, ranked as the wettest on record. Regionally, below-average precipitation in autumn over the Barents Sea contrasted above-average precipitation over northern Europe, pointing to an eastward shift in storm tracks relative to average conditions. The Alaskan Panhandle shifted from having above-average precipitation in autumn to below-average precipitation in winter. This reflects a westward location of low pressure from over the Gulf of Alaska in autumn to over the Aleutian Islands in winter (see Fig. 3 in essay *Surface Air Temperature*). The summer dryness was especially apparent over large parts of Eurasia and northern Canada, likely contributing to the frequent Canadian forest fires. Figure 1 shows seasonal precipitation totals derived from ERA5 reanalysis during the 2024/25 water year expressed as departures from the 1991-2020 means.

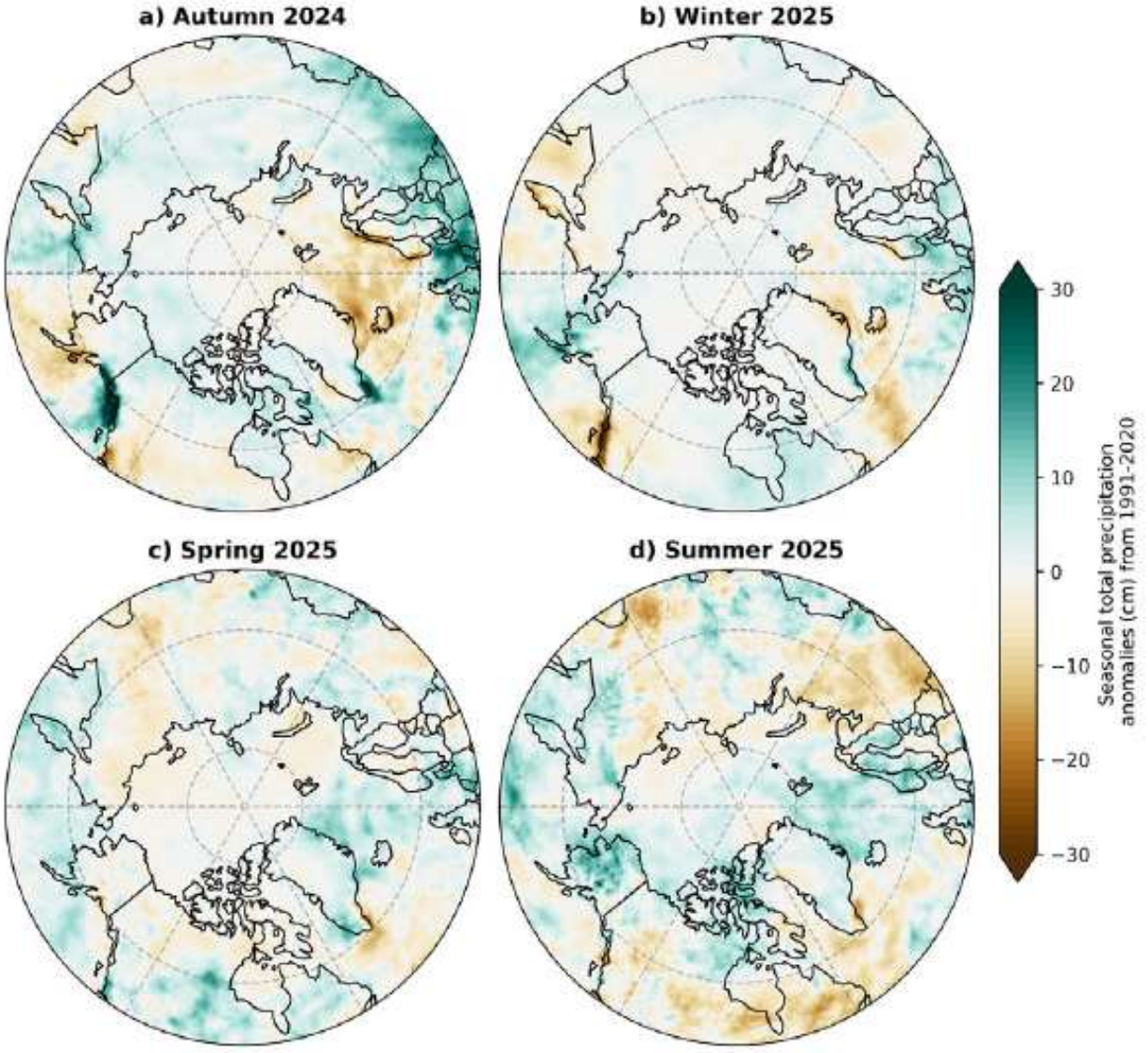

Fig. 1. Precipitation anomalies (using 1991-2020 baseline) for autumn (OND) 2024, winter (JFM) 2025, spring (AMJ) 2025, and summer (JAS) 2025. Green shades denote above-normal precipitation and brown shades denote below-normal precipitation. Data source: ERA5 reanalysis.

Heavy precipitation events

For any given year, regionally heavy precipitation events can approach or exceed previous records, even in a stable climate. Following the approach of previous Arctic Report Cards, Fig. 2 shows heavy precipitation events during the 2024/25 water year in terms of ranks of the maximum 5-day precipitation events (Rx5) in each season (relative to the 1950-2023 period). The standout feature is the comparatively higher density of heavy precipitation events across the Arctic in winter compared with the other seasons. One feature of special note is the band of heavy precipitation events in winter stretching northward from south of the Aleutian Islands across Alaska. Much of that precipitation was related to a large northward pulse of moisture (an “atmospheric river”) from 22-25 January. The associated southerly winds also contributed to warmer-than-average surface air temperatures across

these areas (see essay *Surface Air Temperature*). Note also the band of heavy precipitation in summer over northern Alaska.

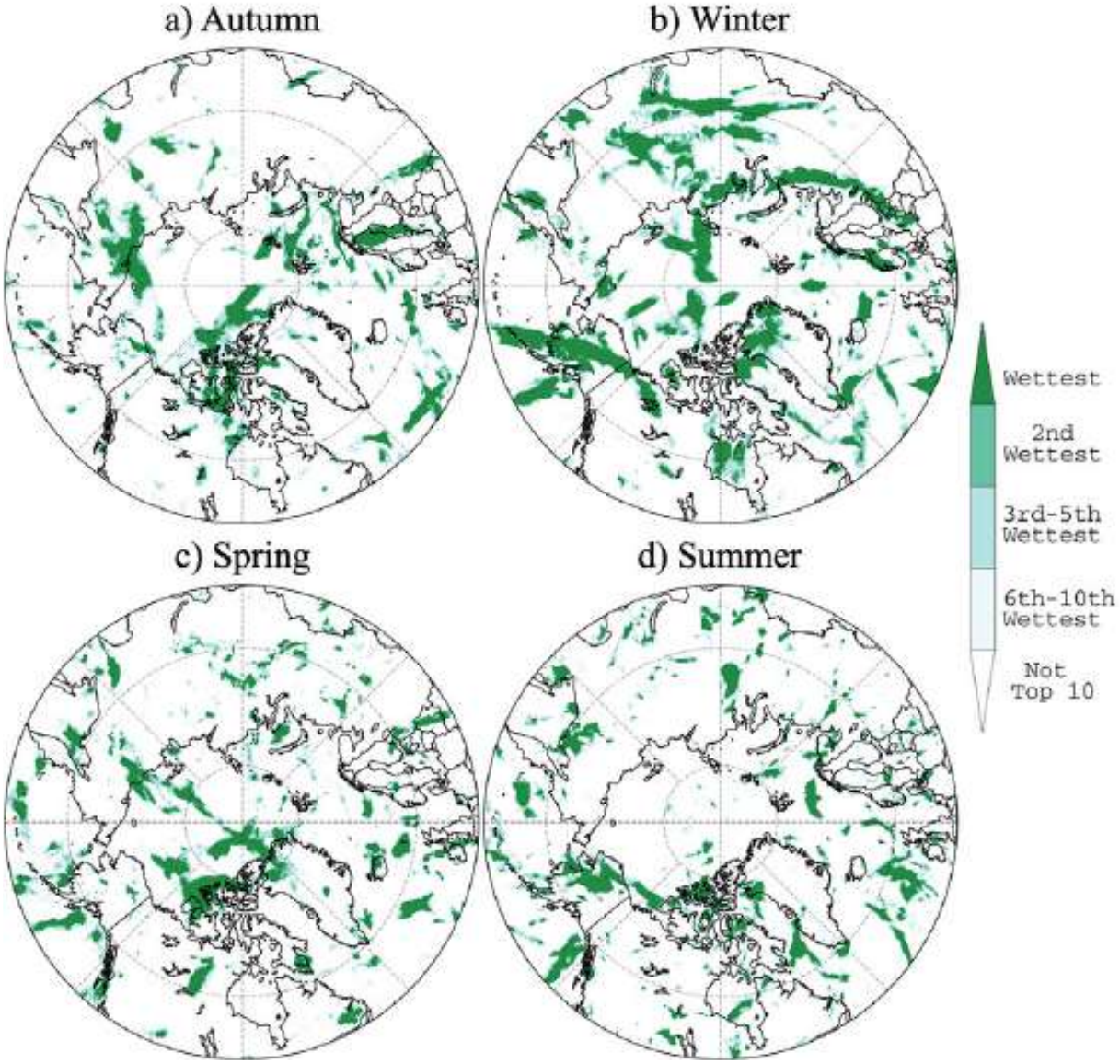

Fig. 2. Ranks of maximum 5-day precipitation for each season during the 2024/25 water year relative to years from 1950-2023: (a) autumn (OND), (b) winter (JFM), (c) spring (AMJ), and (d) summer. Data source: ERA5 reanalysis, 1950-present.

Historical perspective

The last several Arctic Report Cards have highlighted that, as assessed over the available period of record, there are upward trends in pan-Arctic precipitation in the annual mean average and for each season individually. Previous studies commenting on trends (Box et al. 2021; Yeh et al. 2021; Yu and Zhong 2021; Walsh et al. 2022) emphasize interannual and multiyear variability and large regional variations. There is also evidence of a transition from solid to liquid precipitation in the warmer parts of the Arctic (Box et al. 2021).

Following previous Arctic Report Cards, the Arctic precipitation time series from ERA5 (as a percentage of 1991-2020 averages for the region poleward of 60° N) is plotted along with the corresponding time series from the station-based dataset of the Global Precipitation Climatology Center (GPCC) during 1950/51-2024/25 (Fig. 3). The ERA5 data cover ocean areas as well as land, while the GPCC dataset is for land only. While the percent anomaly time series are generally similar, there are some substantial differences for individual years due to the absence of coverage over the Arctic Ocean in GPCC and inherent uncertainties in each data source.

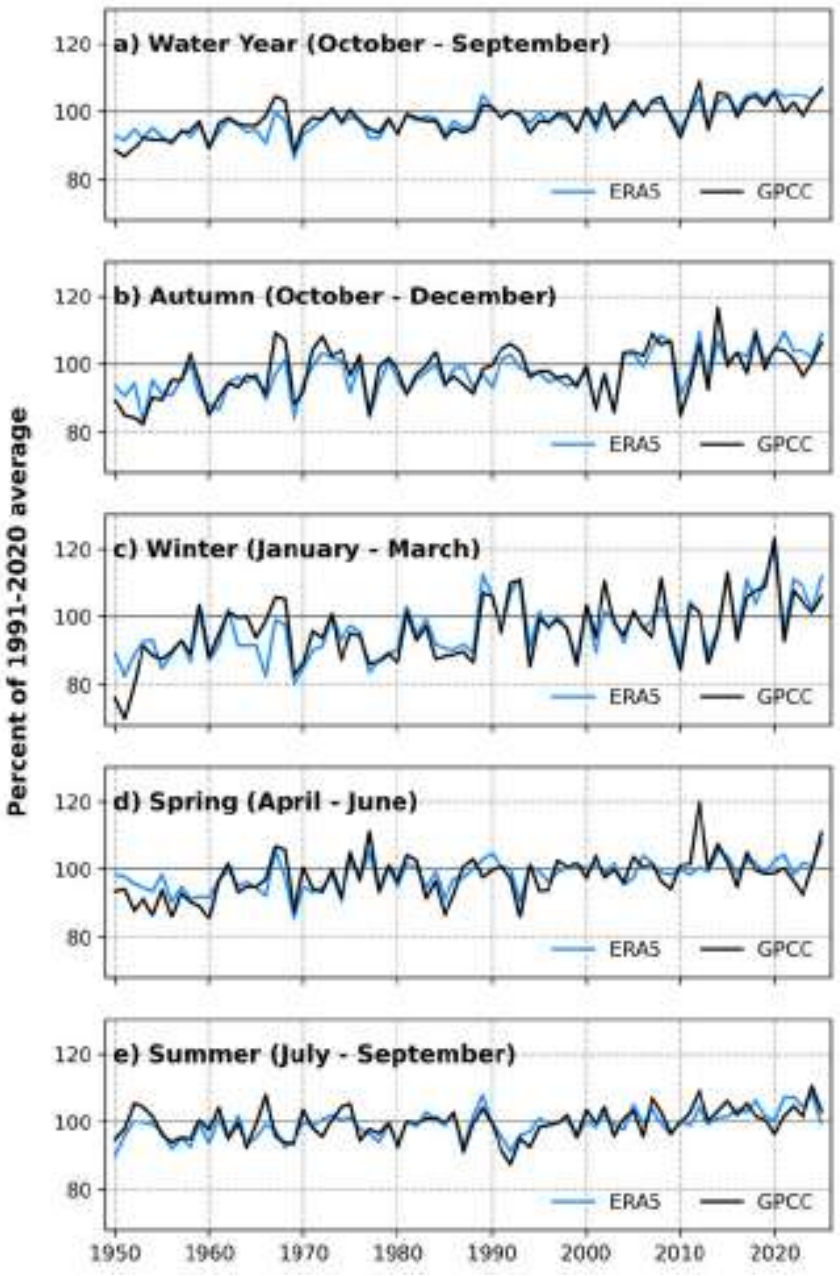

Fig. 3. Time series of Arctic (60-90° N) precipitation for water-years from 1950/51 through 2024/25 expressed as a percentage of the 1991-2020 average (shown by the horizontal black lines at 100%). Results are from ERA5 (blue lines) and GPCC 1.0° data (black lines). ERA5 values are for land plus ocean; GPCC values are for land only. The GPCC Full Data version is used from 1950-2020, the GPCC monitoring product for January 2021-July 2025 and the GPCC First Guess product for August-September 2025.

The record-high rank of annual mean precipitation for the 2024/25 water year, as well as the high ranks for individual seasons (a record-high for spring), served to reinforce the conclusion that precipitation for the Arctic region overall is increasing. Based on the ERA5 precipitation time series for the region poleward of 60° N that includes the 2024/25 water year, the trend in annual mean precipitation stands at 0.75 cm per decade. Corresponding seasonal trends are 0.22 cm per decade for autumn, 0.23 cm per decade for winter, 0.13 cm per year for spring, and 0.09 cm per decade for summer. Autumn and winter hence show the strongest seasonal trends. In terms of percent change relative to the 1991-2020 average, winter is strongest (2.25 % per decade). Autumn is 1.67 % per decade, summer is 1.04% per decade, spring is 1.11% per decade, and the water year as a whole is 1.47% per decade.

The spatial pattern of annual trends, 1950-2025, is quite revealing (Fig. 4). Positive trends of up to 0.3 cm per year are apparent over the North Atlantic sector of the Arctic and extending into the Barents Sea. The strong positive trends along the Norwegian coast and parts of the southeast coast of Greenland point to orographic effects—forced uplift and cooling of moist air. Strong positive trends along the Alaska coast are also consistent with orographic uplift. Pointing further to the spatial heterogeneity of trends, reductions in precipitation are seen in other areas, such as parts of northern Eurasia and Canada.

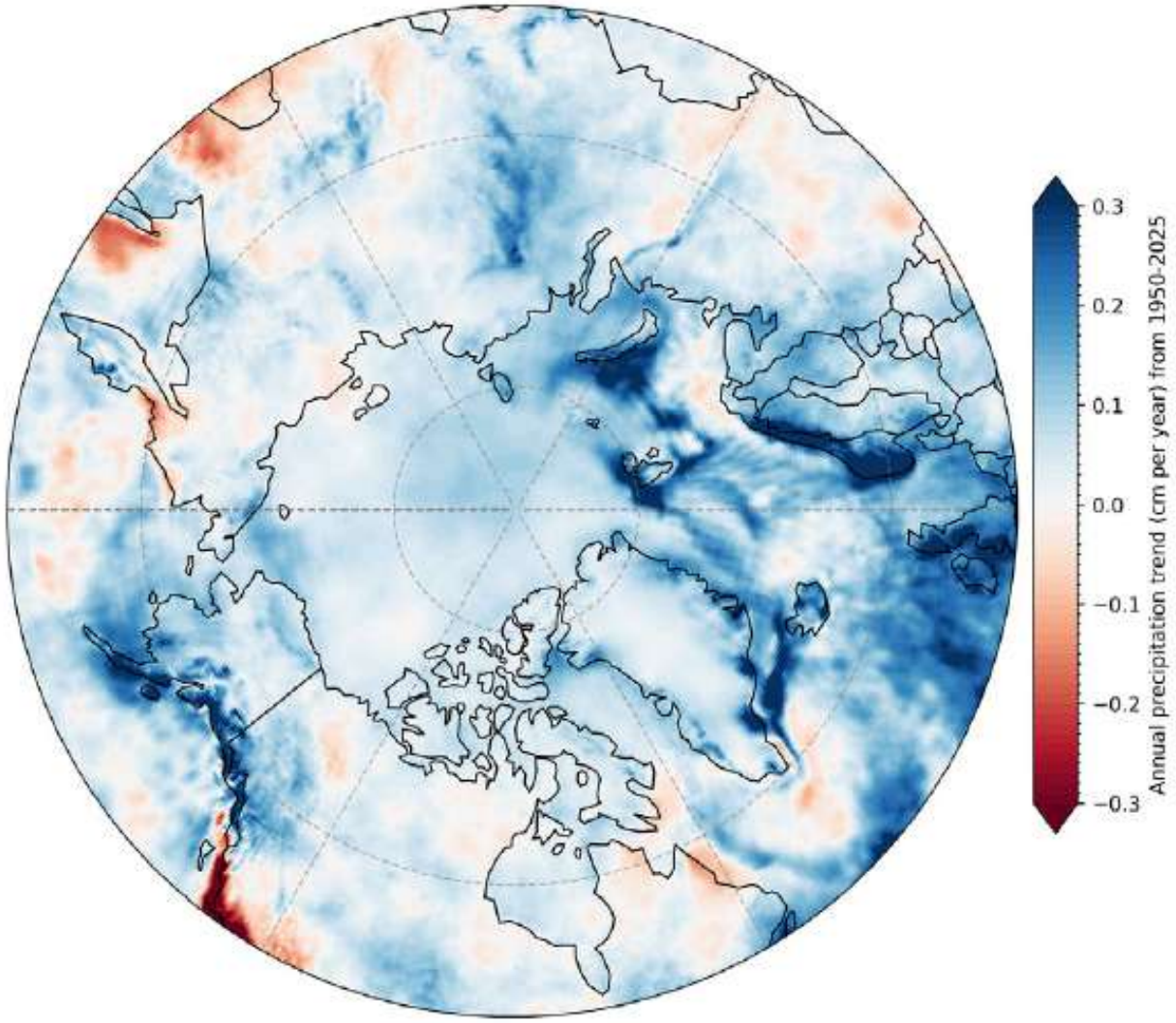

Fig. 4. Linear trends in annual precipitation from 1950-2025 from ERA5 in cm per year.

Methods and data

Because of the challenges of collecting in situ precipitation gauge measurements in the Arctic, we use gridded precipitation fields from both the ERA5 atmospheric reanalysis of the European Centre for Medium Range Weather Forecasts (ECMWF) (Hersbach at al. 2020) and the Global Precipitation Climatology Centre's GPCC Full Data Version Data Version 2022 (Becker et al. 2013; https://opendata.dwd.de/climate_environment/GPCC/html/fulldata-daily_v2022_doi_download.html). ERA5 data are available from January 1940 onward, but the quality of the output is more reliable starting in 1979 (Hersbach et al. 2020), after which modern satellite data are assimilated into the analysis and forecast system. ERA5 is the latest atmospheric reanalysis effort and performs slightly better than other atmospheric reanalyses at matching observed precipitation totals from Arctic extreme events (Loeb et al. 2022). Given the model-derived nature of ERA5, comparisons are made with the GPCC's full data product, a monthly gridded gauge-based product available from 1891 onward (Schneider et al. 2022). Our comparisons of pan-Arctic precipitation computed from these two sources is limited to the post-1950 period because both products were impacted by missing data during World War II.

References

Becker, A., P. Finger, A. Meyer-Christoffer, B. Rudolf , K. Schamm, U. Schneider, and M. Ziese, 2013: A description of the global land-surface precipitation data products of the Global Precipitation Climatology Centre with sample applications including centennial (trend) analysis from 1901-present. *Earth Syst. Sci. Data*, **5**, 71-99, https://doi.org/10.5194/essd-5-71-2013.

Box, J. E., and Coauthors, 2021: Recent developments in Arctic climate observation indicators. *AMAP Arctic Climate Change Update 2021: Key Trends and Impacts*, Arctic Monitoring and Assessment Programme (AMAP), Tromso, Norway, 7-29, https://www.amap.no/documents/doc/amap-arctic-climate-change-update-2021-key-trends-and-impacts/3594.

Christensen, T. R., and Coauthors, 2021: Multiple ecosystem effects of extreme weather events in the Arctic. *Ecosystems*, **24**, 122-136, https://doi.org/10.1007/s10021-020-00507-6.

Dou, T. F., S. F. Pan, R. Bintanja, and C. D. Xiao, 2022: More frequent, intense, and extensive rainfall events in a strongly warming Arctic. *Earth's Future*, **10**(10), e2021EF002378, https://doi.org/10.1029/2021ef002378.

Fox, S., A. Crawford, M. McCrystall, J. Stroeve, J. Lukovich, N. Loeb, J. Natanine, and M. Serreze, 2023: Extreme Arctic weather and community impacts in Nunavut: A case study of one winter's storms and lessons for local climate change preparedness. *Weather Clim., Soc.*, **15**, 881-892, https://doi.org/10.1175/wcas-d-23-0006.1.

Hansen, B. B., and Coauthors, 2014: Warmer and wetter winters: characteristics and implications of an extreme weather event in the High Arctic. *Environ. Res. Lett.*, **9**, 114021, https://doi.org/10.1088/1748-9326/9/11/114021.

Hersbach, H., and Coauthors, 2020: The ERA5 global reanalysis. *Quart. J. Roy. Meteor. Soc.*, **146**, 1999-2049, https://doi.org/10.1002/qj.3803.

Loeb, N. A., A. Crawford, J. C. Stroeve, and J. Hanesiak, 2022: Extreme precipitation in the eastern Canadian Arctic and Greenland: An evaluation of atmospheric reanalyses. *Front. Env. Sci.*, **10**, 866929, https://doi.org/10.3389/fenvs.2022.866929.

Schneider, U., P. Finger, E. Rustemeier, M. Ziese, and S. Hänsel, 2022: Global precipitation analysis products of the GPCC, Global Precipitation Climatology Centre, https://opendata.dwd.de/climate_environment/GPCC/PDF/GPCC_intro_products_v2022.pdf.

Serreze, M. C., and Coauthors, 2021: Arctic rain on snow events: bridging observations to understand environmental and livelihood impacts. *Environ. Res. Lett.*, **16**(10), 105009, https://doi.org/10.1088/1748-9326/ac269b.

Walsh, J. E., S. Bigalke, S. A. McAfee, R. Lader, M. C. Serreze, and T. J. Ballinger, 2022: Precipitation. *Arctic Report Card 2022*, M. L. Druckenmiller, R. L. Thoman, and T. A. Moon, Eds., https://doi.org/10.25923/n07s-3s69.

Ye, H., D. Yang, A. Behrangi, S. L. Stuefer, X. Pan, E. Mekis, Y. Dibike, and J. E. Walsh, 2021: Precipitation characteristics and changes. *Arctic Hydrology, Permafrost and Ecosystems* (D. Yang and D. L. Kane, Eds.), Springer Nature Switzerland, https://doi.org/10.1007/978-3-030-50930-9_2.

Yu, L., and S. Zhong, 2021: Trends in Arctic seasonal and extreme precipitation in recent decades. *Theor. Appl. Climatol.*, **145**, 1541-1559, https://doi.org/10.1007/s00704-021-03717-7.

November 21, 2025

Terrestrial Snow Cover

https://doi.org/10.25923/cfhv-c239

L. R. Mudryk[1], A. Elias Chereque[2], C. Derksen[1], K. Luojus[3], and B. Decharme[4]

[1]Climate Research Division, Environment and Climate Change Canada, Toronto, ON, Canada
[2]Department of Physics, University of Toronto, Toronto, ON, Canada
[3]Arctic Research Centre, Finnish Meteorological Institute, Helsinki, Finland
[4]Centre National de Recherches Météorologiques, Météo-France, Toulouse, France

Headlines

- Snowpack at the peak of the 2024/25 snow season was higher than normal over much of the Arctic and remained high through May.
- Despite the higher-than-normal snowpack remaining in May, by June snow cover extent dropped below normal, consistent with values typical of the past 15 years.
- June snow cover extent over the Arctic today is half of what it was six decades ago.
- Loss of snow cover directly contributes to amplified warming in the Arctic, while also affecting permafrost deterioration, timing of freshwater availability, and ecosystem health.

Overview

Snow cover in the Arctic helps to regulate the climate and maintain the health of the established ecosystem. Reductions in snowpack depth or coverage reduce the amount of insulation between the ground and the air, which can, for example, alter ground temperatures and affect permafrost conditions (Goodrich 1982). Winter snowpack also functions as a temperature-stable habitat for small animals, vegetation, and microbial life (Jones et al. 2011). Even following the snow cover season, the timing of snowmelt has impacts on river discharge timing and magnitude, surface and sub-surface water availability, vegetation phenology, and fire risk (Meredith et al. 2019). Loss of snow cover also contributes to amplified Arctic warming through the surface albedo feedback (Forster et al. 2021).

In this essay, multiple data sets derived from satellite observations and snowpack models driven by historical weather conditions are used to assess Arctic seasonal snow cover (see *Methods and data*). Collectively, this approach provides a reliable picture of Arctic snow cover variability over the last five to six decades. We characterize snow conditions across the Arctic land surface using three quantities: how much total land area is covered by snow (snow cover extent – SCE), how much of the year snow covers the land surface (snow cover duration – SCD), and how much total water is stored in solid form by the snowpack (snow water equivalent – SWE; the product of snow depth and density). We examine each of these quantities in turn for the 2024/25 Arctic snow season (August 2024 to July 2025).

Snow cover extent and duration

Snow cover extent anomalies over the 1967-2025 period are shown separately for the North American and Eurasian sectors of the Arctic in Fig. 1. In 2025, Arctic SCE was close to normal across both the Eurasian and North American sectors during May but by June had dropped below normal (baseline

periods listed in figure captions). Weekly SCE anomalies (Fig. 2) indicate that Eurasian Arctic SCE was already below normal in April (Fig. 2a; see also the discussion of SWE below), and while it recovered slightly during May, by June it dropped to values typical of recent years (typical recent values illustrated in Fig. 2 by the average anomalies seen over the 2010-24 period). Across North America, SCE was very close to normal until the end of May (Fig. 2b), after which it fell sharply to values even lower than those typical of recent years.

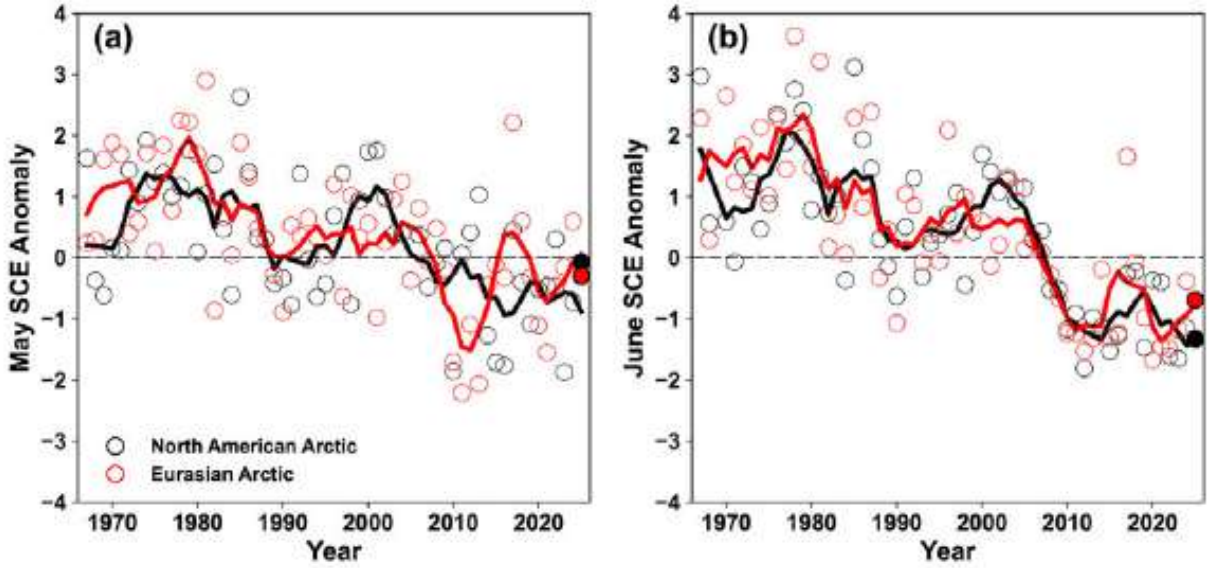

Fig. 1. Standardized monthly Arctic snow cover extent anomalies (circles) from 1967 to 2025 for (a) May, and (b) June for the Eurasian (red) and North American (black) sectors. Filled circles highlight 2025 anomalies. Lines depict 5-year running averages of the anomalies. Anomalies relative to the 1991-2020 baseline. Source: NOAA Climate Data Record of Northern Hemisphere SCE; available from 1967 to present.

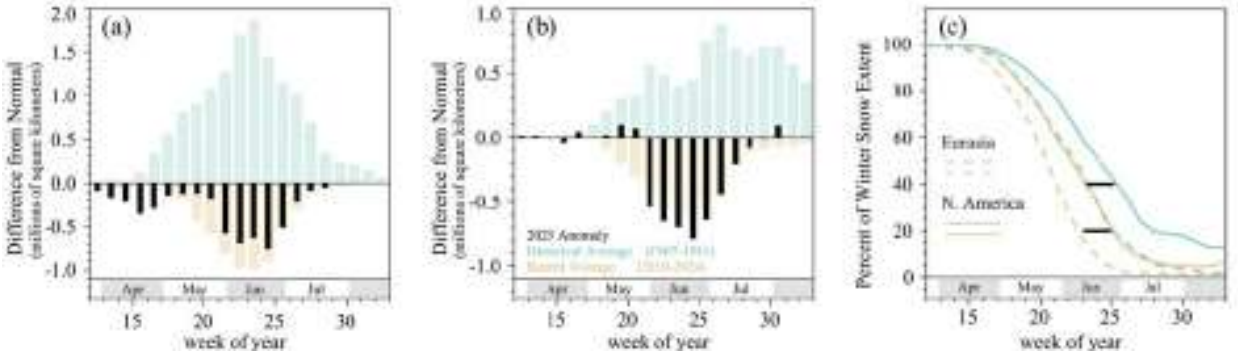

Fig. 2. Weekly Arctic snow cover extent anomalies from April to July 2025 (black) for the (a) Eurasian and (b) North American sectors. Also depicted are average anomalies for the historical 1967-81 period (green) and the recent 2010-24 period (brown). Panel (c) shows the difference in snowmelt timing between the historical and recent time periods for both sectors of the Arctic using the same colors as in (a) and (b). Black horizontal lines in panel (c) depict differences of two weeks in snowmelt timing. Anomalies relative to 1991-2020 baseline. Source: NOAA Climate Data Record of Northern Hemisphere SCE; available from 1967 to present.

Corresponding SCD anomalies (Fig. 3) indicate a mix of early and late snow onset over Eurasia but primarily late onset over North America, except for central Alaska (Fig 3a). Snow melt at the end of the 2024/25 snow season was earlier than normal over northern Europe and eastern Siberia, but later than normal over the central portion of the continent (Fig 3b). Across the North American Arctic, melt was later than normal over the western parts of the region but earlier than normal over the central and

eastern parts. Across broad portions of the southern Canadian Arctic Archipelago the 2024/25 snow season ranked as the shortest in the 27-year record.

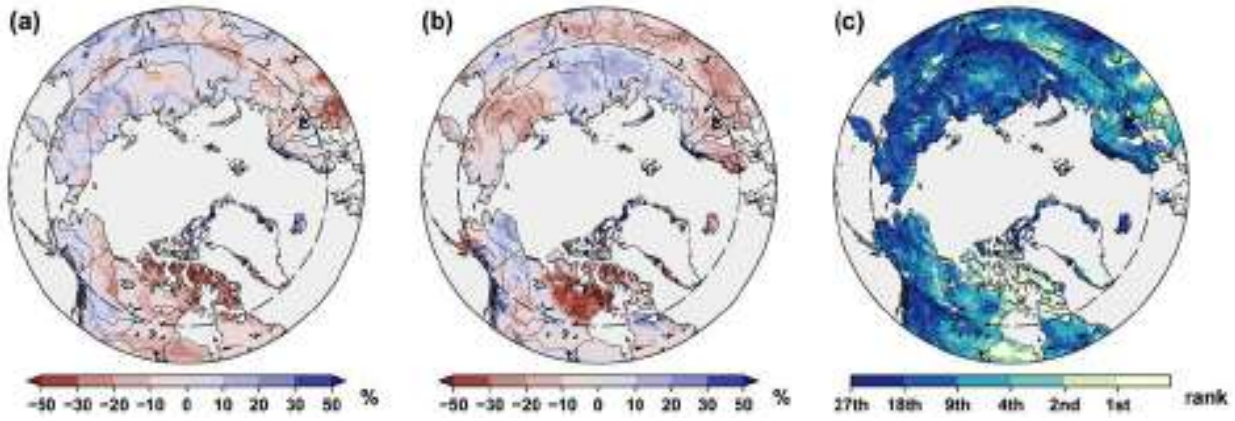

Fig. 3. Snow cover duration anomalies during the 2024/25 snow season (units of % difference relative to annual average number of snow-free days in the baseline period) split into (a) snow onset (August 2024 to January 2025); and (b) snow melt (February 2025 to July 2025). In both (a) and (b) red (blue) indicates decreases (increases) in the number of days with snow cover (equivalent to increases (decreases) in the number of snow-free days). In (a) these changes are aligned with a later (earlier) start to the snow season while in (b) these changes are aligned with earlier (later) melt at the end of the snow season. Ranks of full snow season length (combined onset and melt) shown in (c) where 1st rank indicates the 2024/25 season was the shortest in the available record and 27th indicates the 2024/25 season was the longest. The dashed circle marks the latitude 60° N. Anomalies relative to a baseline period of snow seasons from 1998/99 to 2022/23. Source: IMS Daily Northern Hemisphere Snow and Ice Analysis at 24 km; available from 1998 to present.

Snow mass and snow water equivalent

Snow mass across the Arctic typically peaks each year during April, when snowfall has accumulated since the preceding autumn but before increasing temperatures during May and June lead to melt. Snow mass anomalies for April 2025 (Fig. 4) were above the 1991-2020 baseline across both the North American and Eurasian Arctic. The spatial patterns of monthly SWE (Fig. 5) illustrate how this accumulation varied regionally from just before peak (March) through to the end of the melt period (June). Higher-than-normal SWE anomalies are apparent across broad portions of both continents in March and remain through both April and May. For Eurasia, the absence of SWE over parts of northern Europe in April is consistent with the below-normal SCE during April (Fig. 2a). By June the SWE remaining across much of the rest of Eurasia is also gone, consistent with the sharp decrease in SCE during the last week of May (Fig. 2b) and June SCE anomalies (Fig. 1). For North America during June, the western portion of the Canadian Arctic Archipelago has strongly above-normal SWE while in the eastern portion and Baffin Island SWE is below normal.

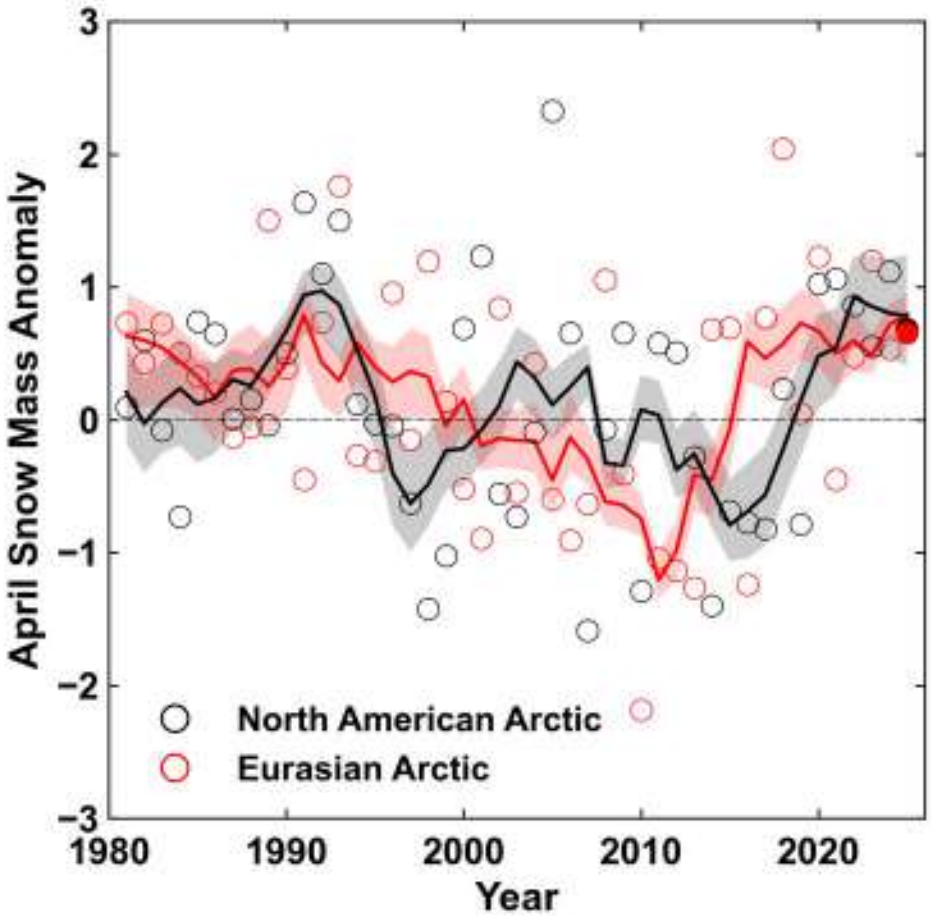

Fig. 4. Standardized Arctic snow mass anomalies (circles) during April from 1981 to 2025 for the Eurasian (red) and North American (black) sectors. Filled circles highlight 2025 anomalies (which nearly overlap). Lines depict 5-yr running averages with shading showing the spread amongst individual data sets. Anomalies relative to 1991-2020 baseline. Source: gridded snow products as described in *Methods and data*.

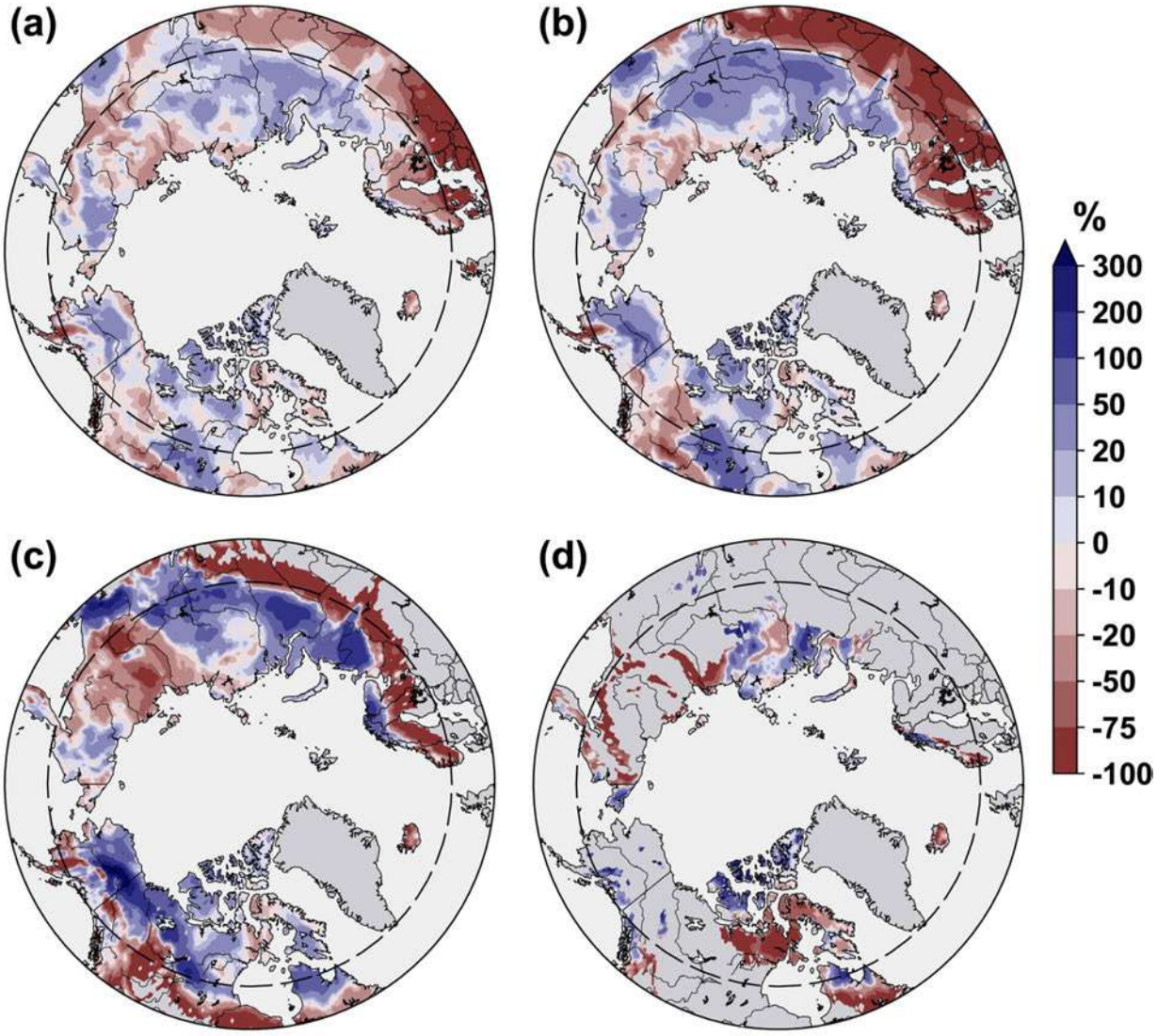

Fig. 5. Monthly snow water equivalent anomalies towards the end of the 2024/25 snow season (units of % difference from the baseline period) for (a) March, (b) April, (c) May, and (d) June. The dashed circle marks the latitude 60° N. Anomalies represent the ensemble mean from a suite of four independent gridded snow products (see *Methods and data*) relative to the 1991-2020 baseline.

Long-term changes and summary

For the Arctic as a whole, May SCE has declined 15% since 1967 (-2.5 %/dec) while June SCE has declined 50% since 1967 (-8.7 %/dec). The onset of snow melt over the recent period (2010-24) has occurred 1-2 weeks earlier during May and June compared to historical conditions (1967-81) for both the Eurasian and North American Arctic sectors (Fig. 2c). Corresponding declines in snow mass for the pan-Arctic region (total SWE over the region) are also large and significant in May and June (snow mass has declined by about 13% and 33%, respectively, since 1981), but during April, near the annual snow mass peak, the decline is small (about 3% since 1981) and not significant. This small April trend may reflect the complex regional picture of snowpack changes expected across the Arctic under climate change. While peak snowpack is expected to decrease on the western portions of both the North American and

Eurasian Arctic, increases are expected over the eastern portions due to increased precipitation in the form of snowfall (Brown et al. 2017; also see essay *Precipitation* for a description of how pan-Arctic precipitation has increased).

In summary, peak seasonal snowpack during the 2024/25 snow season was above average across both continents. Over parts of Eurasia, snow cover extent was already below normal in April, and it remained below normal throughout the remainder of the season (Fig. 2a). Over broad portions of North America, above-normal SWE persisted for most of May, keeping snow cover extent near normal until the end of the month when it dropped even lower than values typically seen over the recent period (Fig. 2b).

Methods and data

SCE anomalies (Figs. 1 and 2) were calculated from the NOAA Climate Data Record of Northern Hemisphere SCE (Robinson et al. 2012) using a 1991-2020 baseline period. Weekly anomalies of total snow cover area over land were computed separately for the North American and Eurasian Arctic sectors (land regions at latitudes > 60° N). For Fig. 1, the data were grouped by month and standardized (each observation was differenced from the mean and divided by the standard deviation and thus unitless) using the baseline period to calculate both the mean and standard deviation.

SCD fields (Fig. 3) were calculated from the IMS Daily Northern Hemisphere Snow and Ice Analysis at 24 km (U.S. National Ice Center 2008). Anomalies in the total number of days with snow cover were computed separately for each half of the snow season: August 2024 to January 2025, referred to as "onset period," and February 2025 to July 2025, referred to as "melt period." IMS availability starts in 1998, so a 1998/99 to 2022/23 baseline period was used. Anomalies for each of the two seasons were presented as percent differences from the climatological number of snow-free days in the baseline period.

Snow mass and SWE data (Figs. 4 and 5) were derived from four daily frequency data sets: (1) the European Space Agency Snow Climate Change Initiative (CCI) SWE version 3.1 product, a combination of satellite passive microwave brightness temperatures and climate station snow depth observations (Luojus et al. 2024); (2) SWE output from the Modern-Era Retrospective Analysis for Research and Applications version 2 (MERRA-2, GMAO 2015); (3) SWE output from the ERA5-Land analysis (Muñoz Sabater 2019); and (4) SWE output from the Crocus physical snowpack model (Decharme and Barbu 2024) driven by ERA5 meteorological forcing. Monthly SWE anomalies were calculated for each product relative to the 1991-2020 baseline period and the ensemble-mean SWE field was presented as percent differences from its average over the baseline period (Fig. 5). For April, snow mass was derived by aggregating the SWE field of each product across Arctic land regions (> 60° N) for both North American and Eurasian sectors. For each data product, these snow mass values were standardized relative to the baseline period and then averaged to produce an ensemble-mean time series. Greenland is not represented consistently among the SWE data products and is not added to the SCE of either Arctic sector nor is it included in calculations of snow mass.

Acknowledgments

Some data generated using modified ERA5-Land information (Muñoz Sabater 2019) downloaded from Copernicus Climate Change Service. Neither the European Commission nor ECMWF is responsible for any use that may be made of the Copernicus information or data it contains.

References

Brown, R., and Coauthors, 2017: Arctic terrestrial snow cover. *Snow, Water, Ice and Permafrost in the Arctic (SWIPA) 2017*. pp. 25-64. Arctic Monitoring and Assessment Programme (AMAP), Oslo, Norway.

Decharme, B., and A. Barbu, 2024: Crocus-ERA5 daily snow product over the Northern Hemisphere at 0.25° resolution (Version 2023), Zenodo, accessed 29 September 2025, https://doi.org/10.5281/zenodo.10943718.

Forster, P., and Coauthors, 2021: The earth's energy budget, climate feedbacks, and climate sensitivity, climate change. In Climate change 2021 – The physical science basis: Working Group I Contribution to the Sixth Assessment Report of the Intergovernmental Panel on Climate Change, V. Masson-Delmotte and others, Eds., Cambridge University Press, 923-2054, https://doi.org/10.1017/9781009157896.009.

GMAO (Global Modeling and Assimilation Office), 2015: MERRA-2tavg1_2d_lnd_Nx:2d, 1-Hourly, Time-Averaged, Single-Level, Assimilation, Land Surface Diagnostics V5.12.4, Goddard Earth Sciences Data and Information Services Center (GESDISC), accessed: 13 August 2025, https://doi.org/10.5067/RKPHT8KC1Y1T.

Goodrich, L. E., 1982: The influence of snow cover on the ground thermal regime. *Can. Geotech. J.*, **19**(4), 421-432, https://doi.org/10.1139/t82-047.

Jones, H. G., J. W. Pomeroy, D. A. Walker, and R. W. Hoham, 2011: Snow ecology: An interdisciplinary examination of snow-covered ecosystems. Cambridge University Press, https://books.google.ca/books?id=7LhicgAACAAJ.

Luojus, K. M., and Coauthors, 2024: ESA Snow Climate Change Initiative (Snow_cci): Snow Water Equivalent (SWE) level 3C daily global climate research data package (CRDP) (1979-2022), version 3.1. NERC EDS Centre for Environmental Data Analysis, accessed: 13 August 2025, https://doi.org/10.5285/9d9bfc488ec54b1297eca2c9662f9c81.

Meredith, M., and Coauthors, 2019: Polar Regions. *IPCC Special Report on the Ocean and Cryosphere in a Changing Climate*, H. -O. Pörtner, and co-editors, Cambridge University Press, Cambridge, UK and New York, NY, USA, 203-320, https://doi.org/10.1017/9781009157964.005.

Muñoz Sabater, J., 2019: ERA5-Land hourly data from 1950 to present. Copernicus Climate Change Service (C3S) Climate Data Store (CDS), accessed 18 July 2025, https://doi.org/10.24381/cds.e2161bac.

Robinson, D. A., T. W. Estilow, and NOAA CDR Program, 2012: NOAA Climate Data Record (CDR) of Northern Hemisphere (NH) Snow Cover Extent (SCE), Version 1 [r01]. NOAA National Centers for Environmental Information, accessed: 12 August 2025, https://doi.org/10.7289/V5N014G9.

U.S. National Ice Center, 2008: IMS Daily Northern Hemisphere Snow and Ice Analysis at 1 km, 4 km, and 24 km Resolutions, Version 1. NSIDC: National Snow and Ice Data Center, Boulder, CO, USA, accessed: 13 August 2025, https://doi.org/10.7265/N52R3PMC.

December 4, 2025

Greenland Ice Sheet

https://doi.org/10.25923/rbsh-t897

K. Poinar[1], J. E. Box[2], B. E. Smith[3], T. G. Askjaer[4], T. L. Mote[5], B. D. Loomis[6], B. C. Medley[6], K. D. Mankoff[7,8], and R. S. Fausto[2]

[1]University at Buffalo, Buffalo, NY, USA
[2]Geological Survey of Denmark and Greenland, Copenhagen, Denmark
[3]University of Washington, Seattle, WA, USA
[4]Danish Meteorological Institute, Copenhagen, Denmark
[5]Department of Geography, University of Georgia, Athens, GA, USA
[6]Goddard Space Flight Center, NASA, Greenbelt, MD, USA
[7]Goddard Institute of Space Studies, NASA, New York, NY, USA
[8]Autonomic Integra, New York, NY, USA

Headlines

- The mass balance of the Greenland Ice Sheet for 2025 was -129 ± 50 Gt, showing less loss than the 2003-24 annual average of -219 ± 16 Gt but continuing the long-term trend of net loss.
- Above-average snowfall and below-average melt, despite above-average ice discharge (all compared to the 1991-2020 average), contributed to the ice sheet losing less mass this year than typical.
- This loss of ice contributes to global sea-level rise, alters regional ocean circulation in the North Atlantic, and changes nutrient levels in local marine food webs.
- Sustained, routine measurement of the mass balance of the Greenland Ice Sheet is crucial for understanding current changes and projecting future changes, which support effective local to global planning and adaptation.

Introduction

The Greenland Ice Sheet is susceptible to climate change. Total loss of the Greenland Ice Sheet would raise global sea levels by approximately seven meters (Morlighem et al. 2017). Greenland ice loss affects human societies and environments globally, including through coastal erosion, saltwater intrusion, habitat change, tidal flooding, heightened storm surges, and permanent seawater inundation. Local and regional impacts of negative Greenland Ice Sheet mass balance include potential disruption of North Atlantic thermohaline circulation, which portends local Arctic sea ice expansion and northern European cooling (van Westen et al. 2024). Enhanced runoff also changes nutrient fluxes into marine environments, affecting marine food webs and fisheries (Hendry et al. 2019).

Net loss of ice from the Greenland Ice Sheet has occurred every year since the late 1990s (Mouginot et al. 2019; Mankoff et al. 2020; Fig. 1a). We summarize the observed mass change and the factors driving it for 2025.

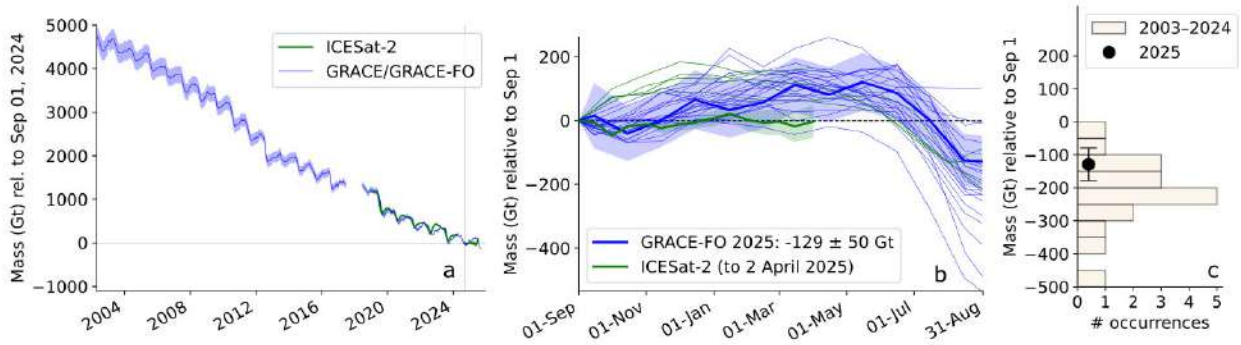

Fig. 1. (a) Full observational record of the mass balance of the Greenland Ice Sheet from GRACE/GRACE-FO (blue) and ICESat-2 (green), with measurement uncertainties shaded. (b) Mass balance over the 2025 mass balance year (GRACE-FO, blue) and through 2 April (ICESat-2, green) (bold lines) and 2003-24 (thinner lines). (c) Histogram of annual mass balance from 2003-24 from GRACE/GRACE-FO, with the GRACE-FO 2025 mass balance of -129 ± 50 Gt in black.

Ice-sheet mass balance

The Greenland Ice Sheet gains mass primarily through snowfall and loses it primarily through runoff and ice discharge (calving of icebergs and melting of glacier marine termini) into the ocean. The sum of these quantities (and including other minor mass change contributors) is the ice-sheet mass balance: the net gain or loss of ice over a period, typically one year. We report on the 2025 mass balance year, 1 September 2024 through 31 August 2025.

The Gravity Recovery and Climate Experiment Follow-on (GRACE-FO) satellite mission measured a 2025 mass balance of -129 ± 50 Gt (Fig. 1b). The observed mass balance was less negative than the 2003-24 annual average measured by GRACE/GRACE-FO of -219 ± 16 Gt (mean ± 1 st. dev.; Fig. 1c).

The Ice, Cloud, and land Elevation Satellite-2 (ICESat-2) mission measures the surface height of the ice sheet over time, which we convert to mass change. Adequate data were not available to evaluate the full 2025 mass balance year. From 1 September 2024 to 2 April 2025, however, this ICESat-2 method measured a mass balance of -2 ± 56 Gt (mean ± 1 st. dev.; Fig. 1b), which underestimates the annual loss because the period does not include the melt season. The ICESat-2 partial-year mass balance is 102 Gt below the independent GRACE-FO measurement over the same time period (Fig. 1b) and is slightly below the ICESat-2 1 September-2 April average of +21 ± 40 Gt (mean ± 1 st. dev) over 2020-23. The ICESat-2 annual average for full mass balance years (2020-24) was -134 ± 62 Gt (mean ± 1 st. dev) and follows a steady trend of year-over-year ice loss (Fig. 1a).

Contributions to the observed loss of ice mass

Surface mass balance (SMB) comprises mass input to the ice sheet from snowfall and refrozen rainfall, minus mass loss from surface runoff, sublimation, and evaporation. SMB is influenced by air temperature, precipitation, melt, and surface reflectivity (albedo), for which we summarize observations over the 2025 mass balance year.

In situ rain and snowfall (hereafter, “precipitation”) is observed at 11 coastal and 10 inland ice sheet stations (see *Methods and data*). Precipitation totals observed at coastal stations during the 2025 mass balance year were generally above the 1991-2020 average. Autumn (September-November 2024)

precipitation was slightly below average, while winter (December 2024-February 2025) precipitation was significantly above average at coastal stations, especially in the northeast, but near average at inland stations. Spring (March-May 2025) precipitation was close to average. Summer (June-August 2025) precipitation was above average, as also shown in the precipitation analysis (see essay *Precipitation*, Fig. 1). Several inland stations recorded notable June snowfall amounts (Fig. 2).

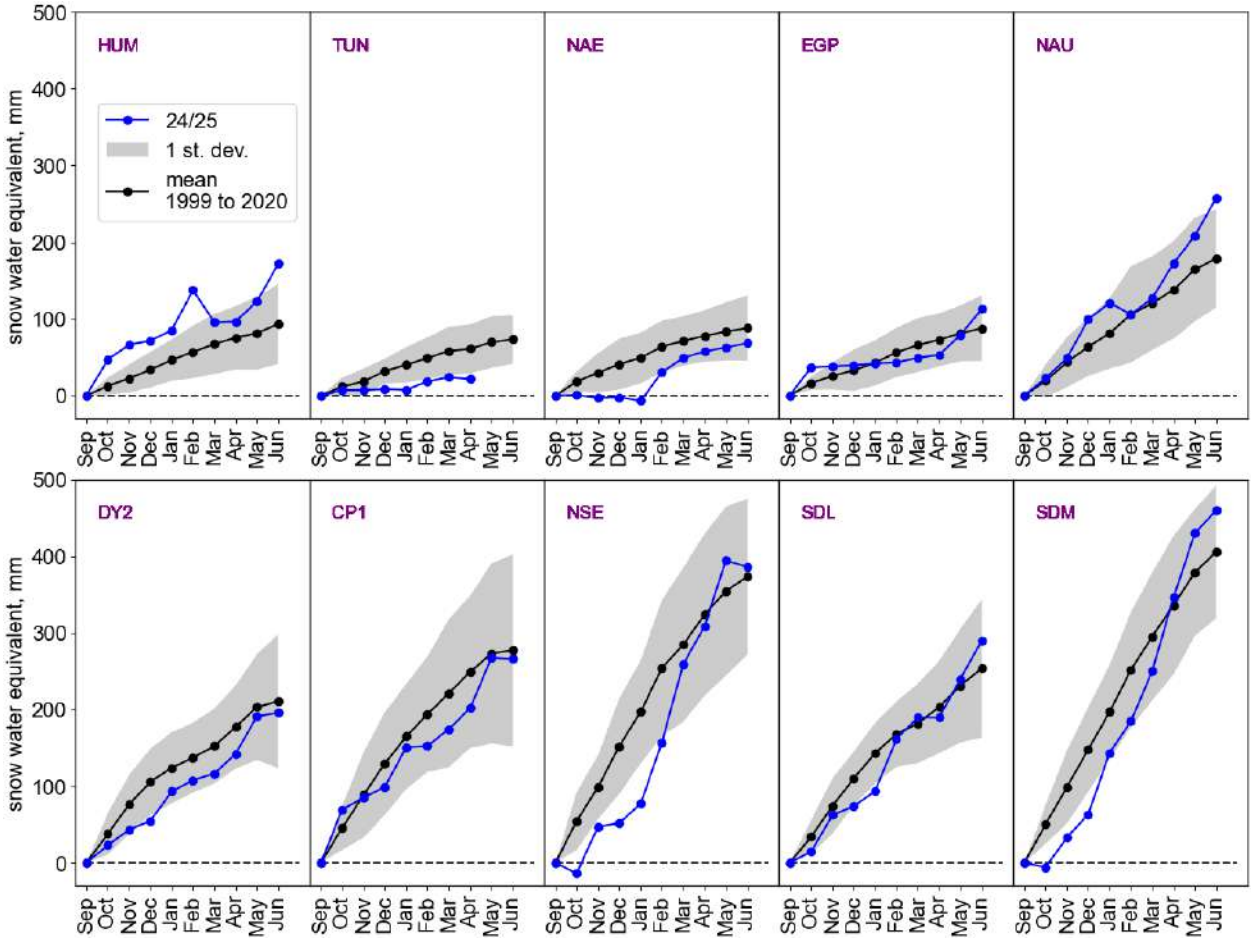

Fig. 2. Snowfall accumulation measured at PROMICE GC-Net stations during 2024/25 (blue; see Fig. 3 for locations), compared to 1999-2020 (black/gray).

Monthly mean air temperatures measured at 34 weather stations across Greenland (see *Methods and data*) during the 2025 mass balance year were generally above the 1991-2020 average (Fig. 3). Autumn, winter, and spring temperatures were above average, especially in the north and west. Summit Station reached a record high monthly mean temperature in April, and a heat wave in late May pushed temperatures well above average on the east coast. Altogether, spring temperatures were above average. These warm patterns ended by June; summer temperatures were close to average.

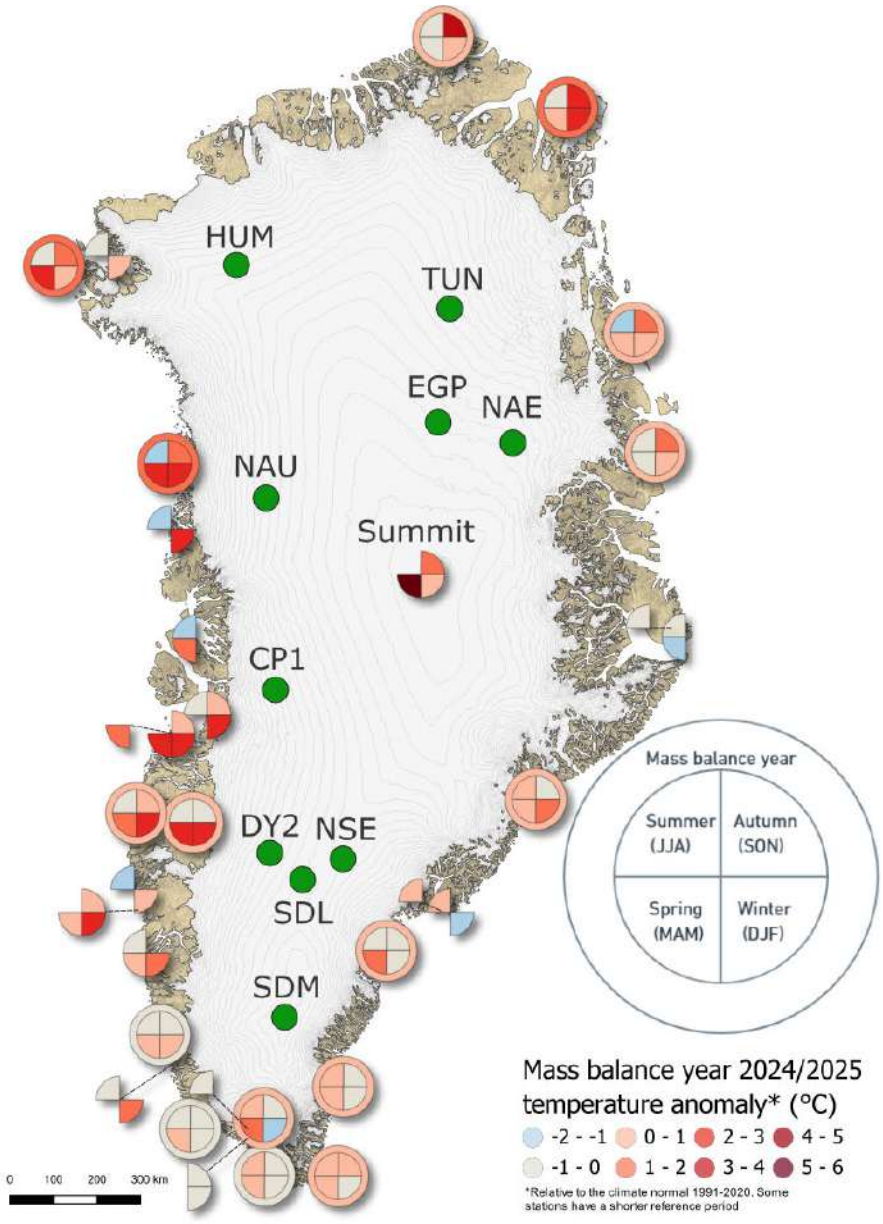

Fig. 3. Temperature anomaly in the four seasons (colored pie charts) and the total 2025 mass balance year (surrounding colored circles, when all four seasons are available) at coastal weather stations. Locations of inland weather stations operated by PROMICE GC-Net (Fig. 2) are in green.

Temperature and snow cover influence ice melt. The overall extent of ice sheet surface melt was close to the 1991-2020 average (Fig. 4a), although this manifested as an above-average number of observed melt days in most locations (Fig. 4b). The above-average summertime snow accumulation likely helped limit the melt extent by raising the albedo, which helps protect the ice sheet from melting by reflecting sunlight away. Early in the melt season (May-June), albedo was near or below average, but summer snowfall raised (brightened) it above the average. Albedo dropped below average in late August, coincident with observed smoke from North American wildfires along the west coast of Greenland. Particulates from smoke, if deposited on the ice, can lower the albedo and enhance melt (Keegan et al. 2014).

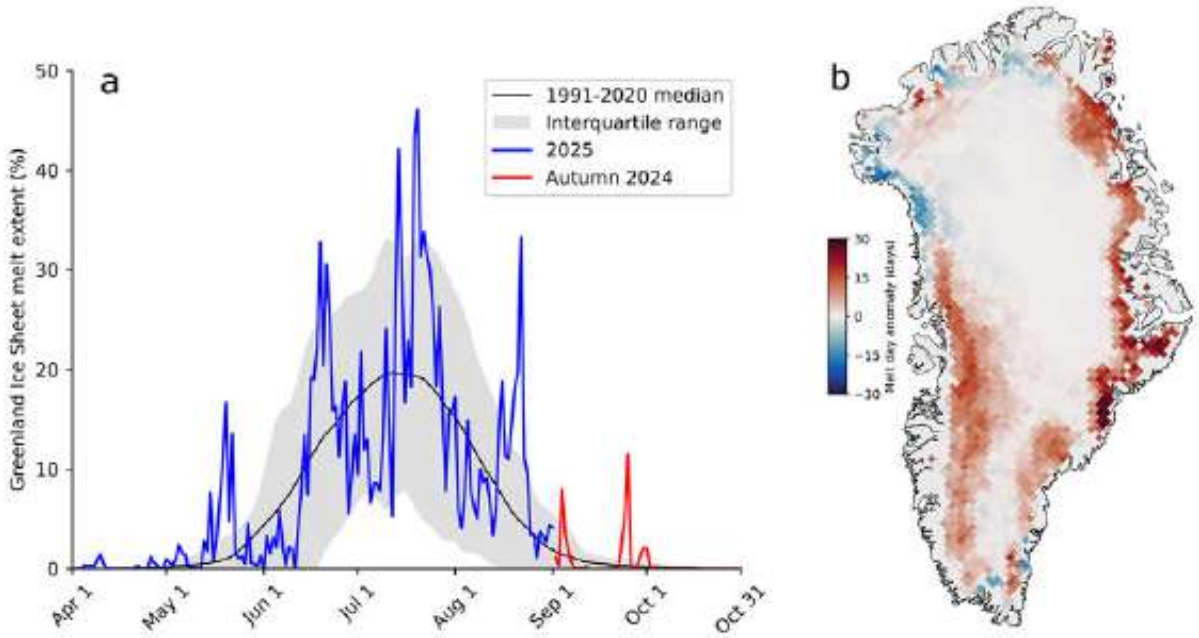

Fig. 4. (a) Daily surface melt extent over the 2025 mass balance year (omitting November-March), including autumn 2024 (red) and spring/summer 2025 (blue). (b) Number of surface melt days from 1 April to 31 August 2025, as an anomaly with respect to 1991-2020.

The mass of ice flowing out of Greenland's glaciers into the ocean is termed ice discharge. At the ice-ocean boundary, ice either calves off as icebergs or melts directly into the ocean. An ice sheet that is in balance loses the same amount of ice through discharge as it gains from SMB. On the Greenland Ice Sheet, however, solid ice discharge has exceeded SMB every year since the mid-1990s. We report an approximation of ice discharge obtained by measuring ice flux through specific gates across the ice sheet (Mankoff et al. 2020). In the 2025 mass balance year through 20 August 2025, this discharge was 491 ± 17 Gt/yr (mean ± 1 st. dev.; Fig. 5), approximately 1 st. dev. above the 1991-2020 mean of 458 ± 27 Gt/yr.

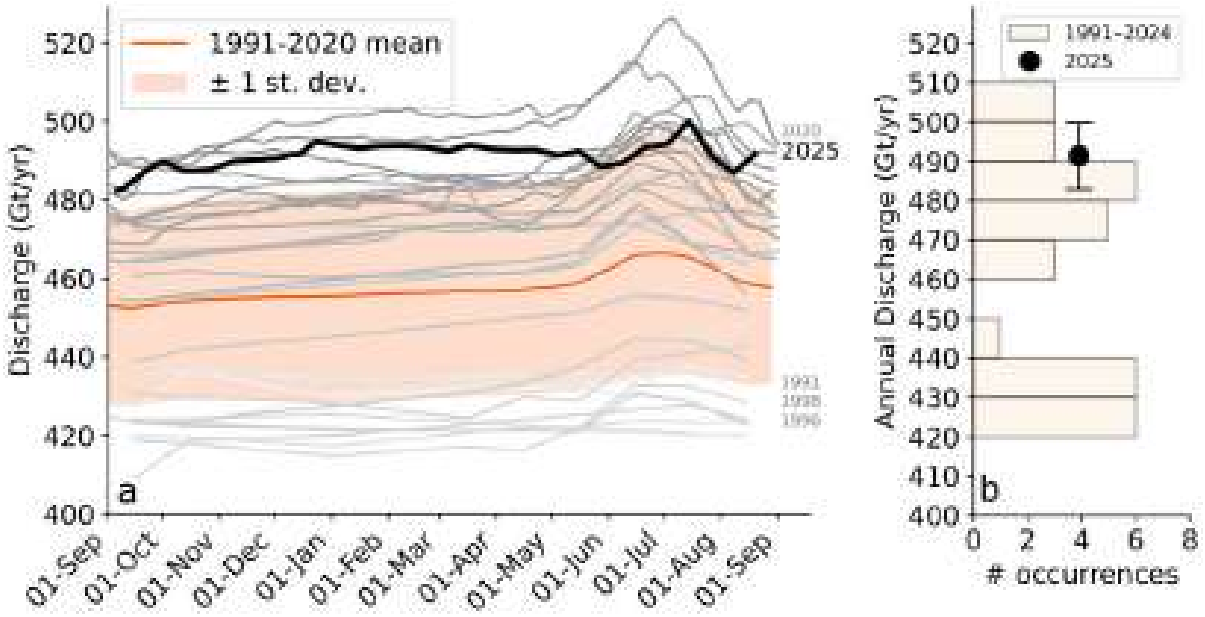

Fig. 5. (a) Solid ice discharge across the Greenland Ice Sheet observed over the mass balance years 1991-2020 (gray lines) with mean ± 1 st. dev. (orange) and 2025 (black line). (b) Histogram of the average annual discharge from 1991-2024, with 2025 discharge in black.

Methods and data

The GRACE (Gravity Recovery and Climate Experiment, mid-2002-17) and GRACE-FO (Follow On, 2018-present) satellite missions detect gravity anomalies to measure changes in ice mass (GRACE/GRACE-FO Level-2: JPL RL06.1 doi:10.5067/GFL20-MJ061; Technical Notes 13 & 14: https://podaac.jpl.nasa.gov/gravity/gracefo-documentation). We apply a regional averaging kernel (Wahr et al. 1998) to the Level-2 products that is consistent with the Jet Propulsion Laboratory and Goddard Space Flight Center mascon solutions (Watkins et al. 2015; Loomis et al. 2019). The source data include peripheral glaciers that are not part of the Greenland Ice Sheet. We scale our results by 0.84 to exclude these glaciers (Colgan et al. 2015).

Changes in ice surface elevation measured by ICESat-2 reflect ice mass change as well as changes in firn air content and SMB. We calculate mass change by correcting quarterly ICESat-2 elevation measurements (Smith et al. 2023) for these anomalies (Medley et al. 2022), then following the processing strategy for ICESat-2 level-3B products (Smith 2023) to calculate non-SMB-driven elevation change. We then add monthly SMB to estimate total mass change. We approximate the error as 0.14 times the SMB anomaly estimates (Medley et al. 2022).

Weather data are obtained from 20 Danish Meteorological Institute (DMI) land-based weather stations, 12 stations owned by Mittarfeqarfiit A/S, and Summit Station courtesy of NSF/NOAA GEOSummit. Ten automatic weather station transects from the Programme for Monitoring of the Greenland Ice Sheet (PROMICE) at the Geological Survey of Greenland and Denmark (GEUS) provide temperatures and SMB measurements, following Fausto et al. (2021).

Surface melt duration and extent are derived from daily Special Sensor Microwave Imager/Sounder (SSMIS) 37 GHz, horizontally polarized passive microwave radiometer satellite data (Mote 2007). On 24 September 2025, this instrument was decommissioned, and with it the capability to produce this melt product (see essay *Assessing the State of the Arctic Observing Network*).

Ice discharge rates are derived by PROMICE from measurements of ice surface velocity from Sentinel-1, estimates of ice thickness and density, and the assumption of plug flow (Mankoff et al. 2020). We estimate discharge at gates a few kilometers upstream of each terminus, which omits frontal advance or retreat, as well as ice loss from melting between the gates and termini.

Acknowledgments

Sentinel-3 albedo data processing was supported by the European Space Agency (ESA) EO Science for Society contract CCN 4000125043/18/I-NB and the ESA Network of Resources via Polar View and Polar TEP.

Jacob C. Yde, Western Norway University of Applied Sciences, Sogndal, Norway provided information on local and regional impacts of ice melt.

References

Colgan, W., and Coauthors, 2015: Hybrid glacier Inventory, Gravimetry and Altimetry (HIGA) mass balance product for Greenland and the Canadian Arctic. *Remote Sens. Environ.*, **168**, 24-39, https://doi.org/10.1016/j.rse.2015.06.016.

Fausto, R. S., and Coauthors, 2021: Programme for Monitoring of the Greenland Ice Sheet (PROMICE) automatic weather station data. *Earth Syst. Sci. Data*, **13**(8), 3819-3845, https://doi.org/10.5194/essd-13-3819-2021.

Hendry, K. R., and Coauthors, 2019: The biogeochemical impact of glacial meltwater from Southwest Greenland. *Prog. Oceanogr.*, **176**, 102126, https://doi.org/10.1016/j.pocean.2019.102126.

Keegan, K. M., M. R. Albert, J. R. McConnell, and I. Baker, 2014: Climate change and forest fires synergistically drive widespread melt events of the Greenland Ice Sheet. *Proc. Natl. Acad. Sci. U.S.A.*, **111**(22), 7964-7967, https://doi.org/10.1073/pnas.1405397111.

Loomis, B. D., S. B. Luthcke, and T. J. Sabaka, 2019: Regularization and error characterization of GRACE mascons. *J. Geodesy*, **93**, 1381-1398, https://doi.org/10.1007/s00190-019-01252-y.

Mankoff, K. D., A. Solgaard, W. Colgan, A. P. Ahlstrøm, S. A. Khan, and R. S. Fausto, 2020: Greenland ice sheet solid ice discharge from 1986 through March 2020. *Earth Syst. Sci. Data*, **12**(2), 1367-1383, https://doi.org/10.5194/essd-12-1367-2020.

Medley, B., T. A. Neumann, H. J. Zwally, B. E. Smith, and C. M. Stevens, 2022: Simulations of firn processes over the Greenland and Antarctic ice sheets: 1980-2021. *Cryosphere*, **16**, 3971-4011, https://doi.org/10.5194/tc-16-3971-2022.

Morlighem, M., and Coauthors, 2017: BedMachine v3: Complete bed topography and ocean bathymetry mapping of Greenland from multibeam echo sounding combined with mass conservation. *Geophys. Res. Lett.*, **44**(21), 11051-11061, https://doi.org/10.1002/2017GL074954.

Mote, T. L., 2007: Greenland surface melt trends 1973-2007: Evidence of a large increase in 2007. *Geophys. Res. Lett.*, **34**(22), L22507, https://doi.org/10.1029/2007GL031976.

Mouginot, J., and Coauthors, 2019: Forty-six years of Greenland Ice Sheet mass balance from 1972 to 2018. *Proc. Natl. Acad. Sci.*, **116**(19), 9239-9244, https://doi.org/10.1073/pnas.1904242116.

Smith, B., 2023: Algorithm Theoretical Basis Document (ATBD) for Land-ice DEM (ATL14) and Land-ice height change (ATL15). NASA Goddard Space Flight Center, https://nsidc.org/sites/default/files/documents/technical-reference/icesat2_atl14_atl15_atbd_v003.pdf.

Smith, B., S. Dickinson, B. P. Jelley, T. A. Neumann, D. Hancock, J. Lee, and K. Harbeck, 2023: ATLAS/ICESat-2 L3B Slope-Corrected Land Ice Height Time Series, Version 6 [Data Set]. NASA National Snow and Ice Data Center Distributed Active Archive Center, Boulder, CO, USA, accessed: 25 August 2025, https://doi.org/10.5067/ATLAS/ATL11.006.

van Westen, R. M., M. Kliphuis, and H. A. Dijkstra, 2024: Physics-based early warning signal shows that AMOC is on tipping course. *Sci. Adv.*, **10**(6), eadk1189, https://doi.org/10.1126/sciadv.adk1189.

Wahr, J., M. Molenaar, and F. Bryan, 1998: Time variability of the Earth's gravity field: Hydrological and oceanic effects and their possible detection using GRACE. *J. Geophys. Res. Solid Earth*, **103**(B12), 30205-30229, https://doi.org/10.1029/98JB02844.

Watkins, M. M., D. N. Wiese, D. N. Yuan, C. Boening, and F. W. Landerer, 2015: Improved methods for observing Earth's time variable mass distribution with GRACE using spherical cap mascons. *J. Geophys. Res. Solid Earth*, **120**(4), 2648–2671, https://doi.org/10.1002/2014JB011547.

January 31, 2026

Sea Ice

https://doi.org/10.25923/mmxf-0r86

W. N. Meier[1], A. Petty[2], S. Hendricks[3], A. Bliss[4], L. Kaleschke[3], D. Divine[5], S. Farrell[6], S. Gerland[5], D. Perovich[7], R. Ricker[8], X. Tian-Kunze[3], and M. Webster[9]

[1]National Snow and Ice Data Center, Cooperative Institute for Research in Environmental Sciences, University of Colorado Boulder, Boulder, CO, USA
[2]Earth System Science Interdisciplinary Center, University of Maryland, College Park, MD, USA
[3]Alfred Wegener Institute, Helmholtz Centre for Polar and Marine Research, Bremerhaven, Germany
[4]Cryospheric Sciences Laboratory, Goddard Space Flight Center, NASA, Greenbelt, MD, USA
[5]Norwegian Polar Institute, Fram Centre, Tromsø, Norway
[6]Department of Geographical Sciences, University of Maryland, College Park, MD, USA
[7]Thayer School of Engineering, Dartmouth College, Hanover, NH, USA
[8]NORCE Norwegian Research Centre, Tromsø, Norway
[9]Polar Science Center, Applied Physics Laboratory, University of Washington, Seattle, WA, USA

Headlines

- The lowest annual Arctic maximum extent in the 47-year satellite record occurred in March 2025, followed by the 10th lowest minimum extent in September 2025.
- In the first Arctic Report Card, 2005 was reported as the record lowest minimum extent, but that 2005 extent now ranks 20th lowest in the 47-year record.
- The last 20 years have been characterized by lower extent and a younger and thinner ice cover than in previous decades.
- Changing sea ice extent and thickness is allowing increased marine traffic and prompting reevaluations of national security concerns.

Introduction

Arctic sea ice forms the frozen interface between the polar ocean and atmosphere. Its high albedo due to its bright, near-white surface reduces the absorption of solar energy, and as a physical barrier sea ice modulates the heat and moisture transfer between the atmosphere and ocean. Sea ice plays a key role in polar ecosystems, providing an essential habitat for marine life and is an essential component of life and culture in Indigenous communities of the North. Changes in sea ice extent and seasonality have already impacted the Arctic ecosystem and peoples who rely on resources from the ocean (e.g., George et al. 2020). Additionally, the presence of sea ice historically limited economic and other activities in the Arctic; as the ice declines, maritime traffic is increasing and driving a reevaluation of resource extraction and national security activities in the Arctic (Zhao et al. 2024).

The Arctic sea ice environment has substantially changed since the publication of the first Arctic Report Card in 2006, which reported on 2005 sea ice conditions. At the end of summer 2025, the ice cover was younger, thinner and 28% less extensive than in 2005. The profound changes in sea ice since 2005 are opening the Arctic to more human activity and bringing to the fore concerns about safety, security, and the environment.

Sea ice extent

Sea ice extent, derived from sea ice concentration fields and defined as the total area covered by ice of at least 15% concentration, is an iconic indicator of long-term Arctic sea ice conditions. The primary source of extent observations is the 47-year record derived from satellite-borne passive microwave sensors, beginning in 1979.

After the annual minimum in September 2024, extent increased more slowly than average through mid-October, particularly in the Beaufort and Chukchi Seas on the Pacific side of the Arctic, as well as in the Barents and Kara Seas on the Atlantic side. Sea ice developed rapidly in the East Siberian and Laptev Seas in late October when the Siberian coast was iced in. Freeze-up was very slow in Hudson Bay, with record or near-record low extent from November through January. Extent was also near-record low in the Bering Sea and the Sea of Okhotsk in February and March (Fig. 1). This corresponded with record and near-record high surface air temperatures (see essay *Surface Air Temperature*). Other regions of the Arctic saw less extreme anomalies (relative to the 1991-2020 average) but were nonetheless lower than average throughout the winter. Arctic-wide, monthly extent was either lowest or second lowest from December through March, culminating in a record low annual maximum extent in March 2025 (Fig. 2; Table 1).

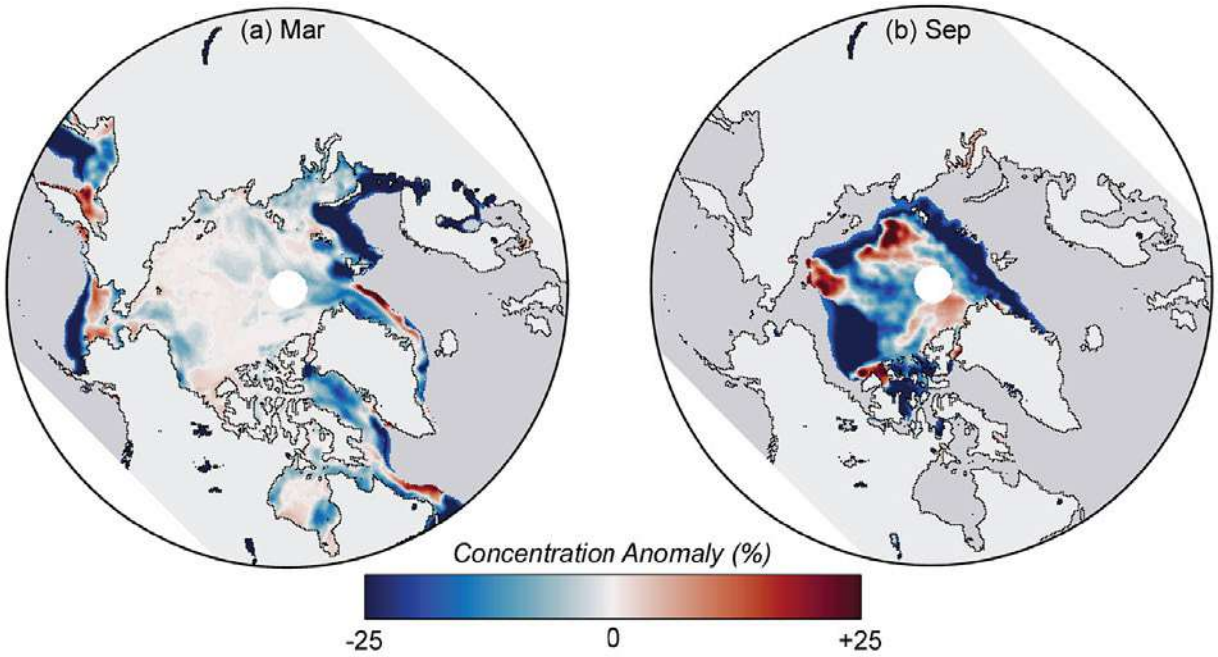

Fig. 1. Sea ice concentration anomaly for (a) March 2025 and (b) September 2025 relative to the 1991-2020 average. The extreme negative anomalies (less than -25%) indicate regions where there is ice in the climatology, but no ice present in 2025.

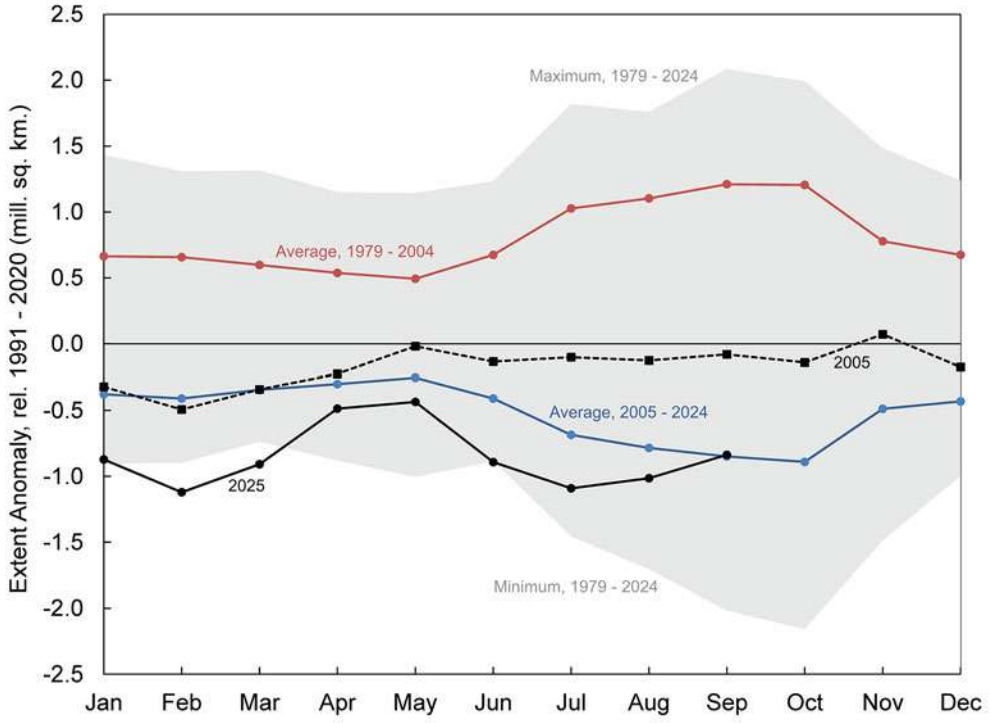

Fig. 2. Monthly average sea ice extent anomaly relative to 1991-2020 for: 2025 (black solid line), 2005 (black dashed line), average 2005-24 (blue), average 1979-2004 (red), and the maximum and minimum range (gray shading) for 1979-2024.

Table 1. March and September 2025 Arctic sea ice extent (monthly averages and annual daily maximum/minimum) and related statistics. Ranking is from least (1) to most (47) sea ice over the 47-year period.

	March Monthly Average	**March** Daily Maximum	**September** Monthly Average	**September** Daily Minimum
Extent (10^6 km^2)	14.12	14.31	4.75	4.60
Rank (out of 47 years)	1	1	11	10
1991-2020 average (10^6 km^2)	15.03	15.26	5.58	5.37
Anomaly rel. 1991-2020 average (10^6 km^2)	-0.91	-1.05	-0.83	-0.78
Trend, 1979-2025 (km^2/yr)	-38,000	-40,300	-76,100	-76,900
Trend, 1979-2005 (km^2/yr)	-37,700	-40,300	-54,400	-53,800

However, the record low maximum extent was followed by a slow start to the melt season with very little ice loss through April. Ice loss then accelerated with early open water areas developing in the Laptev and Kara Seas, resulting in record low ice extent in May in the Laptev Sea. The Bering Sea ice

retreated rapidly in May. Compared to recent years, the Beaufort Sea was relatively slow to lose ice early in the melt season, with above-average extent into July; however, in late July and throughout August, ice rapidly melted in the Beaufort Sea. In contrast to record low extent in 2024, ice conditions in the Canadian Archipelago and Northwest Passage were lower than normal, but not extreme. Overall, ice loss throughout the summer season led to the 10th lowest minimum extent in September 2025 (Fig. 2). In the first Arctic Report Card, 2005 was reported as the record lowest minimum extent. That 2005 annual minimum extent now ranks 20th lowest in the 47-year record (Table 1); only 2006 was higher in the 20 years of the report.

Melt onset of sea ice

The summer melt season begins when liquid water first appears on the sea ice surface—often within the overlying snowpack—and is known as the melt onset date. Following melt onset, more advanced stages of surface melt, such as melt ponds, develop, further reducing surface albedo. In the spring and early summer when solar radiation nears its annual peak, the timing of melt onset becomes an important control on the absorption of heat in the ice-ocean system throughout the summer. In the Arctic, melt onset generally varies with latitude, occurring in March at lower latitudes and in early to mid-June in the central Arctic near the North Pole. Melt onset is sensitive to weather conditions, including cyclones and intrusions of warm, moist air, which contribute to interannual variability of melt onset timing at the regional scale.

In 2025, the average melt onset date for the marine areas of the Arctic was 21 May 2025 (Fig. 3a), two days earlier than in 2024. Compared to the 1991-2020 average, melt onset dates in 2025 were anomalously early in the Canadian Arctic Archipelago, much of the Laptev Sea, and parts of the Atlantic sector (Fig. 3b). In contrast, an anomalously late melt onset occurred in the central Arctic surrounding the North Pole and in much of the Pacific sector, including the East Siberian Sea, which is a region where sea ice extent survived the melt season in many recent years. Overall, Arctic melt onset dates are occurring earlier at a rate of 4.1 days per decade. The 2025 melt onset date occurred two weeks earlier than the melt onset observed at the beginning of the satellite melt onset date record in 1979.

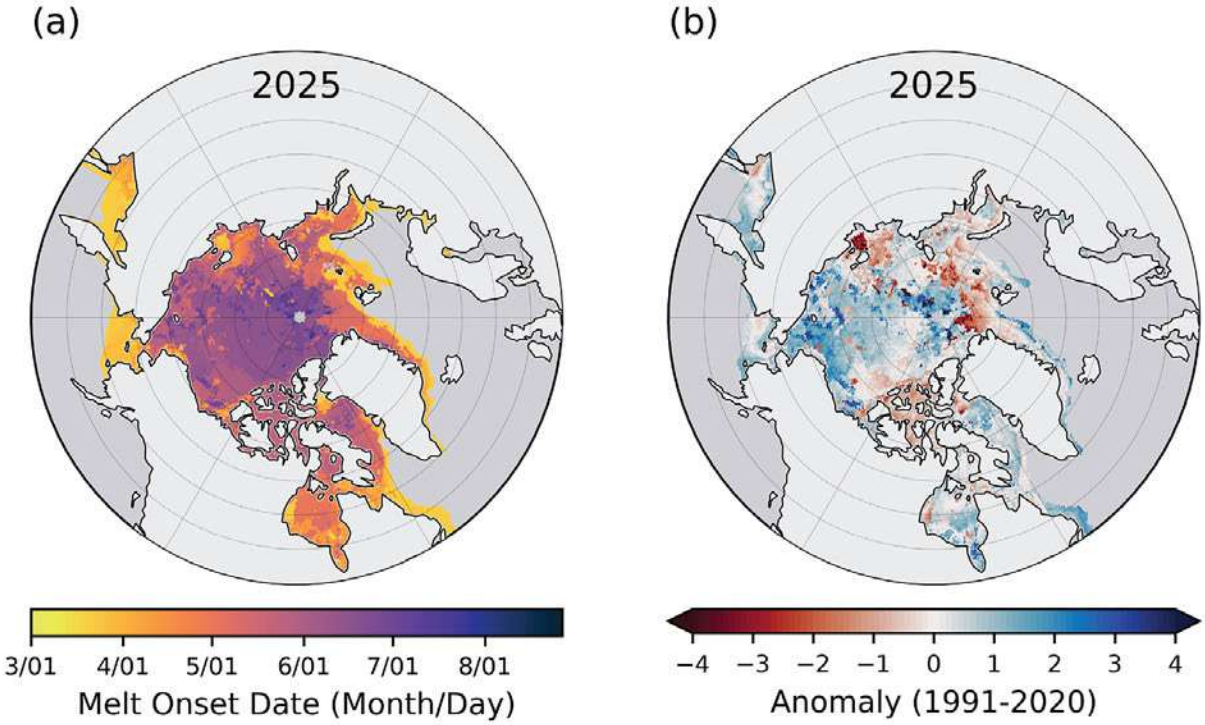

Fig. 3. (a) Arctic sea ice melt onset dates for 2025 and (b) 2025 normalized anomalies relative to the 1991-2020 average (anomaly divided by standard deviation), where blue indicates late onset. [Data updated from Bliss (2023)].

Sea ice age

For sea ice, age is a proxy for thickness because multi-year ice generally grows thicker through successive winter periods. As in the last several years, multi-year ice (i.e., ice that has survived at least one summer melt season) in 2025 was largely constrained to the region near the north coast of Greenland and the Canadian Archipelago (Fig. 4). The Arctic sea ice today is far younger than in the 1980s and 1990s and is even substantially younger than 2005, with 47% less multi-year ice. There is almost no old (>4 years) multi-year ice remaining in the Arctic, just 95,000 km^2 at the September 2025 minimum. This is a reduction of 72% from the average of 326,000 km^2 over the Arctic Report Card period, 2005-24, and a reduction of 95% from the average of 1.72 million km^2 for the earlier 20 years, 1985-2004.

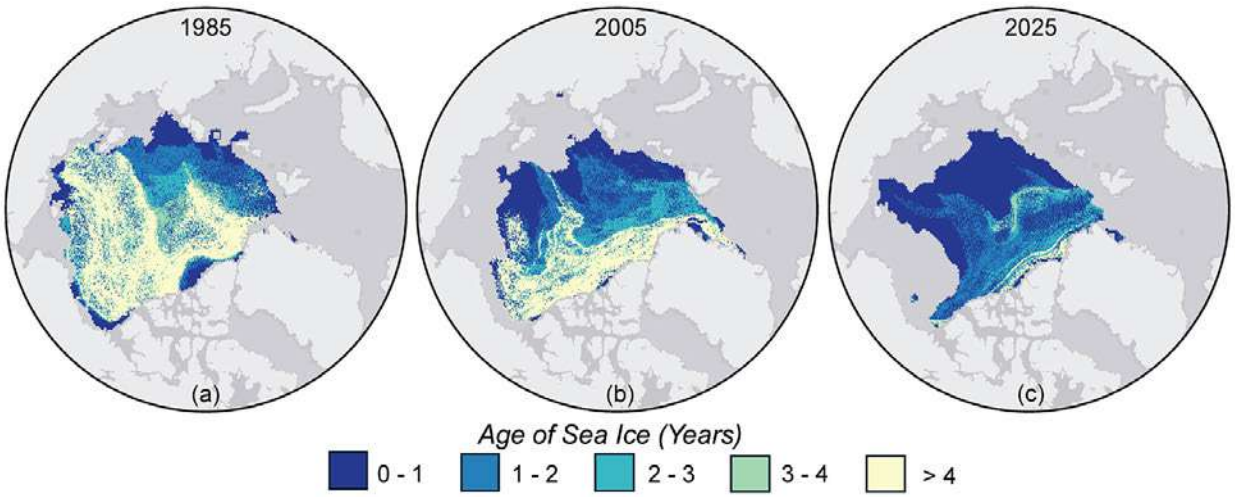

Fig. 4. Sea ice age during the week of the annual minimum ice extent in (a) 1985, (b) 2005, and (c) 2025.

Sea ice thickness

Quantitative estimates of sea ice thickness based on satellite altimetry began in 2010 and have been used to directly track this important metric. At the end of the winter growth season, the April 2025 thickness (Fig. 5a) in the Arctic had the typical pattern of thicker ice along the northern coast of Greenland and the Canadian Archipelago due to deformation and advection across the pole, though this also corresponds to the region of older ice noted above. The thickness anomaly pattern for April 2025 shows a substantial amount of spatial variability (Fig. 5b). The sea ice growth season began with the Laptev, Kara, and Barents Seas having thicker ice than the 2011-21 average and other regions being thinner than average (Fig. 5c). Ice growth through the winter was robust and by April all regions were either average or thicker than the 2011-21 average. However, there were areas within some regions with thinner than average ice.

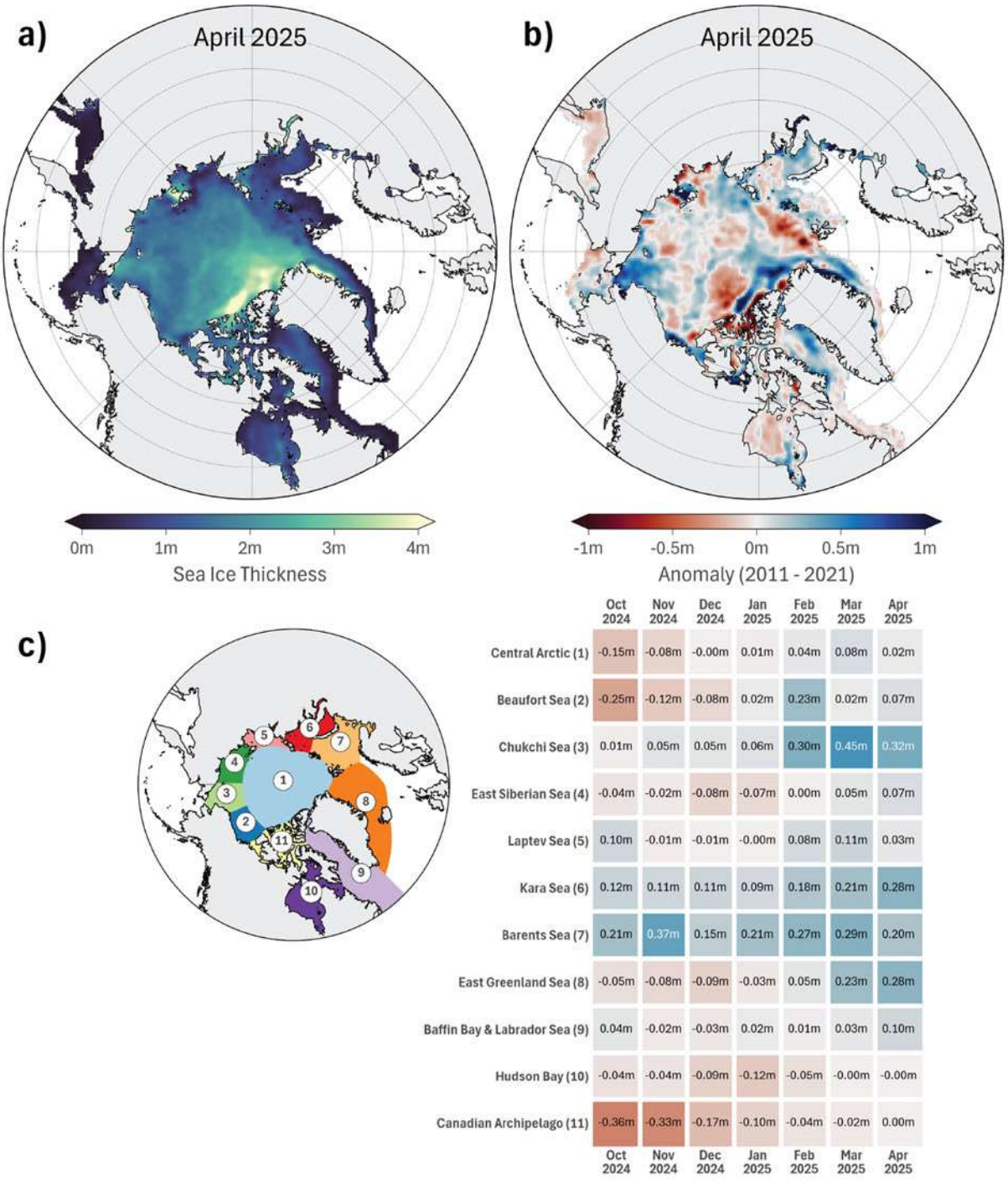

Fig. 5. Arctic sea ice in April 2025: (a) sea ice thickness from CryoSat-2/Sentinel-3/SMOS (b) sea ice thickness anomaly relative to April 2011-April 2021 average. (c) Regional monthly mean sea ice thickness anomalies in 2024/25 winter season relative to October 2011-April 2021 average.

Methods and data

Sea ice extent values are from the NSIDC Sea Ice Index (Fetterer et al. 2025), based on passive microwave derived sea ice concentrations from the NASA Team algorithm (Cavalieri et al. 1996), though

other high-quality products exist (e.g., Lavergne et al. 2019). For 2025, the algorithm was adapted for data from the JAXA Advanced Microwave Scanning Radiometer 2 (AMSR2) to create a consistent NASA Team product (Stewart et al. 2025).

Sea ice age data are from the EASE-Grid Sea Ice Age, Version 4 (Tschudi et al. 2019a) and Quicklook Arctic Weekly EASE-Grid Sea Ice Age, Version 1 (Tschudi et al. 2019b) archived at the NASA Snow and Ice Distributed Active Archive Center (DAAC) at NSIDC. Age is calculated via Lagrangian tracking of ice parcels using weekly sea ice motion vectors. Only the oldest age category is preserved for each grid cell.

Melt onset dates were derived from passive microwave satellite observations using the Advanced Horizontal Range Algorithm (Drobot and Anderson 2001; Bliss 2023). A sharp increase in the daily time series of brightness temperatures occurs when liquid water develops on the frozen sea ice surface, with the date of this brightness jump indicating the melt onset date.

Weekly CryoSat-2 estimates have been combined with thin ice (<1 m) estimates from the ESA Soil Moisture Ocean Salinity (SMOS) instrument and Sentinel-3 A/B data to obtain an optimal estimate across thin and thick ice regimes (Ricker et al. 2017) on a 25-km resolution EASE2 grid. Optimal interpolation is used to fill data gaps in the weekly CryoSat-2 fields and to merge the CryoSat-2 and SMOS estimates. The results here are from Version 206 (ESA 2023).

Acknowledgments

W. Meier thanks the NSIDC DAAC and the NASA ESDIS projects for support.

References

Bliss, A. C., 2023: Passive microwave Arctic ice melt onset dates from the advanced horizontal range algorithm 1979-2022. *Sci. Data*, **10**, 857, https://doi.org/10.1038/s41597-023-02760-5.

Cavalieri, D. J., C. L. Parkinson, P. Gloersen, and H. J. Zwally, 1996 (updated yearly): Sea Ice Concentrations from Nimbus-7 SMMR and DMSP SSM/I-SSMIS Passive Microwave Data, Version 1. NASA National Snow and Ice Data Center Distributed Active Archive Center, Boulder, CO, USA, accessed 1 September 2025, https://doi.org/10.5067/8GQ8LZQVL0VL.

Drobot, S. D., and M. R. Anderson, 2001: An improved method for determining snowmelt onset dates over Arctic sea ice using Scanning Multichannel Microwave Radiometer and Special Sensor Microwave/Imager data. *J. Geophys. Res.*, **106**(D20), 24033-24049, https://doi.org/10.1029/2000JD000171.

European Space Agency, 2023: SMOS-CryoSat L4 Sea Ice Thickness, Version 206. ESA Earth Online, accessed 1 September 2025, https://doi.org/10.57780/sm1-4f787c3.

Fetterer, F., K. Knowles, W. N. Meier, M. Savoie, A. K. Windnagel, and T. Stafford, 2025 (updated daily): Sea Ice Index, Version 4. NSIDC: National Snow and Ice Data Center, Boulder, CO, USA, accessed 2 October 2025, https://doi.org/10.7265/a98x-0f50.

George, J. C., S. E. Moore, and J. G. M. Thewissen, 2020: Bowhead whales: recent insights into their biology, status and resilience. *Arctic Report Card 2020*, R. L. Thoman, J. Richter-Menge, and M. L. Druckenmiller, Eds., https://doi.org/10.25923/cppm-n265.

Lavergne, T., and Coauthors, 2019: Version 2 of the EUMETSAT OSI SAF and ESA CCI sea-ice concentration climate data records. *Cryosphere*, **13**, 49-78, https://doi.org/10.5194/tc-13-49-2019.

Ricker, R., S. Hendricks, L. Kaleschke, X. Tian-Kunze, J. King, and C. Haas, 2017: A weekly Arctic sea-ice thickness data record from merged CryoSat-2 and SMOS satellite data. *Cryosphere*, **11**, 1607-1623, https://doi.org/10.5194/tc-11-1607-2017.

Stewart, J. S., W. N. Meier, R. Marowitz, D. J. Scott, and H. Wilcox, 2025: AMSR2 Daily Polar Gridded Sea Ice Concentrations, Version 2. NASA National Snow and Ice Data Center Distributed Active Archive Center, Boulder, CO, USA, accessed 2 October 2025, https://doi.org/10.5067/W13AO54SS7CW.

Tschudi, M., W. N. Meier, J. S. Stewart, C. Fowler, and J. Maslanik, 2019a: EASE-Grid Sea Ice Age, Version 4. NASA National Snow and Ice Data Center Distributed Active Archive Center, Boulder, CO, USA, accessed 5 September 2025, https://doi.org/10.5067/UTAV7490FEPB.

Tschudi, M., W. N. Meier, and J. S. Stewart, 2019b: Quicklook Arctic Weekly EASE-Grid Sea Ice Age, Version 1. NASA National Snow and Ice Data Center Distributed Active Archive Center, Boulder, CO, USA, accessed 2 October 2025, https://doi.org/10.5067/2XXGZY3DUGNQ.

Zhao, P., Y. Li, and Y. Zhang, 2024: Ships are projected to navigate whole year-round along the North Sea route by 2100. *Commun. Earth Environ.*, **5**, 407, https://doi.org/10.1038/s43247-024-01557-7.

December 10, 2025

Sea Surface Temperature

https://doi.org/10.25923/pz7y-3b10

M. -L. Timmermans[1] and Z. M. Labe[2]

[1]Department of Earth and Planetary Sciences, Yale University, New Haven, CT, USA
[2]Climate Central, Princeton, NJ, USA

Headlines

- In the marginal seas of the Arctic Ocean's Atlantic sector, August 2025 mean sea surface temperatures (SSTs) were as much as ~7°C warmer than 1991-2020 August mean values.
- Anomalously cool August 2025 SSTs (~1-2°C cooler) were observed in parts of the marginal seas of the Arctic Ocean's Pacific sector.
- August mean SSTs show warming trends for 1982-2025 in almost all Arctic Ocean regions that are ice-free in August, with mean SST increases of ~0.3°C per decade in the region north of 65° N.
- Warming Arctic SSTs alter local ecosystems and accelerate sea-ice loss, with wide-ranging global climate and societal consequences.

Introduction

Arctic Ocean sea-surface temperatures (SSTs) in the summer are primarily influenced by the amount of incoming solar radiation absorbed by the sea surface and by the flow of warm waters into the Arctic from the North Atlantic and North Pacific Oceans. Solar warming of the Arctic Ocean surface is influenced by the sea-ice distribution (with greater warming occurring in ice-free regions), cloud cover, and upper-ocean stratification. Inflows of relatively warm Arctic river waters can provide an additional heat source in coastal regions.

Arctic SST is a key indicator of the strength of the ice-albedo feedback during a given summer melt season. As the brighter, more reflective sea-ice retreats, more solar energy is absorbed by the darker ocean surface, which in turn warms the water and accelerates further ice melt. In addition, higher summer SSTs are associated with delayed autumn sea-ice freeze-up and increased ocean heat storage throughout the year. Marine ecosystems are also influenced by SSTs, which affect the timing and development of primary production cycles, available habitat, and other factors, such as the occurrence of harmful algal blooms (see essays *Primary Productivity* and *Warming of the Bering and Chukchi Seas*). These ecological changes influence fisheries, food security, and human health, particularly for Arctic communities that rely on marine resources (e.g., Quakenbush et al. 2024; Schoen et al. 2023). More recently, Arctic marine heatwaves have emerged as a significant concern, further stressing already vulnerable ecosystems (e.g., Gou et al. 2025).

2025 sea surface temperature

The SST data analyzed span June 1982 through August 2025, with 1991-2020 used as the climatological reference period ("normal") (see *Methods and data*). Here, we focus most closely on August 2025 mean

SSTs in context with the climatological record. August mean SSTs provide the most appropriate representation of Arctic Ocean summer SSTs because sea-ice extent and concentration are near a seasonal low at this time of year, and there is not yet the influence of surface cooling and subsequent sea-ice growth that typically takes place in the latter half of September.

August 2025 mean SSTs were as high as ~12°C in parts of the Barents and Kara Seas (within the Arctic Ocean's Atlantic sector) with somewhat cooler values ~ -1-7°C in other Arctic basin marginal regions (Fig. 1a,b). August 2025 mean SSTs were anomalously warm compared to the 1991-2020 August mean in the Barents, Kara, and Laptev Seas: SSTs were around 1-4°C higher, with SST anomalies as high as ~7°C in the Kara Sea (Fig. 1c). In the Arctic's Pacific sector, the Beaufort and northern Chukchi Seas had anomalously cold SSTs (August 2025 mean values ~1-2°C lower than the 1991-2020 mean), while the southern Chukchi Sea and the Bering Sea were anomalously warm (SSTs ~1-2°C higher). This general pattern of August 2025 SST anomalies is consistent with regional patterns of anomalously warm surface-air temperatures in the Kara and Laptev Sea regions and cold surface-air temperatures in the Beaufort Sea region in summer 2025 (see essay *Surface Air Temperature*).

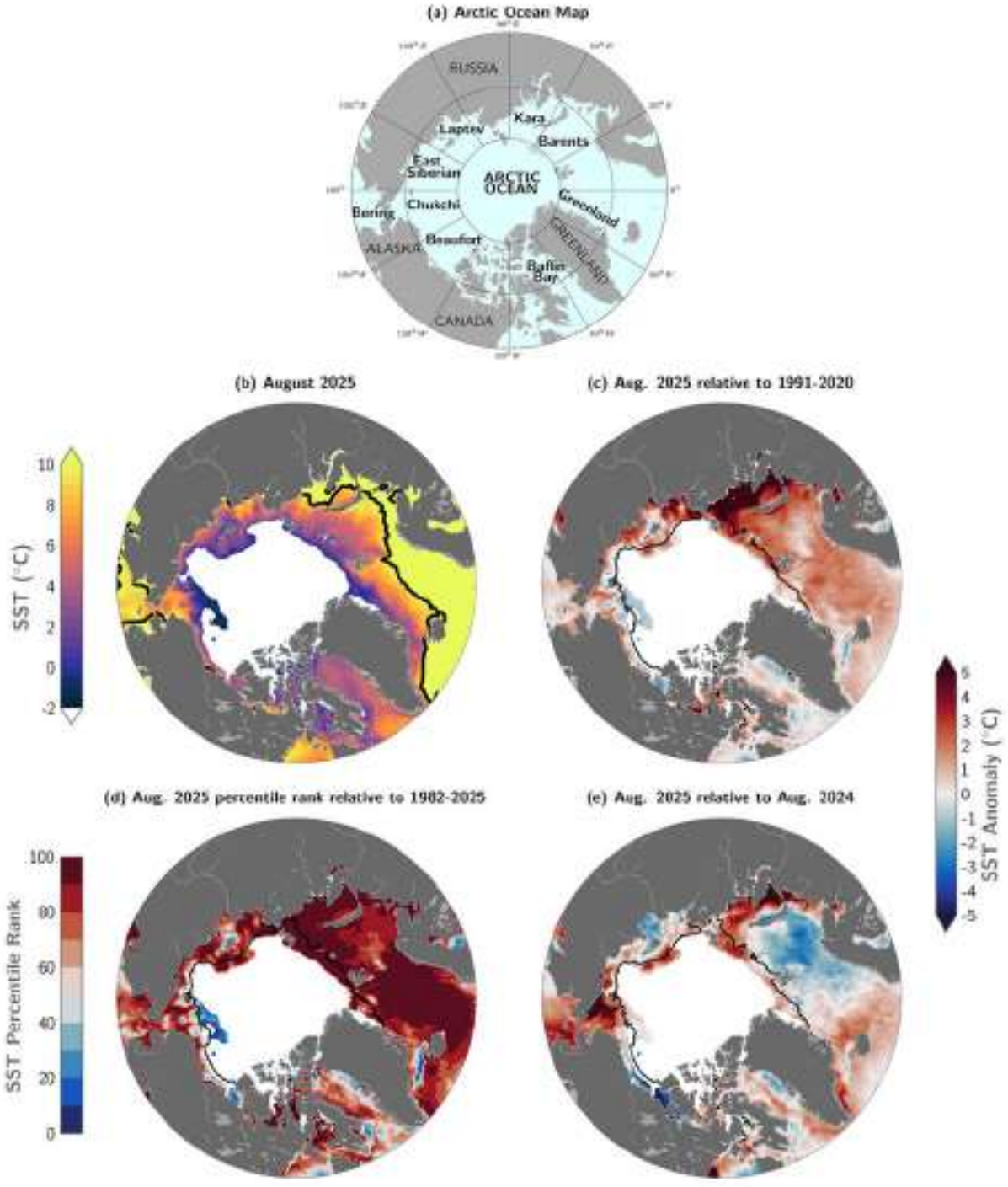

Fig. 1. (a) Arctic Ocean map showing relevant marginal sea locations and geographic features. (b) Mean sea-surface temperature (SST; °C) in August 2025. Black contours indicate the 10°C-SST isotherm. (c) SST anomalies (°C) in August 2025 relative to the August 1991-2020 mean. (d) August 2025 SST percentile rank relative to the August values in 1982-2025. (e) Difference between August 2025 SSTs and August 2024 SSTs (negative values indicate where 2025 was cooler). White shading in all panels is the August 2025 mean sea-ice extent. Black lines in (c-e) indicate the August 1991-2020 median ice edge.

In most Arctic regions, August 2025 SSTs ranked among the warmest recorded in the 1982-2025 period (70th to 100th percentile; Fig. 1d), although regional SST anomalies differ significantly from year to year. The Kara and Chukchi Seas had considerably higher SSTs in August 2025 compared to August 2024, with differences of up to 9°C (Fig. 1e). By contrast, August 2025 SSTs were up to a few degrees cooler than 2024 SSTs in the Barents and southern Beaufort Seas.

SST patterns in August 2025 were indicated by developments in June and July. Above-normal SSTs in the Arctic's Atlantic sector were also observed in June and July 2025 (Fig. 2). This is consistent with relatively warm summer 2025 surface-air temperatures in the region (see essay *Surface Air Temperature*). Below-normal SSTs in the Bering Sea in June and July (Fig. 2a,b) were consistent with the relatively late ice retreat from the Pacific sector (see essay *Sea Ice*), suggesting a weaker ice-albedo feedback that can be initiated by warm Pacific inflows to the Arctic. The transition from below-normal to above-normal SSTs from June to August in the Bering Strait region corresponded with the transition from anomalously cool surface air temperatures in spring to warm in summer (see essay *Surface Air Temperature*).

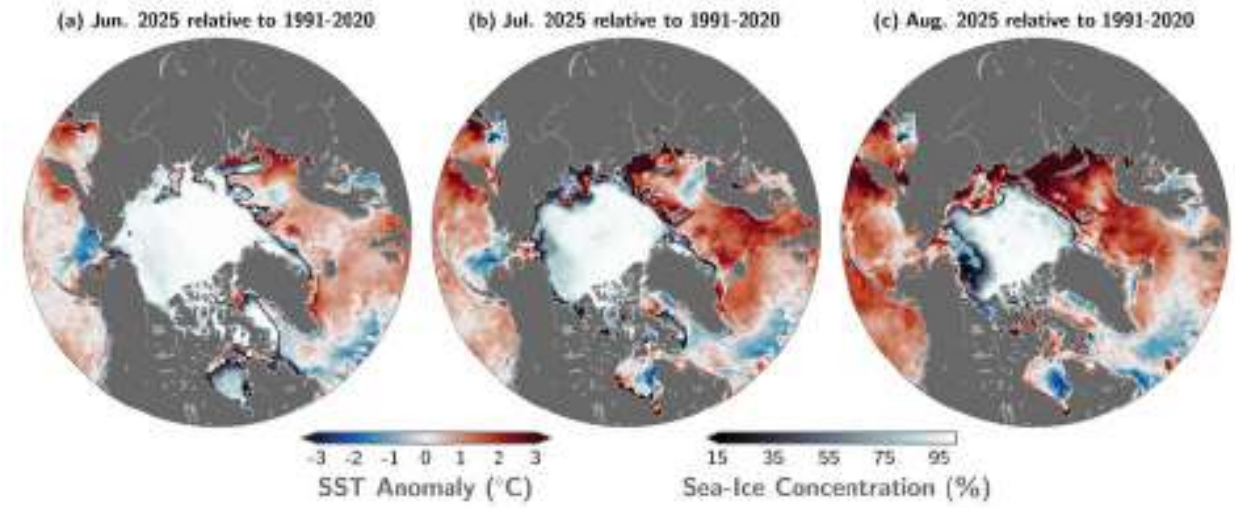

Fig. 2. Sea-surface temperature (SST) anomalies (°C) for (a) June 2025, (b) July 2025, and (c) August 2025 relative to the 1991-2020 mean for the respective months. Note a difference in the color bar scale compared to Fig. 1c,e. The mean sea-ice concentration for the corresponding month is also shown.

The Arctic Ocean has experienced significant mean August SST warming from 1982 to 2025, with statistically significant (95% confidence interval) linear trends in almost all regions (Fig. 3a). Mean August SSTs for the entire region of the Arctic Ocean north of 65° N exhibit a linear warming trend of 0.3 ± 0.1°C/decade, matching the Northern Hemisphere trend (Fig. 3b). Similarly, the North Pacific and North Atlantic (between 50° N and 65° N) show warming trends of 0.4 ± 0.1°C/decade over the same period. The global mean SST trend is also not statistically distinct, with mean August SSTs exhibiting a linear trend of 0.20 ± 0.02°C/decade over the 1982 to 2025 period. In the context of these long-term trends, August 2025 mean Arctic Ocean SST was the second warmest on record, exceeded only in August 2007. Globally averaged SSTs for August 2025 were the third warmest on record, following August 2023 and August 2024 (Mercator Ocean International 2025).

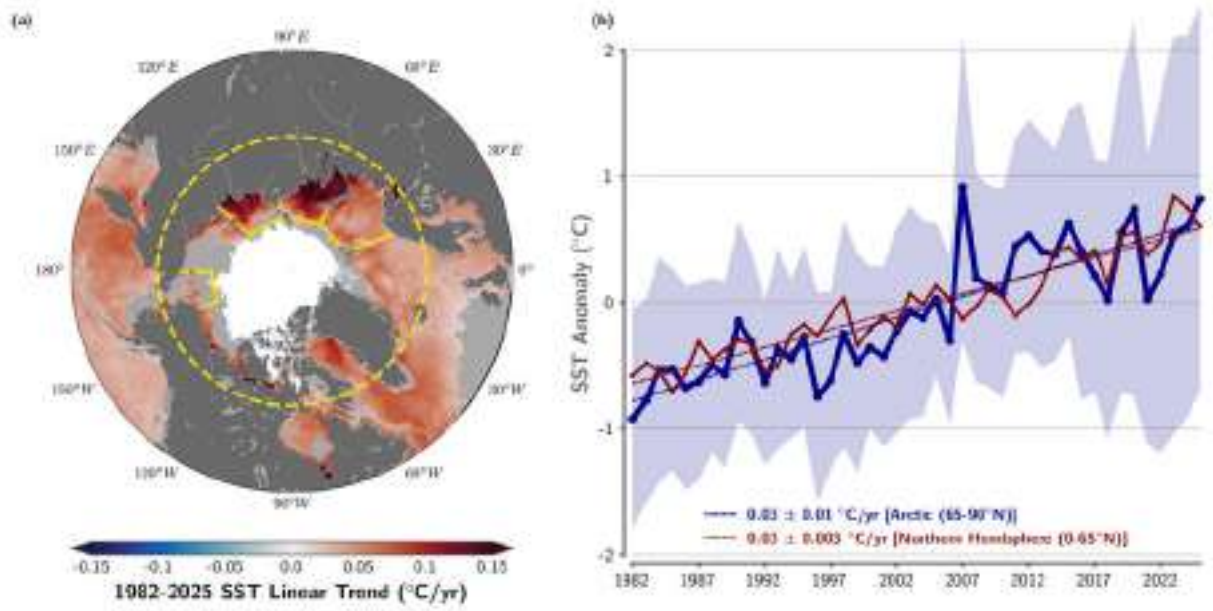

Fig. 3. (a) Linear sea-surface temperature (SST) trend (°C/yr) for August of each year from 1982 through 2025. The trend is only shown for values that are statistically significant at the 95% confidence interval; the region is shaded light gray otherwise. White shading indicates regions that are ice covered (> 15% sea ice concentration) in all years, 1982 through 2025. The dashed yellow circle marks 65° N (the Arctic Ocean region), and other solid yellow line boundaries delineate the Barents, Kara, Laptev, and Chukchi Seas (see *Methods and data*). (b) Area-averaged SST anomalies (°C) for August of each year (1982-2025) relative to the 1991-2020 August mean for the Arctic Ocean north of 65° N (blue line) (shading indicates ±1 standard deviation of the regional mean SST anomaly field) and south of 65° N in the Northern Hemisphere (red line). The dotted lines show the corresponding linear SST anomaly trends over 1982-2025, and numbers in the legends indicate the trends with 95% confidence intervals.

Regionally, the Kara and Laptev Seas show the strongest warming trends in the Arctic Ocean (Fig. 3a), with August SST linear trends in these seas of 0.12 ± 0.03°C/yr and 0.08 ± 0.02°C/yr, respectively (Fig. 4a,b). In the Kara Sea, August 2025 mean SSTs were the warmest on record. Statistically significant linear trends (0.06 ± 0.02°C/yr) in August SST are also observed in the Barents Sea (Fig. 4c). On the other hand, there is no statistically significant trend in the Chukchi Sea, which is notably influenced by anomalously cool August SSTs in recent years (Fig. 4d). Beginning around 2007, there is some indication of an intensification of the warming trends in the Barents, Kara, and Laptev Seas (Atlantic sector of the Arctic Ocean; Fig. 4a-c). However, changepoint analysis of these regional SST records yields variable results across the seas, and no statistically robust shift is detected to date. A longer time series will be necessary to determine whether these apparent changes represent a sustained shift in the warming trajectory.

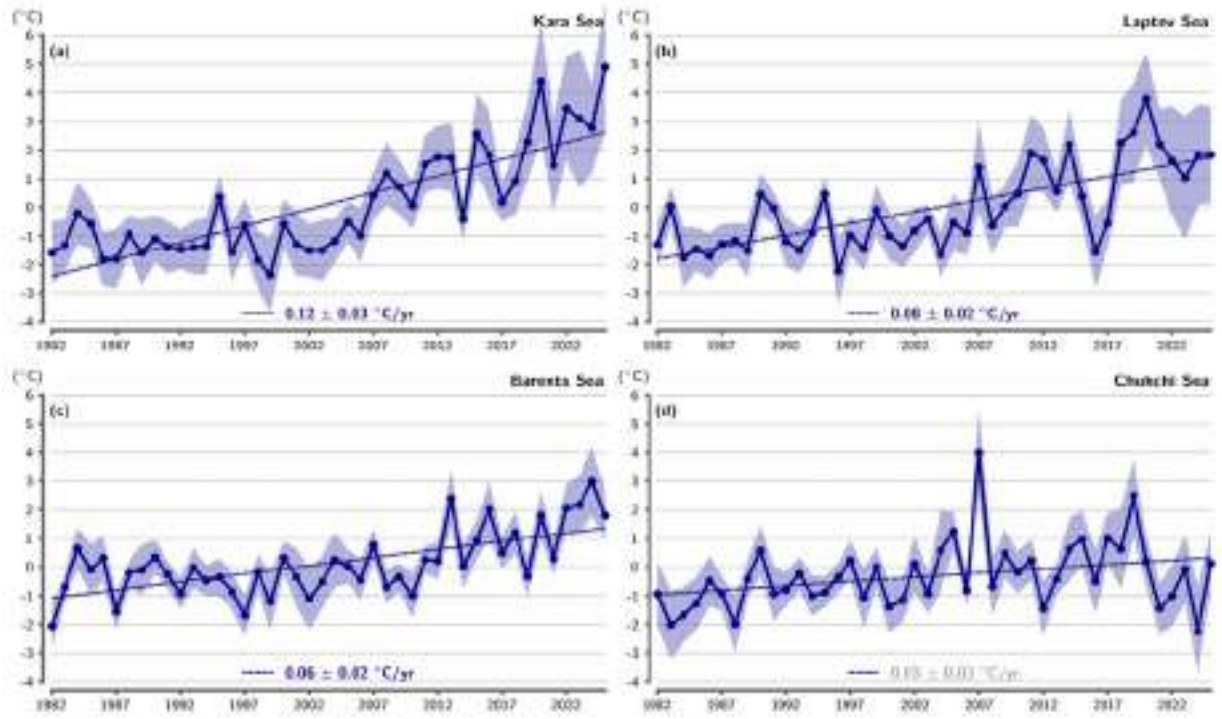

Fig. 4. Area-averaged SST anomalies (°C) for August of each year (1982-2025) relative to the 1991-2020 August mean for (a) the Kara Sea, (b) the Laptev Sea, (c) the Barents Sea, and (d) the Chukchi Sea regions shown by blue boundaries in Fig. 3a (see also *Methods and data*). The dotted lines show the linear SST anomaly trends over 1982-2025, and numbers in the legends indicate the trends in °C/year (with 95% confidence intervals; trends that are not statistically significant are labeled in grey). Blue shading indicates ±1 standard deviation of the regional mean SST anomaly fields.

Methods and data

The SST data presented here are from the 0.25° × 0.25° NOAA Optimum Interpolation Sea Surface Temperature (OISST) Version 2.1 product, a blend of in situ and satellite measurements (Reynolds et al. 2002, 2007; Huang et al. 2021a,b); https://psl.noaa.gov/data/gridded/data.noaa.oisst.v2.highres.html (NOAA 2024). The datafile "sst.mon.mean.nc" (comprising monthly means from the daily data) was retrieved from https://downloads.psl.noaa.gov/Datasets/noaa.oisst.v2.highres/ (accessed 3 September 2025). Note that in January 2023, OISST Version 2.1 replaced the 1° × 1° NOAA OISST Version 2, which was analyzed in Arctic Report Cards before 2023; while overall SST trends and patterns are similar between versions, the difference merits caution when comparing Arctic Report Cards across years (for further details, see Timmermans and Labe 2023).

For setting a proxy SST in sea-ice covered regions, OISST Version 2.1 sets SST equal to the freezing temperature (computed using a climatological sea-surface salinity) where ice concentrations are greater than 35% (see Banzon et al. 2020). Therefore, uncertainty in inferring SSTs (and SST trends) may be significant in the vicinity of the sea-ice edge, which varies in location each year, and when sea ice covers a significant portion of the region of interest.

Sea-ice concentration data are the Near-Real-Time NOAA/NSIDC Climate Data Record of Passive Microwave Sea Ice Concentration, Version 3 (https://nsidc.org/data/g10016/versions/3) (Peng et al. 2013; Meier et al. 2021a,b). The 1991-2020 median ice edge is derived from the NOAA/NSIDC Climate Data

Record of Passive Microwave Sea Ice Concentration, Version 5 (https://nsidc.org/data/g02202/versions/5) with a threshold of 15% concentration defined as the ice edge.

Boundaries shown in Fig. 3a for the regional time series (Fig. 4) are as follows: Kara Sea: 70-80° N, 50-100° E; Chukchi Sea: 65-75° N, 180-202° E; Laptev Sea: 70-80° N, 100-139° E; Barents Sea: 66.5-80° N, 20-60° E.

Acknowledgments

M. -L. Timmermans acknowledges support from the National Science Foundation Office of Polar Programs and the Office of Naval Research. We thank Dr. Kristina Dahl (Climate Central) for reviewing the essay. NOAA OI SST V2 High Resolution Dataset data provided by the NOAA PSL, Boulder, Colorado, USA, from their website at https://psl.noaa.gov.

References

Banzon, V., T. M. Smith, M. Steele, B. Huang, and H. -M. Zhang, 2020: Improved estimation of proxy sea surface temperature in the Arctic. *J. Atmos. Ocean. Tech.*, **37**, 341-349, https://doi.org/10.1175/JTECH-D-19-0177.1.

Gou, R., K. K. E. Wolf, C. J. M. Hoppe, L. Wu, and G. Lohmann, 2025: The changing nature of future Arctic marine heatwaves and its potential impacts on the ecosystem. *Nat. Climate Change*, **15**, 162-170, https://doi.org/10.1038/s41558-024-02224-7.

Huang, B., C. Liu, V. Banzon, E. Freeman, G. Graham, B. Hankins, T. Smith, and H. -M. Zhang, 2021a: Improvements of the Daily Optimum Interpolation Sea Surface Temperature (DOISST) Version 2.1. *J. Climate*, **34**(8), 2923-2939, https://doi.org/10.1175/JCLI-D-20-0166.1.

Huang, B., C. Liu, E. Freeman, G. Graham, T. Smith, and H. -M. Zhang, 2021b: Assessment and Intercomparison of NOAA Daily Optimum Interpolation Sea Surface Temperature (DOISST) Version 2.1. *J. Climate*, **34**(18), 7421-7441, https://doi.org/10.1175/JCLI-D-21-0001.1.

Meier, W. N., F. Fetterer, A. K. Windnagel, and J. S. Stewart, 2021a: NOAA/NSIDC Climate Data Record of Passive Microwave Sea Ice Concentration, Version 4. [1982-2021]. NSIDC: National Snow and Ice Data Center, Boulder, CO, USA, accessed 4 September 2025, https://doi.org/10.7265/efmz-2t65.

Meier, W. N., F. Fetterer, A. K. Windnagel, and J. S. Stewart, 2021b: Near-Real-Time NOAA/NSIDC Climate Data Record of Passive Microwave Sea Ice Concentration, Version 2. [1982-2021], NSIDC: National Snow and Ice Data Center, Boulder, CO, USA, accessed 4 September 2025, https://doi.org/10.7265/tgam-yv28.

Mercator Ocean International, 2025: Ocean Temperature Bulletin – August 2025. European Union, Copernicus Marine Service. https://www.mercator-ocean.eu/bulletin/ocean-temperature-bulletin-august-2025/, accessed 17 September 2025.

NOAA, 2024: Optimum Interpolation Sea Surface Temperature (OISST) high resolution dataset, version 2.1. NOAA/PSL, accessed 4 September 2025, https://psl.noaa.gov/data/gridded/data.noaa.oisst.v2.highres.html.

Peng, G., W. N. Meier, D. J. Scott, and M. H. Savoie, 2013: A long-term and reproducible passive microwave sea ice concentration data record for climate studies and monitoring. *Earth Syst. Sci. Data*, **5**, 311-318, https://doi.org/10.5194/essd-5-311-2013.

Quakenbush, L., A. Bryan, J. Crawford, J. Olnes, and R. Stimmelmayr, 2024: Ice seals of Alaska. *Arctic Report Card 2024*, T. A. Moon, M. L. Druckenmiller, and R. L. Thoman, Eds., https://doi.org/10.25923/4488-8843.

Reynolds, R. W., N. A. Rayner, T. M. Smith, D. C. Stokes, and W. Wang, 2002: An improved in situ and satellite SST analysis for climate. *J. Climate*, **15**, 1609-1625, https://doi.org/10.1175/1520-0442(2002)015<1609:AIISAS>2.0.CO;2.

Reynolds, R. W., T. M. Smith, C. Liu, D. B. Chelton, K. S. Casey, and M. G. Schlax, 2007: Daily high-resolution-blended analyses for sea surface temperature. *J. Climate*, **20**, 5473-5496, https://doi.org/10.1175/2007JCLI1824.1.

Schoen, E. R., K. G. Howard, J. M. Murphy, D. E. Schindler, P. A. H. Westley, and V. R. von Biela, 2023: Divergent responses of western Alaska salmon to a changing climate. *Arctic Report Card 2023*, R. L. Thoman, T. A. Moon, and M. L. Druckenmiller, Eds., https://doi.org/10.25923/f2hv-5581.

Timmermans, M. -L., and Z. M. Labe, 2023: Sea surface temperature. *Arctic Report Card 2023*, R. L. Thoman, T. A. Moon, and M. L. Druckenmiller, Eds., https://doi.org/10.25923/e8jc-f342.

January 26, 2026

Arctic Ocean Primary Productivity: The Response of Marine Algae to Climate Warming and Sea Ice Decline

https://doi.org/10.25923/c7gy-pp78

K. E. Frey[1], L. V. Stock[2], C. Garcia[3], L. W. Cooper[4], and J. M. Grebmeier[4]

[1]Graduate School of Geography, Clark University, Worcester, MA, USA
[2]Cryospheric Sciences Laboratory, Goddard Space Flight Center, NASA, Greenbelt, MD, USA
[3]Arctic Research Program, Global Ocean Monitoring and Observing Program, NOAA, Silver Spring, MD, USA
[4]Chesapeake Biological Laboratory, University of Maryland Center for Environmental Science, University of Maryland, Solomons, MD, USA

Headlines

- Satellite estimates of ocean primary productivity (i.e., the rate at which marine algae transform dissolved inorganic carbon into organic material) show higher values for 2025 (relative to the 2003-22 mean) for eight of nine regions assessed across the Arctic.
- All regions, except for the Amerasian Arctic (the combined Chukchi Sea, Beaufort Sea, and Canadian Archipelago), continue to exhibit positive trends in ocean primary productivity during 2003-25, with the largest percent changes in the Eurasian Arctic (+80.2%), Barents Sea (+33.8%), and Hudson Bay (+27.1%).
- While higher primary productivity may enhance carbon availability to food webs in some cases, important negative impacts to ecosystem health also result from trophic mismatches that stymie the movement of carbon through the food chain as well as the increasing prevalence of harmful algal blooms.

Introduction

Arctic marine primary productivity, the fundamental process by which marine algae convert dissolved inorganic carbon into organic material through photosynthesis, forms the foundation of the marine food web and plays a critical role in global carbon cycling. This biological engine is highly sensitive to changes in sea ice cover (see essay *Sea Ice*), ocean temperature (see essay *Sea Surface Temperature*), and nutrient availability, all of which are being altered by ongoing Arctic warming. As the Arctic is warming at nearly four times the global average rate (Rantanen et al. 2022), marine primary productivity continues to exhibit complex regional and temporal responses across the Arctic Ocean.

Recent in-situ observations reveal multifaceted primary productivity changes. While many regions show increased productivity owing to thinner and more light-transmissive sea ice, expanded ice-free areas, and enhanced nutrient upwelling (Ardyna et al. 2020), the highest localized productivity remains associated with the retreating ice edge (Castagno et al. 2023). Organic matter from ice-associated algae continues to play a critical year-round role in Arctic ecosystems (Koch et al. 2023). However, increased stratification and shifts from larger diatoms to smaller flagellates may inhibit long-term production or

efficient energy transfer (Li et al. 2009). The diverse sectors of the Arctic Ocean also respond uniquely to environmental changes, from the Atlantic-influenced Eurasian Basin (see essay *Atlantification of the Arctic Ocean*) experiencing increased Atlantic water inflow and warming, to the Pacific-dominated Chukchi Sea receiving variable nutrient inputs through Bering Strait. These regional variations are further complicated by increasing riverine discharge delivering both nutrients and chromophoric (i.e., colored) dissolved organic matter (CDOM), which can either enhance or inhibit productivity depending on local conditions (Lewis and Arrigo 2020; Mathew et al. 2025).

Increasing primary productivity in Arctic regions has both ecological and societal relevance as an indicator of ecosystem health. Higher productivity may enhance carbon availability to food webs, potentially benefiting zooplankton and benthic populations. However, concurrent trends of reduced ice cover, warming seawater, and enhanced stratification can cause shifts in the timing and species composition of phytoplankton blooms, which can negatively impact ecosystem dynamics by causing trophic mismatches (and therefore reduced utilization of carbon through the food chain). Furthermore, sea-ice obligate species at higher trophic levels (e.g., Arctic cod, Pacific walruses, and several species of ice seals) can be severely impacted by declining sea ice regardless of food availability. Adding to these challenges, recent warming in the Pacific Arctic has increased the occurrence of algal species that synthesize toxins that can be transmitted through the food web and potentially affect the health of subsistence-based coastal communities (Anderson et al. 2022). Observing and understanding changes in regional primary productivity across the Arctic are essential for predicting ecosystem trajectories, managing marine resources, and understanding food security issues across human societies (Huntington et al. 2022).

Satellite remote sensing provides critical synoptic observations for tracking productivity patterns across the vast Arctic Ocean. The Moderate Resolution Imaging Spectroradiometer (MODIS)-Aqua satellite record, now spanning over two decades (2003-25), enables detection of localized productivity hotspots, phenological shifts, and long-term trends that otherwise would be impossible to capture through shipboard observations alone (Frey et al. 2023a). In this year's assessment, we utilized the extended MODIS-Aqua record to present satellite-derived estimates of Arctic Ocean primary productivity for 2025, examining regional variations and contextualizing current conditions over the 23-year observational record.

Chlorophyll-*a*

We present satellite-based estimates of algal chlorophyll-*a* (occurring in all species of phytoplankton) based on ocean color and subsequently provide calculated primary production estimates (below). Observed patterns in chlorophyll-*a* (Fig. 1), which are spatially and temporally heterogeneous across the Arctic Ocean, are often associated with the timing of the seasonal break-up and retreat of sea ice cover (Fig. 2) (see essay *Sea Ice*): high chlorophyll-*a* percentages (i.e., relative to the 2003-22 average) tend to occur in regions where the break-up is relatively early, while low percentages tend to occur in regions where the break-up is delayed. May 2025 (Fig. 1a) showed clear higher-than-average chlorophyll-*a* concentrations along the sea ice edge in the Greenland Sea, with distributions of lower-than-average values in the Barents and Bering Seas. During June 2025 (Fig. 1b), higher-than-average chlorophyll-*a* concentrations continued in the Greenland Sea and emerged in portions of the Barents, Kara, and Bering Seas. During July 2025 (Fig. 1c), higher-than-average values were apparent in the western Barents, Kara, Laptev, and Bering Seas, with lower-than-average values developing in the Greenland and central Barents Seas. During August 2025 (Fig. 1d), spatial patterns remained heterogeneous showing higher-than-average values in the Kara and western Barents Seas, with noteworthy lower-than-average values

clustered in the eastern Barents, Laptev, East Siberian, Chukchi, and Beaufort Seas. Examples of clear connections between chlorophyll-*a* and sea ice include: (1) a likely strong sea ice edge bloom in the eastern Greenland Sea during May (Fig. 1a) associated with higher-than-average sea ice concentrations adjacent to the west (Fig. 2a); and (2) high chlorophyll-*a* concentrations in the Kara Sea during June (Fig. 1b) geographically coincident with lower-than-average sea ice cover across the region (Fig. 2b).

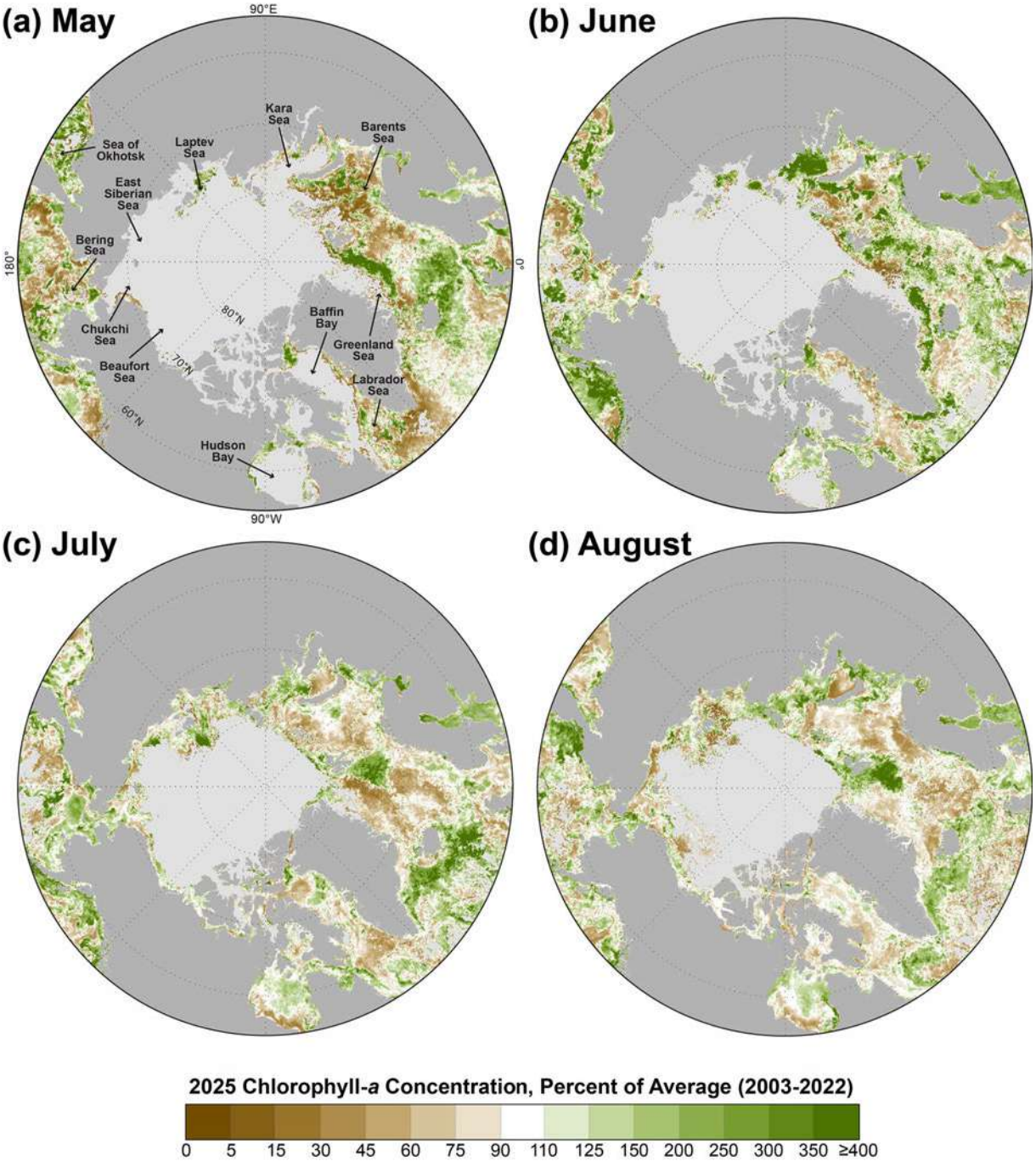

Fig. 1. Mean monthly chlorophyll-*a* concentrations during 2025, shown as a percent of the 2003-22 average for (a) May, (b) June, (c) July, and (d) August. The light gray regions represent areas where no data are available (owing to either the presence of sea ice or cloud cover). The color scale bar uses unequal intervals ranging from 5 to 50 percentage units, where the largest intervals are used for values greater than 125%. Data source: MODIS-Aqua Reprocessing 2022.0.2, chlor_a algorithm: https://oceancolor.gsfc.nasa.gov/.

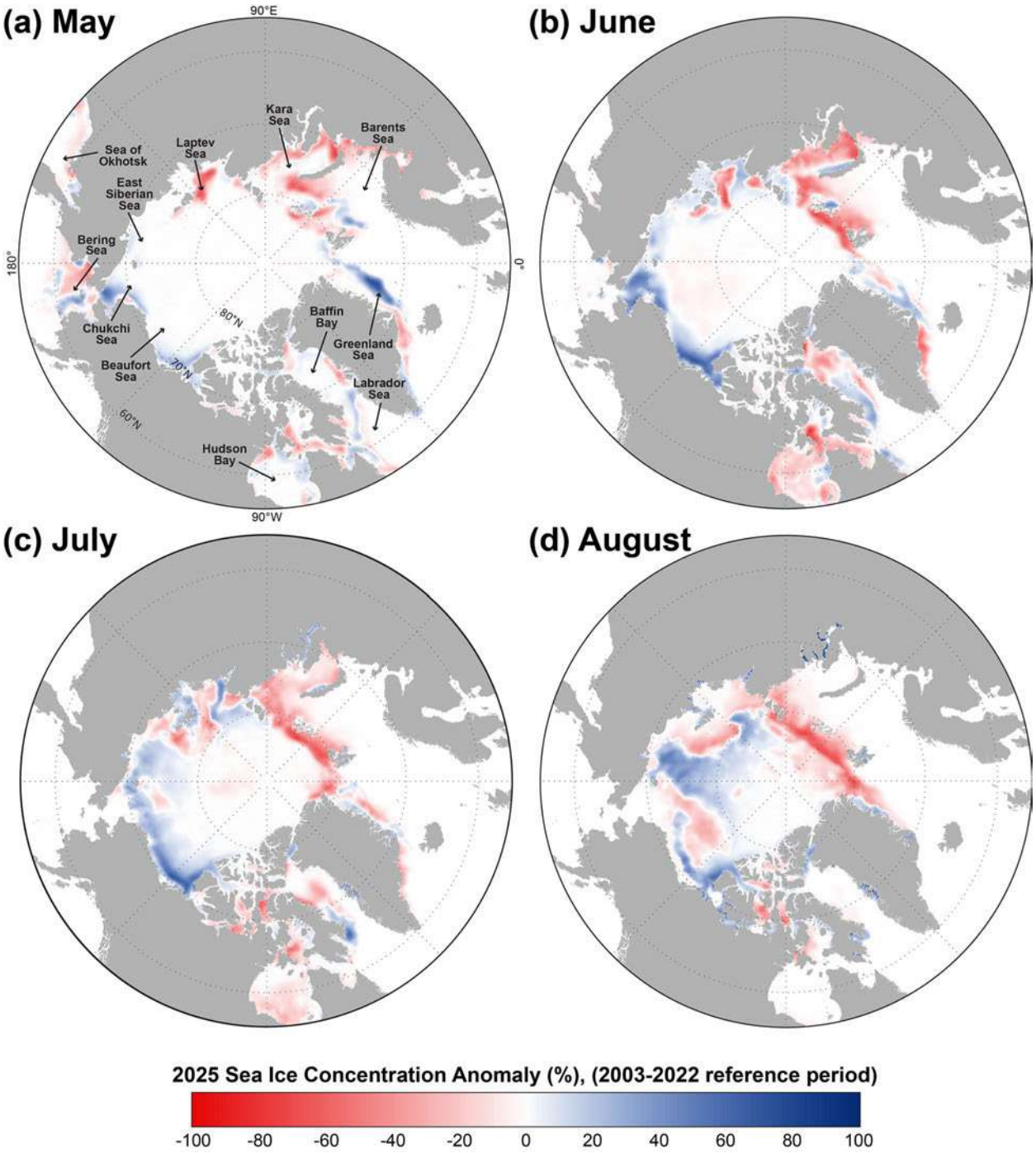

Fig. 2. Sea ice concentration anomalies (%) in 2025 (compared to a 2003-22 mean reference period) for (a) May, (b) June, (c) July, and (d) August. Data source: SSM/I and SSMIS passive microwave data, calculated using the Goddard Bootstrap (SB2) algorithm (Comiso et al. 2017).

Primary production

While chlorophyll-*a* concentrations give an estimate of the total standing stock of algal biomass, rates of primary production provide a different perspective since not all algae in the water column are necessarily actively producing. The mean annual (March through September) primary productivity

across the Arctic shows important spatial patterns, most notably that rates decrease northward as sea ice becomes more prevalent and nutrients become less available (Fig. 3a). Spatial trends in annual primary productivity (Fig. 3b) are a particularly useful tool for understanding hotspots of change. Statistically significant increases in primary productivity appear clustered in the Norwegian Sea, Barents Sea, Kara Sea, Laptev Sea, southeastern Chukchi Sea, and northern Bering Sea south of St. Lawrence Island (Fig. 3b). Positive trends adjacent to the Eurasian coastline may reflect river-derived, light-absorbing CDOM variability rather than true productivity increases (e.g., Zoffoli et al. 2025)—a critical caveat for interpreting regional increases there. There is almost no evidence of significant negative trends in primary productivity across the Arctic (Fig. 3b). Investigations of 2025 annual primary productivity (Fig. 3c), as well as 2025 compared to the 2003-22 average (Fig. 3d), show the strongest higher-than-average annual productivity along the sea ice edge in the northern Greenland, Barents, and Kara Seas of the eastern Arctic. The strongest lower-than-average annual productivity values are juxtaposed in the western Arctic across the Chukchi and Beaufort Seas (Fig. 3d). This clearly aligns with observed hemispheric contrasts in 2025 sea ice conditions (Fig. 2), where sea ice cover was lower-than-average in the eastern Arctic and higher-than-average in the western Arctic, most notably during June (Fig. 2b), July (Fig. 2c), and August (Fig. 2d).

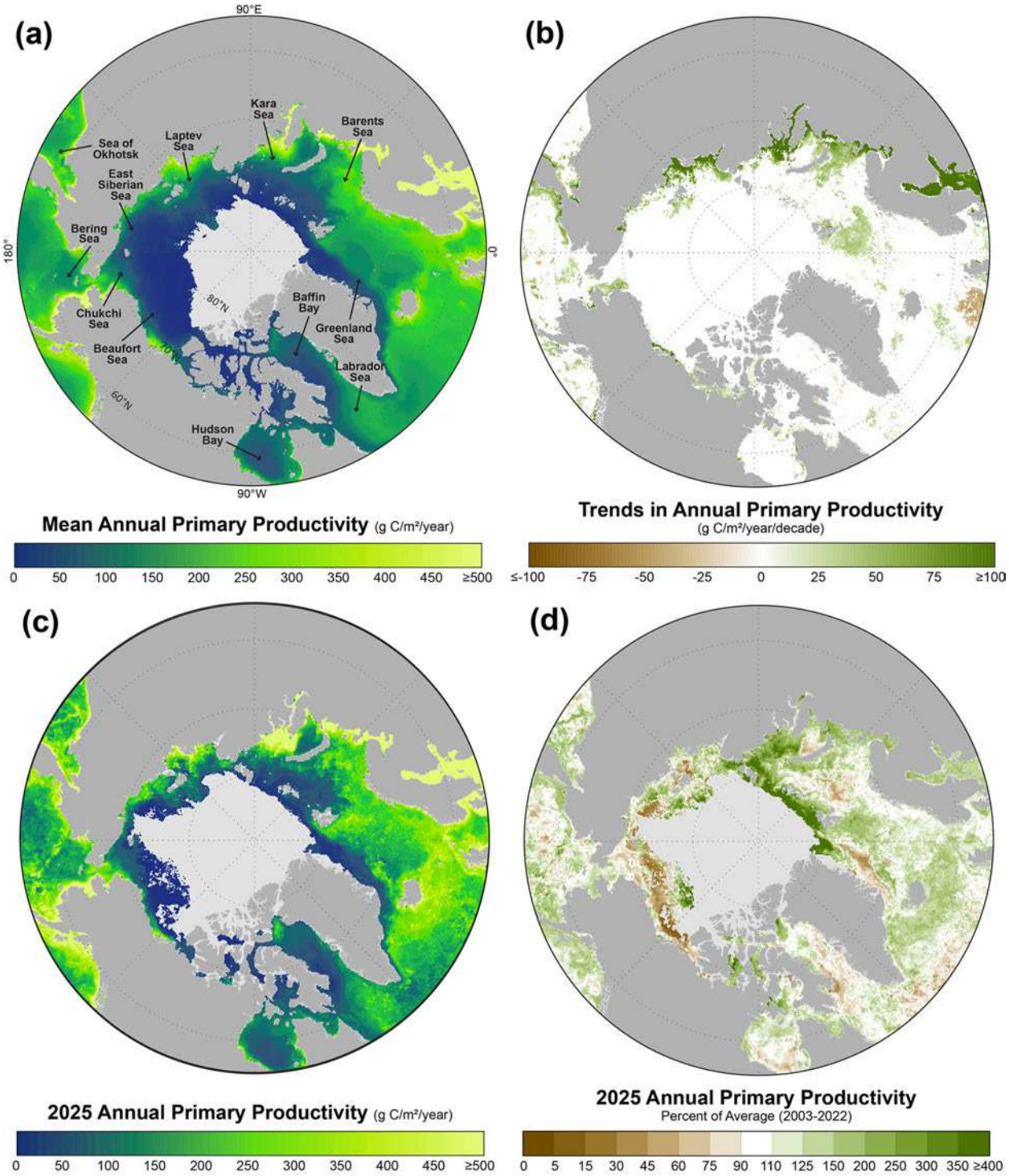

Fig. 3. For the pan-Arctic region: (a) mean annual (March-September only) primary productivity (2003-25); (b) trends in annual productivity (over 2003-25) where only those trends that are statistically significant (p<0.05) are shown; (c) annual primary productivity for 2025 only; and (d) 2025 annual primary productivity anomalies (shown as a percent of the 2003-22 average). In a, c, and d, light gray indicates no data owing to the presence of sea ice. Additional information regarding these data can be found in Table 1. September 2025 chlorophyll-*a* data (inputs into the primary productivity algorithm) were only available as Near Real Time (not final) data at the timing of this publication. See *Methods and data* section for details of how primary productivity was calculated.

Overall estimates of ocean primary productivity in 2025 for nine regions and across the Northern Hemisphere (relative to the 2003-22 reference period) were assessed (Fig. 4, Table 1). The Eurasian Arctic region includes the Kara, Laptev, and East Siberian Seas. The Amerasian Arctic region includes the Chukchi Sea, Beaufort Sea, and Canadian Archipelago. The North Atlantic region is confined between ~45-55° N. Our results show above-average primary productivity for 2025 in eight of the nine regions assessed, with only the Amerasian Arctic exhibiting lower-than-average values (Fig. 4, Table 1). Positive trends in primary productivity continued in all regions (except for the Amerasian Arctic) during the 2003-25 period. Those trends that are statistically significant (p<0.05) occurred in six of the nine regions: Eurasian Arctic (80.2% increase), Sea of Okhotsk (24.4% increase), Bering Sea (26.3% increase), Barents Sea (33.8% increase), Hudson Bay (27.1% increase), and Baffin Bay/Labrador Sea (10.4% increase). Annual net primary production was also calculated for the Arctic region, defined as 60-90° N (Fig. 5), which shows a trend over the 2003-25 time period of 21.6 Tg C/yr (Mann-Kendall significance p<0.0001). The percent increase over the 23-year time series is estimated to be 30.5%. In summary, while observations of primary productivity show complex interannual and spatial patterns over the 2003-25 period, we continue to observe overall positive trends across most Arctic regions.

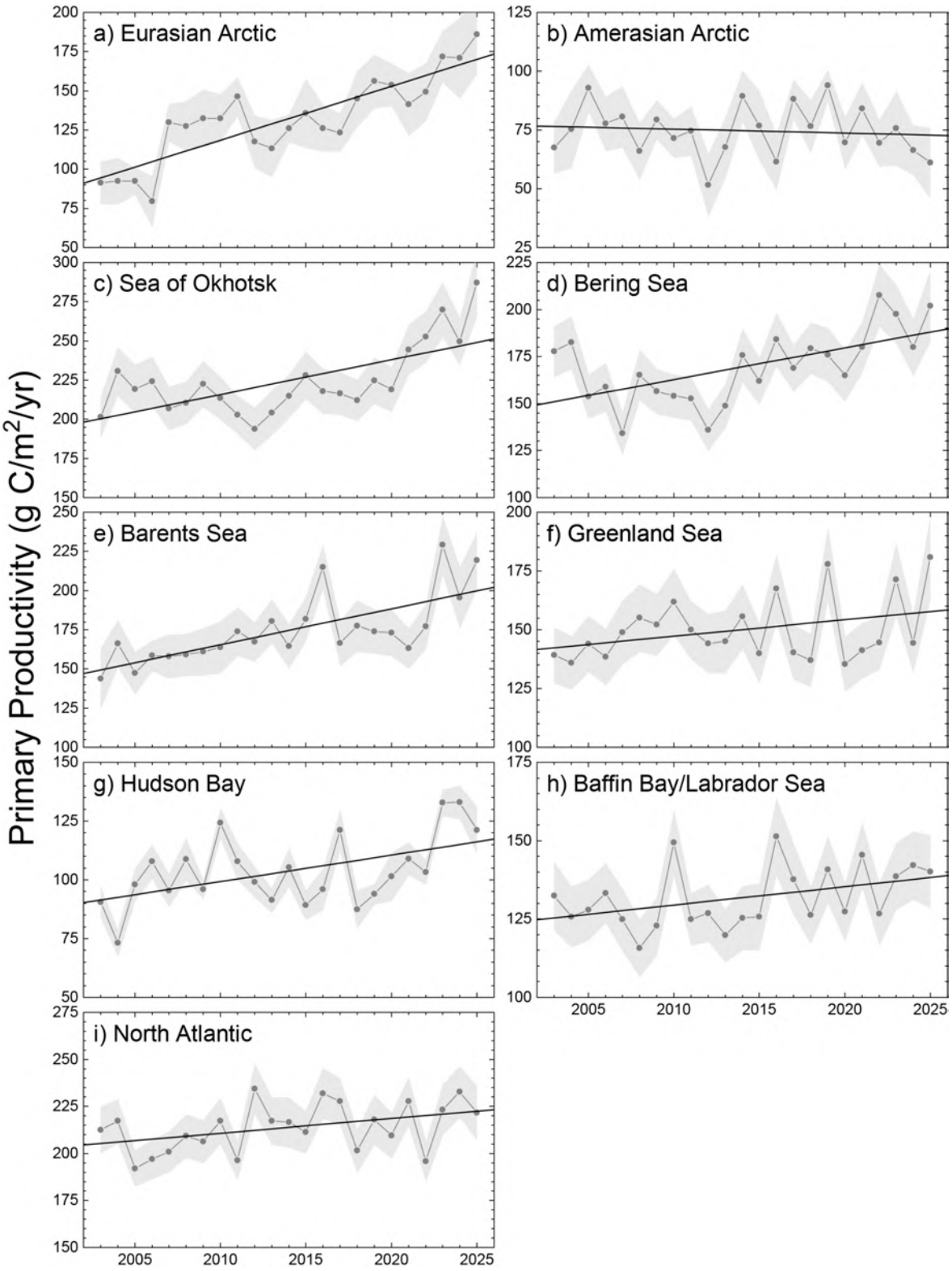

Fig. 4. Primary productivity (2003-25, March-September only) in nine different regions of the Northern Hemisphere (for a definition of the regions see Comiso 2015). The statistical significance of the trends (based on the Mann-Kendall test), *p*-values, and additional information regarding these data can be found in Table 1. September 2025 chlorophyll-*a* data (inputs into the primary productivity algorithm) were only available as Near Real Time (not final) data at the timing of this publication. See *Methods and data* section for primary productivity calculation details.

Table 1. Linear trends, statistical significance, and percent change in primary productivity (2003-25) and primary productivity anomalies for 2025 (March-September) in the nine regions as shown in Fig. 4. Values in bold are statistically significant (p<0.05) using the Mann-Kendall test for trend. The percentage change was estimated from the linear regression of the 23-year time series. The units for the Total Arctic differ because they represent annual net primary production across the Arctic (60-90° N) (as shown in Fig. 5) rather than average regional production rates (as shown in Fig. 4). September 2025 chlorophyll-*a* data (inputs into the primary productivity algorithm) were only available as Near Real Time (not final) data at the timing of this publication.

Region	**2003-25** Trend (g C/m^2/yr/ decade)	**2003-25** Mann-Kendall p-value	**2003-25** % Change	**2025** Anomaly (g C/m^2/yr) from the 2003-22 reference period	**2025** Primary Productivity (% of the 2003-22 average)
Eurasian Arctic	**34.40**	<0.0001	80.2	60.52	148.2
Amerasian Arctic	-1.03	0.566	-3.0	-8.60	88.6
Sea of Okhotsk	**22.19**	0.004	24.4	69.05	131.7
Bering Sea	**17.97**	0.005	26.3	46.53	128.0
Barents Sea	**22.93**	<0.0001	33.8	50.64	130.0
Greenland Sea	7.27	0.172	11.2	35.71	124.2
Hudson Bay	**11.24**	0.039	27.1	21.28	121.3
Baffin Bay/Labrador Sea	**5.93**	0.044	10.4	10.18	107.8
North Atlantic	7.85	0.050	8.4	9.67	104.6
Total Arctic (>60° N)	**21.6***	<0.0001	30.5	478.90**	127.3

*units are Tg C/yr; **units are Tg C

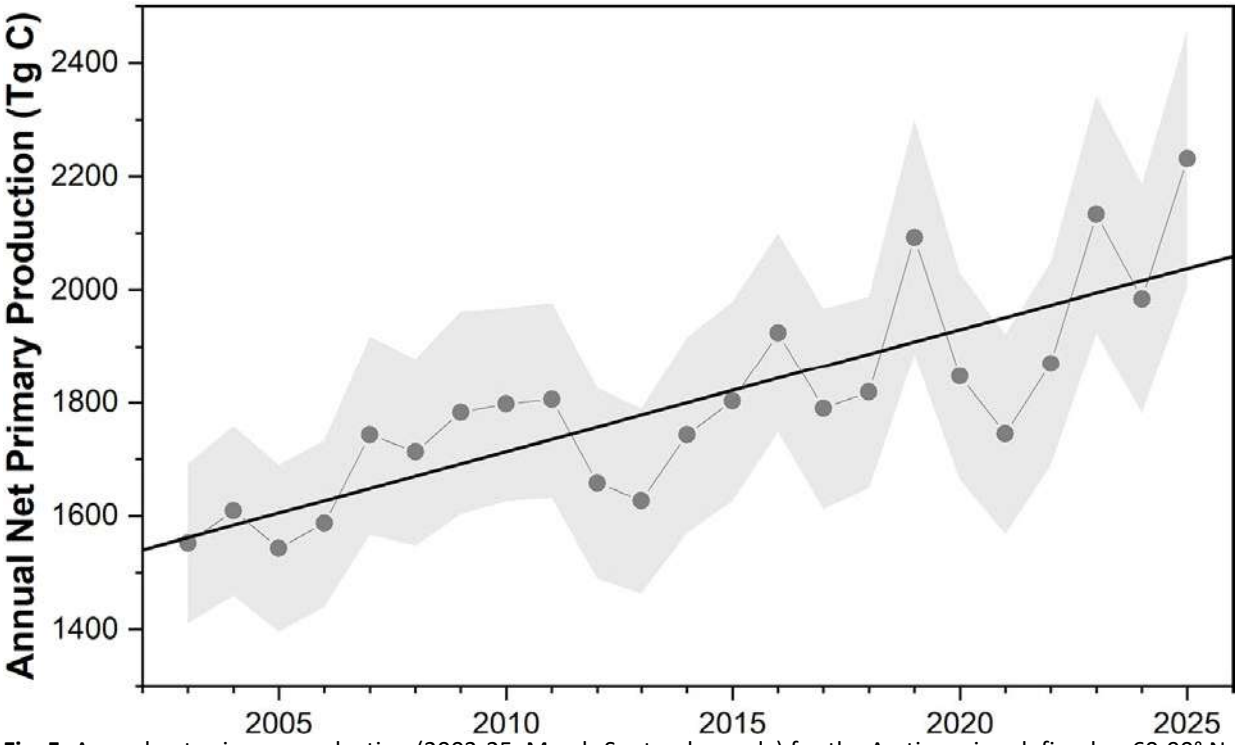

Fig. 5. Annual net primary production (2003-25, March-September only) for the Arctic region defined as 60-90° N. The trend over the 2003-25 time period is 21.6 Tg C/yr. The percentage change estimated from the linear regression over the 23-year time series is 30.5%. September 2025 chlorophyll-*a* data (inputs into the primary productivity algorithm) were only available as Near Real Time (not final) data at the timing of this publication. See *Methods and data* section for primary productivity calculation details.

Methods and data

Measurements of the algal pigment chlorophyll (specifically, chlorophyll-*a*) serve as a proxy for algal biomass present in the ocean as well as overall plant health. The complete, updated MODIS-Aqua satellite record of chlorophyll-*a* concentrations within northern polar waters for the years 2003-25 serves as a time-series against which individual years can be compared. Satellite-based chlorophyll-*a* data across the pan-Arctic region were derived using the MODIS-Aqua Reprocessing 2022.0.2 (November 2024) chlor_a algorithm: https://oceancolor.gsfc.nasa.gov/. For this report, we show mean monthly chlorophyll-*a* concentrations calculated as a percentage of the 2003-22 average. This same reference period (2003-22) has been utilized for the last three consecutive Arctic Ocean Primary Productivity Arctic Report Card essays (i.e., Frey et al. 2023b; Frey et al. 2024; *this essay*) ever since the MODIS-Aqua satellite record accrued 20 years of data. Satellite-based sea ice concentrations were derived from the Special Sensor Microwave/Imager (SSM/I) and Special Sensor Microwave Imager/Sounder (SSMIS) passive microwave instruments, calculated using the Goddard Bootstrap (SB2) algorithm (Comiso et al. 2017). Primary productivity data were derived using chlorophyll-*a* concentrations from MODIS-Aqua data (Reprocessing 2022.0.2, chlor_a algorithm), the NOAA 1/4° daily Optimum Interpolation Sea Surface Temperature dataset (or daily OISST), incident solar irradiance, mixed layer depths, and additional parameters. Primary productivity values were calculated based on the Vertically Generalized Production Model (VGPM) algorithm described by Behrenfeld and Falkowski (1997) as applied by Frey et al. (2023a). We included only pixels with less than 10% sea ice concentration, balancing ice contamination concerns against capturing the productive sea ice-edge. We define annual productivity as productivity over the March-September period. The 2025 annual primary

productivity percent of average (compared to 2003-22) was calculated the same way as for chlorophyll-*a*, as described above. Spatial trends of primary productivity (Fig. 3b) were calculated using a Theil-Sen median trend estimator, and regional (and total Arctic) linear trends/percent change (Table 1, Figs. 4 and 5) were calculated through ordinary least squares regression. The statistical significance of all trends (p<0.05) was determined using the Mann-Kendall trend test. The MODIS-Aqua Reprocessing 2022.0.2 (https://oceancolor.gsfc.nasa.gov/data/reprocessing/r2022.0.2/aqua/) that took place in November 2024 includes revised data from 2022-present in response to satellite orbital shifts and resulting declines in data accuracy. As such, values and trends shown in our time series analyses this year (e.g., Table 1, Figs. 1, 3, 4, and 5) are updated from previous Arctic Report Card essays based on these newly revised data for 2022 onwards.

Importantly, our estimates exclude sea ice algae and under-ice phytoplankton blooms, which can be significant (Ardyna et al. 2020). Furthermore, it is known that satellite observations can underestimate production under stratified conditions when a deep chlorophyll maximum is present. The variable distribution of sediments and CDOM (owing to riverine delivery, coastal erosion, and sea ice dynamics) can also affect the accuracy of satellite-based estimations of chlorophyll-*a* and primary productivity in Arctic waters (Lewis and Arrigo 2020; Zoffoli et al. 2025). As such, in-situ observations continue to provide important overall context for changes to and drivers of primary productivity across Arctic marine ecosystems. This is particularly relevant given the vulnerabilities of satellite systems to finite temporal extents where in-situ observations can help to accurately dovetail data from different satellite platforms.

Acknowledgments

K. Frey acknowledges financial support from the U.S. National Science Foundation (NSF) Arctic Observing Network (AON) Program (Grants 1917434 and 2336480). Support for J. Grebmeier and L. Cooper was provided through NSF AON (Grant 1917469) and the NOAA Global Ocean Monitoring and Observing, Arctic Research Program (CINAR 22309.07_UMCES_Grebmeier). 2025 Near Real Time Goddard Bootstrap (SB2) sea ice concentrations were provided by Angela Bliss (Cryospheric Sciences Laboratory, NASA Goddard Space Flight Center).

References

Anderson, D. M., and Coauthors, 2022: Harmful algal blooms in the Alaskan Arctic: An emerging threat as the ocean warms. *Oceanography*, **35**(3/4), 130-139, https://doi.org/10.5670/oceanog.2022.121.

Ardyna, M., and Coauthors, 2020: Under-ice phytoplankton blooms: Shedding light on the “invisible” part of Arctic primary production. *Front. Mar. Sci.*, **7**, 608032, https://doi.org/10.3389/fmars.2020.608032.

Behrenfeld, M. J., and P. G. Falkowski, 1997: Photosynthetic rates derived from satellite-based chlorophyll concentration. *Limnol. Oceanogr.*, **42**(1), 1-20, https://doi.org/10.4319/lo.1997.42.1.0001.

Castagno, A. P., T. J. W. Wagner, M. R. Cape, C. W. Lester, E. Bailey, C. Alves-de-Souza, R.A. York, and A. H. Fleming, 2023: Increased sea ice melt as a driver of enhanced Arctic phytoplankton blooming. *Glob. Change Biol.*, **29**(17), 5087-5098, https://doi.org/10.1111/gcb.16815.

Comiso, J. C., 2015: Variability and trends of the global sea ice cover and sea level: Effects on physicochemical parameters. *Climate Change and Marine and Freshwater Toxins*, L. M. Botana, M. C. Lauzao, and N. Vilarino, Eds., De Gruyter, Berlin, Germany, https://doi.org/10.1515/9783110333596-003.

Comiso, J. C., W. N. Meier, and R. Gersten, 2017: Variability and trends in the Arctic Sea ice cover: Results from different techniques. *J. Geophys. Res.-Oceans*, **122**, 6883-6900, https://doi.org/10.1002/2017JC012768.

Frey, K. E., J. C. Comiso, L. W. Cooper, C. Garcia, J. M. Grebmeier, and L. V. Stock, 2023b: Arctic ocean primary productivity: The response of marine algae to climate warming and sea ice decline. *Arctic Report Card 2023*, R. L. Thoman, T. A. Moon, and M. L. Druckenmiller, Eds., https://doi.org/10.25923/nb05-8w13.

Frey, K. E., J. C. Comiso, L. V. Stock, L. N. C. Young, L. W. Cooper, and J. M. Grebmeier, 2023a: A comprehensive satellite-based assessment across the Pacific Arctic Distributed Biological Observatory shows widespread late-season sea surface warming and sea ice declines with significant influences on primary productivity. *PLoS ONE*, **18**(7), e0287960, https://doi.org/10.1371/journal.pone.0287960.

Frey, K. E., L. V. Stock, C. Garcia, L. W. Cooper, and J. M. Grebmeier, 2024: Arctic ocean primary productivity: The response of marine algae to climate warming and sea ice decline. *Arctic Report Card 2024*, T. A. Moon, M. L. Druckenmiller, and R. L. Thoman, Eds., https://doi.org/10.25923/9ex0-t425.

Huntington, H. P., and Coauthors, 2022: Societal implications of a changing Arctic Ocean. *Ambio*, **51**, 298-306, https://doi.org/10.1007/s13280-021-01601-2.

Koch, C. W., and Coauthors, 2023: Year-round utilization of sea ice-associated carbon in Arctic ecosystems. *Nat. Commun.*, **14**, 1964, https://doi.org/10.1038/s41467-023-37612-8.

Lewis, K. M., and K. R. Arrigo, 2020: Ocean color algorithms for estimating chlorophyll *a*, CDOM absorption, and particle backscattering in the Arctic Ocean. *J. Geophys. Res.- Ocean*s, **125**, e2019JC015706, https://doi.org/10.1029/2019JC015706.

Li, W. K., F. A. McLaughlin, C. Lovejoy, and E. C. Carmack, 2009: Smallest algae thrive as the Arctic Ocean freshens. *Science*, **326**, 539-539, https://doi.org/10.1126/science.1179798.

Mathew, S., J. -K. Hong, J. -H. Kim, M. Chen, and J. Hur, 2025: Terrestrial inputs of nutrients and dissolved organic carbon to the Arctic Ocean and their influence on primary production. *Mar. Environ. Res.*, **209**, 107182, https://doi.org/10.1016/j.marenvres.2025.107182.

Rantanen, M., A. Y. Karpechko, A. Lipponen, K. Nordling, O. Hyvärinen, K. Ruosteenoja, T. Vihma, and A. Laaksonen, 2022: The Arctic has warmed nearly four times faster than the globe since 1979. *Commun. Earth Environ.*, **3**, 168, https://doi.org/10.1038/s43247-022-00498-3.

Zoffoli, M. L., and Coauthors, 2025: CIAO: A machine-learning algorithm for mapping Arctic Ocean Chlorophyll-*a* from space. *Sci. Remote Sens.*, **11**, 100212, https://doi.org/10.1016/j.srs.2025.100212.

November 21, 2025

Tundra Greenness

https://doi.org/10.25923/0k84-kn78

G. V. Frost[1], M. J. Macander[1], U. S. Bhatt[2], L. T. Berner[3,4], J. J. Assmann[5], A. Bartsch[6], J. W. Bjerke[7,8], H. E. Epstein[9], B. C. Forbes[10], M. J. Lara[11,12], E. López-Blanco[13], R. Í. Magnússon[14], P. M. Montesano[15,16], C. S. R. Neigh[15], K. M. Orndahl[4], G. K. Phoenix[17], G. Schaepman-Strub[5], H. Tømmervik[7], C. Waigl[18], D. A. Walker[19], D. Yang[20], and Q. Zhou[15,21]

[1]Alaska Biological Research, Inc., Fairbanks, AK, USA
[2]Geophysical Institute, University of Alaska Fairbanks, Fairbanks, AK, USA
[3]Department of Natural Sciences, University of Alaska Southeast, Juneau, AK, USA
[4]School of Informatics, Computing and Cyber Systems, Northern Arizona University, Flagstaff, AZ, USA
[5]Department of Evolutionary Biology and Environmental Studies, University of Zurich, Zurich, Switzerland
[6]b.geos GmbH, Korneuburg, Austria
[7]Norwegian Institute for Nature Research, FRAM – High North Research Centre for Climate and the Environment, Tromsø, Norway
[8]Tromsø Arctic-Alpine Botanical Garden, The Arctic University Museum of Norway, UiT The Arctic University of Norway, Tromsø, Norway
[9]Department of Environmental Sciences, University of Virginia, Charlottesville, VA, USA
[10]Arctic Centre, University of Lapland, Rovaniemi, Finland
[11]Department of Plant Biology, University of Illinois, Urbana, IL, USA
[12]Department of Geography, University of Illinois, Urbana, IL, USA
[13]Department of Ecoscience and Arctic Research Centre, Aarhus University, Roskilde, Denmark
[14]Plant Ecology and Nature Conservation Group, Wageningen University & Research, Wageningen, Netherlands
[15]Goddard Space Flight Center, NASA, Greenbelt, MD, USA
[16]ADNET Systems, Inc., Bethesda, MD, USA
[17]School of Biosciences, University of Sheffield, Sheffield, UK
[18]International Arctic Research Center, University of Alaska Fairbanks, Fairbanks AK, USA
[19]Institute of Arctic Biology, University of Alaska Fairbanks, Fairbanks, AK, USA
[20]Environmental Sciences Division, Oak Ridge National Laboratory, Oak Ridge, TN, USA
[21]Science Systems and Applications, Inc., Lanham, MD, USA

Headlines

- In 2025, the circumpolar mean maximum tundra greenness value was the third highest in the high-resolution 26-year MODIS satellite record, continuing a sequence of record or near-record high values since 2020.
- First detected in the late 1990s, the “greening of the Arctic” is a long-term increase in the productivity and abundance of tundra vegetation that remains evident in all available long-term satellite records.

- Tundra greenness is increasing across most of the Arctic due to rapid warming, but there are many localized areas of decline that reflect disturbances such as wildfire and extreme weather events.
- Tundra greening has far-reaching impacts to Arctic landscapes, wildlife habitats, biodiversity, permafrost conditions, and the livelihood of Arctic people, with implications for global climate and the carbon cycle.

Introduction

Earth's northernmost continental landmasses and island archipelagos are home to the Arctic tundra biome, which collectively encompasses a 5.1 million km^2 region bounded by the Arctic Ocean to the north and the boreal forest biome to the south (Raynolds et al. 2019). While Arctic tundra ecosystems are treeless and lack the vertical structure of forests, they present rich variation across spatial scales, reflecting both broad latitudinal climate gradients as well as landscape-scale differences in soil, hydrology, permafrost conditions, wildlife habitat use, and more (Fig. 1). For thousands of years, Arctic ecosystems have accumulated large amounts of carbon, as cold temperatures greatly slow decomposition and a large proportion of vegetation biomass becomes preserved in permafrost. In recent decades, the Arctic has warmed dramatically (see essay *Surface Air Temperature*), far exceeding the global rate of warming and placing the circumpolar region at the forefront of global climate and environmental change. Today, the circumpolar region lies at the crossroads of multiple feedback mechanisms that connect the living Arctic with a warming climate, declining nearshore sea ice, changing seasonal snow cover, thawing permafrost soils that contain large amounts of carbon, and industrial development (Bartsch et al. 2025; Vonk et al. 2025). Some of the most compelling evidence of broad-scale changes in this remote region comes from long-term satellite observations that began in 1982. By the late 1990s, Earth-observing satellites began to detect a sharp increase in the productivity of tundra vegetation, a phenomenon known today as "the greening of the Arctic."

Fig. 1. The composition and structure of tundra vegetation varies depending on landscape characteristics as well as climate. Tundra shrubs tend to be prominent in riverine corridors and well drained upland landscapes (upper left; Seward Peninsula, Alaska). Coastal tundra supports highly productive herbaceous vegetation that, in turn, supports large concentrations of migratory waterbirds (upper right; Baldwin Peninsula, Alaska). Living vegetation plays a critical role in protecting underlying permafrost, but permafrost disturbances can abruptly transform the land surface (lower left; thermo-erosional gully, Seward Baldwin Peninsula, Alaska). Field studies are crucial to determining the drivers and consequences of Arctic greening (lower right, northeastern Greenland). Alaska photos credit G. V. Frost, Greenland photo credit J. J. Assmann.

Spaceborne monitoring of tundra greenness

The earliest consistent spaceborne record of Arctic vegetation began in 1982 with the launch of the Advanced Very High Resolution Radiometer (AVHRR) sensor; however, funding for the AVHRR-derived Global Inventory Modeling and Mapping Studies 3g V1.2 dataset (GIMMS-3g+), which long underpinned reports of Arctic greening, ceased in 2025 after 43 years of record (see essay *Assessing the State of the Arctic Observing Network*). At present, the Moderate Resolution Imaging Spectroradiometer (MODIS) and the Landsat series of satellites provide the longest active spaceborne records of tundra greenness. MODIS is nearing the end of its service life, but continuity of this important record will be maintained by its successor, the Visible Infrared Imaging Radiometer Suite (VIIRS). All of these instruments monitor vegetation greenness using the Normalized Difference Vegetation Index (NDVI), a spectral metric of plant biomass that exploits the unique way in which green vegetation absorbs and reflects visible and near-infrared light. We summarize greenness observations for each growing season by calculating the

Maximum NDVI (MaxNDVI), representing vegetation biomass at the height of the Arctic summer, typically during July and August.

All three long-term records show increasing annual maximum tundra greenness (MaxNDVI) across most of the circumpolar Arctic during 1982-2024 (GIMMS-3g+) and 2000-25 (MODIS and Landsat), respectively (Fig. 2). MODIS (Fig. 3a), GIMMS-3g+ (Fig. 3b), and Landsat (not shown) all display widespread greening trends in continental Eurasia and North America, except for portions of southwestern Alaska, and central and northeastern Siberia where flat or negative ("browning") trends are evident. Trends in the Canadian Arctic Archipelago are somewhat mixed, which may be partly due to different observational periods among sensors, as well as observational challenges posed by the very short growing season, persistent cloudiness, and high interannual variability in snowmelt and surface water in High Arctic environments (Zemlianskii et al. 2025). Regional contrasts in greening highlight the complexity of Arctic change and the rich web of interactions that exist between tundra ecosystems and the local properties of sea ice (see essay *Sea Ice*), permafrost, seasonal snow (see essay *Terrestrial Snow Cover*), soil composition and moisture, microtopography, disturbance processes, wildlife, and human activities (Frost et al. 2025). Understanding the underlying drivers of complex Arctic trends is important for improved monitoring and prediction of tundra ecosystem functions and the consequences of Arctic change on the global carbon cycle.

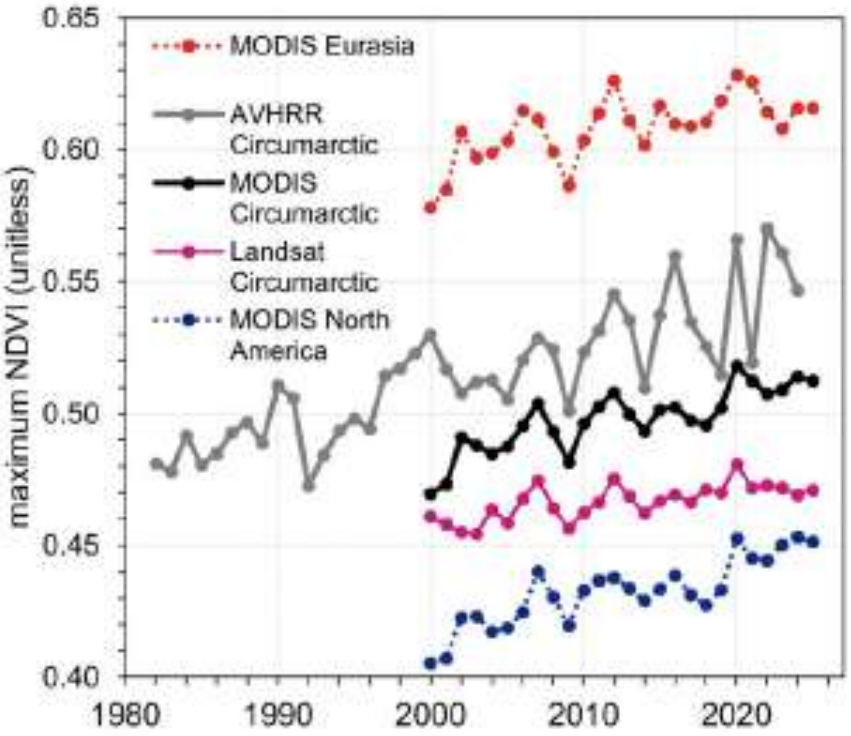

Fig. 2. Time-series of mean MaxNDVI for Arctic tundra from the MODIS MCD13A1 v6.1 (2000-25) dataset for the Eurasian Arctic (red), North American Arctic (blue), and the circumpolar Arctic (black), and from the Landsat Collection 2 (2000-25; pink) and AVHRR GIMMS-3g+ (1982-2024; gray) datasets.

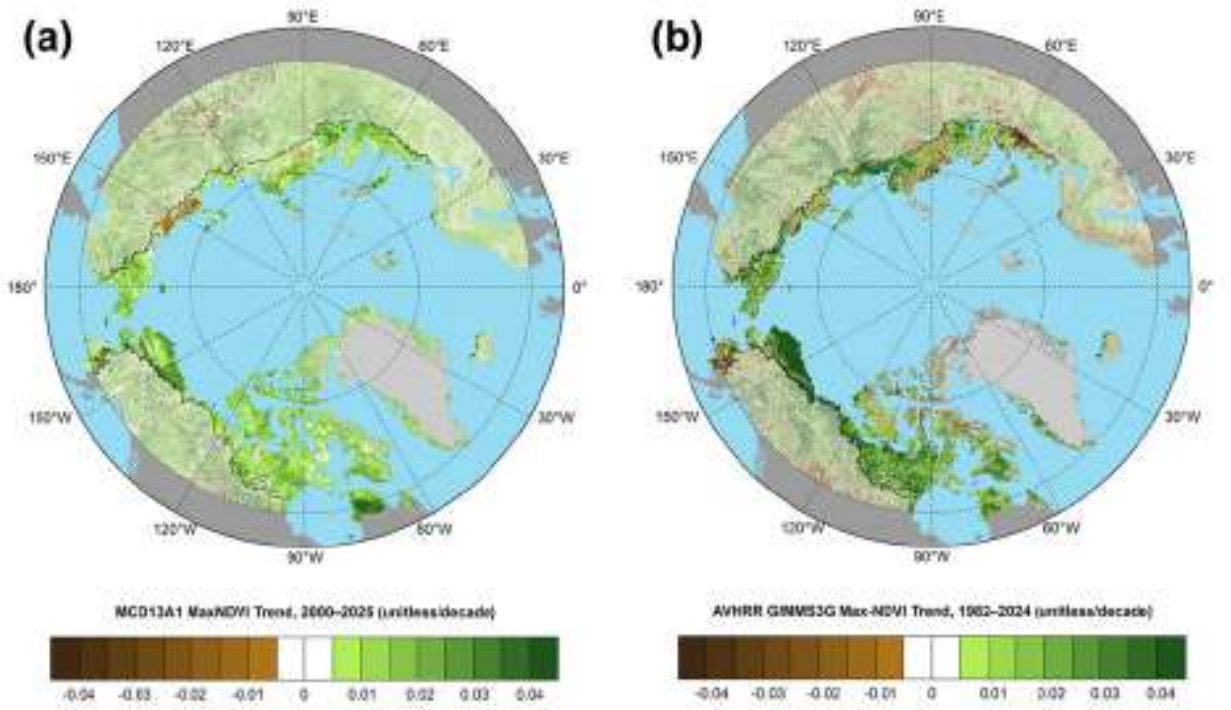

Fig. 3. Magnitude of the MaxNDVI trend calculated as the change per decade using ordinary least squares regression for Arctic tundra (solid colors), and boreal forest north of 60° latitude (muted colors) during (a) 2000-25 based on the MODIS MCD13A1 v6.1 dataset, and (b) 1982-2024 based on the no longer active AVHRR GIMMS 3-g+ dataset.

The neighboring boreal forest biome (see Fig. 3) occupies large swaths of northern Eurasia and North America and has also emerged as a focal point of global environmental change. Patches of positive and negative greenness trends are widely interspersed, reflecting the biome's active disturbance regime and differential responses of boreal forests as a function of latitude. Browning has generally prevailed in the warmer southern boreal zone, where warming temperatures have promoted drought-stress and increased wildfire; however, greening has been widespread in colder parts of the biome along the northern forest-tundra ecotone (Berner and Goetz 2022).

In 2025, the MODIS-observed circumpolar average MaxNDVI value was nearly identical (-0.2%) compared to 2024 and represents the third highest value in the 26-year record for that sensor. This continued a sequence of record or near-record high values that began in 2020, with the five highest MaxNDVI values in the 26-year MODIS record being observed since that year. Tundra greenness was much higher than normal across most of the North American Arctic, particularly in northern Alaska, Quebec, and Labrador (Fig. 4). The Eurasian Arctic, however, featured a mixture of positive and negative departures from normal, a pattern that has recurred for the last several years. Nonetheless, the long-term trend in MODIS-observed tundra greenness is strongly positive (greening) for most of the circumpolar region. The last circumpolar average MaxNDVI value from GIMMS-3g+ in 2024 was the fifth highest in the 43 years of record for that sensor; although no longer maintained, this dataset provides the most unequivocal signal of long-term Arctic greening, with four of the five highest MaxNDVI values in the 43-year record all observed since 2020 (Fig. 2).

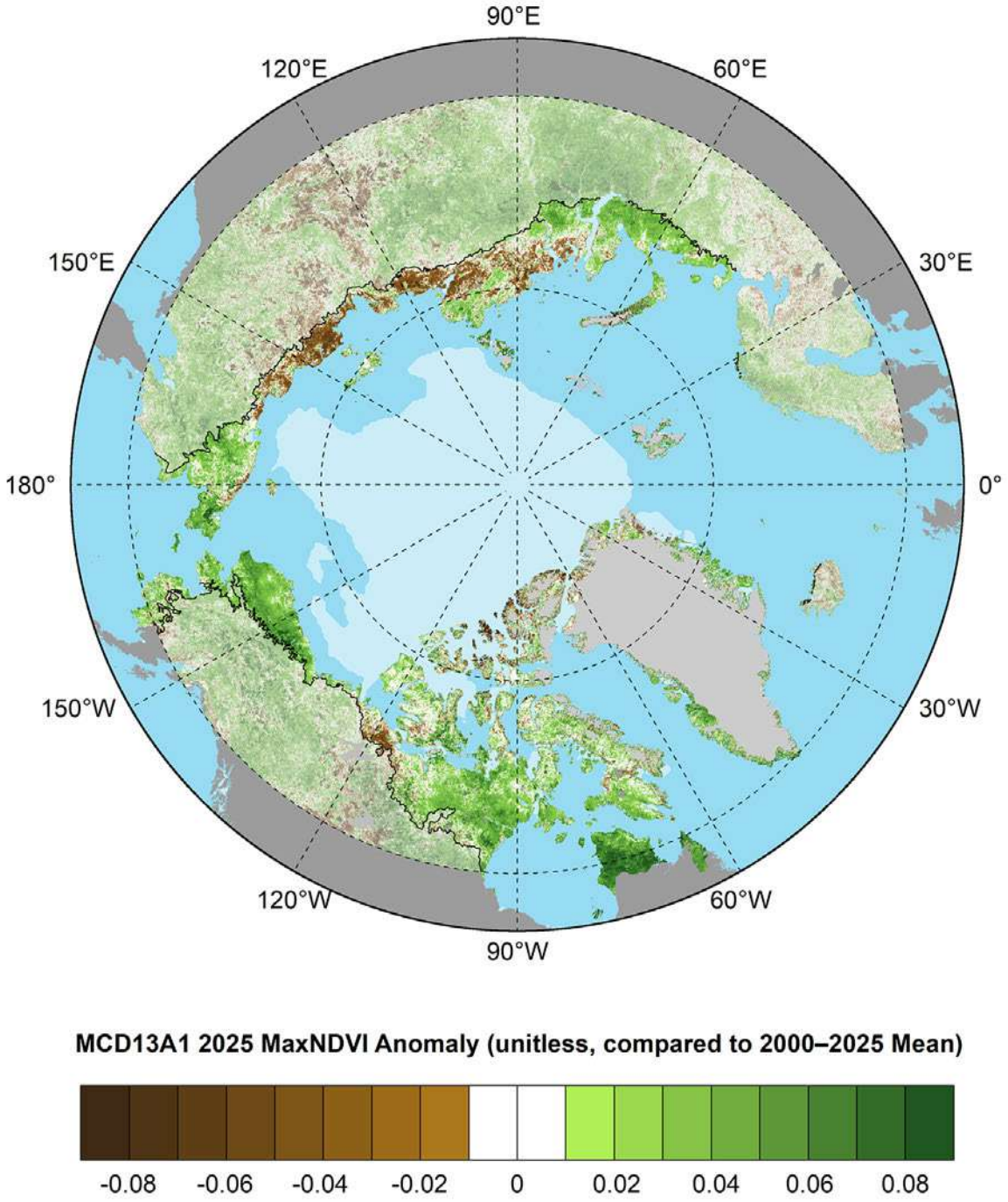

Fig. 4. Circumpolar MaxNDVI anomalies for the 2025 growing season for Arctic tundra (solid colors) and boreal forest north of 60° latitude (muted colors) relative to mean values (2000-25) from the MODIS MCD13A1 v6.1 dataset. The 2025 mean August sea-ice extent is indicated by light shading.

Drivers and consequences of Arctic greening

Earth-observing satellites provide foundational datasets for monitoring Arctic environmental change and help to overcome the long-standing access barriers posed by the region's remoteness, as well as new

ones arising from the cessation of international cooperation in the Russian Arctic and cutbacks in funding and logistical support for Arctic research and spaceborne monitoring capabilities in the United States and the European Union. Nonetheless, field studies provide crucial information needed to connect spaceborne observations with patterns and drivers of change (or stability) on the ground. Increases in the abundance, distribution, and height of Arctic shrubs are a major component of Arctic greening (Frost et al. 2025). The development of taller plant canopies is particularly impactful in tundra ecosystems, with important consequences for biodiversity, seasonal snow cover, permafrost temperatures, biogeochemical cycling, forage availability for animals, and human land uses (García Criado et al. 2025; Shuman et al. 2025; Rearden and Fienup-Riordan 2014). However, while changes to the Arctic climate have generally favored greening, ecological disturbances, extreme events, and other causes of browning (a decline in productivity that is opposite to greening) are also increasing in frequency (Phoenix et al. 2025). For example, greening trends in many parts of the Arctic have been partially offset by increasing wildfires during the past two decades, and permafrost thaw can produce strong local "hotspots" of browning associated with thermokarst and changes in surface water extent (Assmann et al. 2025). Understanding the regional variability of complex Arctic greening trends and attributing its drivers continues to be a subject of multidisciplinary scientific research (Fig. 1).

Methods and data

The satellite record of Arctic tundra greenness began in 1982 using AVHRR, a sensor that collects daily observations; while this sensor continues to operate, the AVHRR-derived Global Inventory Modeling and Mapping Studies 3g V1.2 dataset (GIMMS-3g+) (Pinzon et al. 2023) that long underpinned Arctic greenness monitoring is no longer funded after 43 years of record (1982-2024). Therefore, we also report observations from the Moderate Resolution Imaging Spectroradiometer (MODIS) and the Landsat series of satellites, which are higher spatial resolution systems that provide circumpolar greenness observations since 2000. The latter two records generally display less interannual variability in MaxNDVI than the legacy GIMMS-3g+ dataset, likely reflecting their higher spatial resolution and improved calibration (Frost et al. 2025). For MODIS, we computed tundra greenness trends for 2000-25 with a higher spatial resolution of 500 m, combining 16-day Vegetation Index products from Terra (MOD13A1, version 6.1) and Aqua (MYD13A1, version 6.1) (Didan 2021a,b), referred to here as MCD13A1. Landsat provides tundra greenness data at a much higher spatial resolution of 30 m; we computed time-series of greenness from Landsat Collection 2 (Crawford et al. 2023) using the methods of Berner and Goetz (2022). Circumpolar maps depicting greenness trends (AVHRR and MODIS only) cover the Arctic tundra biome, as well as boreal forest and non-Arctic tundra above 60° N latitude. For time-series plots, data were masked to include only ice-free land within the extent of the Circumpolar Arctic Vegetation Map (Raynolds et al. 2019). MODIS and Landsat data were further masked to exclude permanent water based on the 2015 MODIS Terra Land Water Mask (MOD44W, version 6). We summarize the GIMMS-3g+, MODIS, and Landsat records for Maximum NDVI (MaxNDVI), the peak yearly value that is typically observed during the months of July and August.

References

Assmann, J. J., C. Akandil, E. Plekhanova, A. Le Moigne, S. V. Karsanaev, T. C. Maximov, and G. Schaepman-Strub, 2025: High variation in the surface extent of freshwater ponds creates dynamic Arctic tundra landscapes in the lowlands of Eastern Siberia. *Environ. Res. Lett.*, **20**, 114041, https://doi.org/10.1088/1748-9326/ae0fb1.

Bartsch, A., and Coauthors, 2025: Similarities between sea ice area variations and satellite-derived terrestrial biosphere and cryosphere parameters across the Arctic. *Cryosphere*, **19**(10), 4929-4967, https://doi.org/10.5194/tc-19-4929-2025.

Berner, L. T., and S. J. Goetz, 2022: Satellite observations document trends consistent with a boreal forest biome shift. *Global Change Biol.*, **28**(10), 3275-3292, https://doi.org/10.1111/gcb.16121.

Crawford, C. J., and Coauthors, 2023: The 50-year Landsat collection 2 archive. *Sci. Remote Sens.*, **8**, 100103, https://doi.org/10.1016/j.srs.2023.100103.

Didan, K., 2021a: MODIS/Terra Vegetation Indices 16-Day L3 Global 500m SIN Grid V061 [Data set]. NASA EOSDIS Land Processes Distributed Active Archive Center, accessed 29 August 2023, https://doi.org/10.5067/MODIS/MOD13A1.061.

Didan, K., 2021b: MODIS/Aqua Vegetation Indices 16-Day L3 Global 500m SIN Grid V061 [Data set]. NASA EOSDIS Land Processes Distributed Active Archive Center, accessed 29 August 2023, https://doi.org/10.5067/MODIS/MYD13A1.061.

Frost, G. V., and Coauthors, 2025: The changing face of the Arctic: four decades of greening and implications for tundra ecosystems. *Front. Environ. Sci.*, **13**, 1525574, https://doi.org/10.3389/fenvs.2025.1525574.

García Criado, M., and Coauthors, 2025: Plant diversity dynamics over space and time in a warming Arctic. *Nature*, **642**, 653-661, https://doi.org/10.1038/s41586-025-08946-8.

Phoenix, G. K., and Coauthors, 2025: Browning events in Arctic ecosystems: Diverse causes with common consequences. *PLOS Climate*, **4**, e0000570, https://doi.org/10.1371/journal.pclm.0000570.

Pinzon, J. E., E. W. Pak, C. J. Tucker, U. S. Bhatt, G. V. Frost, and M. J. Macander, 2023: Global Vegetation Greenness (NDVI) from AVHRR GIMMS-3G+, 1981-2022 [Data set]. ORNL DAAC, Oak Ridge, TN, USA, https://doi.org/10.3334/ORNLDAAC/2187.

Raynolds, M. K., and Coauthors, 2019: A raster version of the Circumpolar Arctic Vegetation Map (CAVM). *Remote Sens. Environ.*, **232**, 111297, https://doi.org/10.1016/j.rse.2019.111297.

Rearden, A., and A. Fienup-Riordan, 2014: Nunamta ellamta-llu ayuqucia: What Our Land and World Are Like. Alaska Native Language Center 656pp.

Shuman, I. N. C., S. P. Serbin, A. M. Erb, C. B. Schaaf, and D. Yang, 2025: Fine-scale vegetation composition and structure shape spatiotemporal variation in surface albedo across a low Arctic tundra landscape. *Environ. Res. Ecol.*, **4**(4), 045001, https://doi.org/10.1088/2752-664X/ae04ef.

Vonk, J. E., and Coauthors, 2025: The land-ocean Arctic carbon cycle. *Nat. Rev. Earth Environ.*, **6**, 86-105, https://doi.org/10.1038/s43017-024-00627-w.

Zemlianskii, V., K. Ermokhina, N. Rietze, R. Heim, J. Assmann, J. Rüthi, N. Loginova, and G. Schaepman-Strub, 2025: Finding northernmost baselines: high variability of above-ground biomass on Eurasian polar desert islands. *Environ. Res. Ecol.*, **4**(3), 035006, https://doi.org/10.1088/2752-664X/adf447.

Glaciers and Ice Caps Outside Greenland

https://doi.org/ 10.25923/f47r-hd76

G. Wolken[1,2], D. Burgess[3], B. Wouters[4], L. M. Andreassen[5], J. Kohler[6], B. Luks[7], F. Pálsson[8], L. Thomson[9], and T. Thorsteinsson[10]

[1]University of Alaska Fairbanks, Fairbanks, AK, USA
[2]Alaska Division of Geological and Geophysical Surveys, Fairbanks, AK, USA
[3]Geological Survey of Canada, Ottawa, ON, Canada
[4]Department of Geoscience and Remote Sensing, Delft University of Technology, Delft, The Netherlands
[5]Section for Glaciers, Ice and Snow, Norwegian Water Resources and Energy Directorate, Oslo, Norway
[6]Norwegian Polar Institute, Tromsø, Norway
[7]Institute of Geophysics, Polish Academy of Sciences, Warsaw, Poland
[8]Institute of Earth Sciences, University of Iceland, Reykjavík, Iceland
[9]Queen's University, Kingston, ON, Canada
[10]Icelandic Meteorological Office, Reykjavík, Iceland

Headlines

- During the 2022/23 and 2023/24 mass balance years, Arctic glaciers and ice caps continued their widespread mass loss. Glaciers in Arctic Scandinavia and Svalbard experienced their most negative mass balance year on record in 2023/24.
- Since the mid-20th century, Arctic glaciers and ice caps have undergone relentless thinning, with long-term measurements on glaciers in Alaska showing an average of over 38 meters of water equivalent thinning, which is contributing steadily to global sea level rise.
- Ongoing glacier loss threatens Arctic communities by reducing water supplies, driving destructive floods, and increasing landslide and tsunami hazards that endanger people, infrastructure, and coastlines.

Introduction

The Arctic contains 60% of the world's mountain glaciers and ice caps by area, excluding the Greenland and Antarctic ice sheets (RGI Consortium 2023) (Fig. 1). While Arctic glaciers and ice caps' potential long-term sea level contribution is smaller than that of the Greenland and Antarctic ice sheets, they are more responsive to climate variability and have been a leading contributor to recent sea level rise due to persistent atmospheric warming (The GlaMBIE Team 2025; Hugonnet et al. 2021; Wouters et al. 2019; Box et al. 2019).

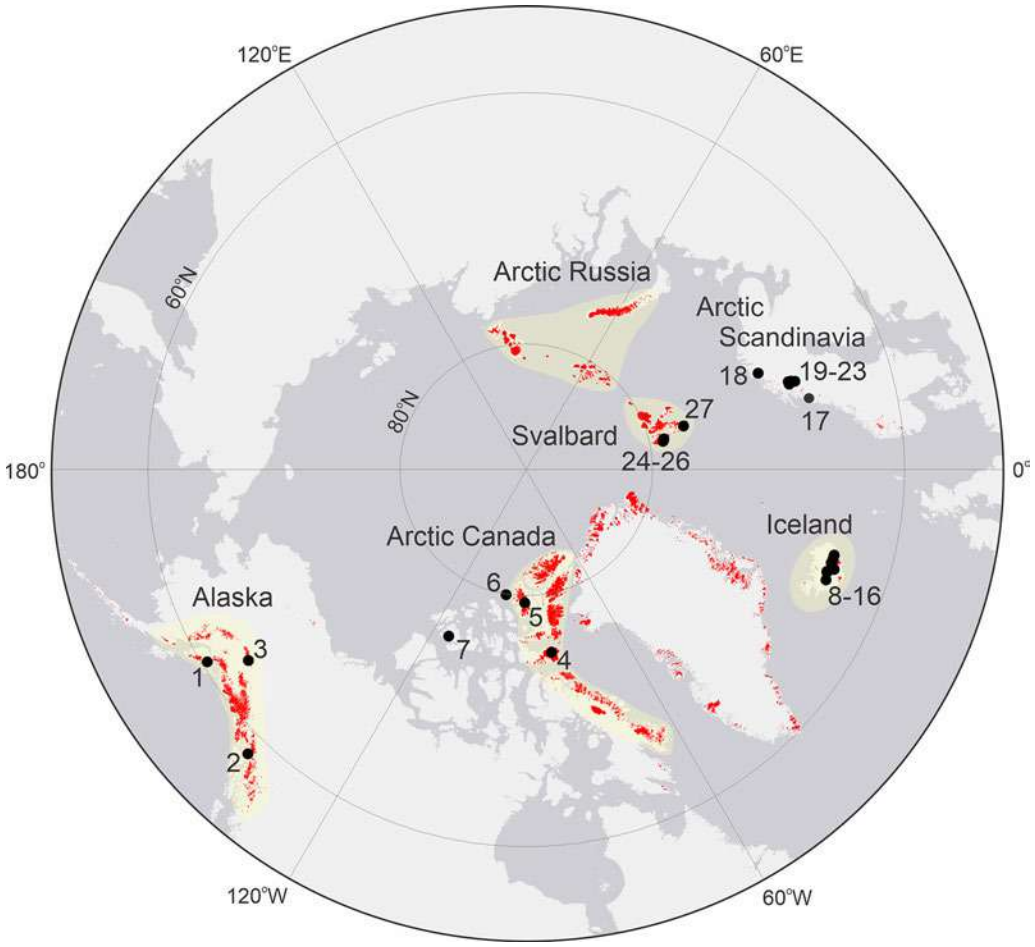

Fig. 1. Arctic glaciers and ice caps (red), including ice caps in Greenland that are separate from the ice sheet. Yellow shaded regions delineate the GRACE- and GRACE-FO-derived mass anomaly domains used to estimate changes in annual glacier mass balance for heavily glacierized Arctic regions. Black dots indicate the 27 long-term Arctic glacier monitoring sites, with numbers linked to the glacier/ice cap names in Table 1.

With amplified warming at high northern latitudes (see essay *Surface Air Temperature*; Masson-Delmotte et al. 2021), the annual mass loss of Arctic glaciers and ice caps has tripled since the mid-1990s (Zemp et al. 2019). While observations of Arctic glaciers and ice caps from balance year 2024/25 are not yet available, observations from mass balance years 2022/23 and 2023/24 highlight both regional and interannual variability, yet the overall trajectory remains one of widespread and significant ice loss.

Recent observations and regional contrasts

Mass changes in glaciers and ice caps result from the balance between inputs, primarily snow accumulation, and outputs, which include surface melt and runoff, as well as iceberg calving for tidewater- or lake-terminating glaciers. The net, or total, mass balance reflects the difference between these processes. Our analysis of the 27 monitored Arctic glaciers excludes losses from iceberg calving, which occurs only at Kongsvegen, Hansbreen, and Devon Ice Cap (Table 1; Fig. 1). Accordingly, we report the climatic mass balance (B_{clim}), the difference between annual snow accumulation and annual runoff, expressed as the mean annual thickness change (mm water equivalent, w.e.) averaged over the glacier or ice cap surface.

Table 1. Measured climatic mass balance (B_{clim}) for 25 glaciers in Alaska (3), Arctic Canada (4), Iceland (9), Svalbard (3), and Arctic Scandinavia (6) in 2022/23 and 2023/24, together with the 1991-2020 mean and standard deviation for each of the 27 monitored glaciers (* indicates one or more years of data missing from the record; – indicates no data reported). Negative (positive) values for B_{clim} indicate mass loss (gain). Numbers in left hand column correspond to glacier locations in Fig. 1.

Region	Glacier (record length, years)	Bclim Mean (mm w.e./yr) (1991-2020)	Bclim Std. Dev. (mm w.e./yr) (1991-2020)	Bclim (mm w.e./yr) (2022/23)	Bclim (mm w.e./yr) (2023/24)
Alaska					
1	Wolverine(59)	-770	984	-1090	-700
2	Lemon Creek(72)	-1195	839	-2360	-1120
3	Gulkana(59)	-767	817	-400	-380
Arctic Canada					
4	Devon Ice Cap(64)	-257	215	-377	-158
5	Meighen Ice Cap(63)	-326	422	-615	-442
6	Melville S. Ice Cap(62)	-458	487	-1482	-300
7	White(62)	-341	323	-653	-452
Iceland					
8	Langjökull S. Dome(28)	-1248	842*	-1430	-1005
9	Hofsjökull E(36)	-980	840	-1210	-880
10	Hofsjökull N(37)	-824	706	-1070	-980
11	Hofsjökull SW(36)	-956	951	-690	-480
12	Köldukvislarjökull(33)	-467	708*	-740	-80
13	Tungnaarjökull(33)	-1142	781*	-1529	-1370
14	Dyngjujökull(27)	-44	792*	-308	-50
15	Brúarjökull(32)	-238	622*	-713	-60
16	Eyjabakkajökull(33)	-700	766*	-1417	-510
Arctic Scandinavia					
17	Engabreen(55)	-62	972	-1101	-3855
18	Langfjordjokelen(34)	-953	771*	-1651	-4060
19	Marmaglaciaren(34)	-494	568*	-1256	-2573
20	Rabots(41)	-533	648*	-1565	-2804
21	Riukojietna(36)	-701	734*	-1347	-3458
22	Storglaciaren(79)	-235	747	-812	-2846
23	Tarfalaglaciaren(20)	-331	1170*	-	-
Svalbard					
24	Midre Lovenbreen(57)	-497	407	-972	-1955
25	Austre Broggerbreen(58)	-618	450	-948	-2048
26	Kongsvegen(38)	-146	404	-673	-1491
27	Hansbreen(33)	-419	470	-	-

In the 2023/24 balance year (October 2023 to September 2024), all 25 of the monitored glaciers for which we have data (i.e., data were not available for 2 of the 27) recorded negative mass balances,

consistent with the 2022/23 balance year (Table 1; WGMS 2025). This decline was most severe in Arctic Scandinavia and Svalbard, which experienced a precipitous drop in land ice since 2021. Both regions had their most negative mass balance year on record in 2023/24 (Kjøllmoen et al. 2025; Schuler et al. 2025), with melt increasing by an average of 1486% in Arctic Scandinavia and 482% in Svalbard relative to the 1991-2020 mean. This enhanced melt coincided with a persistent warm air mass over northern Scandinavia and the Barents Sea that produced record high seasonal temperatures since 1950 (Ballinger et al. 2024).

This dramatic thinning is underscored by data from monitored Arctic glaciers. For example, Arctic Scandinavia's Langfjordjokelen and Engabreen saw their climatic mass balances decrease, respectively, from -1651 and -1101 mm w.e. in 2022/23 to -4060 and -3855 mm w.e. in 2023/24. Similarly, Svalbard's Midre Lovenbreen and Austre Broggerbreen went from -972 and -948 mm w.e. to -1955 and -2048 mm w.e. during the same period. While Alaska, Arctic Canada, and Iceland also showed negative anomalies in 2022/23, with melt increases of 30%, 112%, and 115%, respectively, they experienced less melt (i.e., positive anomalies) in 2023/24 relative to the 1991-2020 mean.

Long-term mass loss and global contribution

Observations from the 2023/24 balance year confirm the ongoing multi-decadal trend of surface mass loss for glaciers and ice caps across the Arctic (Fig. 2). Since the mid-20th century, long-term records show that Alaska's glaciers have experienced the greatest thinning, exceeding 38 m w.e. by 2024. Arctic Scandinavia follows with over 32 m w.e. of loss, while Iceland and Svalbard have also undergone significant cumulative thinning of 29 m w.e. and 27 m w.e., respectively. Arctic Canada has lost 16 m w.e. These widespread negative balances further demonstrate that these glaciers are highly sensitive to climate warming and are significant contributors to sea-level rise (Box et al. 2018).

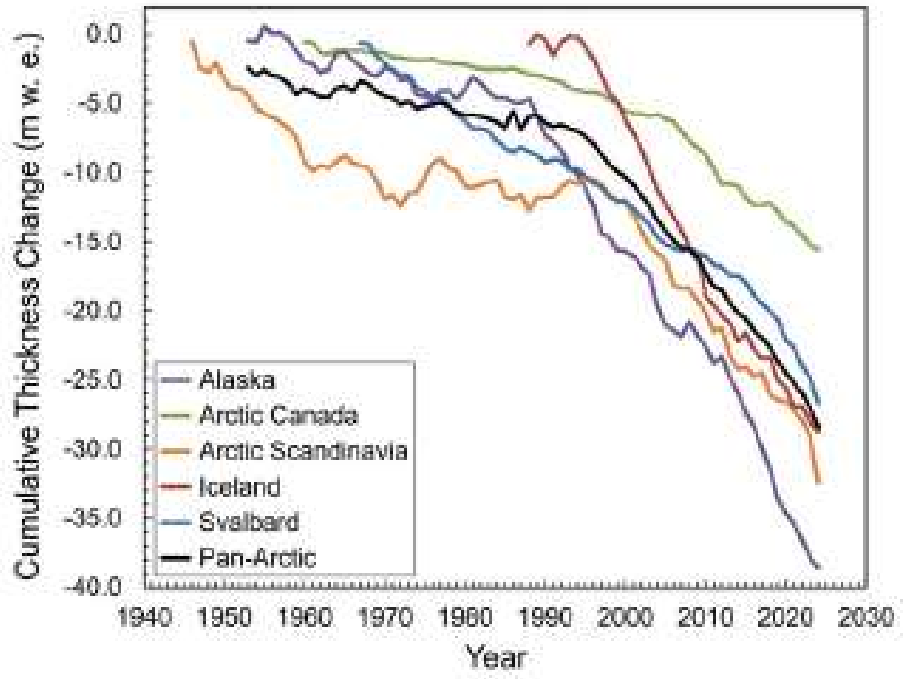

Fig. 2. Cumulative B_{clim} in meters of water equivalent (m w.e.) for 27 monitored glaciers in 5 Arctic regions and for the Arctic as a whole (Pan-Arctic mean). Note the variable time periods over which cumulative changes are measured.

Gravity anomaly measurements from the combined GRACE (2002-16) and GRACE-FO (2018-25) satellite missions show that Pan-Arctic glaciers and ice caps lost mass at an average rate of -181 ± 21 Gt per year since 2002 (Figs. 1 and 3). This loss corresponds to a contribution of 0.55 ± 0.06 mm per year to global mean sea level rise. Although the magnitude of change varies by region, all records exhibit a persistent downward trend, highlighting the widespread and ongoing retreat of Arctic glaciers and ice caps outside Greenland.

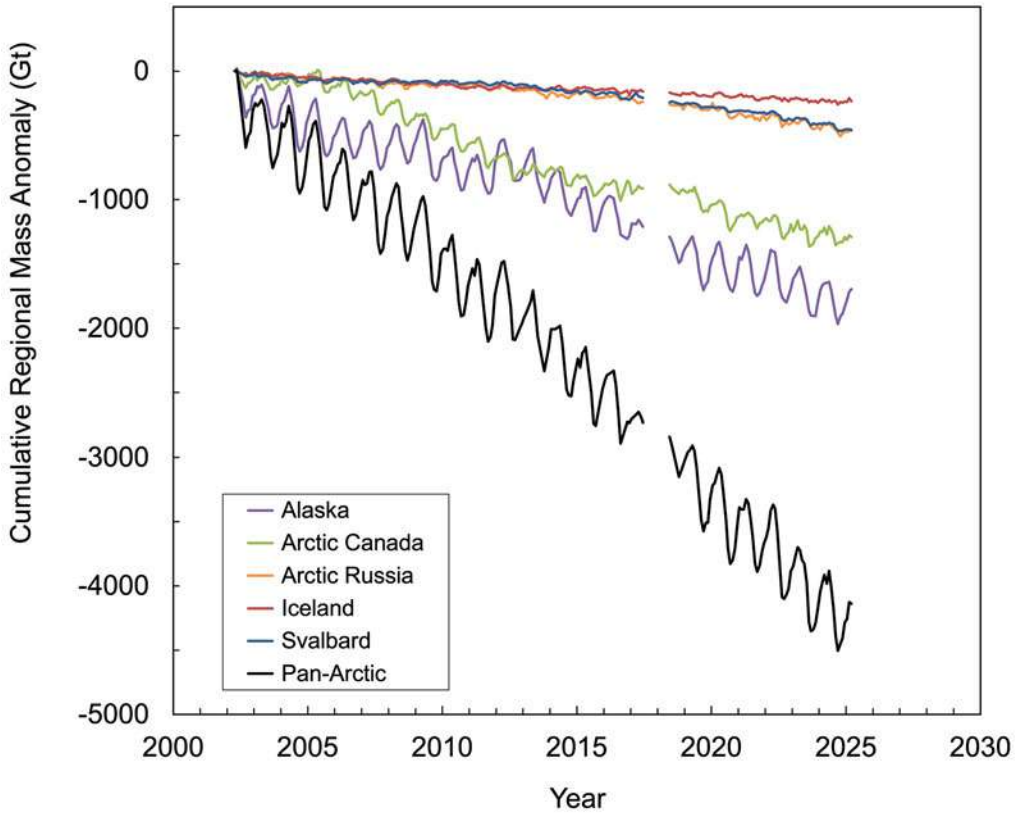

Fig. 3. Cumulative changes in regional total stored water (Gt) for 2002-25 derived from GRACE and GRACE-FO satellite gravimetry for the five regions shown in Fig. 1 and for the total of these five regions (Pan-Arctic). An instrumental data gap exists for July 2017 to May 2018.

During the 2023/24 balance year, Pan-Arctic glaciers and ice caps lost -151 ± 20 Gt of mass, contributing 0.42 ± 0.06 mm to global mean sea level rise. Regional differences were evident: while most areas continued to lose mass, Arctic Canada diverged from the broader Arctic pattern and recorded a slightly positive regional balance for the year. The overall Pan-Arctic losses were driven largely by sustained reductions in Alaska (36% of the Arctic total), Arctic Russia (31%), Svalbard (30%), and Iceland (7%), and countered by a small gain in Arctic Canada (5%). Mass balance data for 2024/25 and GRACE-derived regional anomalies are not yet available, but preliminary indicators suggest contrasting regional dynamics. In Alaska, the onset of summer melt was delayed in 2025 (see essays *Surface Air Temperature* and *Terrestrial Snow Cover*), potentially moderating annual losses. In contrast, Arctic Canada recorded only minimal mass gain during winter 2024/25, setting the stage for a strongly negative mass balance in 2024/25.

Direct societal impacts

Observations of the Arctic system, including glaciers and ice caps, support a multitude of societal impacts (see essay *Assessing the State of the Arctic Observing Network*). The societal dimensions of Arctic glacier mass loss are wide-ranging, from driving global sea level rise to having direct, regional effects in the Arctic. In the Arctic, this mass loss directly impacts communities and threatens public safety and infrastructure. At the local scale, a key impact is water availability. For example, the decline of ice in Ausuiktuq (Grise Fiord), Arctic Canada directly affects the local community's water availability. Since the 1970s, this community has depended on an intermittent stream primarily fed by snowmelt and glacier runoff, supplemented by manually collected glacier ice. However, as glaciers and remnant ice patches disappear over the coming decades, a crucial mid- to late-summer water supply will be lost. This change will significantly shorten the already brief period during which meltwater is available, intensifying seasonal scarcity. In response, the community plans to temporarily relocate the water intake to a nearby catchment basin holding remnant glacier ice. Given the current warming trends across the Arctic, this new source, while initially more reliable, is anticipated to be short-lived. The community continues to blend traditional knowledge and modern technology to adapt to these escalating water challenges.

Another critical concern is geohazards associated with glacier-loss (Wolken et al. 2021). A notable example is the Mendenhall Glacier near Juneau in southeastern Alaska. Here, a retreating tributary glacier has created a basin for meltwater that is impounded by the larger Mendenhall Glacier. This has resulted in annual glacial lake outburst floods (GLOFs) since 2011 (Kienholz et al. 2020), which are becoming more frequent and severe, leading to widespread flooding resulting in property damage and loss of homes and infrastructure in Juneau, Alaska. Glacier mass loss is also contributing to slope destabilization and a rise in tsunamigenic landslides throughout the Arctic. The August 2025 landslide at South Sawyer Glacier in Alaska's Tracy Arm fiord is a prime example of how these cascading hazards can pose a risk to people and infrastructure far from the initial slope failure. The unstable rock mass, with an estimated volume of ~100 million cubic meters (~130 million cubic yards), failed catastrophically and slid into the water near and onto the terminus of South Sawyer Glacier (USGS 2025). The resulting tsunami caused water to run-up slopes opposite the landslide to a height of nearly 500 meters (1600 feet) and was recorded as far away as Juneau, where a tide gauge measured a wave height of 36 cm (14 inches) above the tide.

Methods and data

Data were obtained from the World Glacier Monitoring Service (WGMS 2025) with updates from Norwegian Water Resources and Energy Directorate (NVE) and Geological Survey of Canada. Bias corrections were applied to B_{clim} for Hofsjökull glaciers (N, E, and SW), Iceland using methods outlined in Jóhannesson et al. (2013). Regional climatic mass balances were derived as arithmetic means for all monitored glaciers within each region for each year, and these means were summed over the period of record and interpreted as cumulative thickness changes.

Cumulative changes in regional total stored water (Gt) for 2002-25 were derived from GRACE and GRACE-FO satellite gravimetry for the five regions shown in Fig. 1 and for the total of these five regions (i.e., Pan-Arctic). A July 2017 to May 2018 data gap exists between retrieval periods. The data processing involved several steps. First, common post-corrections to the Level-2 data were applied, including the addition of degree-1 coefficients which are not directly observed by the satellites. To reduce correlated

noise in the GRACE data, an adaptation of a method by Wouters and Schrama (2007) was used. This involved fitting a 3rd order polynomial to the monthly time series of all Stokes coefficients to preserve the long-term variability. After restoring this variability, a 150 km Gaussian smoothing filter was applied to the resulting Stokes coefficients to further reduce remaining noise. Finally, to retrieve the mass changes for the glacier regions, the processed coefficients were converted into maps of equivalent water height anomalies using a "mascon" (mass concentration) approach based on a global 0.5° × 0.5° grid.

References

Ballinger, T. J., and Coauthors, 2024: Surface air temperature. *Arctic Report Card 2024*, T. A. Moon, M. L. Druckenmiller, and R. L. Thoman, Eds., https://doi.org/10.25923/mjhx-3j40.

Box, J., and Coauthors, 2019: Key indicators of Arctic climate change: 1971-2017. *Environ. Res. Lett.*, **14**, 045010, https://doi.org/10.1088/1748-9326/aafc1b.

Box, J. E., W. T. Colgan, B. Wouters, D. O. Burgess, S. O'Neel, L. I. Thomson, and S. H. Mernild, 2018: Global sea-level contribution from Arctic land ice: 1971-2017. *Environ. Res. Lett.*, **13**, 125012, https://doi.org/10.1088/1748-9326/aaf2ed.

Hugonnet, R., and Coauthors, 2021: Accelerated global glacier mass loss in the early twenty-first century. *Nature*, **592**, 726-731, https://doi.org/10.1038/s41586-021-03436-z.

Jóhannesson, T., H Björnsson, E. Magnússon, S. Guðmundsson, F. Pálsson, O. Sigurðsson, T. Thorsteinsson, and E. Berthier, 2013: Ice-volume changes, bias estimation of mass-balance measurements and changes in subglacial lakes derived by lidar mapping of the surface of Icelandic glaciers. *Ann. Glaciol.*, **54**(63), 63-74, https://doi.org/10.3189/2013AoG63A422.

Kienholz, C., and Coauthors, 2020: Deglacierization of a marginal basin and implications for outburst floods, Mendenhall Glacier, Alaska. *Front. Earth Sci.*, **8**, 137, https://doi.org/10.3389/feart.2020.00137.

Kjøllmoen, B. (Ed.), L. M. Andreassen, and H. Elvehøy, 2025: Glaciological investigations in Norway 2024. NVE Rapport 27-2025, 110 pp +app. Norwegian Water resources and Energy Directorate, Oslo, https://publikasjoner.nve.no/rapport/2025/rapport2025_27.pdf.

Masson-Delmotte, V., P. Zhai, A. Pirani, S. L. Connors, C. Péan, S. Berger, N. Caud, Y. Chen, L. Goldfarb, M. I. Gomis, M. Huang, K. Leitzell, E. Lonnoy, J. B. R. Matthews, T. K. Maycock, T. Waterfield, O. Yelekçi, R. Yu, and B. Zhou, eds., 2021: Climate Change 2021: The Physical Science Basis. Contribution of Working Group I to the Sixth Assessment Report of the Intergovernmental Panel on Climate Change. Cambridge University Press, Cambridge, UK and New York, NY, USA, 2391 pp., https://doi.org/10.1017/9781009157896.

RGI Consortium, 2023: Randolph Glacier Inventory – A Dataset of Global Glacier Outlines, Version 7.0. Boulder, CO, USA. NSIDC: National Snow and Ice Data Center, Online access: https://doi.org/10.5067/f6jmovy5navz.

Schuler, T. V, R. E. Benestad, K. Isaksen, H. P. Kierulf, J. Kohler, G. Moholdt, and L. S. Schmidt, 2025: Svalbard's 2024 record summer: An early view of Arctic glacier meltdown? *Proc. Natl. Acad. Sci.*, **122**(34), e2503806122, https://doi.org/10.1073/pnas.2503806122.

The GlaMBIE Team, 2025: Community estimate of global glacier mass changes from 2000 to 2023. *Nature*, **639**, 382-388, https://doi.org/10.1038/s41586-024-08545-z.

U.S. Geological Survey (USGS), 2025: 2025 Tracy Arm Landslide-Generated Tsunami. U.S. Geological Survey, Landslide Hazards Program, 14 August 2025, https://www.usgs.gov/programs/landslide-hazards/science/2025-tracy-arm-landslide-generated-tsunami#overview.

WGMS, 2025: Fluctuations of Glaciers Database. World Glacier Monitoring Service (WGMS), Zurich, Switzerland, https://doi.org/10.5904/wgms-fog-2025-02b.

Wolken, G. J., and Coauthors, 2021: Glacier and permafrost hazards. *Arctic Report Card 2021*, T. A. Moon, M. L. Druckenmiller, and R. L. Thoman, Eds., https://doi.org/10.25923/v40r-0956.

Wouters, B., and E. J. O. Schrama, 2007: Improved accuracy of GRACE gravity solutions through empirical orthogonal function filtering of spherical harmonics. *Geophys. Res. Lett.*, **34**, L23711, https://doi.org/10.1029/2007GL032098.

Wouters, B., A. S. Gardner, and G. Moholdt, 2019: Global glacier mass loss during the GRACE Satellite Mission (2002-2016). *Front. Earth Sci.*, **7**, 96, https://doi.org/10.3389/feart.2019.00096.

Zemp, M., and Coauthors, 2019: Global glacier mass changes and their contributions to sea-level rise from 1961 to 2016. *Nature*, **568**, 382-386, https://doi.org/10.1038/s41586-019-1071-0.

November 24, 2025

Atlantification of the Arctic Ocean

https://doi.org/ 10.25923/8q4y-bg95

I. V. Polyakov[1], R. B. Ingvaldsen[2,3], and B. A. Bluhm[3]

[1]International Arctic Research Center and College of Natural Science and Mathematics, University of Alaska Fairbanks, Fairbanks, AK, USA
[2]Institute of Marine Research, Bergen, Norway
[3]Department of Arctic and Marine Biology, UiT The Arctic University of Norway, Tromsø¸, Norway

Headlines

- Atlantification—an influx of anomalous water properties and biota from lower latitudes—now reaches the central Arctic Ocean, with its fingerprint detected in the western Amerasian Basin and advancing toward Alaska.
- Atlantification weakens Arctic Ocean stratification, enhancing heat transfer to the surface and undermining sea ice resilience.
- Rapid atlantification drives Arctic change, altering ocean properties, reshaping ecosystems, and threatening climate stability.

Introduction

Oceanic currents play an important role in the Arctic region by bringing oceanic heat to the Arctic Ocean from the lower latitude regions (Fig. 1). In the early 1890s, Nansen and his crew aboard the *Fram* made the first measurements in the Eurasian Basin, observing that warm, salty water from the Atlantic Ocean flows northward into the Arctic Ocean at 150-800 meters depth. They also observed near-freezing and relatively fresh water in the upper ~50 m and a layer with large vertical salinity and density gradients (called the Arctic halocline) overlying the Atlantic Water (AW) at ~50-150 m depth.

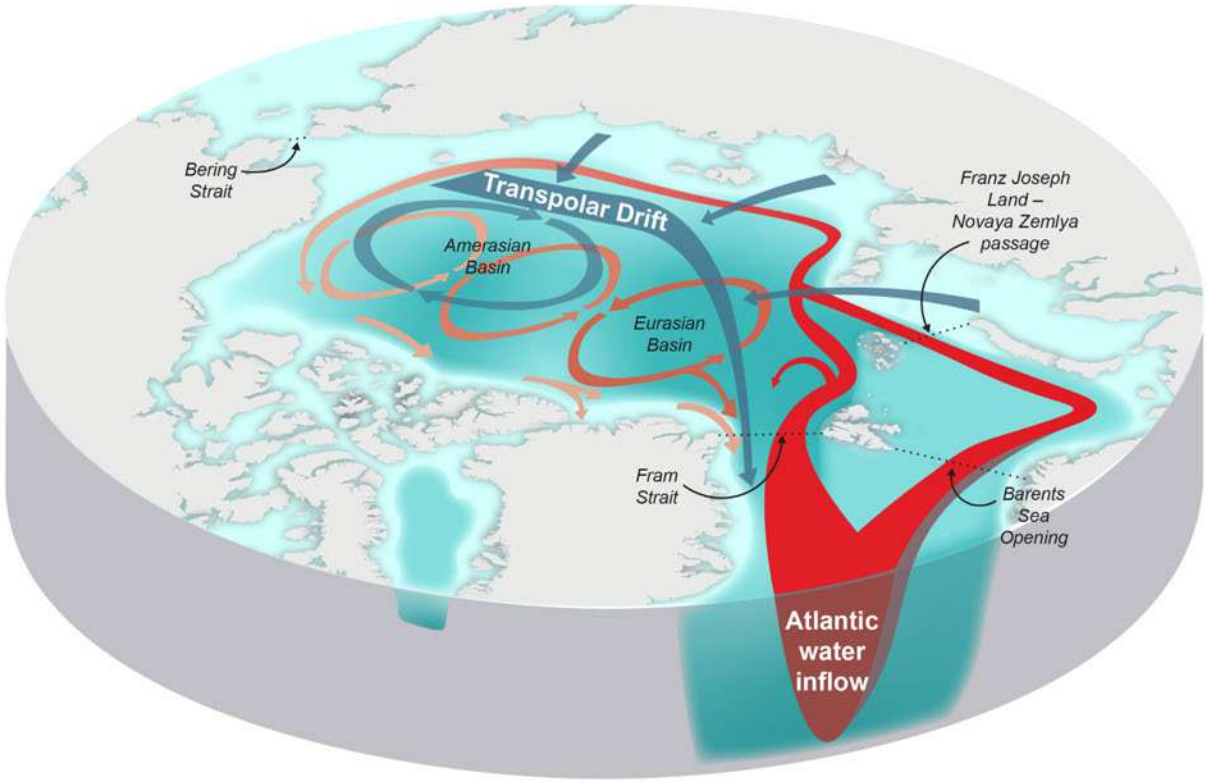

Fig. 1. Circulation of Atlantic Water (red/pink) and surface water (blue) flowing through and within the Arctic Ocean.

Later expeditions showed that changes in the AW layer are often connected to ocean cooling or warming events (Fig. 2) related to the highly variable nature of AW inflows (Fig. 3e-g). System-wide changes in Arctic Ocean basins driven by anomalous AW inflows are referred to as atlantification (e.g., Polyakov et al. 2023; Ingvaldsen et al. 2021). Atlantification has a long historical perspective: a series of studies, including paleoceanographic reconstructions, demonstrate that AW inflows and sea ice conditions have varied over decades to millennia, highlighting the Arctic Ocean's sensitivity to long-term climate variability (e.g., Fig. 2). In 1990, for instance, a warm pulse entered the Eurasian Basin and moved along the deep oceanic pathways, resulting in a strong, up to 1°C, AW warming in the Arctic. Another warm AW pulse was detected in Fram Strait and later in the eastern Eurasian Basin during 1999-2004. This latter pulse peaked in 2007-08, when the average AW temperature was ~0.2°C higher than in the 1990s. After 2007, AW temperature stabilized, showing no significant trend through 2017 (Fig. 2).

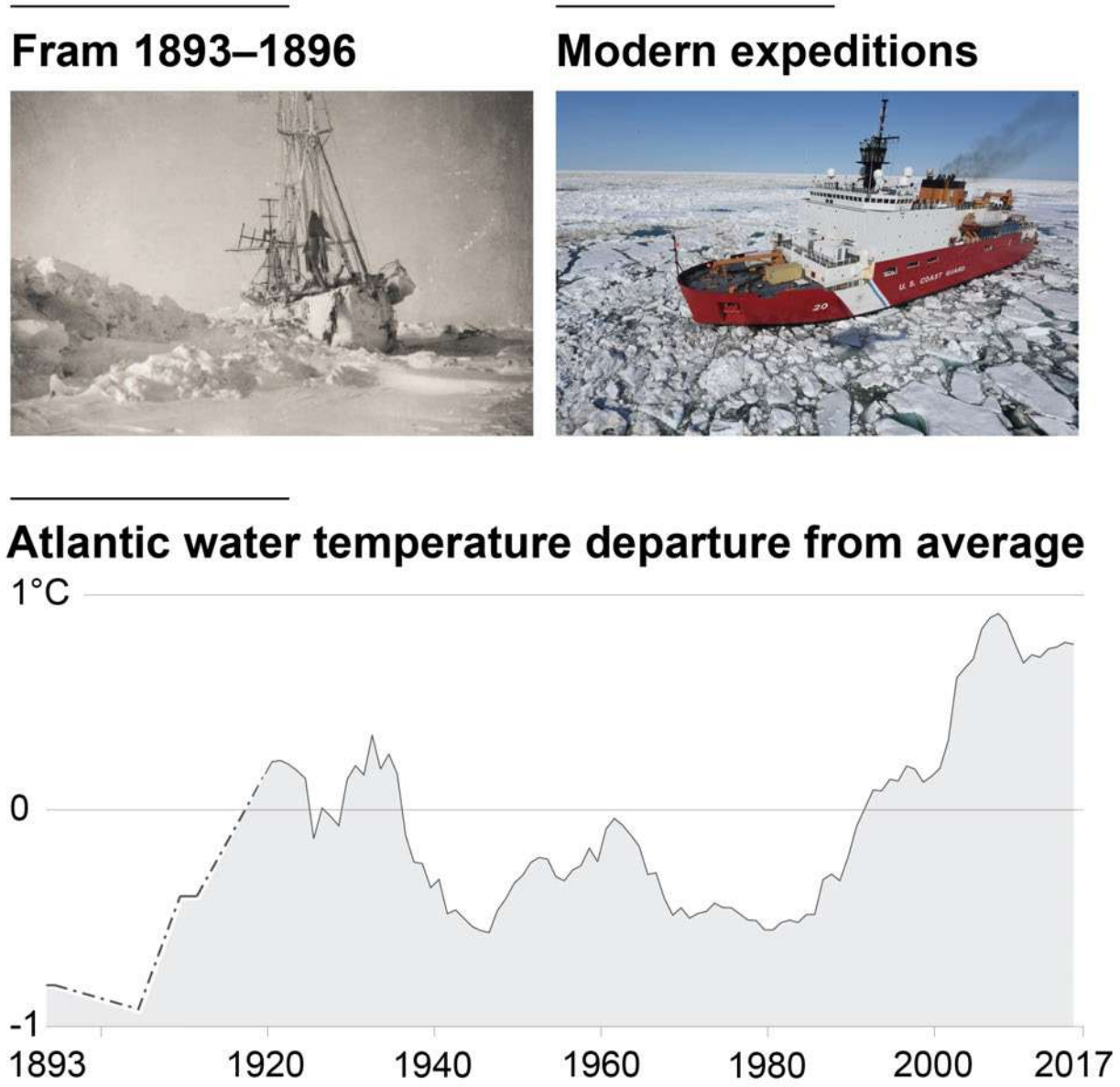

Fig. 2. Atlantic Water temperature anomalies in the Arctic Ocean based on historical data, including Nansen's observations from *Fram* (vessel on the left) in 1893-96 and modern measurements (indicated by icebreaker). The time series have been filtered with a 7-year running average, and the dashed-dotted line indicates sparse observations in the early part of the record. Uncertainties due to limited observations are discussed in Polyakov et al. (2012). See *Methods and data* for data source information.

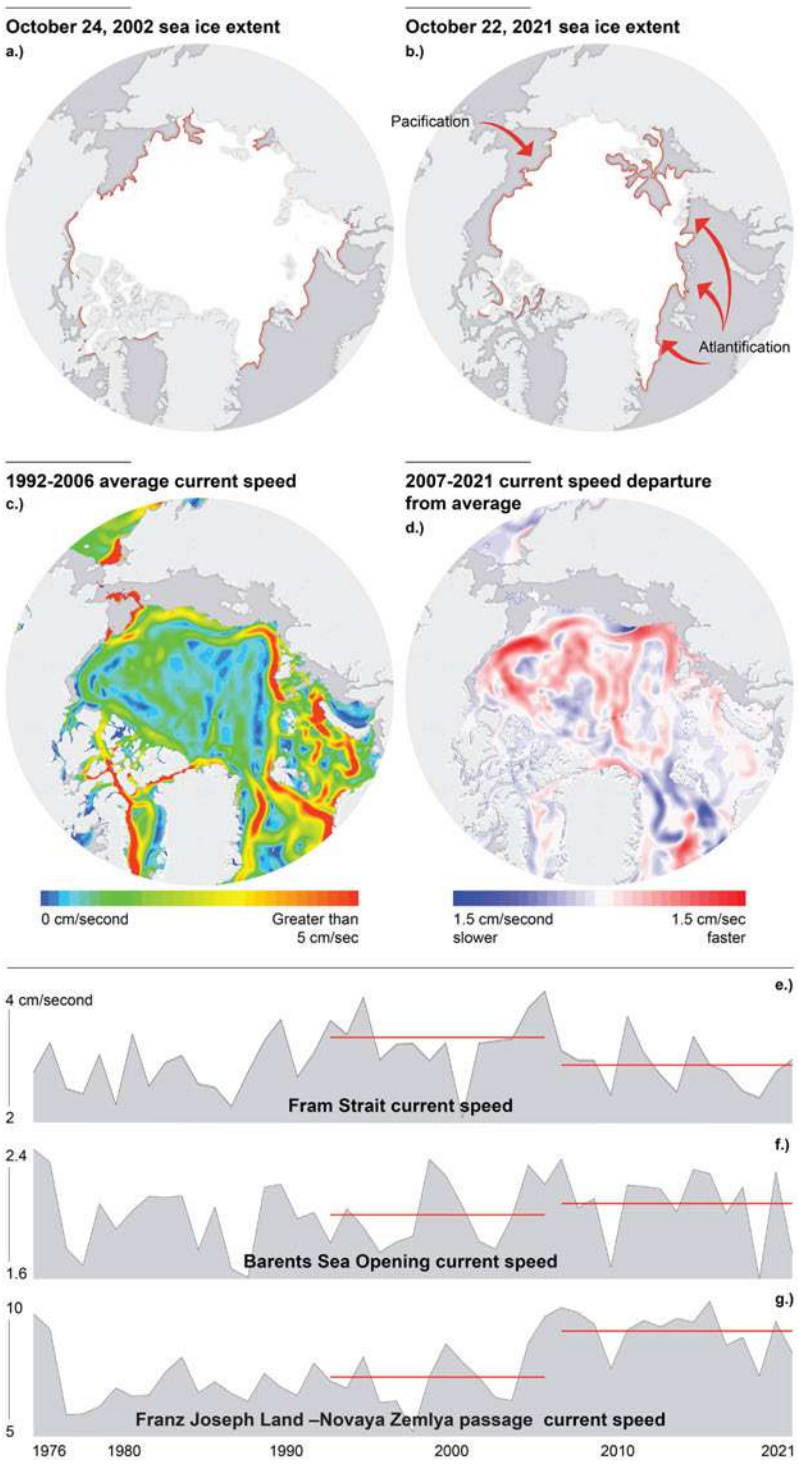

Fig. 3. Changes in Arctic sea ice cover (a, b), upper 50 m oceanic circulation (c, d), and water exchanges through the Arctic gateways (e-g) associated with atlantification. (a, b) Examples of Arctic sea ice concentration (SIC, %) during the start of the freezing season from the early 2000s (a) and early 2020s (b). (c, d) Maps of (c) 1992-2006 annual mean current speed |**U**| and (d) 2007-21 |**U**| anomalies (relative to the 1992-2006 mean) from ocean reanalysis. (e-g) Mooring-based time series of the ocean annual mean current, flowing into the Arctic through Fram Strait (e), the Barents Sea Opening (f), and the Franz Joseph Land-Novaya Zemlya passage (g). Red horizontal lines show means over 1992-2006 and 2007-21.

Arctic halocline changes

Despite >1°C AW warming in the 1990s-2000s, the strong halocline largely insulated the surface and sea ice from the AW heat. The warming did, however, affect the halocline stratification, with stratification weakening in the Eurasian Basin while strengthened in the Amerasian Basin. These trends continued toward present, and overall stronger stratification in the Amerasian Basin since 2007 is consistent with the region's ongoing freshening and deepening of the surface fresh layer due to the intensification of the Arctic high pressure atmospheric system. Boosted regional stratification lowers oceanic heat fluxes, slowing sea-ice losses in the Amerasian Basin (Polyakov et al. 2023).

In contrast, by the mid-2010s, the Eurasian Basin halocline had lost its fundamental role as an effective barrier to AW heat, having experienced a ~30% decline in stability over the preceding three decades (Polyakov et al. 2025). Increased upward AW heat transport associated with atlantification has significantly lowered the regional rates of winter sea-ice formation (e.g., Polyakov et al. 2025). The primary contribution of atlantification to high-latitude climate change has been the decline of regional sea ice over the past decade (Fig. 3a,b). Furthermore, sea ice thickness declines caused by atlantification persist across the central Arctic Ocean and are prevalent along the Transpolar Drift (Belter et al. 2021; see essay *Sea Ice*). Atlantification also impacts the strength of upper ocean currents (Fig. 3c,d) and the efficiency of ocean mixing, thereby affecting carbon and nutrient exchanges and thus primary productivity (see essay *Primary Productivity*).

Role of Atlantic Water influxes from the Barents Sea

Changes brought on by atlantification are closely related to the advection of AW over two Arctic gateways: Fram Strait and the Barents Sea (Fig. 1). Alternating decadal phases of atmospheric circulation modulate the relative strength of these two branches (Polyakov et al. 2023). In 2007-21, this circulation pattern weakened the northward inflows, enhanced southward sea-ice export through Fram Strait, and increased the AW inflow from the Barents Sea (Fig. 3e-g). Moreover, since the mid-2000s, the along-track heat losses of the Fram Strait and Barents Sea throughflow has changed (e.g., Moore et al. 2022), suggesting a stronger warming of the AW entering the Arctic from the Barents Sea as compared to Fram Strait.

In addition, the Barents Sea and Nordic regions are the key contributors to the biological component of atlantification, evident in northward changes of boreal species, driving shifts in biological community compositions and food webs (Calvet et al. 2024; Husson et al. 2024; Fig. 4).

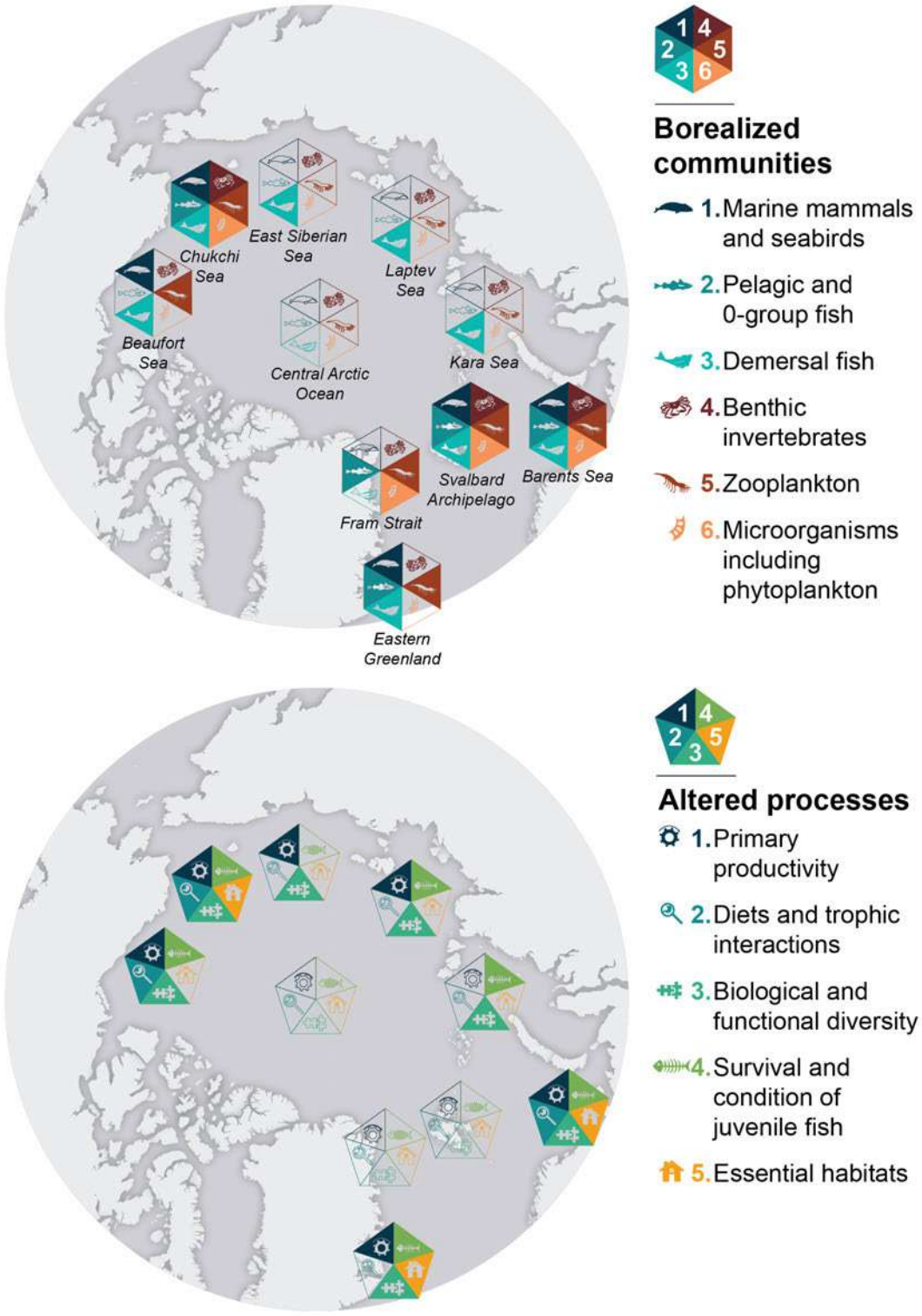

Fig. 4. Borealization of marine communities (top panel) and processes (bottom panel) originating from the sub-Arctic Atlantic and Pacific Seas. Filled triangles show impacts documented in scientific peer-reviewed literature. Borealization is defined as system-wide changes caused by anomalous inflows of sub-Arctic Atlantic- and Pacific-origin waters and biota into the polar basins. Modified from Husson et al. 2024. Pelagic fish live in the water column, demersal fish near the seafloor; 0-group fish are in their first year of growth.

Ocean-heat/sea ice-albedo feedback

Atlantification of the Arctic Ocean can be viewed as occurring in two phases (Fig. 5). Phase 1 involves warming of the ocean interior and shoaling of the (AW)/nitricline—a layer where nutrient concentrations increase with depth—while the halocline remains relatively strong, preventing deep mixing. In Phase 2, the halocline weakens sufficiently to allow deep mixing to occur. The shoaling of AW from approximately 150 m in the early 2000s to up to 70 m in recent years in the eastern Eurasian Basin has coincided with the seasonal disappearance of the halocline, causing fast sea ice loss (Polyakov et al. 2025) and probably an increase in primary production. A positive ocean-heat/sea ice-albedo feedback mechanism is triggered, amplifying atlantification. In this feedback, weaker stratification and enhanced winter ventilation—when cold, dense surface waters formed through sea ice growth and brine rejection sink and mix with underlying layers—of the upper (>100 m) ocean increase the release of AW heat to the sea surface, contributing to sea ice loss (Polyakov et al. 2023). Thinner ice melts more quickly in the following summer, exposing the darker ocean surface sooner and intensifying the sea ice-albedo feedback. Reduced sea ice extent during the succeeding freezing season encourages more powerful currents, which in turn enhances AW ventilation (Polyakov et al. 2020). Stronger coupling between the atmosphere, ice, and ocean in the Eurasian Basin over the past decade has played a critical role in driving this feedback (Polyakov et al. 2020), which has been central to the sustained decline in sea ice cover in the region in recent decades (Fig. 3a,b).

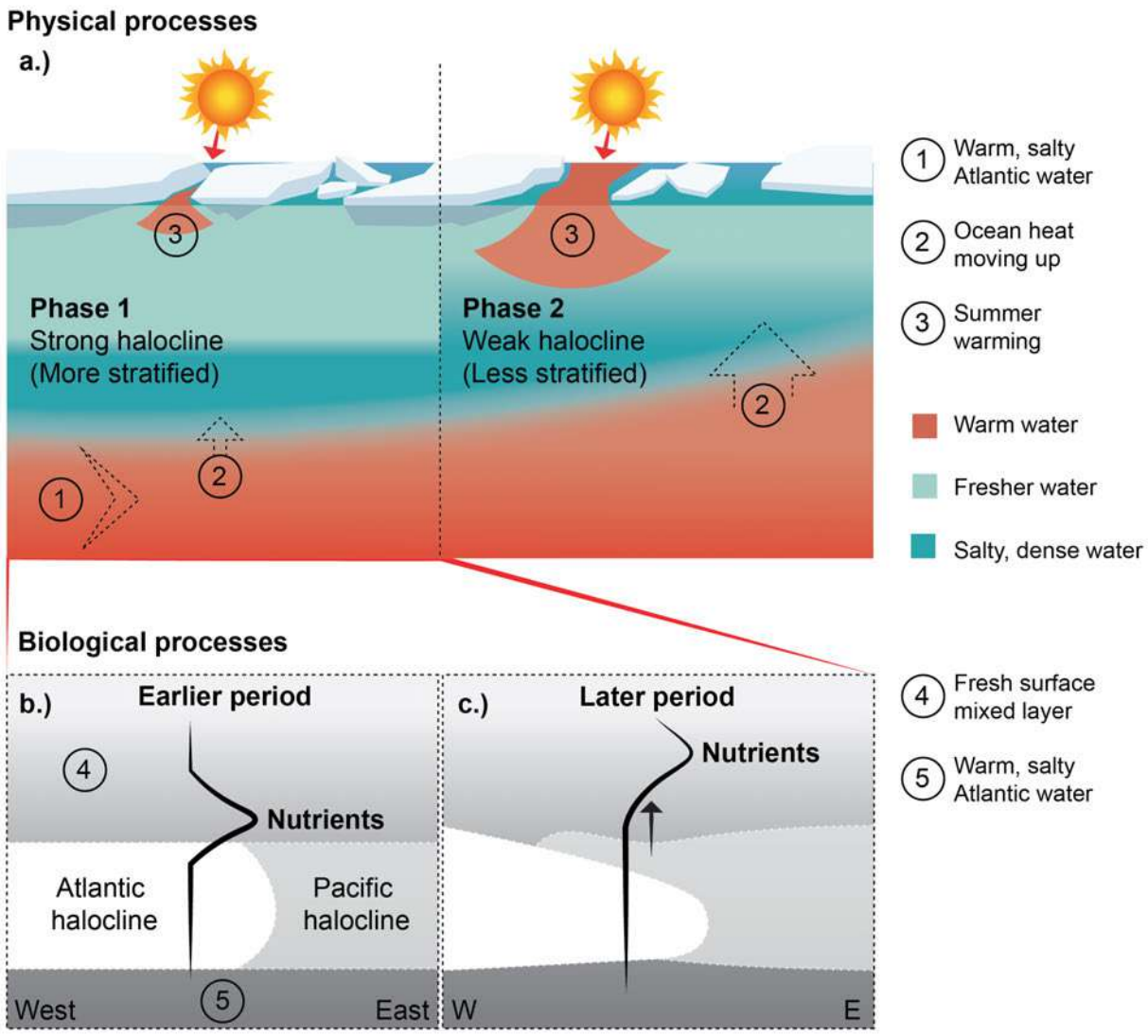

Fig. 5. Physical and biogeochemical changes in the Siberian Arctic Ocean (SAO, north of the Laptev and East Siberian Sea shelves) in response to atlantification. (a) Two phases of atlantification of the Arctic Ocean. The eastward progression of atlantification into the central/eastern SAO toward Alaska lags the western SAO by 5-7 years. (b and c) Diagram illustrating the environmental changes brought about by atlantification in the central and eastern SAO. The vertical arrow in (c) shows that the Chl-*a* maximum shoaled from 2015-16 (earlier period, b) to 2022-23 (later period, c) in response to the incursion of Atlantic halocline waters. Figure modified from Polyakov et al. (2025).

Eastward progression and ramifications of atlantification

CMIP-6 model projections indicate that atlantification is unlikely to extend far into the Amerasian Basin during the current century (Muilwijk et al. 2023). However, there is observational evidence that atlantification is already extending beyond the Eurasian Basin. The transition of the western Amerasian Basin to conditions resembling those observed in the eastern Eurasian Basin 5-7 years earlier is a clear fingerprint of the eastward progression of atlantification (Fig. 5a, Polyakov et al. 2025). The powerful ocean-heat/sea ice-albedo feedback mechanism is the primary cause of these changes (phase 2 of atlantification in Fig. 5a).

In contrast, no evidence of deep ventilation of AW heat was found in the 2021-24 mooring records from the eastern East Siberian Sea. Shoaling of the AW and halocline, however, indicates that this region is experiencing a preconditioning phase (phase 1 of atlantification in Fig. 5a) similar to that found in the Eurasian Basin in the 2000s. This ongoing transition not only mirrors earlier changes but also sets the stage for broader ecosystem impacts. For example, the shoaling of AW and diminishing stability of the halocline resulted in a 70 m vertical elevation of the boundary between the Pacific and Atlantic halocline domains from 2015 to 2023 (Fig. 5b,c). This process lifted nutrient-rich waters into the zone where there is enough light for photosynthesis to occur, potentially enhancing nutrient use and influencing the occurrence of summer surface blooms, as seen in observational records by the relocation of the chlorophyll-*a* (Chl-*a*, a proxy for phytoplankton biomass and primary production) maximum nearer to the surface since 2015, and reflected in model projections of primary production (Fig. 5b,c) (Bluhm et al. 2020, see essay *Primary Productivity*). Thus, even in this early preconditioning stage of atlantification, physical changes had an immediate impact on the state of the local ecosystem. Notably, newly recovered mooring records from winter and spring (February-May) 2025 provide the first evidence of deep ventilation in the eastern East Siberian Sea.

Shifting species distributions and migrations are expected to impact the entire food web. At lower trophic levels, the growing potential and observed occurrence of harmful algal blooms pose concerns for both humans and marine ecosystems (Karlson et al. 2021). At higher levels, expanding commercial (boreal) stocks may demand new monitoring and management strategies, complicated by logistical and geopolitical challenges (Nascimento et al. 2025). In areas where boreal and Arctic species already overlap, competitive and trophic interactions suggest an increasing role for omnivorous predatory fish. Greater mixing of halocline waters could further facilitate species exchange between the Pacific and Atlantic, as has occurred in the past (e.g., Reid et al. 2007).

Concluding note

Climatic and ecological changes linked to Arctic atlantification are complex and far-reaching, already having major impacts on primary production and species distribution in the Pacific Arctic (Ershova et al. 2021). Altered nutrient fluxes and increased high-latitude productivity (Nishino et al. 2023) have led to shifts in species composition and food web structure (Ingvaldsen et al. 2021; Husson et al. 2024). The continued weakening of nutrient, temperature, and light limitations in upstream areas is expected to further accelerate atlantification (Noh et al. 2024), with uncertain but potentially severe consequences for the Arctic system.

Methods and data

A detailed description of the data and methods used in this synthesis can be found in Polyakov et al. (2023, 2025). Conductivity, temperature, density (CTD) data are available online via Pangaea Data Publisher (e.g., https://doi.org/10.1594/PANGAEA.691332), at https://uaf-iarc.org/nabos/data/ (NABOS [Nansen and Amundsen Basins Observational System] project) and https://www2.whoi.edu/site/itp/data/ (ITP [Ice Tethered Profilers] program).

References

Belter, H. J., and Coauthors, 2021: Interannual variability in Transpolar Drift summer sea ice thickness and potential impact of Atlantification. *Cryosphere*, **15**(6), 2575-2591, https://doi.org/10.5194/tc-15-2575-2021.

Bluhm, B. A., and Coauthors, 2020: The Pan-Arctic continental slope: Sharp gradients of physical processes affect pelagic and benthic ecosystems. *Front. Mar. Sci.*, **7**, 544386, https://doi.org/10.3389/fmars.2020.544386.

Calvet, N., B. A. Bluhm, N. Yoccoz, and A. Altenburger, 2024: Shifting invertebrate distributions in the Barents Sea since pre-1900. *Front. Mar. Sci.*, **11**, 1421475, https://doi.org/10.3389/fmars.2024.1421475.

Ershova, E. A., K. N. Kosobokova, N. S. Banas, I. Ellingsen, B. Niehoff, N. Hildebrandt, and H. -J. Hirche, 2021: Sea ice decline drives biogeographical shifts of key *Calanus* species in the central Arctic Ocean. *Global Change Biol.*, **27**(10), 2128-2143, https://doi.org/10.1111/gcb.15562.

Husson, B., and Coauthors, 2024: Borealization impacts shelf ecosystems across the Arctic. *Front. Environ. Sci.*, **12**, 1481420, https://doi.org/10.3389/fenvs.2024.1481420.

Ingvaldsen, R. B., K. M Assmann, R. Primicerio, M. Fossheim, I. V. Polyakov, and A. V. Dolgov, 2021: Physical manifestations and ecological implications of Arctic Atlantification. *Nat. Rev. Earth Environ.*, **2**(12), 874-889, https://doi.org/10.1038/s43017-021-00228-x.

Karlson, B., and Coauthors, 2021: Harmful algal blooms and their effects in coastal seas of Northern Europe. *Harmful Algae*, **102**, 101989, https://doi.org/10.1016/j.hal.2021.101989.

Moore, G. W. K., K. Våge, I. A. Renfrew, and R. S. Pickart, 2022: Sea-ice retreat suggests re-organization of water mass transformation in the Nordic and Barents Seas. *Nat. Commun.*, **13**(1), 67, https://doi.org/10.1038/s41467-021-27641-6.

Muilwijk, M., A. Nummelin, C. Heuzé, I. V. Polyakov, H. Zanowski, and L. H. Smedsrud, 2023: Divergence in climate model projections of future Arctic Atlantification. *J. Climate*, **36**(6), 1727-1748, https://doi.org/10.1175/JCLI-D-22-0349.1.

Nascimento, M. C., F. Fransner, R. Hordoir, M. D. Skogen, R. Primicerio, and T. Pedersen, 2025: Future poleward distribution shifts of community and functional groups in the Barents Sea modelled under different climate and fisheries scenarios. *Mar. Ecol. Prog. Ser.*, **763**, 1-25, https://doi.org/10.3354/meps14868.

Nishino, S., and Coauthors, 2023: Atlantic-origin water extension into the Pacific Arctic induced an anomalous biogeochemical event. *Nat. Commun.*, **14**, 6235, https://doi.org/10.1038/s41467-023-41960-w.

Noh, K. -M., J. -H. Oh, H. -G. Lim, H. Song, and J. -S. Kug, 2024: Role of Atlantification in enhanced primary productivity in the Barents Sea. *Earth's Future*, **12**(1), e2023EF003709, https://doi.org/10.1029/2023EF003709.

Polyakov, I. V., A. V. Pnyushkov, and L. A. Timokhov, 2012: Warming of the intermediate Atlantic Water of the Arctic Ocean in the 2000s. *J. Climate*, **25**(23), 8362-8370, https://doi.org/10.1175/JCLI-D-12-00266.1.

Polyakov, I. V., and Coauthors, 2020: Intensification of near-surface currents and shear in the Eastern Arctic Ocean. *Geophys. Res. Lett.*, **47**(16), e2020GL089469, https://doi.org/10.1029/2020GL089469.

Polyakov, I. V., R. B. Ingvaldsen, A. V. Pnyushkov, U. S. Bhatt, J. A. Francis, M. Janout, R. Kwok, and Ø. Skagseth, 2023: Fluctuating Atlantic inflows modulate Arctic Atlantification. *Science*, **381**(6661), 972-979, https://doi.org/10.1126/science.adh5158.

Polyakov, I. V., and Coauthors, 2025: Atlantification advances into the Amerasian Basin of the Arctic Ocean. *Sci. Adv.*, **11**(8), eadq7580, https://doi.org/10.1126/sciadv.adq7580.

Reid, P. C., D. G. Johns, M. Edwards, M. Starr, M. Poulin, and P. Snoeijs, 2007: A biological consequence of reducing Arctic ice cover: arrival of the Pacific diatom *Neodenticula seminae* in the North Atlantic for the first time in 800 000 years. *Global Change Biol.*, **13**(9), 1910-1921, https://doi.org/10.1111/j.1365-2486.2007.01413.x

November 26, 2025

Warming Waters and Borealization: Restructuring Ecosystem Dynamics in the Northern Bering and Chukchi Seas, 2002-2022

https://doi.org/10.25923/ee1p-zw53

S. P. Wise[1], L. A. K. Barnett[2], S. Gonzalez[3,4], I. Ortiz[5], K. Rand[6,7], A. Spear[2], and J. T. Thorson[7]

[1]Economic and Social Science Research Program, Alaska Fisheries Science Center, NOAA, Seattle, WA, USA
[2]Resource Assessment and Conservation Engineering Division, Alaska Fisheries Science Center, NOAA, Seattle, WA, USA
[3]Climate and Oceanography, Institute of Marine Research, Bergen, Norway
[4]Bjerknes Centre for Climate Research, Bergen, Norway
[5]Cooperative Institute for Climate, Ocean, and Ecosystem Studies, University of Washington, Seattle, WA, USA
[6]Lynker, Leesburg, VA, USA
[7]Resource Ecology and Fisheries Management, Alaska Fisheries Science Center, NOAA, Seattle, WA, USA

Headlines

- Warming bottom waters, declining sea ice, and rising chlorophyll levels in the Chukchi and northern Bering Seas are restructuring Arctic marine ecosystems.
- Recent shifts in key mid-water-dwelling species reflect changing sea ice, prey dynamics, and the movement of species in the Chukchi and northern Bering Seas.
- Changes in Arctic bottom-dwelling species point to emerging borealization of seafloor ecosystems, with some southern species appearing farther north as conditions warm.
- Chukchi and northern Bering Seas ecosystem shifts—driven by warming, sea ice loss, and species redistribution—affect North Pacific commercial fisheries, Arctic food security, and Indigenous subsistence practices.

Introduction

Arctic marine ecosystems have historically relied on strong biological coupling between the surface/midwater (pelagic) and seafloor (benthic), driven by early spring phytoplankton blooms that export carbon to the seafloor. However, climate change may disrupt this linkage, causing ecosystem change. Ocean warming and sea ice loss can increase mixing across the water column and delay phytoplankton blooms relative to the seasonal timing of sea ice retreat (Kikuchi et al. 2020; Nielsen et al. 2024), which can shift more production to pelagic consumption, reducing food for benthic species on which seabirds, walruses, and other animals rely. Additionally, boreal species may move northward with ocean warming, a process known as borealization, with potential influence on Arctic species.

This research synthesizes 21 years of data to understand how warming oceans and disappearing sea ice are reshaping ecosystems in the northern Bering and Chukchi Seas (NBS-CS). The project, Arctic Integrated Ecosystem Research Program Synthesis, funded by the North Pacific Research Board, is a collaboration between the NOAA Arctic Research Program and NOAA Fisheries. Integrated computer modeling of boreal and Arctic taxa (species groups) is advancing, linking ecological monitoring and remote-sensing data to produce robust assessments of species trends under accelerating climate shifts.

To examine possible ecosystem shifts, we synthesized data in the NBS-CS (Fig. 1) from 2002 to 2022 and developed models to deduce trends. Drawing from 7,560 samples, we selected 27 species groups important for people, ecosystems, and fisheries to model (Table 1). These taxa include commercial species—Pacific cod (*Gadus macrocephalus*), walleye pollock (*Gadus chalcogrammus*), yellowfin sole (*Limanda aspera*), and snow crab (*Chionoecetes opilio*)—and taxa serving as prey for commercial species, marine mammals, seabirds, and humans, including Indigenous subsistence hunters and fishers.

Fig. 1. Regions included in this study: U.S. portions of the Chukchi Sea (blue) and northern Bering Sea (red).

Table1. Summary of taxa in this essay, with habitat type, classification, and common name. Most were found in the Chukchi Sea and the northern Bering Sea, except sea stars and basket stars (NBS only), and sea cucumbers and brittle stars (CS only).

Habitat and Classification	Taxa	Common Name
Pelagic zooplankton	*Calanus marshallae/glaciallis*	Copepods
	Calanus hyperboreus	Copepods
	Pseudocalanus spp	Copepods
	Euphausiacea	Krill
	Chaetognatha	Chaetognats
Pelagic invertebrate	*Chrysaora melanaster*	Northern Sea Nettle
Pelagic fish	*Mallotus villosus*	Capelin
	Clupea pallasii	Herring
	Oncorhynchus gorbuscha	Pink Salmon
	Oncorhynchus nerka	Sockeye Salmon
Benthic infauna	*Bivalvia*	Bivalves
	Polychaeta	Bristle worms
	Crustacea	Crustaceans
	Amphipoda	Amphipods
Benthic epifauna	*Chionoecetes opilio*	Snow crab
	Phrynophiurida	Basket stars
	Ophiurida	Brittle stars
	Ascidiacea	Sea squirts
	Strongylocentrotidae	Sea urchins
	Dendrochirotida	Sea cucumbers
	Asteroidea	Sea stars
Epibenthic fish	*Boreogadus saida*	Arctic cod
	Eleginus gracilis	Saffron cod
	Gadus chalcogrammus	Walleye pollock
	Gadus macrocephalus	Pacific cod
	Limanda aspera	Yellowfin sole
	Pleuronectes quadrituberculatus	Alaska plaice

Environmental drivers

In the Chukchi Sea, bottom temperatures in September show no long-term trends due to high variation among years, but temperatures increased from 2013 to 2019; whereas in the northern Bering Sea, temperatures decreased into the late 2000s and early 2010s before increasing (Fig. 2). Spring sea ice declined in both regions during the study period.

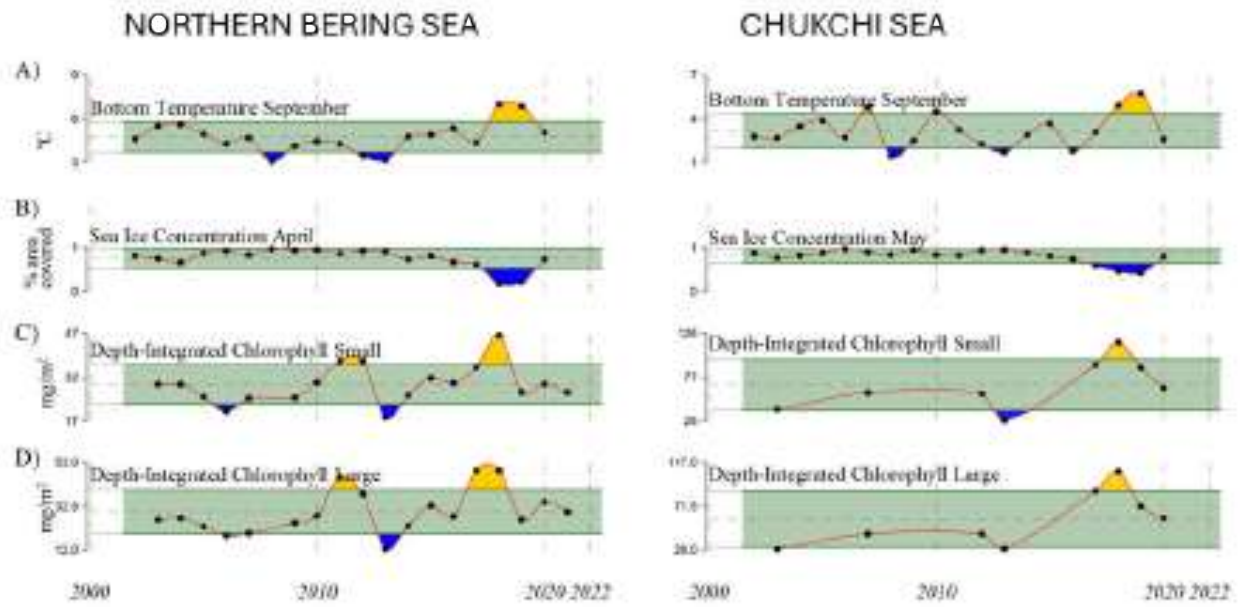

Fig. 2. Environmental conditions/drivers collected within 2002-21 for the northern Bering Sea (left) and Chukchi Sea (right). (A) Bottom temperature in °C (September); (B) Sea ice concentration in % area covered (April/May); (C) Depth-integrated chlorophyll in mg/m^2 (small, < 10 µm Chla); (D) Depth-integrated chlorophyll in mg/m^2 (large, > 10 µm Chla). Yellow/blue shading indicates years when the value was ± 1 st. dev. above/below the mean. Green shade denotes values within ± 1 st. dev. from the mean.

Size-categorized chlorophyll concentrations (indicating plant-like life in the water) increased in the Chukchi Sea and northern Bering Sea from 2013 to 2018 for both large and small sizes (Fig. 2). In the northern Bering Sea, both size classes also increased from 2006 to 2012 before transitioning to a minimum in 2013. These trends were generally consistent with previous observations (Docquier et al. 2024; Frey et al. 2021; Hu et al. 2024).

Pelagic (surface and mid-water) trends

In the Chukchi Sea, most pelagic taxa showed no change in estimated population size (Fig. 3); however, *Pseudocalanus* copepods declined from 2010 to 2012 before increasing across 2013 to 2019, and *Calanus marshallae/glacialis* increased from 2010 to 2016 before declining. These trends are likely due to reduced sea ice and increased northward water transport (Spear and Kimmel, personal communication). Pink salmon (*Oncorhynchus gorbuscha*) and sockeye salmon (*Oncorhynchus nerka*) showed unusual recent high years, which likely reflects population increases related to shifting distributions.

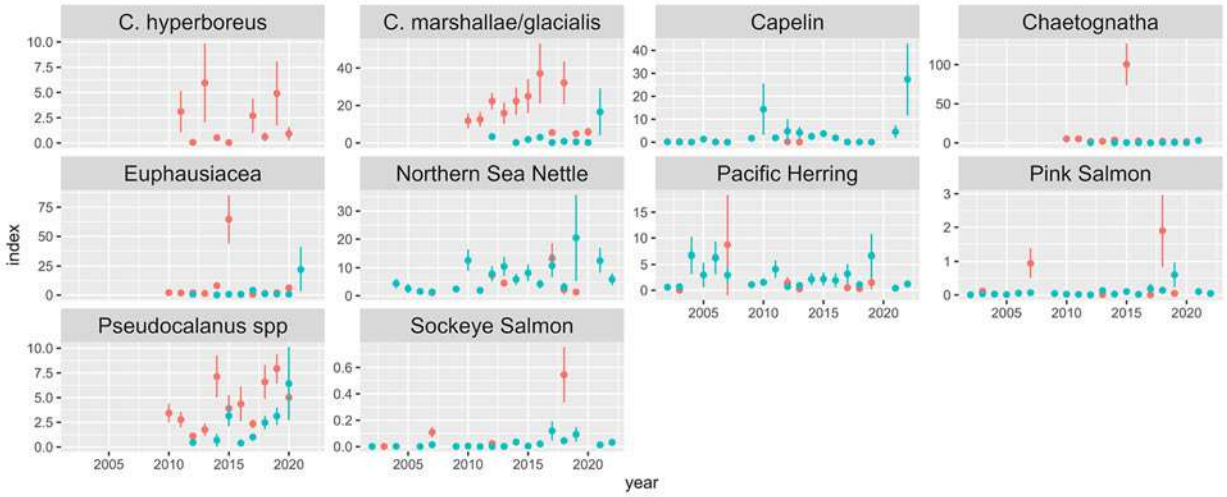

Fig. 3. Estimated area-expanded population size index value (dot) ± 2 standard deviations (vertical lines, y-axis) for pelagic components 2002-22 for the Chukchi Sea (red) and northern Bering Sea (blue). Some confidence intervals are too small to see at this scale but are plotted each year. Index scales match between regions for each taxon. "C" (e.g., C. *hyperboreus*) denotes genus *Calanus*.

In the northern Bering Sea, patterns were mixed (Fig. 3): *Pseudocalanus* increased, while northern sea nettles (*Chrysaora melanaster*) increased slightly overall. Pacific herring (*Clupea pallasii*), pink, and sockeye salmon were largely unchanged. Capelin (*Mallotus villosus*) and *Calanus marshallae/glacialis* had one anomalous high year. The data offer little support that pelagic species increased in response to pelagic-benthic decoupling.

Benthic (sea bottom) trends

In the Chukchi Sea, time series for the benthic infauna (sediment dwelling species) show an increase only in bivalvia (Fig. 4). Typical Arctic epibenthic taxa, species living on or just above the seafloor, had mixed responses (Figs. 4 and 5), and also sparse data in many cases. *Chionoecetes*, including snow crab, decreased over time, while Arctic cod (*Boreogadus saida*) were unchanged, as was the saffron cod (*Eleginus gracilis*) which resides in both Arctic and boreal waters (Arctic-boreal). Of the epibenthic and boreal species, pollock increased while yellowfin sole and Pacific cod were unchanged, as was the Arctic-boreal Alaska plaice (*Pleuronectes quadrituberculatus*). Epibenthic invertebrates, sea cucumbers, sea squirts, and brittle stars showed no trend, while sea urchins slightly decreased.

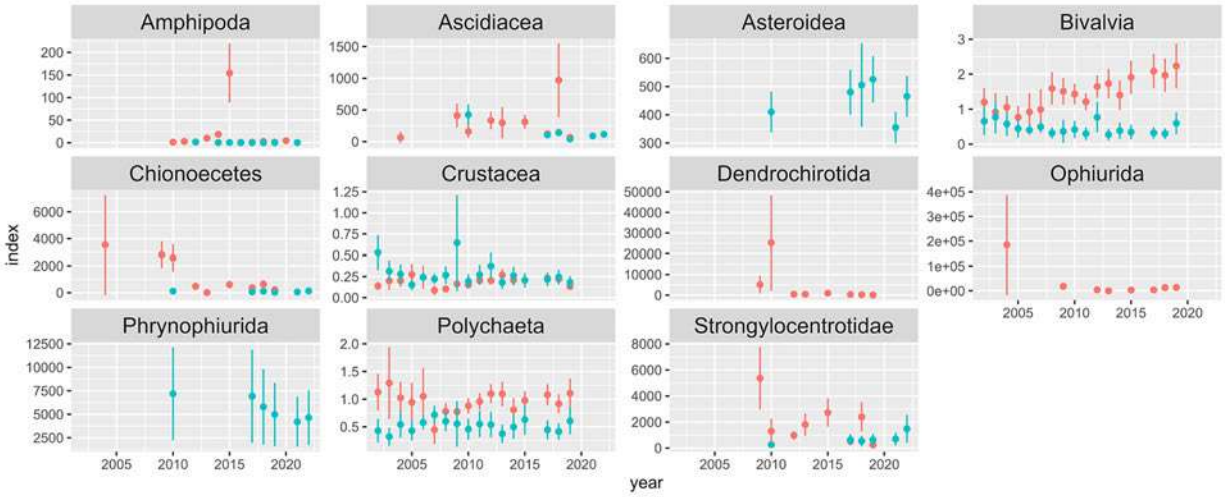

Fig. 4. Estimated area-expanded population size index for infauna and epifauna components 2002-22 (see Fig. 3 caption for details).

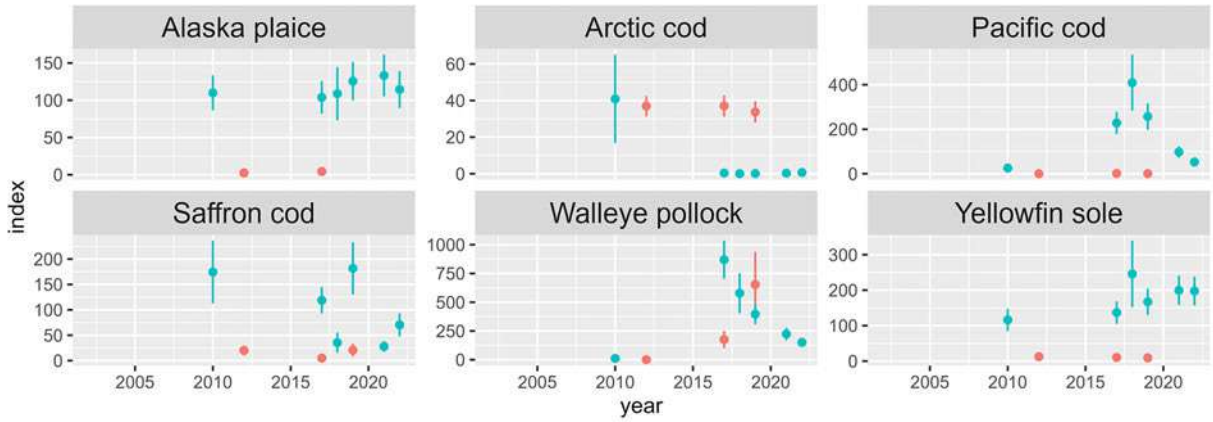

Fig. 5. Estimated area-expanded population size index for epibenthic fish components 2010-22 (see Fig. 3 caption for details).

Among infaunal taxa in the northern Bering Sea, bivalvia and polychaetes showed no overall population trend despite a slight initial decrease for bivalves (Fig. 4). Crustaceans trended downward, with 2009 as an anomalously high year. This is consistent with documentation of decreasing infaunal biomass between 1990 and 2003 (Grebmeier et al. 2006) and amphipods from 1983 to 2000 (Moore et al. 2003). Other epibenthic invertebrates showed no change. Epibenthic fishes were sampled in more years in the northern Bering Sea than the Chukchi Sea (Fig. 5). Two of the Arctic and Arctic-boreal epibenthic fishes in the northern Bering Sea—Arctic cod and saffron cod—declined (although the Arctic cod pattern relies primarily on an anomalously high first survey year) while Alaska plaice was unchanged. Boreal epibenthic fishes—pollock and Pacific cod—increased into the late 2010s before declining, while yellowfin sole slightly increased.

In both regions, epibenthic changes were not consistent with pelagic-benthic decoupling, as we did not observe the reductions in benthic biomass or prey availability that would be expected under such a shift. Instead, changes in species composition marked by increasing boreal-affiliated taxa (e.g., walleye pollock, yellowfin sole) and declining Arctic-boreal and Arctic-affiliated taxa (e.g., saffron cod, snow crab) provide some evidence for borealization.

Borealization

In the Chukchi Sea, one of five typically Arctic taxa time series declined (snow crab). Two of the six boreal taxa increased: *Pseudocalanus* and pollock, while sockeye and pink salmon had recent anomalously high years but showed no consistent long-term trend.

In the northern Bering Sea, the saffron cod population decreased, while Arctic cod remained low after an initial high year. *Calanus marshallae*/*glaciallis* showed no trend aside from a recent high year. Two of the six boreal taxa increased: *Pseudocalanus* and yellowfin sole, while pollock and Pacific cod initially increased into the warm late 2010s and then declined as temperatures moderated.

In summary, approximately one-third of the boreal taxa examined in NBS-CS increased over the time series and one-third experienced recent anomalous highs, and one-third of Arctic taxa declined, which is consistent with borealization. Warming temperatures, declining sea ice, and shifting productivity in the Chukchi and northern Bering Seas drive ecosystem changes with significant implications for fisheries, food security, and Indigenous subsistence.

Methods and data

Data were from surveys and models tracking changes in the Arctic marine environment. Most benthic species data came from the Distributed Biological Observatory (DBO). Plankton and fish data came from the Ecosystem and Fisheries Oceanographic Coordinated Investigations (EcoFOCI) (Mordy et al. 2023). Additional data on fish, invertebrates, and crab came from the NOAA Alaska Fisheries Science Center Groundfish Assessment Program (GAP). Chlorophyll data were from DBO and EcoFOCI surveys (Eisner 2016). Zooplankton were sampled by EcoFOCI (Kimmel et al. 2023). Pelagic fish and jellyfish were sampled by EcoFOCI (Murphy et al. 2023). Infauna were sampled with a Van Veen grab (Grebmeier et al. 2018) on Pacific Marine Arctic Regional Synthesis (PacMARS) (Grebmeier and Cooper 2024) and DBO surveys. Epibenthic fish and invertebrates were sampled in the Chukchi Sea (Iken et al. 2019; Markowitz et al. 2024). Bottom water temperature data were from the Pacific Arctic Regional Ocean Modeling System (Danielson et al. 2020), based on the Regional Ocean Modeling System (Curchitser et al. 2013). Spring sea ice concentration was calculated from the National Snow and Ice Data Center (NSIDC) monthly sea ice index (Fetterer et al. 2017). Trends in environmental variables and chlorophyll were defined by comparing annual values to the standard deviation of the long-term mean (Fig. 2).

Time series of zooplankton, fish, and invertebrate population size were standardized using the R-package *tinyVAST* (Thorson et al. 2025). In total, we fit 44 spatio-temporal generalized linear mixed models (ST-GLMM) for the 27 taxa to estimate the indices of population size (Figs. 3-5). Each ST-GLMM estimated a log-linked Tweedie distribution for biological samples while estimating an annually varying intercept as a fixed effect, a spatial latent variable using the stochastic partial differential equation (SPDE) approximation (Lindgren et al. 2011), and a spatio-temporal variable that follows a random walk over time. After fitting the ST-GLMM, we calculated the epsilon-corrected, area-expanded population size index over a given region (Thorson and Kristensen 2016). Strong trends in estimated population size indices were identified when confidence intervals (2 standard deviations, approximating a 95% CI) had little to no overlap among years.

Acknowledgments

Funding by the North Pacific Research Board through its Arctic Integrated Ecosystem Research Program created the unique opportunity to bring together diverse datasets, perspectives, and disciplines. This work was made possible by a multidisciplinary team and by the vision and sustained commitment of Dr. Elizabeth A. Logerwell. Support for I. Ortiz was provided by the Cooperative Institute for Climate, Ocean, and Ecosystem Studies (CICOES) under NOAA Cooperative Agreement NA20OAR4320271.

References

Curchitser, E. N., H. P. Batchelder, D. B. Haidvogel, J. Fiechter, and J. Runge, 2013: Advances in physical, biological, and coupled ocean models during the US GLOBEC program. *Oceanography*, **26**(4), 52-67, https://doi.org/10.5670/oceanog.2013.75.

Danielson, S. L., and Coauthors, 2020: Oceanic routing of wind-sourced energy along the Arctic continental shelves. *Front. Mar. Sci.*, **7**, 509, https://doi.org/10.3389/fmars.2020.00509.

Docquier, D., F. Massonnet, F. Ragone, A. Sticker, T. Fichefet, and S. Vannitsem, 2024: Drivers of summer Arctic sea-ice extent at interannual time scale in CMIP6 large ensembles revealed by information flow. *Sci. Rep.*, **14**, 24236, https://doi.org/10.1038/s41598-024-76056-y.

Eisner, L., 2016: The Bering Sea: Current status and recent trends. *PICES press*, **24**(1), 51-54.

Fetterer, F., K. Knowles, W. N. Meier, M. Savoie, A. K. Windnagel, and T. Stafford, 2025: Sea Ice Index, G02135, Version 4. NSIDC: National Snow and Ice Data Center, Boulder, CO, USA, accessed 2 October 2025, https://doi.org/10.7265/a98x-0f50.

Frey, K. E., J. C. Comiso, L. W. Cooper, J. M. Grebmeier, and L. V. Stock, 2021: Arctic ocean primary productivity: The response of marine algae to climate warming and sea ice decline. *Arctic Report Card 2021*, T. A. Moon, M. L. Druckenmiller, and R. L. Thoman, Eds., https://doi.org/10.25923/kxhb-dw16.

Grebmeier, J. M., and L. W. Cooper, 2024: Benthic observations and ecosystem connections in the Pacific Arctic over temporal and spatial scales. AGU Fall Meeting Abstracts, Vol. 2024, OS21D-0626, doi: 10.1002/essoar.10515159.1, https://agu.confex.com/agu/agu24/meetingapp.cgi/Paper/1686070.

Grebmeier, J. M., and Coauthors, 2006: A major ecosystem shift in the northern Bering Sea. *Science*, **311**(5766), 1461-1464, https://doi.org/10.1126/science.1121365.

Grebmeier, J. M., K. E. Frey, L. W. Cooper, and M. Kędra, 2018: Trends in benthic macrofaunal populations, seasonal sea ice persistence, and bottom water temperatures in the Bering Strait region. *Oceanography*, **31**(2), 136-151, https://doi.org/10.5670/oceanog.2018.224.

Hu, Z.-Z., M. J. McPhaden, B. Huang, J. Zhu, and Y. Liu, 2024: Accelerated warming in the North Pacific since 2013. *Nat. Climate Change*, **14**(9), 929-931, https://doi.org/10.1038/s41558-024-02088-x.

Iken, K., F. Mueter, J. M. Grebmeier, L. W. Cooper, S. L. Danielson, and B. A. Bluhm, 2019: Developing an observational design for epibenthos and fish assemblages in the Chukchi Sea. *Deep Sea Res. II: Top. Stud. Oceanogr.*, **162**, 180-190, https://doi.org/10.1016/j.dsr2.2018.11.005.

Kikuchi, G., H. Abe, T. Hirawake, and M. Sampei, 2020: Distinctive spring phytoplankton bloom in the Bering Strait in 2018: A year of historically minimum sea ice extent. *Deep Sea Res. II: Top. Stud. Oceanogr.*, **181-182**, 104905, https://doi.org/10.1016/j.dsr2.2020.104905.

Kimmel, D. G., L. B. Eisner, and A. I. Pinchuk, 2023: The northern Bering Sea zooplankton community response to variability in sea ice: Evidence from a series of warm and cold periods. *Mar. Ecol. Prog. Ser.*, **705**, 21-42, https://doi.org/10.3354/meps14237.

Lindgren, F., H. Rue, and J. Lindström, 2011: An explicit link between Gaussian fields and Gaussian Markov random fields: the stochastic partial differential equation approach. *J. Roy. Stat. Soc. B*, **73**(4), 423-498, https://doi.org/10.1111/j.1467-9868.2011.00777.x.

Markowitz, E. H., E. J. Dawson, S. N. Wassermann, C. B. Anderson, S. K. Rohan, N. E. Charriere, and D. E. Stevenson, 2024: Results of the 2023 eastern and northern Bering Sea continental shelf bottom trawl survey of groundfish and invertebrate fauna. NOAA Tech. Memo. NMFS-AFSC-487, U.S. Dept. of Commerce, 242 pp., https://doi.org/10.25923/2mry-yx09.

Moore, S. E., J. M. Grebmeier, and J. R. Davies, 2003: Gray whale distribution relative to forage habitat in the northern Bering Sea: current conditions and retrospective summary. *Can. J. Zool.*, **81**(4), 734-742, https://doi.org/10.1139/z03-043.

Mordy, C. W., and Coauthors, 2023: Progress of Fisheries-Oceanography Coordinated Investigations in the Gulf of Alaska and Aleutian Passes. *Oceanography*, **36**(2-3), 94-100, https://doi.org/10.5670/oceanog.2023.218.

Murphy, J., and Coauthors, 2023: Northern Bering Sea ecosystem and surface trawl cruise report, 2021: NOAA Tech. Memo. NMFS-AFSC-479, U.S. Dept. of Commerce, 136 pp., https://doi.org/10.25923/mbyq-xc41.

Nielsen, J. M., and Coauthors, 2024: Spring phytoplankton bloom phenology during recent climate warming on the Bering Sea shelf. *Prog. Oceanogr.*, **220**, 103176, https://doi.org/10.1016/j.pocean.2023.103176.

Thorson, J. T., K. Y. Aydin, M. L. H. Cheng, B. S. Dias, D. G. Kimmel, and K. Kristensen, 2025: Bottom-up interactions in state-space age-structured models using mass-balance dynamics. *Fish Fish.*, **26**(6), 1048-1064, https://doi.org/10.1111/faf.70016.

Thorson, J. T., and K. Kristensen, 2016: Implementing a generic method for bias correction in statistical models using random effects, with spatial and population dynamics examples. *Fish. Res.*, **175**, 66-74, https://doi.org/10.1016/j.fishres.2015.11.016.

January 30, 2026

Weaving the Seen and Unseen: Stewarding the Arctic Means Sustaining Indigenous Monitoring

https://doi.org/ 10.25923/qrm7-bv68

H. -M. Ladd[1], V. M. Padula[1], A. Bishop[2], B. Robson[1], R. Fried[2], B. Barst[3], S. G. Crawford[4], A. R. Gastaldi[4], D. Melovidov[1], and O. M. Gologergen[2]

[1]Aleut Community of St. Paul Island Tribal Government, St. Paul Island, AK, USA
[2]University of Alaska Anchorage, Anchorage, AK, USA
[3]University of Calgary, Calgary, AB, Canada
[4]University of Alaska Fairbanks, Fairbanks, AK, USA

Headlines

- On St. Paul Island, Alaska, the BRAIDED Food Security Project (Building Research Aligned with Indigenous Determination, Equity, and Decision-making) and the newly established Bering Sea Research Center (BSRC) delivered food safety information directly to the community in 2025, weaving what is seen in harvests with what is unseen with analysis of contaminants in traditional foods.
- For over two decades, the Indigenous Sentinels Network (ISN) has collected observations on weather and wildlife by providing the cyberinfrastructure to Indigenous communities and partners to support data collection and governance.
- Weaving the seen and unseen shows why this work matters: Indigenous-led monitoring through BRAIDED, BSRC, and ISN supports Arctic stewardship and community resilience.

Introduction

Across the Arctic, survival has long depended on close observation of lands and waters. Families watch the sea and skies, reading shifts in currents, winds, and wildlife. Knowledge is inseparable from culture: observing is stewardship, livelihood, and science all at once (Carroll 2024). Community members see when sea ice forms late or breaks up too soon. Harvesters know when fish arrive later or when seals show signs of stress. Elders track shifting winds and the silence where birds once nested. Observations are not anecdotes; they are essential data points for decision-making and survival.

For too long, Arctic research has treated Indigenous peoples as “informants” or “stakeholders.” Yet, Indigenous Sentinels and Guardians— Indigenous experts who, like Australia’s Rangers or Canada’s Guardians, combine Traditional Knowledge and Western science to care for their lands and waters— have always been scientists (Government of Canada 2023; National Indigenous Australians Agency 2025; Fox and Jaypoody 2024). Today, their expertise is essential to resilience and research in the Arctic.

Here, we focus on St. Paul Island—the largest of the Pribilof Islands—home to the Unangax̂ (Aleut) peoples (Fig. 1). The island is shaped by winds up to 60 mph and is one of the world’s most ecologically productive marine ecosystems. Currently, this region is experiencing dramatic environmental impacts (Slats et al. 2019). This article tells the story of two interconnected initiatives led by the Aleut

Community of St. Paul Island (ACSPI) Tribal Government: the BRAIDED Food Security Project (Building Research Aligned with Indigenous Determination, Equity, and Decision-making) and the Indigenous Sentinels Network (ISN). These efforts are more than projects; they are pathways to resilience, rooted in Indigenous leadership and designed to meet the challenges of a changing world.

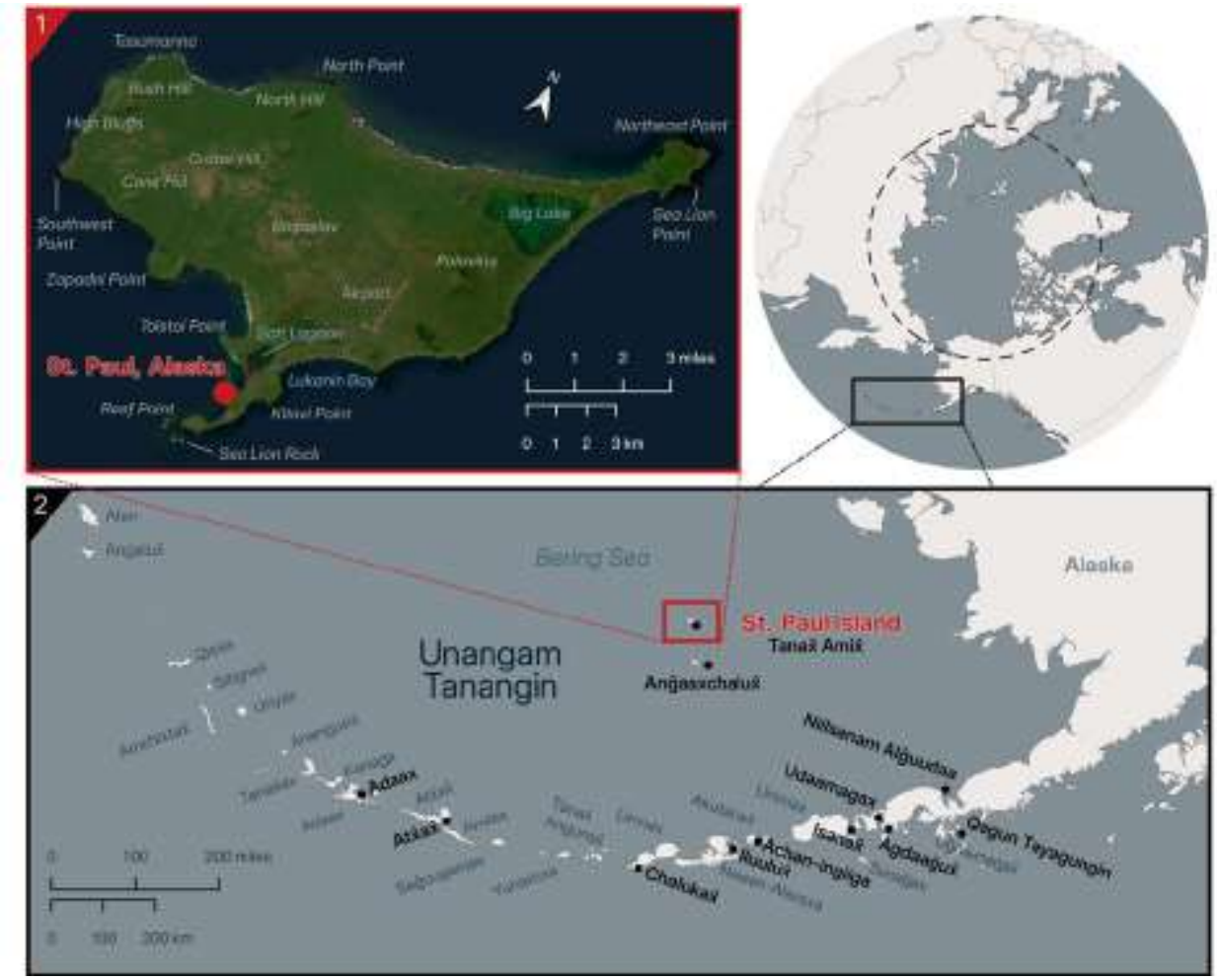

Fig. 1. Map of the Arctic showing (Insert 1): St. Paul Island, the pilot location, the largest of the Pribilof Islands, located at 57.2° N, 170.3° W. The city of St. Paul, Alaska (Tanaŝ Amiŝ) is located on the southern peninsula of the island. (Inset 2): The Aleutian Islands (Unangam Tanangin) with island (blue) and village (black) names in Unangam Tunuu, the Indigenous language of the Aleutian and Pribilof Islands region. Credit: Matthew Druckenmiller.

Background

In the 18th and 19th centuries, Russian and U.S. regimes forcibly relocated Unangaŝ communities to the Pribilof Islands for commercial fur seal harvests (Torrey 1983). After the United States purchased Alaska from Russia in 1867, federal policies in the 1870s continued to exert tight control over Unangaŝ communities on the Pribilofs, reflecting the long arc of colonial management that shaped local governance and resource use (Torrey 1983; Burch 1998). Despite this tragic history, the people of St. Paul Island have remained deeply connected to their environment. From an Indigenous perspective, our ecosystems are a living network of relatives, providers, kin, and teachers who are woven into identities and cultures (Carothers et al. 2021). Impacts to our environments are not only an ecological crisis but

also a cultural one, rooted in both the historic trauma of forced relocation and in the ongoing grief that comes with threats to the right to remain in one's homeland.

Recognizing this reality, the ACSPI has spent decades building local leadership in economic development and research so that St. Paul Island would not just be a site of study but a full partner, with Tribal leadership shaping and governing the work.

Two initiatives now carry this vision forward:

The **BRAIDED Food Security Project** began as a pilot in 2023 to test new ways of monitoring contaminants and strengthen community control over decisions related to food safety. Mercury is a World Health Organization top ten contaminant of concern. BRAIDED aimed to monitor mercury by establishing the Bering Sea Research Center (BSRC) on St. Paul Island. Instead of sending samples off-island—a process requiring expensive shipping from one of the most remote communities in the Bering Sea and long waits for results—Tribal staff can now receive donated tissues from harvesters, process them locally at BSRC, and analyze fish, seals, seabirds, and other harvested foods. The pilot phase, completed in 2025, laid the foundation for the program's continuation and expansion by building the capacity and confidence of Tribal staff to independently assess the health of harvested foods and maintain on-island laboratory operations.

The **ISN** builds on more than 20 years of local innovation. Created and designed by ACSPI, ISN is a suite of software tools supported by training programs that allow Tribes to design and manage their own monitoring programs across the state of Alaska. ISN's foundation is Indigenous Data Sovereignty (IDSov): all data are owned and controlled by the communities that collect them. ISN trains Sentinels and Guardians to collect observations within their communities. ISN data are stored in secure systems, but can also be connected to larger Arctic research networks.

Together, BRAIDED and ISN show what it means for Indigenous communities to lead Arctic research. Four themes woven throughout this work illustrate the impact of Tribally-led research: community-driven monitoring, food safety, IDSov, and training and capacity building.

Community-driven monitoring: Sentinels and Guardians as eyes and ears for lands and waters

Resilience depends on seeing change as it happens. While conventional Arctic science often relies on short-term field seasons, Indigenous peoples live in a deep relationship with place. Implementing monitoring programs that are driven by communities ensures that essential knowledge and observations are informing stewardship of lands and waters in real time (see Figs. 2 and 3).

Fig. 2. Coastal erosion monitoring in Golovin, Alaska, is conducted by local observers documenting shoreline change as part of regional monitoring efforts. Such observations provide critical information for understanding climate impacts in vulnerable communities. Credit: Hannah-Marie Ladd.

Fig. 3. A group of four Sentinels and two NOAA NMFS officials conduct surveys on Northern Fur Seal rookeries on St. Paul Island. Sentinels use long-standing knowledge of rookery behavior, seasonal timing, and seal movement patterns to guide when and where surveys occur, complementing co-management efforts with NOAA NMFS. Together, they monitor population numbers and search for entanglements as part of a co-management agreement to protect this vital marine species. Credit: Hannah-Marie Ladd.

The ISN provides cyberinfrastructure and a supportive network for community-driven monitoring. Outside scientists engage through partnerships that bring in technical expertise, while adhering to community protocols for access and use of data. ISN equips Sentinels and Guardians with tools, technology, and training, including a community-owned database, mobile data-collection apps, and reporting dashboards, that empower them to document their observations (see Figs. 4 and 5). For example, Sentinels often use traditional knowledge of the seasons to determine when to begin monitoring efforts, what species or conditions warrant attention, and how to interpret unusual

observations. The result is science and research that are both more accountable, place-based, and adaptive: local decisions are informed by Traditional Knowledge, lived experiences, and local expertise, data gaps are filled, research is collaborative, and global research benefits from knowledge shared from the frontlines of change.

Fig. 4. An observer logs data into the Anadromous Waters Catalogue (AWC) while surveying a stream in Southcentral Alaska. The AWC supports monitoring of fish habitats, and the Fish Map App, powered by ISN, enhances data collection and community participation in fisheries stewardship. Credit: Lee House.

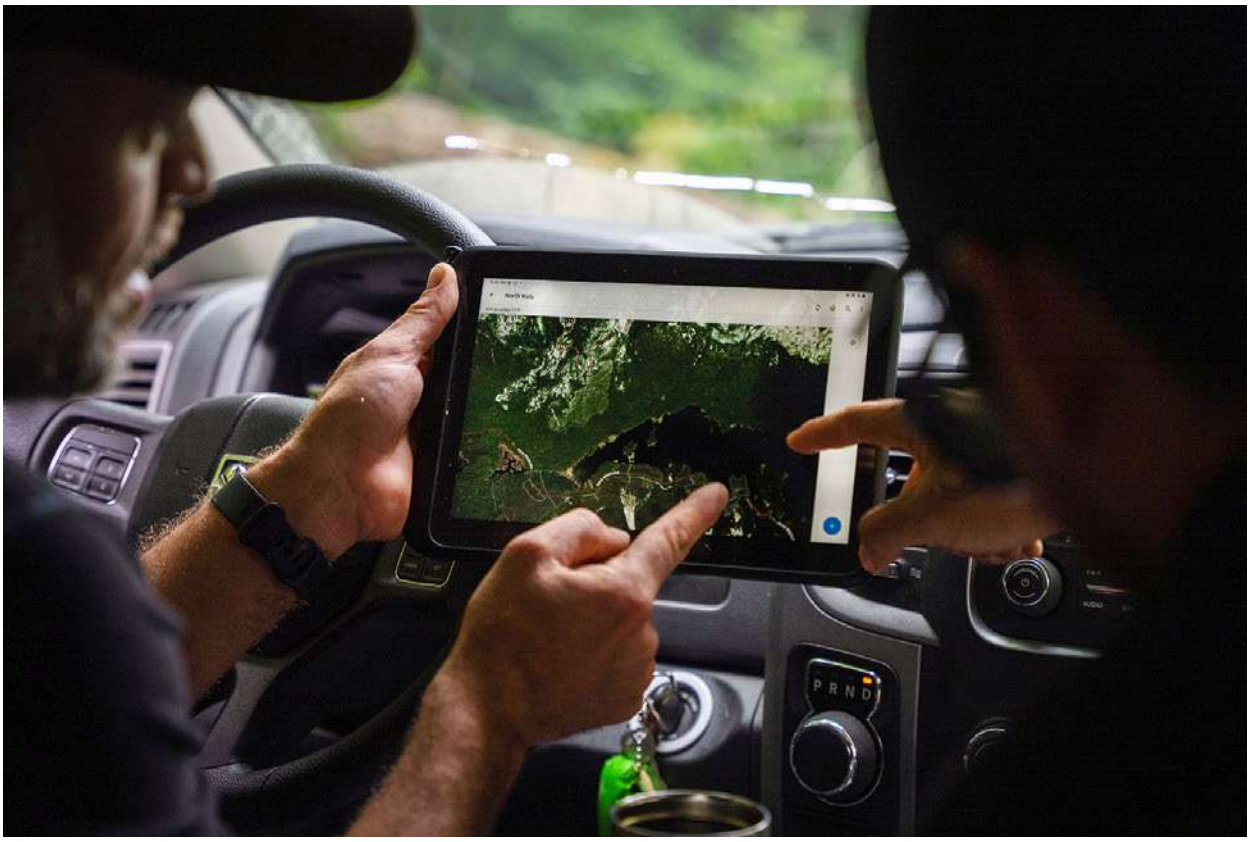

Fig. 5. Observers in Southeast Alaska use GPS tools to log vital data for the AWC. Integrating mobile technology empowers communities to drive data collection and support sustainable fisheries management. Credit: Lee House.

Food safety: Food security is climate security

For Arctic communities, food safety and concerns about contaminants have caused stress and changes in diet. The BRAIDED Project has had a demonstrable positive impact by embedding environmental monitoring and research directly within the ACSPI. The BRAIDED project departs from conventional citizen science by placing community members at the helm of the research process, with scientists acting as collaborators rather than gatekeepers (UAA 2024), strengthening the relevance, quality, and quantity of data being collected. The BRAIDED project has relied on long-standing relationships and trust with university researchers, where earlier partnerships laid the foundation for BRAIDED to take root. By equipping local staff to test harvested foods in the BSRC, scientists have succeeded in increasing trust, timeliness, and community capacity, and are aware that they will eventually 'put themselves out of a job.'

Quantitative outcomes from the first year in 2024 included nearly 100 tested biological samples, ranging from marine mammals to seabirds, analyzed locally by community members (UAA 2024). The samples were tested for mercury contamination using a Nippon MA-Solo direct mercury analyzer, with results uploaded to ISN. While there are no current guidelines for mercury levels in marine mammals in Alaska, BRAIDED supports community interpretation by pairing each result with textual reports and visual summaries presented to the Tribal council, using familiar reference points, such as Alaska fish consumption advisories, to contextualize values. During community presentations, report-backs, and one-on-one conversations, Tribal staff help interpret mercury results for harvesters and families. A formal training course (described below) further introduced participants to how mercury moves through

marine ecosystems and how to interpret results within traditional harvesting practices. Together, these approaches ensure that results are communicated in accessible ways and interpreted locally under Tribal leadership as the program continues to develop.

Data sovereignty: Trust, governance, and resilience

IDSov ensures that information collected about Indigenous peoples, their lands, waters, and knowledge systems remains under their ownership and governance. The FAIR (Findable, Accessible, Interoperable, Reproducible) principles for data management are widely known and broadly endorsed. They emphasize machine readability, "distinct from peer initiatives that focus on the human scholar" (Wilkinson et al. 2016). In contrast, the CARE Principles (Collective Benefit, Authority to Control, Responsibility, Ethics) developed through the Global Indigenous Data Alliance reflect the human side of data and ask researchers to put human well-being at the forefront of open-science and data sharing practices (Carroll et al. 2020).

ISN is designed with IDSov and CARE principles at its core and supports communities and Tribes across Alaska in defining access, ownership, and governance of their data. IDSov is not only about protection; it is also about stewarding data to ensure resilient knowledge systems.

Training and capacity building

Resilience requires training and intergenerational learning; without it, monitoring risks being temporary. In 2024, BRAIDED partnered with Iḷisaġvik College to offer an in-person accredited "One Health" course on St. Paul Island, which emphasized the interconnected health of people, animals, and ecosystems, and brought together Elders, harvesters, youth, and community to explore these connections (UAA 2024).

Course instruction and training included:

- Place-based instruction at the BSRC, using samples from local harvests to teach laboratory procedures.
- Mentorship from trained local Sentinels, ensuring the transfer of skills within the community.
- Integration of Traditional knowledge alongside scientific techniques, grounding in local harvesting methods and emphasizing the nutritional benefits of traditional foods.

Participants demonstrated measurable gains in awareness and understanding of mercury contamination, food safety, and laboratory techniques (National Institute of Food and Agriculture 2024). These findings illustrate that community-driven monitoring is not only scientifically rigorous but a vehicle for (re)building capacity. Both physical infrastructure, like the BSRC, and cyberinfrastructure, like the ISN, anchor capacity and training for generational resilience.

Conclusion

The BRAIDED project and ISN show what is possible when Indigenous communities lead: timely, locally-controlled information, earlier warnings, protected data, and trained local experts. These projects center on Tribal sovereignty and community leadership, not as an added benefit, but as the foundation of Arctic resilience. Supporting them means supporting Arctic resilience. Importantly, support requires more than recognition; it requires investment in several measurable forms:

- Sustained funding for Indigenous-led monitoring programs that go beyond pilot projects, including long-term operational support, staffing, and training.
- Infrastructure support, from community laboratories like the BSRC to digital systems that uphold IDSov and CARE principles, like ISN or other existing databases.
- Workforce development, creating long-term, regenerative jobs for Sentinels and Guardians.
- Partnerships that position Tribes as leaders, not stakeholders, in Arctic research.

Supporting Indigenous-led monitoring is both an ethical imperative and a practical investment in innovation. Arctic resilience depends on shifting power and resources to communities that have cared for their lands and waters for millennia. BRAIDED and ISN show us how. Now it is time to scale up, strengthen, and sustain this work for St. Paul Island, for the Bering Sea, for the Arctic, and for all the ecosystems that support and sustain us.

This work was funded by USDA-NIFA (project accession #1031690).

References

Burch, E. S., 1998: The Eskimo and Aleut peoples: Their history and cultural traditions. Arctic Research Consortium of the United States (ARCUS), Fairbanks, AK.

Carothers, C., and Coauthors, 2021: Indigenous peoples and salmon stewardship: a critical relationship. *Ecol. Soc.*, **26**(1), 16, https://doi.org/10.5751/ES-11972-260116.

Carroll, S. R., 2024: Indigenous peoples breathing data back. TEDxUArizona. [Available online at https://www.youtube.com/watch?v=jPS_3mZXWXw]

Carroll, S. R., I. Garba, O. L. Figueroa-Rodríguez, J. Holbrook, R. Lovett, S. Materechera, M. Parsons, K. Raseroka, D. Rodriguez-Lonebear, R. Rowe, R. Sara, J. D. Walker, J. Anderson, and M. Hudson, 2020: The CARE principles for Indigenous data governance. *Data Sci. J.*, **19**, 43, https://doi.org/10.5334/dsj-2020-043.

Fox, S., and M. Jaypoody, 2024: The original researchers: Hunters are scientists deserving sustained support. *Arctic Report Card 2024*, T. A. Moon, M. L. Druckenmiller, and R. L. Thoman, Eds., https://doi.org/10.25923/af21-r537.

Government of Canada, 2023: Indigenous Guardians. Environment and Climate Change Canada. Accessed 22 September 2025, https://www.canada.ca/en/environment-climate-change/services/environmental-funding/indigenous-guardians.html.

National Indigenous Australians Agency, 2025: Indigenous Rangers Program (IRP). Australian Government. Accessed 22 September 2025, https://www.niaa.gov.au/our-work/environment-and-land/indigenous-rangers-program-irp.

National Institute of Food and Agriculture (NIFA), 2024: BRAIDED Food Security – Building research aligned with Indigenous determination, equity, and decision-making. USDA NIFA Project report.

Slats, R., C. Oliver, R. Bahnke, H. Bell, A. Miller, D. Pungowiyi, J. Merculief, N. Menadelook Sr., J. Ivanoff, and C. Oxereok, 2019: Voices from the front lines of a changing Bering Sea: An Indigenous Perspective

for the 2019 Arctic Report Card. M. L. Druckenmiller, R. Daniel, and M. Johnson, Eds. *Arctic Report Card 2019*, J. Richter-Menge, M. L. Druckenmiller, and M. Jeffries, Eds., https://arctic.noaa.gov/report-card/report-card-2019/voices-from-the-front-lines-of-a-changing-bering-sea/.

Torrey, B. B., 1983: Slaves of the harvest. St. Paul Island, AK: TDX Corp.

University of Alaska Anchorage (UAA), 2024: BRAIDED Food Security Project: Building research aligned with Indigenous determination, equity, and decision-making. University of Alaska Anchorage Project booklet.

Wilkinson, M. D., and Coauthors, 2016: The FAIR Guiding Principles for scientific data management and stewardship. *Sci. Data*, **3**, 160018, https://doi.org/10.1038/sdata.2016.18.

December 4, 2025

Rusting Rivers: Assessing the Causes and Consequences in Alaska and Across the Arctic

https://doi.org/10.25923/f3tr-5759

J. A. O'Donnell[1], M. P. Carey[2], J. C. Koch[2], C. Baughman[2], K. Hill[3], T. Evinger[4], A. Pruitt[4], C. Thompson[3], E. Graham[5], and B. A. Poulin[4]

[1]National Park Service, Arctic Network, Anchorage, AK, USA
[2]U.S. Geological Survey, Alaska Science Center, Anchorage, AK, USA
[3]National Park Service, Arctic Network, Fairbanks, AK, USA
[4]Department of Environmental Toxicology, University of California Davis, Davis, CA, USA
[5]Geophysical Institute, University of Alaska Fairbanks, Fairbanks, AK, USA

Headlines

- In Arctic Alaska, surface waters have changed from clear to orange in over 200 watersheds, with most changes occurring within the past decade. Evidence suggests this "rusting" is an emerging issue due to iron release from thawing permafrost soils.
- Rusting rivers have degraded water quality and habitat, with increased acidity and toxic trace metal concentrations contributing to a loss of aquatic biodiversity in headwater streams.
- Ongoing research aims to understand the causes and consequences of rusting rivers, particularly regarding impacts to drinking water supplies for rural communities and subsistence fisheries.

Introduction

Terrestrial and aquatic ecosystems of the Arctic are undergoing rapid change due to the impacts of a changing climate and ecosystem disturbances. One climate-driven disturbance, permafrost thaw, is altering watershed hydrology and biogeochemical cycles (e.g., carbon cycling), with implications for coastal waters and marine ecosystems. Recent ground-based, aerial, and satellite observations from remote watersheds of northern Alaska indicate that hundreds of streams and rivers have shifted from pristine, clear water to an orange “rusting” condition, with many sites changing over the past decade (O’Donnell et al. 2024). This abrupt change appears to be an unanticipated consequence of permafrost thaw in the Arctic, and represents an emergent risk to water quality and aquatic life (Miner et al. 2021).

The leading hypothesis describing this recent phenomenon is that permafrost thaw is exposing previously inaccessible mineral deposits, such as sulfide minerals (e.g., pyrite), to chemical weathering. These abiotic processes in the subsurface generate acid, sulfate, and metals that are transported by groundwater flow to stream ecosystems. Rusting rivers indicate the presence of oxidized iron particles, but laboratory analyses indicate that orange-colored streams also have elevated concentrations of toxic trace metals like copper, aluminum, and zinc. In this essay, we discuss the spatial and temporal patterns of rusting rivers, the broader historical context of permafrost thaw and weathering processes, and the implications for water quality and fisheries across the Circum-Arctic region.

Occurrence and causes of rusting rivers

In a 2024 study, we reported on the emergence of 75 streams in Alaska's Brooks Range that had turned from clear to orange (O'Donnell et al. 2024). Since then, we have compiled additional observations from more than 200 streams and rivers that are discolored (Fig. 1; Hill 2024). These rusting rivers are visually striking (Fig. 2a,c,e) and are readily detected using satellite imagery. Using historical satellite imagery, we showed that most of these streams have changed color in the past 10 years. This shift coincides with a dramatic increase in air and ground temperatures across the region, indicating that recent permafrost thaw is a likely driver (Swanson et al. 2021).

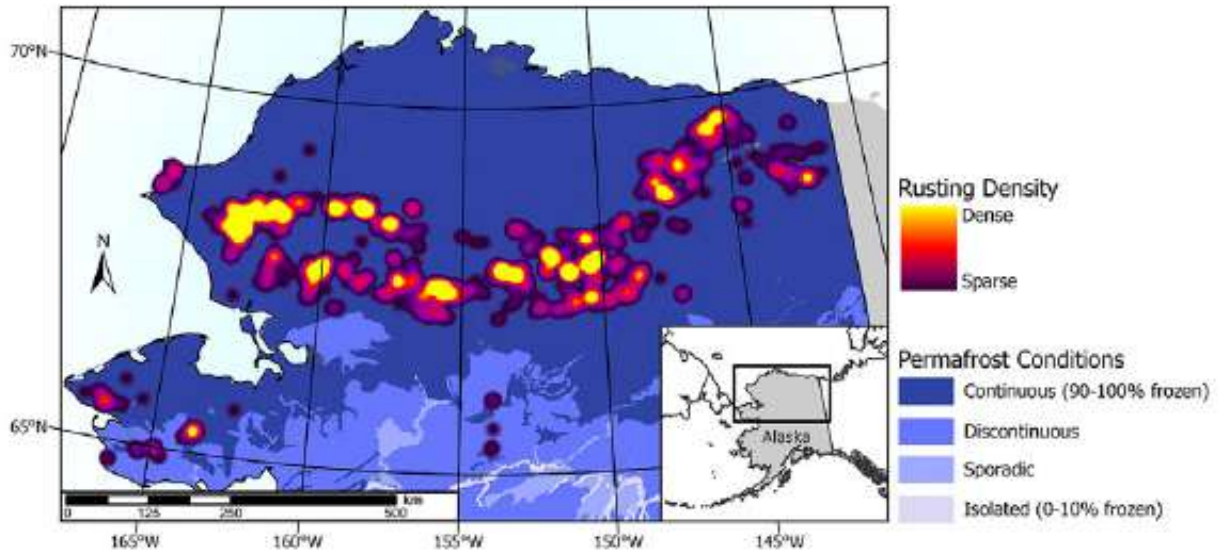

Fig. 1. Heat map depicting density of rusting rivers in northern Alaska based on in situ and satellite observations from 2007-24. The base map depicts permafrost zones as classified by Jorgenson et al. (2008).

A more in-depth analysis of a U.S. Geological Survey (USGS) Landsat satellite time series for a subset of streams indicated that (1) rusting initiated around 2018 and has continued, and (2) some streams had prior periods of rusting and recovered to clear-water conditions (Fig. 2b,d,f). It is currently unknown what drives interannual and seasonal patterns of stream discoloration. The winter of 2017/18 was also a year of deep snowpack (Mudryk et al. 2018; see essay *Snow Cover*), which can accelerate thaw. Further, seasonal variation in stream flow can influence stream color, with high flow conditions diluting the appearance of iron oxides. There are certainly rusting rivers that precede this recent period of warming. However, the abrupt increase in the number of rusting rivers and the broad spatial extent of these observations (more than 1000 km west to east) suggest regional climate drivers and soil thaw are likely to have caused the emergence of these discolored waters.

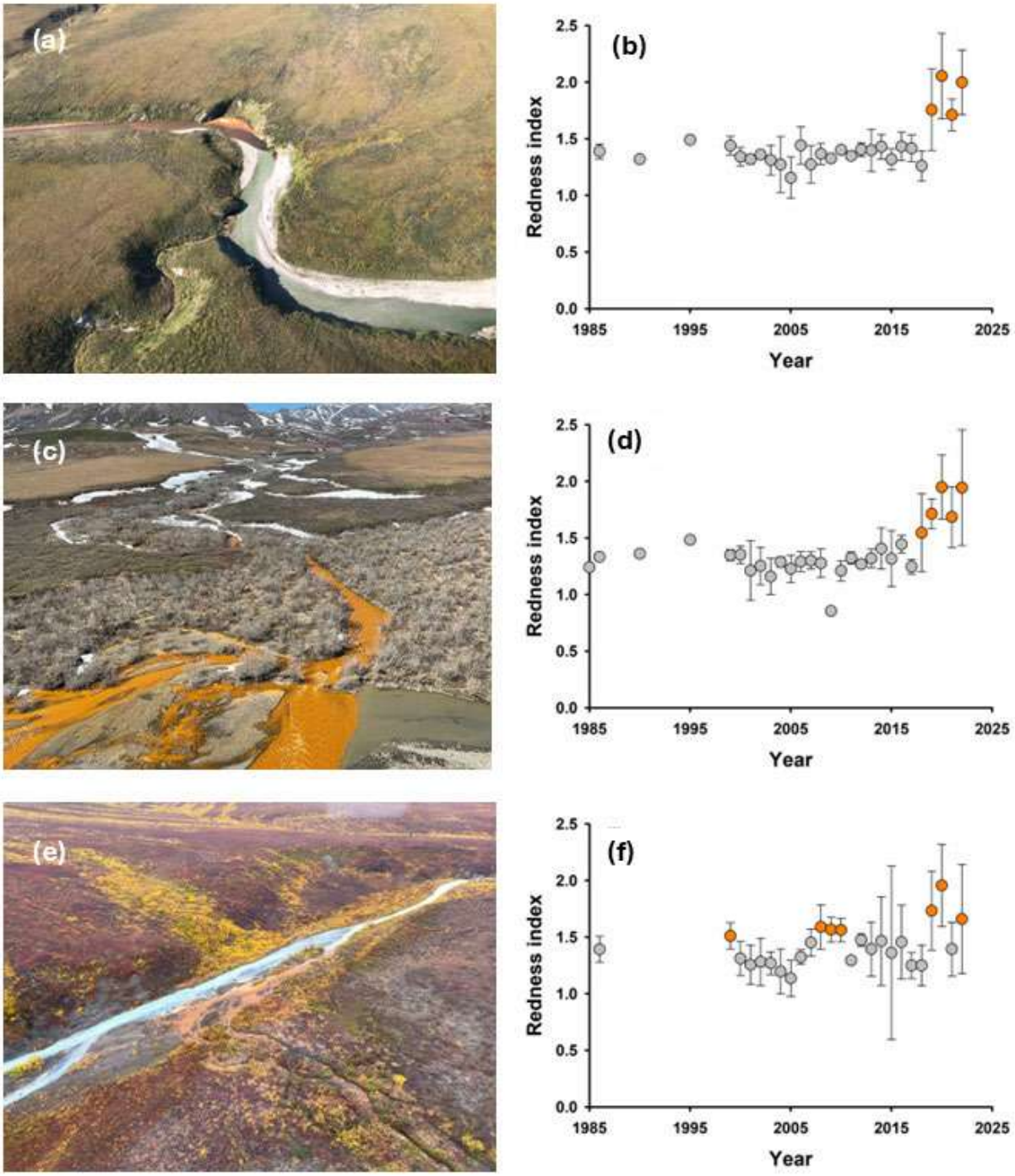

Fig. 2. Photographs of rusting rivers and time series plots of Redness Index for watersheds in Alaska's Brooks Range, including the Agashashok River (Noatak National Preserve, panels a, b), the Kugururok River (Noatak National Preserve, panels c, d), and Anaktok Creek, a tributary of the Salmon Wild and Scenic River in Kobuk Valley National Park (panels e, f). The time-series data were generated from Landsat satellite images using average Redness Index values for summer months of each year from 1985 through 2022. Redness index, which represents the presence of iron oxides, was calculated as the ratio of surface reflectance of the red and blue bands. The orange circles with mean (± standard deviation) Redness Index values > 1.5 indicate waters discolored by iron particles. Grey circles represent mean Redness Index values < 1.5, indicating clear water or streams unimpacted by iron mobilization. Photo credits: Jonathan O'Donnell/NPS, Michael Carey/USGS, and Joshua Koch/USGS.

Much of the rusting we observed was due to acid rock drainage—chemical weathering that releases iron, acid, sulfate, and trace metals (e.g., copper, zinc, and others) into surface waters (Fig. 3). Rusting rivers are common in the continuous permafrost zone (Fig. 1) and in alpine and rocky watersheds of the Brooks Range where sulfide minerals like pyrite are present. Acid rock drainage waters often emerge via groundwater seeps that develop on terrestrial hillslopes and drain into streams and rivers. As the climate warms and permafrost thaws, groundwater can be rerouted to deep soil layers where it can drive chemical weathering reactions and the mobilization of acid and toxic metals (Fig. 4). Widespread talik formation (i.e., the development of year-round unfrozen layers in permafrost soils) may be an important contributor to this phenomenon (Farquharson et al. 2022). While acid rock drainage appears to be the dominant process contributing to stream impairment, rusting rivers can also be caused by microbial mobilization of soil iron stocks in response to permafrost thaw, shifting soil drainage, and changing redox conditions (Barker et al. 2023; Fig. 4). This microbial pathway can cause streams to turn orange from iron particulates, but these streams do not have elevated toxic metal concentrations as in the case of acid rock drainage.

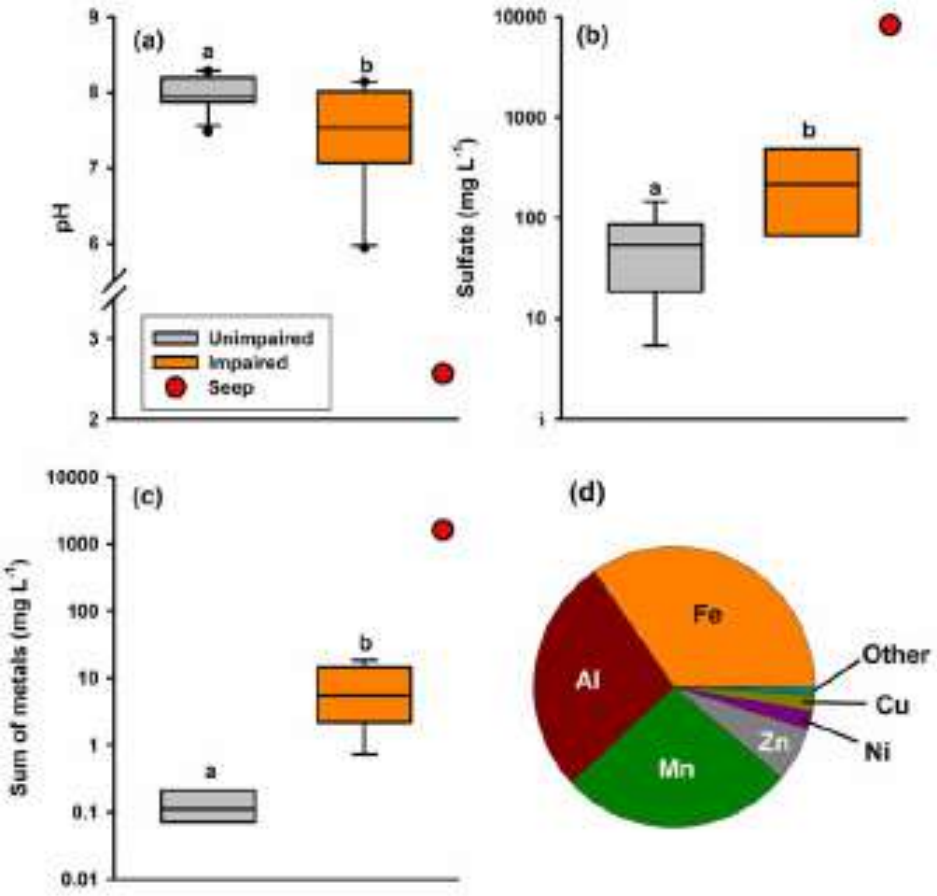

Fig. 3. Summary of geochemical observations from impaired rusting rivers, unimpaired reference sites, and impaired groundwater seeps. (a) Impaired sites and groundwater seeps are more acidic (i.e., have low pH) than unimpaired clearwater sites. (b) Impaired sites and seeps have higher sulfate concentrations than unimpaired sites, indicating the chemical weathering of sulfide minerals (e.g., pyrite). (c) The sum of total metals is higher in impaired sites and seeps than in unimpaired sites. Note: panels (b) and (c) are plotted in log scale. (d) The pie chart presents the average distribution of metals from impaired, rusting rivers. Major metals like iron (Fe), aluminum (Al), and manganese (Mn) dominate. However, concentrations of toxic travel metals, such as zinc (Zn), nickel (Ni), copper (Cu), and others, are also present at high concentrations.

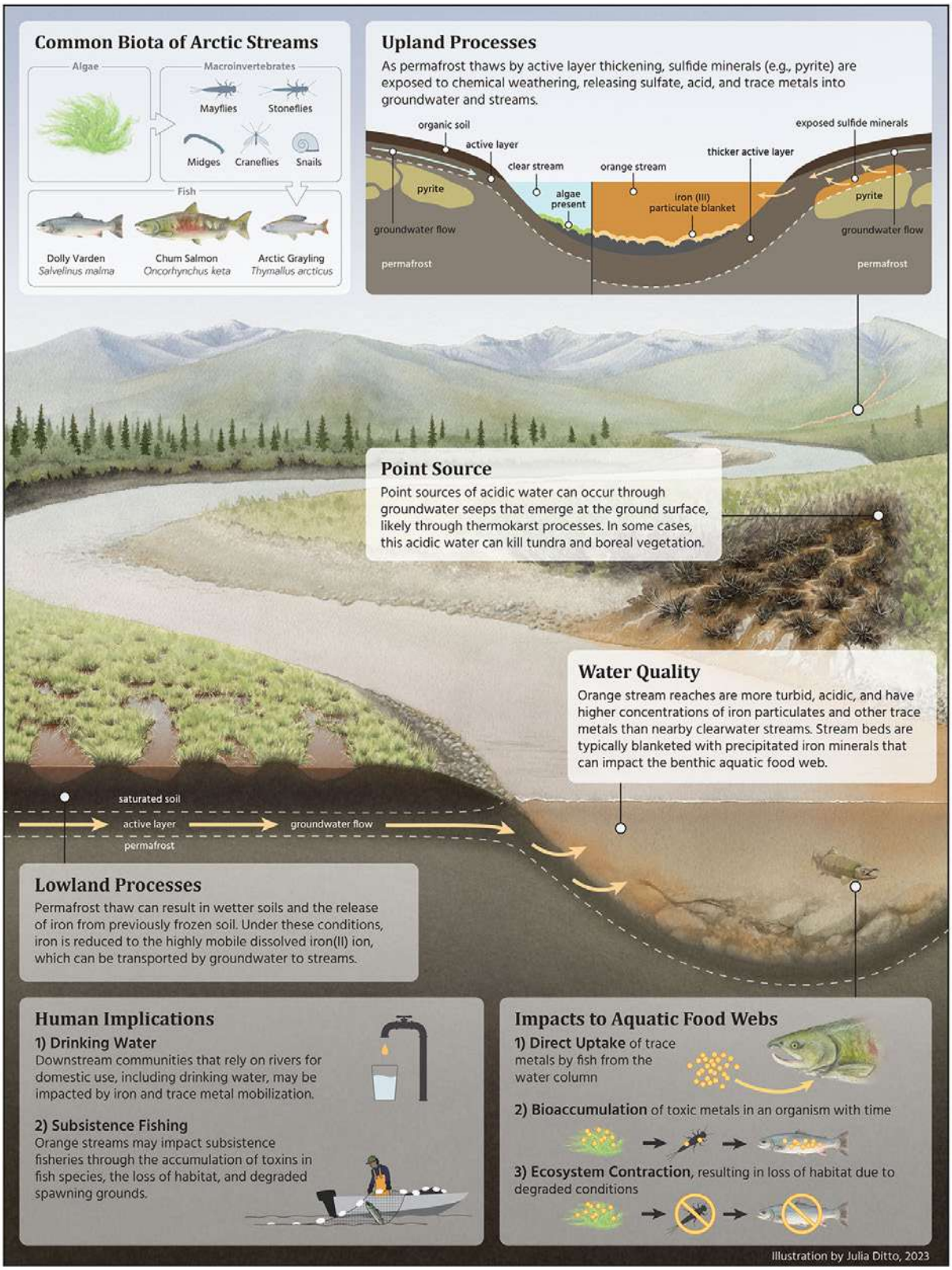

Fig. 4. Conceptual illustrations of hypothesized processes contributing to rusting rivers in northern Alaska and their impacts. Illustration by Julia Ditto, 2023

Observations of iron mobilization from Alaska's North Slope and in peatlands of northern Sweden are likely due to microbial mobilization of iron, not acid rock drainage, in part due to their topographic setting in lowland tundra (Barker et al. 2023; Patzner et al. 2020). Depending on the setting, these lowland rusting rivers could have occurred throughout recent history during periods of soil wetting and drying, and in the absence of permafrost thaw. Whatever mechanisms may be occurring, the increased flux of iron from rivers to the coast could increase marine primary productivity, which is limited in part by iron availability (see essay *Primary Productivity*).

Why river rusting matters

Arctic rivers provide habitat for a broad array of fish, many of which are critical for subsistence, sport, and commercial fisheries. Climate change is already impacting high-latitude fish species, including Pacific salmon (*Oncorhynchus* spp.), due to effects of warming on marine and freshwater ecosystems (see essay *Warming Waters and Borealization*). Adding to those concerns, mobilization of iron and toxic metals to Arctic streams in northern Alaska may degrade water quality, reduce habitat, and bioaccumulate in aquatic food webs.

Within Kobuk Valley National Park, we observed a sharp decrease in stream biodiversity at an existing monitoring location when a headwater tributary of the Akillik River changed from clear to orange between early and late summer of the same year (O'Donnell et al. 2024). We documented the complete loss of fish species, juvenile Dolly Varden (*Salvelinus malma*) and Slimy Sculpin (*Cottus cognatus*), after an abrupt increase in stream acidity. The loss of fish coincided with a steep decrease in benthic (bottom dwelling) macroinvertebrate diversity and algal biomass on the stream bed. While the underlying causes for this decline in biodiversity are unknown, evidence from the Salmon Wild and Scenic River in Kobuk Valley National Park indicates that many rusting rivers exceed chronic metal exposure criteria established by the U.S. Environmental Protection Agency (EPA; Sullivan et al. 2025).

Beyond the effects on fish, rusting rivers may impact drinking water supplies to rural communities. Some metals, such as cadmium, nickel, and manganese, exceeded either EPA drinking water criteria or World Health Organization guidelines in orange-colored streams (O'Donnell et al. 2024). At a minimum, this disturbance may present taste issues for drinking water that require enhanced water filtration to mitigate the increase in metals. In rural Alaska, climate and permafrost thaw present direct threats to water resources. Disturbance along river corridors, including bank erosion and retrogressive thaw slumps (i.e., landslides caused by thawing permafrost soils), can profoundly affect water quality through deposition of sediments, nutrients, and ions in river water. The observed presence of dissolved and particulate metals through processes described here present a similar challenge to drinking water access in remote Alaska, particularly for villages near rusting rivers.

These findings of water quality degradation in northern Alaska clarify broader implications for the Circum-Arctic region and waters draining landscapes undergoing permafrost thaw and deglaciation (see essay *Glaciers and Ice Caps*). Recent work has documented the relationship between permafrost thaw and sulfide chemical weathering in the Yukon and Mackenzie rivers in western Canada and Alaska (Kemeny et al. 2023). Another recent review highlighted concerns for water quality across the northern permafrost region due to these underlying processes (Skierszkan et al. 2024). Other studies have documented rusting and metal mobilization in watersheds undergoing mountain permafrost thaw or glacier melt, as in temperate regions of the Alps and tropical regions of Peru (Santofimia et al. 2017; Wanner et al. 2023). These global observations point toward the broader loss of the cryosphere as an

issue driving water quality impairment. Additional research could help better understand the causes and consequences of this emerging environmental issue.

Methods and data

Detailed field, remote sensing, and analytical methods can be found in O'Donnell et al. (2024). USGS and the National Park Service have published data releases for observations of rusting rivers (Hill 2024), stream and river chemistry (Koch et al. 2023), and aquatic biota (Carey et al. 2023). Additional photographs of rusting rivers are hosted by the USGS. A five-minute video documenting rusting rivers was produced by the University of California Davis and can be accessed via YouTube. Any use of trade, firm, or product names is for descriptive purposes only and does not imply endorsement by the U.S. Government.

References

Barker, A. J., T. D. Sullivan, W. B. Baxter, R. A. Barbato, S. Gallaher, G. E. Patton, J. P. Smith, and T. A. Douglas, 2023: Iron oxidation-reduction processes in warming permafrost soils and surface waters expose a seasonally rusting Arctic watershed. *ACS Earth Space Chem.*, **7**(8), 1479-1495, https://doi.org/10.1021/acsearthspacechem.2c00367.

Carey, M. P., J. C. Koch, J. A. O'Donnell, and A. Riddle-Berntsen, 2023: Length, weight, energy density, and isotopic values of fish from rivers in Northwest Alaska, 2015-2019. U.S. Geological Survey data release, accessed 24 September 2025, https://doi.org/10.5066/P9WGRX66.

Farquharson, L. M., V. E. Romanovsky, A. Kholodov, and D. Nicolsky, 2022: Sub-aerial talik formation observed across the discontinuous permafrost zone of Alaska. *Nat. Geosci.*, **15**, 475-481, https://doi.org/10.1038/s41561-022-00952-z.

Hill, K., 2024: Orange streams observations: geographic coordinates and maps. National Park Service, Fairbanks, Alaska, accessed 23 August 2025, https://irma.nps.gov/DataStore/Reference/Profile/2303647.

Jorgenson, M. T., and Coauthors, 2008: Permafrost characteristics of Alaska. Proceedings of the Ninth International Conference on Permafrost, Fairbanks, University of Alaska, pp. 121-122.

Kemeny, P. C., and Coauthors, 2023: Arctic permafrost thawing enhances sulfide oxidation. *Global Biogeochem. Cycles*, **37**(11), e2022GB007644, https://doi.org/10.1029/2022GB007644.

Koch, J. C., B. Poulin, J. A. O'Donnell, M. P. Carey, and T. Evinger, 2023: Chemistry of orange and reference streams in Northwestern Alaska, 2022. U. S. Geological Survey data release, accessed 24 September 2025, https://doi.org/10.5066/P9DZSQ43.

Miner, K. R., J. D'Andrilli, R. Mackelprang, A. Edwards, M. J. Malaska, M. P. Waldrop, and C. E. Miller, 2021: Emergent biogeochemical risks form Arctic permafrost degradation. *Nat. Climate Change*, **11**, 809-819, https://doi.org/10.1038/s41558-021-01162-y.

Mudryk, L., R. Brown, C. Derksen, K. Luojus, B. Decharme, and S. Helfrich, 2018: Terrestrial snow cover. *Arctic Report Card 2018*, https://arctic.noaa.gov/report-card/terrestrial-snow-cover-5/.

O'Donnell, J. A., and Coauthors, 2024: Metal mobilization from thawing permafrost to aquatic ecosystems is driving rusting of Arctic streams. *Commun. Earth Environ.*, **5**, 268, https://doi.org/10.1038/s43247-024-01446-z.

Patzner, M. S., and Coauthors, 2020: Iron mineral dissolution releases iron and associated organic carbon during permafrost thaw. *Nat. Commun.*, **11**, 6329, https://doi.org/10.1038/s41467-020-20102-6.

Santofimia, E., E. López-Pamo, E. J. Palomino, E. González-Toril, and Á. Aguilera, 2017: Acid rock drainage in Nevado Pastoruri glacier area (Huascarán National Park, Perú): hydrochemical and mineralogical characterization and associated environmental implications. *Environ. Sci. Pollut. Res.*, **24**, 25243-25259, https://doi.org/10.1007/s11356-017-0093-0.

Skierszkan, E. K., J. W. Dockrey, and M. B. J. Lindsay, 2024: Metal mobilization from thawing permafrost is an emergent risk to water resources. *ACS EST Water*, **5**(1), 20-32, https://doi.org/10.1021/acsestwater.4c00789.

Sullivan, P. F., R. J. Dial, D. J. Cooper, C. Diamond, C. J. Tino, D. D. Gregory, R. E. Wong, and T. W. Lyons, 2025: Wild, scenic, and toxic: Recent degradation of an iconic Arctic watershed with permafrost thaw. *Proc. Natl. Acad. Sci.*, **122**(37), e2425644122, https://doi.org/10.1073/pnas.2425644122.

Swanson, D. K., P. J. Sousanes, and K. Hill, 2021: Increased mean annual temperatures in 2014-2019 indicate permafrost thaw in Alaskan national parks. *Arct. Antarct. Alp. Res.*, **53**(1), 1-19, https://doi.org/10.1080/15230430.2020.1859435.

Wanner, C., H. Moradi, P. Ingold, M. A. Cardenas Bocanegra, R. Mercurio, and G. Furrer, 2023: Rock glaciers in the Central Eastern Alps – How permafrost degradation can cause acid rock drainage, mobilization of toxic elements and formation of basaluminite. *Global Planet. Change*, **227**, 104180, https://doi.org/10.1016/j.gloplacha.2023.104180.

November 24, 2025

Assessing the State of the Arctic Observing Network: Strengths, Gaps and Risks to Systems that Track Arctic Change

https://doi.org/ 10.25923/m8k4-9558

S. Starkweather[1,2], M. B. Armstrong[3], and H. Shapiro[4]

[1]Cooperative Institute for Research in Environmental Sciences, University of Colorado Boulder, Boulder, CO, USA
[2]Physical Sciences Laboratory, NOAA, Boulder, CO, USA
[3]Sea Grant Knauss Fellowship, Arctic Research Program, Global Ocean Monitoring and Observing Program, NOAA, Silver Spring, MD, USA
[4]UIC Science, Utqiaġvik, AK, USA

Headlines

- Internationally coordinated Arctic observing infrastructure and data-sharing capabilities deliver critical information that supports decision-making from local to global scales, including through contributions to scientific assessments such as the Arctic Report Card.
- Persistent gaps in Arctic observing systems limit our ability to fully understand and respond to changing conditions. For example, sparse precipitation gauges in complex terrain cause underestimates, hindering assessments of how shifting precipitation affects river discharge and complicating management strategies.
- The resilience of the internationally supported Arctic Observing Network depends on sustaining investments, protecting specialized expertise, and ensuring continuity of both satellite and in situ observing systems and the high-quality data products derived from them.

Tracking Arctic change with the Arctic Observing Network

For 20 years, the Arctic Report Card (ARC) has vividly depicted the profound transformations of Arctic systems and their far-reaching consequences for societies in the region and beyond (see *ARC 2025 Executive Summary*). Accurate and timely observations of these rapid, system-wide changes are essential, making the internationally coordinated Arctic Observing Network (AON) a crucial foundation for assessments such as the ARC. This essay for the 20th anniversary Report Card provides an updated assessment of the AON, focusing on its strengths, persistent gaps, and risks in supporting scientific assessments typified by the ARC.

The AON refers to an international system of observing, data collection, and sharing, independently supported by a diverse range of actors, including governments, universities, regional organizations, and communities. The concept was conceived to collectively confront the significant challenges that conventional monitoring systems face in the Arctic, with the goal of better “linking and supplementing” diverse efforts through coordination, integration, and strategic investment (NRC 2006). The international Sustaining Arctic Observing Networks (SAON) initiative was established in 2011 to facilitate

AON's progress by establishing inventories of relevant assets, enabling data sharing, and collectively addressing gaps.

In addition to the need for better integration, collective challenges for SAON's partners include sparse ground-based observations, unreliable infrastructure, and limited telecommunications-factors that hinder in situ data collection and timely access (Cherry and Delamere 2025; NSTC 2022). Satellites play an essential role in providing services such as weather forecasting, wildfire detection, coastal mapping, and supporting scientific assessments that inform management and adaptation actions. However, they also face limitations: geostationary coverage degrades above 60° N, frequent cloud cover and limited daylight mask many signals, and, in some cases, resolution is inadequate in space and/or time (Cherry and Delamere 2025).

Indigenous Knowledge systems, with deep roots tracking change and supporting holistic decision-making for millennia (Daniel 2019), speak to the need for stronger support of community-led monitoring (e.g., Glenn-Borade et al. 2023) and effective co-production of knowledge partnerships (Ellam Yua et al. 2022; Rudolf et al. 2025). Indigenous-led monitoring is an essential contribution to the AON, yet this recognition must be paired with meaningful investment (see essay *Weaving the Seen and Unseen*) and inclusion of Indigenous leadership in advancing the AON, both of which have been slow to emerge.

In Europe, SAON's goals have been advanced under the Horizon 2020 program via EU-PolarNet, INTAROS, and Arctic PASSION (see *AON Glossary* for all acronyms). In the U.S., SAON's goals are advanced through the U.S. Arctic Observing Network (US AON) initiative, which coordinates across multiple federal agencies and non-federal partners to improve observing and data systems. Using its BENEFIT framework and software tool (Marowitz et al. 2025)—**Benefit Evaluation, Network Exploration, Find gaps, Improve Together**—the initiative assesses societal benefits, identifies strengths, recommends actions, and documents status. Inspired by systems engineering methods applied to federal observing systems (e.g., U.S. GEO 2024), US AON's BENEFIT framework has been adapted through Arctic-centered, grassroots, and internationally coordinated methods. BENEFIT measures AON performance against benchmarks specified in SAON's International Arctic Observing Assessment Framework (IAOAF; IDA 2017), which organizes key objectives for observing systems into twelve Societal Benefit Areas (SBAs; Box 1) and serves to align SAON's partners.

Box 1. Societal Benefit Areas of the International Arctic Observing Assessment Framework. SAON's partners generated this framework that organizes more than 150 key objectives for Arctic observations into the 12 Societal Benefit Areas defined here. This framework acts as an international benchmark for evaluating observation value, enabling a coordinated societal benefit-based approach to advance the AON in support of informed decision-making and adaptation planning in the rapidly changing Arctic.

1. Disaster Preparedness: Preparing for, preventing, mitigating, responding to, and recovering from natural and human-made disasters and emergencies.

2. Environmental Quality: Mitigating impacts on ecosystem functions and biodiversity, monitoring the effects of transboundary pollutants in the Arctic, and managing waste.

3. Food Security: Ensuring food accessibility, availability, sustainability, safety, and exchange networks for Arctic populations and communities.

4. Fundamental Understanding of Arctic Systems: Advancing understanding of Arctic social, economic, and environmental systems to reduce uncertainty and identify drivers.

5. Human Health: Tracking, forecasting, preventing, mitigating, and responding to threats to physical and mental health in Arctic communities.

6. Infrastructure and Operations: Ensuring safe and efficient operation of built and service infrastructure throughout its life cycle in the Arctic.

7. Marine and Coastal Ecosystems and Processes: Understanding, managing, and monitoring marine and coastal resources, ecosystems, and biogeochemical processes.

8. Natural Resources: Supporting sustainable and responsible discovery, extraction, and processing of renewable and non-renewable natural resources and their impacts.

9. Resilient Communities: Sustaining and preserving the vitality, security, and livelihoods of Arctic communities amid changing environmental conditions.

10. Sociocultural Services: Maintaining the environment's role in cultural life, preserving heritage, integrating knowledge, and understanding socioeconomics.

11. Terrestrial and Freshwater Ecosystems and Processes: Understanding, managing, and monitoring terrestrial and freshwater resources, ecosystems, and biogeochemical processes.

12. Weather and Climate: Improved forecasts, climate projections, and timely warnings for safety, socioeconomic benefits, and informed decision-making.

As AON is a work in progress, there is no authoritative inventory internationally or within the U.S., though relevant AON assets have been outlined in high-level reports (e.g., NSTC 2022; EU-PolarNet 2 2022) and are being assembled under the Registry of Polar Observing Networks initiative. As a proxy for a clear inventory, the US AON engages with AON-relevant programs, projects, and efforts like the ARC to link the performance of observing systems to the societal benefits they provide.

To produce the findings in this essay, ARC authors who contributed during 2021-24 were invited to participate in a BENEFIT assessment of their most recent essays, each of which evaluates a physical, ecological, or integrated indicator. Authors of 15 ARC essays participated in all or part of this assessment of strengths, gaps, and risks to the AON (see *Methods and data* section).

Strengths: Supporting societal benefits

The strengths of the AON can be understood through its performance and relevance in supporting efforts like the ARC. Overall, participating authors rated AON performance as high (Fig. 1), with a composite score of 76/100, indicating that as of ARC 2024, the network "fully satisfies" requirements for the ARC scientific assessments included in this work. Their criticality ratings underscore the importance of satellite systems, as they provide the spatial and temporal coverage, consistency, and timeliness essential for ARC essays. **Ecological indicators** were less consistently supported by the AON than **physical** or **integrated indicators**. This was particularly true for emerging ecological topics—such as *Beavers* and *Pollinators*—whose performance was lower than those tracking species already embedded in regulatory regimes like *Geese*, *Ice Seals*, and *Caribou*, which are closely tracked to inform harvest limits and, in the case of geese, vectors for disease risks like avian influenza.

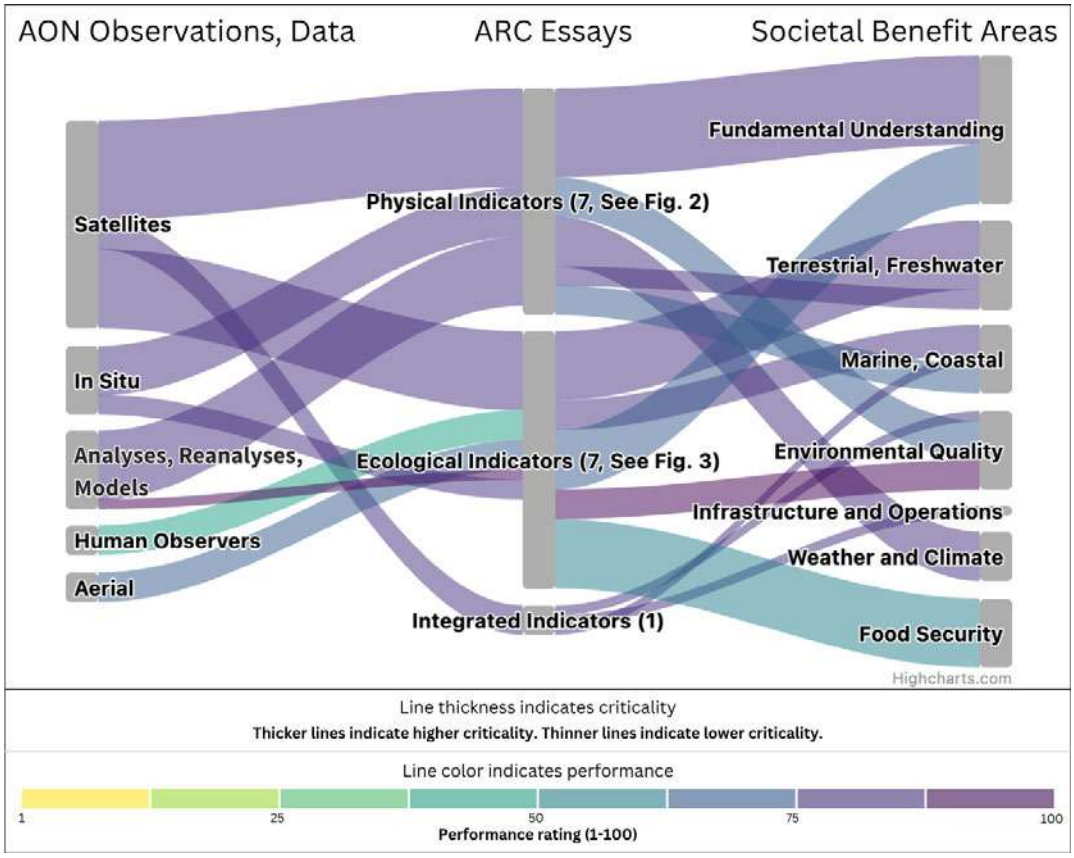

Fig. 1. Societal benefits of the AON for indicators: This figure, read left to right, illustrates the value chain linking AON observations and data to indicators in the ARC essays, and Arctic Societal Benefit Areas, grouped by indicator type, with the number indicating the count of essays assessed in each category. Colors indicate composite performance scores; line thickness indicates weighted and composited criticality. Performance and criticality scores are provided by the essay authors (see *Methods and data*). Observing systems are grouped by satellites, aerial, human and in situ observations. Analyses, reanalyses, and models are also used as inputs to ARC essays with the latter two being derived directly from observations.

Essays tracking physical components of the Arctic system (Fig. 2) provided robust support for scientific understanding [SBAs 4, 7, 11]. These essays also showed high relevance toward the management-relevant key objectives within the Weather and Climate [12] and Environmental Quality [2] SBAs, particularly in advancing our understanding of the changing ecosystem characteristics of snow cover, sea ice, and land ice. Gene Petrescu of NOAA's Arctic Test Bed summarizes the ARC impact on regional operations as "putting the weather and ice conditions of the past year into context for climate-related messaging."

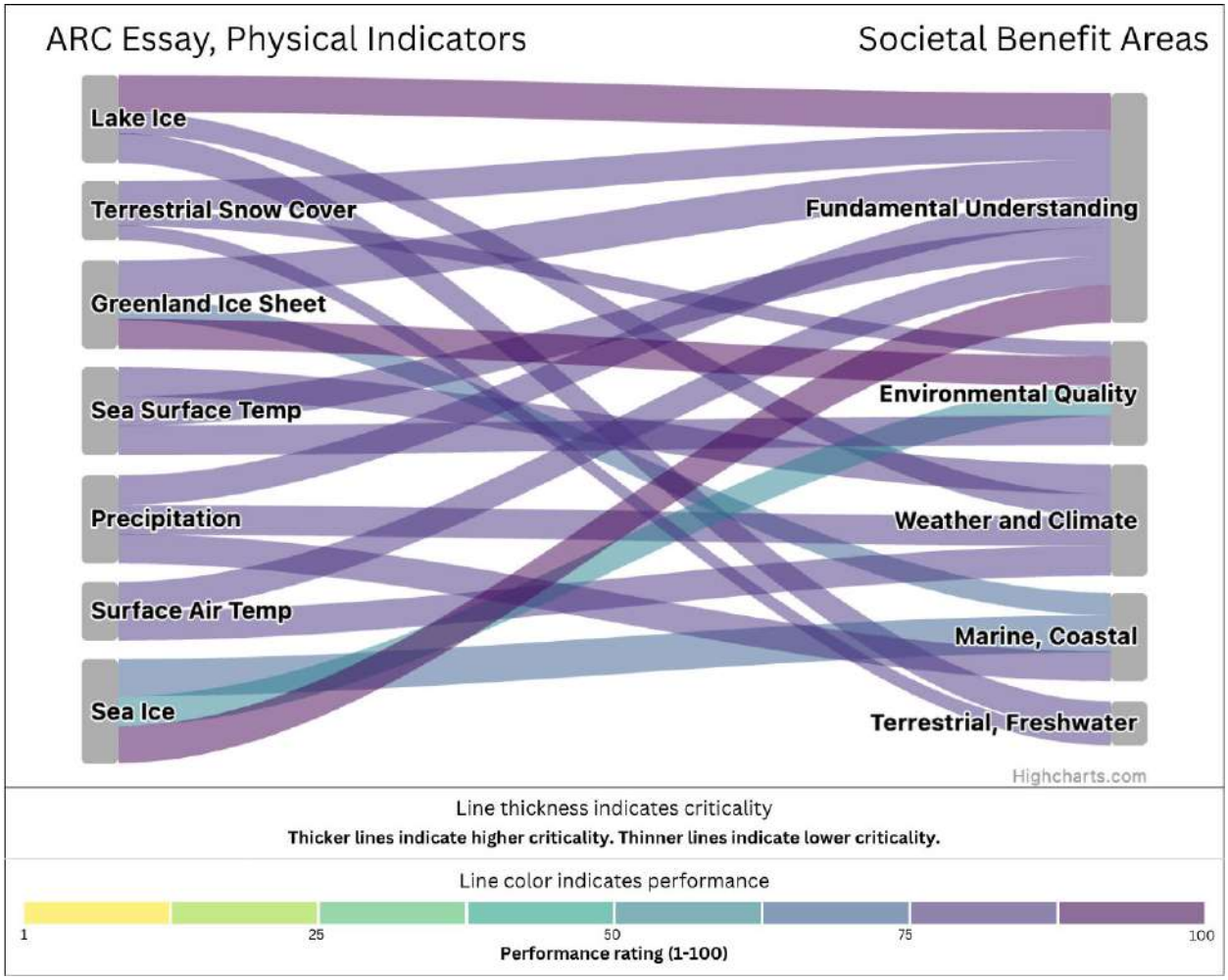

Fig. 2. Societal benefits supported by ARC essay physical indicators: This depiction of the assessed societal benefits for physical indicators provides greater detail on the specific strengths identified and the level of AON performance for the five most relevant SBAs for physical indicators.

Essays tracking ecological change (Fig. 3) demonstrated strong support for scientific understanding [SBAs 4, 7, 11], while also showing strong relevance for regionally critical issues, including Food Security [3], through providing timely updates on subsistence species, their food chains, and ecosystem health.

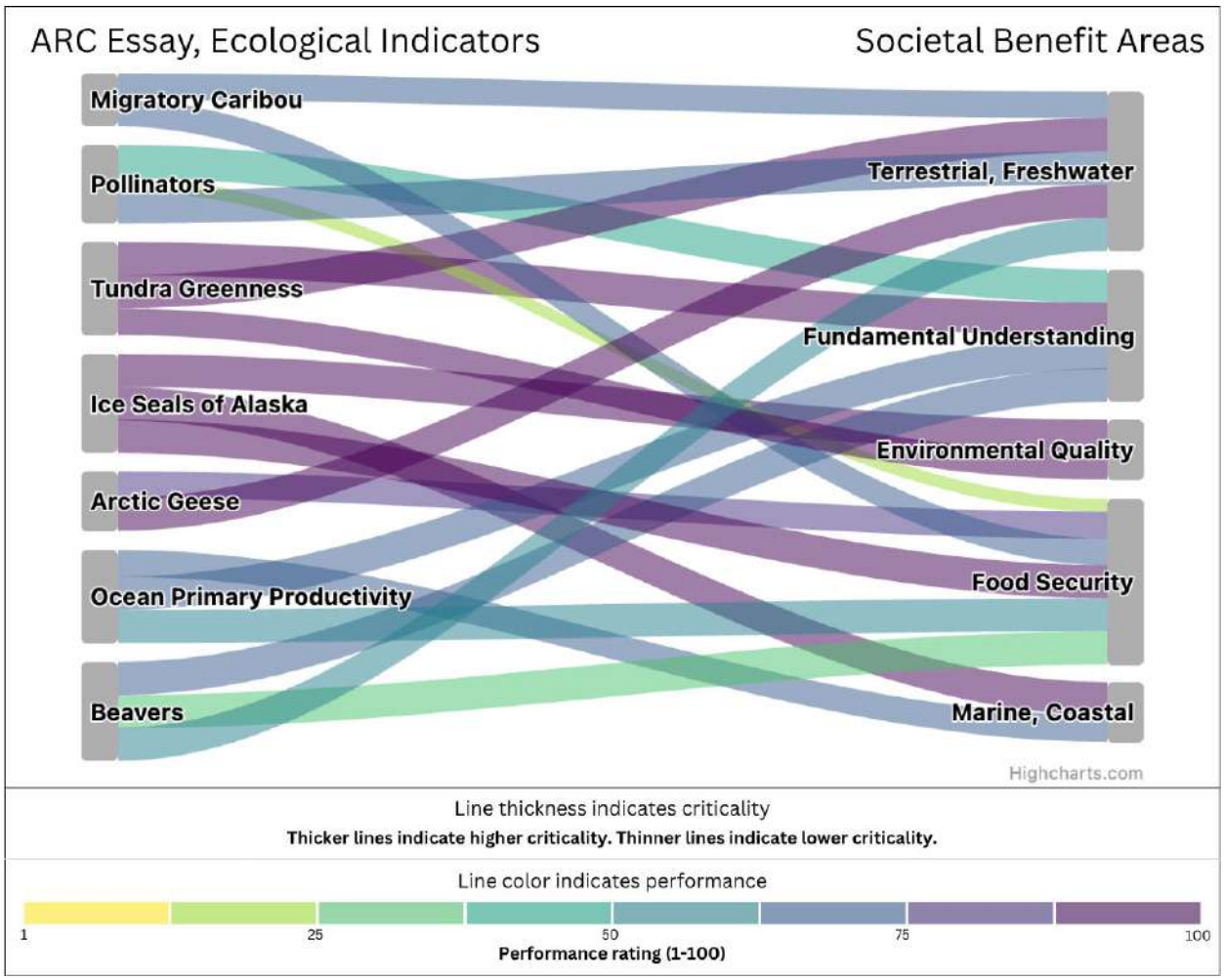

Fig. 3. Societal benefits supported by ARC essay ecological indicators: This depiction of the assessed societal benefits for ecological indicators provides greater detail on the specific strengths identified and the level of AON performance for the five most relevant SBAs for ecological indicators. Natural Resource Management and Community Resilience SBAs were also identified as relevant, but did not rise to the same level as those pictured here.

While this assessment included only one topic integrating social and ecosystem change (Fig. 1)—*Marine Ship Traffic*, it suggests that **integrated indicators** extend the societal relevance of the AON and the ARC [SBAs 2, 6, 7].

Gaps: Understanding the impact of data limitations

To understand AON limitations, ARC essay authors assessed the observing systems and data products underlying ARC essays. These systems and products were rated against ideal performance, and where ratings fell short, authors described underlying gaps (Table 1). Gaps may occur at any stage in the AON value chain, including data collection or processing, and manifest in derived products such as reanalyses. Gaps reflect the difference between current and desired capabilities. This analysis synthesizes gaps across physical, ecological, and integrated essays to inform future efforts.

Table 1. Summary of key observational gaps across Arctic observing systems grouped by indicator type: physical (blue), ecological (green), and integrated (orange).

Indicator Type	Essay Topic	Gaps
Physical Indicators	**Sea Ice**	Need for more small-scale observations and better sampling of properties (e.g., impurities in snow and ice), alongside improved satellite data resolution and coverage, especially near coasts and for melt ponds. Reducing uncertainties in thickness estimations is crucial, particularly regarding snow cover and the availability of summer retrievals.
	Greenland Ice Sheet	Low spatial resolution at the ice sheet edge, significant uncertainties in coastal ice sheet elevation, and limited site variation for in situ data collection.
	Precipitation	Much of the Arctic terrestrial drainage remains ungauged, with a lack of coverage in high elevations and other data-sparse regions, alongside a sharp decline in reporting gauges over recent decades. The sparse network is prone to precipitation undercatch errors that are difficult to correct, and short-term forecasts from reanalyses like ERA5 remain uncertain, particularly over high latitudes. Key datasets such as GPCC lack marine coverage, and while integration with reanalysis or satellite products (e.g., MSWEP) could improve monitoring, high-latitude ocean areas have yet to be properly evaluated.
	Sea Surface Temperature	Subsurface ocean temperature data are incomplete. Spatial resolution of satellite-derived SST is limited, especially in coastal regions where SST variability is significant.
	Terrestrial Snow Cover	Need for higher resolution in higher latitudes and mountain regions for global snow water equivalent products. Larger uncertainty in snow cover extent trends during fall and winter due to coarse resolution, difficulty distinguishing snow from clouds, and inconsistent temporal coverage has resulted in limited analysis for these seasons.
	Surface Air Temperature	Sparse station coverage and relatively few weather stations add uncertainty to the early portion of the record for GHCNm data. Similarly, sparse surface air temperature observations in the Arctic before the satellite era increase uncertainty in the early years of the ERA5 reanalysis record.
	Lake Ice	Data from in situ ice sensors have good coverage but are still limited. GMASI (Autosnow Ice) data are useless in winter but adds value in summer, and is useful for detecting snow under warm clouds in spring where surface stations are unavailable.

Indicator Type	Essay Topic	Gaps
Ecological Indicators	**Tundra Greenness**	The metric of tundra greenness used in the ARC is the Normalized Difference Vegetation Index (NDVI), a spectral metric that is linked to the abundance of green vegetation. While this metric has a long history of use and provides a period of record exceeding 40 years, it is a spectral proxy and is subject to some limitations. Alternative metrics, like ground-based metrics, exist that could eventually provide more robust assessments of Arctic change, but these metrics remain in their infancy and do not have a sufficient period of record to provide a meaningful "big picture" of conditions and change across the Arctic tundra biome.
	Ocean Primary Productivity	Satellite estimates exclude sea ice algae and under-ice phytoplankton blooms. They can also underestimate primary productivity under highly stratified conditions. There also remain challenges in distinguishing between clouds, snow, and ice in polar regions with AVHRR data, leading to high uncertainty in surface parameter retrieval. Inadequate spatial density of ship, Argo, and buoy observations affects the quality and comprehensiveness of data in those areas.
	Geese	Visual estimates often underestimate and sample only a part of a species' range. Research is ongoing to expand banding and apply aerial imagery surveys to more species and populations, but improvements are still needed in image analysis to reduce manual effort.
	Pollinators	Need for long-term monitoring in various Arctic locations, along with improved support and technologies for identifying insect material to the species level. Additionally, there are spatial and temporal gaps in monitoring, as well as gaps in data for certain taxa, like flies, and in understanding responses to stressors.
Integrated Indicators	**Ship Traffic**	Deficiencies in the comprehensiveness of antennae available to generate AIS signals and the omission of certain ships and ship-types from AIS tracking make the dataset incomplete.

Within **physical indicators**, common gaps include limited spatial resolution, particularly in coastal zones and mountainous areas, and a lack of in situ data needed to validate satellite products. For example, *Precipitation* essay authors indicated a lack of gauge coverage in higher elevations and other data-sparse regions, which can result in precipitation undercatch errors. Expanding gauge coverage would improve understanding of how changing precipitation patterns affect river discharge, flood events, and other consequential metrics.

Among **ecological and integrated indicators**, common gaps include reliance on proxy or indirect metrics, limited spatial and temporal coverage, and sparse in situ data. For example, species monitoring (e.g., *Arctic Geese* and *Pollinators*) often underrepresents full ranges due to limited geographic coverage and

reliance on visual estimates. Similarly, *Tundra Greenness* estimates remain constrained by the limited spatial coverage of field measurements needed to validate satellite observations. *Ocean Primary Productivity* estimates are limited to areas with less than 10% of sea ice concentration, excluding primary production from sea ice algae or under-ice phytoplankton blooms, and are further constrained by sparse in situ observations.

Despite clear strengths, persistent gaps limit the AON's ability to fully support Arctic assessments and decision-making, particularly at finer scales. Closing gaps would improve confidence in key indicators of Arctic change, enabling a shift from broad regional assessments toward finer scale, more locally relevant insights that help Arctic communities understand changing conditions, support safer and more effective operations for commercial and industrial sectors such as fisheries, and improve global weather, climate, and ecosystem predictions. These limitations point to the need for sustained investment in resolution, coverage, validation, and cross-system integration.

Risks: Sustaining a resilient observing system

ARC essay authors were surveyed about current risks to the AON, recognizing that the future of Arctic observing could include improvements or degradations to capabilities. Many responses noted recent or proposed changes to U.S. federal staffing and budget levels. Of the 31 observing systems in this assessment, 23 are either primarily supported by U.S. federal agencies or jointly supported by U.S. federal agencies and international partners (e.g., the International Arctic Buoy Program). Additionally, U.S. federal agencies create 8 out of 10 assessed datasets that synthesize observations into analysis and reanalysis products. Notably, agencies like NOAA, NASA, NSF, and DOI, which drive data collection and value-added efforts, face significant staff and budget reductions. For example, 4000 NASA staff left between January and July 2025 (Duster 2025).

Because the U.S. contributes significantly to Arctic observing, changes in the federal budget and staffing could impact the AON and products like the ARC. Risks to funding and staffing, alongside aging infrastructure, may compound existing AON gaps, jeopardizing long-term trend analyses and undermining decision-making. For **physical indicators**, these include potential reductions in satellite missions, data processing efforts, and in situ measurements (Table 2). **Ecological indicators** face many of the same potential impacts (e.g., see essay *Tundra Greenness*). Agency staffing and funding uncertainties have already led to canceled grants and personnel shortages impacting ecological research (Table 2), which has greater in-field requirements than physical research. Arctic fieldwork is 4-10 times more expensive than similar work in lower latitudes (Mallory et al. 2018).

Table 2. Risks to physical indicators (blue) and ecological indicators (green) and the observing and data products that support them.

Indicator Type	Essay Topic	What is at risk and criticality information	Further explanation of risk
Physical Indicators	**Surface Air Temperature**	No risks noted	—
	Precipitation	Meteorological Stations Collecting Precipitation Data - a highly critical observing system for the Precipitation essay	Potential impacts as precipitation data are collected or funded by agencies or programs facing major budget cuts

Indicator Type	Essay Topic	What is at risk and criticality information	Further explanation of risk
	Sea Ice	CryoSat-2, SMOS, and ICESat-2 - the three primary observing systems contributing to sea ice thickness estimates, of medium to medium-high criticality to the Sea Ice essay. DMSP SSM/I-SSMIS - This is a medium-low criticality input to three datasets, all of which support the Sea Ice essay	CryoSat-2, SMOS, and ICESat-2 - All past their nominal mission lifetime. Constrained agency budgets and staffing could impact new instrumentation and/or data products development. DMSP SSM/I-SSMIS - This observing system is explicitly identified for decommissioning. It will be replaced by new passive microwave sensors. This transition introduces inconsistencies, which require staff time and expertise to recalibrate the data and make sure it is as consistent as possible with the long-term record.
	Greenland Ice Sheet	DMSP SSM/I-SSMIS - This is a highly critical observing system supporting a single dataset within the Greenland Ice Sheet essay	DMSP SSM/I-SSMIS - See "Sea Ice" description above.
	Sea Surface Temperature	OISST - The highest criticality dataset for the Sea Surface Temperature essay DMSP SSM/I-SSMIS - This is a medium-low criticality observing system for two datasets underlying the Sea Surface Temperature essay	OISST - The generation and availability of this data product may be affected by the proposed fiscal 2026 budget cuts to U.S. federal agencies. Additionally, the satellite and in situ observing systems that support the OISST may be impacted. DMSP SSM/I-SSMIS - See "Sea Ice" description above.
	Lake Ice	NIC IMS - The highest criticality, and only, dataset for the Lake Ice essay	NIC IMS - Creation of this dataset relies on human analysts, which contributes to its high performance. The generation and availability of this data product may be affected by proposed FY 2026 budget cuts at U.S. federal agencies.

Indicator Type	Essay Topic	What is at risk and criticality information	Further explanation of risk
Ecological Indicators	**Tundra Greenness**	AVHRR GIMMS-3g - The highest criticality dataset for the Tundra Greenness essay. MODIS - High-criticality observing system for the Tundra Greenness essay.	AVHRR GIMMS-3g - will not be updated for 2025 or future years due to funding cuts at NASA GSFC. Potential replacement datasets exist, but have shortcomings in this context. MODIS - The sunsetting of MODIS was expected, and a transition to VIIRS has been planned.
	Ocean Primary Productivity	MODIS - The highest criticality observing system for the Primary Productivity essay.	MODIS - The sunsetting of MODIS was expected, and a transition to VIIRS and PACE has been planned. This transition introduces inconsistencies, which require in situ measurements, staff time, and expertise to make sure it is as consistent as possible with the long-term record.
	Geese	All observing systems for goose population status monitoring were noted as at risk.	Risk of losing adequately trained staff, particularly experienced pilots, alongside continued funding reductions. Due to staffing shortages and funding uncertainty, summer 2025 goose monitoring and fieldwork activities were canceled at multiple locations. This follows years of static funding, which results in decreased funds due to inflation. In some proposed FY 2026 budgets, many of these programs, such as the USGS's Ecosystem Mission Area and Cooperative Research Units and the USFWS's North American Wetland Conservation Act and Migratory Bird Joint Venture Programs, among others, were slated for either reduced funding or elimination.

Indicator Type	Essay Topic	What is at risk and criticality information	Further explanation of risk
	Pollinators	CBMP Arctic Pollinator Expert Network, an international collaboration related to Arctic pollinators, is at risk.	Funded by agencies or programs facing major budget cuts.
	Beavers	A-BON - an organization created to "coordinate research and action among stakeholders" related to beavers in the circumpolar Arctic, is at risk.	Funding opportunities with the NSF-AON program, which has supported the A-BON, are on pause for the 2025 calendar year (McManus 2025).

Given the international nature of the AON, changes to any contributing country's capabilities affect efforts to leverage and coordinate observations across the Arctic. While not all programs may be affected by proposed budget cuts, our assessment shows that potential AON degradations could have broader impacts, for instance, impeding flooding predictions using in situ gauges, icebreaker navigation using sea ice data, or community adaptation plans using ecological data. Additionally, a lack of adequate monitoring information could prevent regulatory bodies from meeting legal mandates (e.g., *Arctic Geese*). Having robust assessments of how observing programs generate societal benefit by supporting baseline understanding and decision making can help countries and organizations respond strategically to changing investments.

Conclusions

The Arctic Report Card exemplifies the vital societal relevance of sustained, high-quality, internationally coordinated observations of Arctic change. Its annual summaries not only deepen conceptual understanding of a rapidly transforming Arctic region but also provide essential context for informed decision-making at regional, national, and global scales, as illustrated by this year's societal impact summary featured in the *Glaciers and Ice Caps* essay.

In the absence of a formal AON inventory, the ARC provides a meaningful way to evaluate relevant aspects of the AON's fitness; this essay details the strengths, gaps, and risks related to this. Yet, as highlighted in 2020 (Starkweather et al. 2020) and reaffirmed here, the ARC focuses on topics where the AON is already robust enough to support strong scientific analysis. There are other assessment-worthy topics not reflected here that would, if included, likely degrade the AONs overall performance rating for assessments, so the AON performance assessed in regard to these ARC topics should be considered an upper estimate.

The AON concept emerged to link sustained efforts, advance innovation, and foster effective partnerships to ensure that observing systems improve in response to societal needs. Sustaining and advancing the AON will require consistent investment, international collaboration, and continued application of fitness testing tools such as BENEFIT assessment. These efforts are critical to ensure that Arctic observing systems deliver lasting value to science, policy, and society.

Methods and data

ARC essay authors provided structured feedback on the connection between the AON's strengths, gaps, and risks and their ARC essay. Ratings included assessing connection to SBAs (see *Strengths* section) as well as listing contributing data sets and their respective observing system inputs. Standard rubrics guided the authors through quantitative ratings of performance (scaled from 0-100, with 76-90 equating to "fully satisfactory") and criticality; authors also provided rating rationales. All essay authors for the 2021-24 ARC were invited to participate; 15 responded. Some completed all aspects of the assessment, while others responded only to portions of the assessment, and others opted out.

This essay's authors used Notebook LM (NLM), which is an AI powered by Google's Gemini 1.5 Pro large language model. NLM uses only the sources provided for synthesis, which included each participating author's most recent ARC essay and the SBA framework. The query asked NLM to identify up to three of the most relevant SBAs and up to five key objectives per societal benefit area. Each choice was first reviewed by this essay's authors; ARC essay authors were then invited to review and amend the choices. Several authors amended the initial choices, and others concurred with the AI's selection.

Assessment data are encoded in the BENEFIT tool and is accessible via [usaon.org].

Acknowledgments

S. Starkweather is grant-funded by NOAA's Global Ocean Monitoring and Observing Program/Arctic Research Program. M. B. Armstrong's work is supported by NOAA's Global Ocean Monitoring and Observing Program/Arctic Research Program and Virginia Sea Grant. H. Shapiro is supported by UIC Science on the IARPC Secretariat team; funding is provided by the National Science Foundation.

References

Cherry, J., and J. Delamere, 2025: Alaska Next Generation Workshop Report (2024). Alaska Next Generation Satellite Workshop, 1-87, https://doi.org/10.25923/tj84-5204.

Daniel, R., 2019: Understanding our environment requires an indigenous worldview. *Eos*, **100**, https://doi.org/10.1029/2019EO137482.

Duster, C., 2025: Nearly 4,000 NASA employees opt to leave agency through deferred resignation program. National Public Radio, https://www.npr.org/2025/07/26/nx-s1-5481304/nasa-employees-deferred-resignation-program.

Ellam Yua, J. Raymond-Yakoubian, R. Aluaq Daniel, and C. Behe, 2022: A framework for co-production of knowledge in the context of Arctic research. *Ecol. Soc.*, **27**(1), 34, https://doi.org/10.5751/ES-12960-270134.

EU-PolarNet 2, 2022: Procedure for ongoing collection and collation of European Polar observing capacities and activities (Deliverable 6.1), https://eu-polarnet.eu/docs/d6-1-procedure-for-ongoing-collection-and-collation-of-european-polar-observing-capacities-and-activities/.

Glenn-Borade, R. T., B. Adams, R. Schaeffer, C. SimsKayotuk, G. Omnik, J. M. Leavitt, and D. D. W. Hauser, 2023: Nunaaqqit Savaqatigivlugich: Working with communities to observe the Arctic. *Arctic*

Report Card 2023, R. L. Thoman, T. A. Moon, and M. L. Druckenmiller, Eds., https://doi.org/10.25923/2sx6-kx89.

Institute for Defense Analyses (IDA), 2017: International Arctic Observations Assessment Framework. IDA Science and Technology Policy Institute, Washington, DC, U.S.A., and Sustaining Arctic Observing Networks, Oslo, Norway, 1-69, https://www.arcticobserving.org/news/268-international-arctic-observations-assessment-framework-released.

Mallory, M. L., H. G. Gilchrist, M. Janssen, H. L. Major, F. Merkel, J. F. Provencher, and H. Strøm, 2018: Financial costs of conducting science in the Arctic: examples from seabird research. *Arct. Sci.*, **4**(4), 624-633, https://doi.org/10.1139/as-2017-0019.

Marowitz, R., M. Fisher, H. Shapiro, and S. Starkweather, 2025: U.S. Arctic Observation Network Benefit Tool, Version v2.7.2 Software. Zenodo, accessed 29 September 2025, https://doi.org/10.5281/zenodo.8403759.

McManus, J., 2025: An update to the NSF Arctic Observing Network (AON) program. National Science Foundation, https://www.nsf.gov/funding/information/dcl-update-nsf-arctic-observing-network-aon-program.

National Research Council (NRC), 2006: Toward an integrated Arctic Observing Network. The National Academies Press, 128 pp., https://doi.org/10.17226/11607.

National Science and Technology Committee (NSTC), 2022: On the need to establish and maintain a sustained Arctic Observing Network, 42 pp., https://www.iarpccollaborations.org/uploads/cms/documents/usaon-report-20221215.pdf.

Rudolf, M. H. C., S. F. Trainor, J. O'Connor, E. Figus, and R. Hum, 2025: Factors in and perspectives of achieving co-production of knowledge with Arctic Indigenous Peoples. *Commun. Sci.*, **4**(2), e2023CSJ000074, https://doi.org/10.1029/2023CSJ000074.

Starkweather, S., H. Shapiro, S. Vakhutinsky, and M. L. Druckenmiller, 2020: The observational foundation of the Arctic Report Card – a 15-year retrospective analysis on the Arctic Observing Network (AON) and insights for the future system. *Arctic Report Card 2020*, R. L. Thoman, J. Richter-Menge, and M. L. Druckenmiller, Eds., https://doi.org/10.25923/ahj5-z336.

United States Group on Earth Observations (U.S. GEO), 2024: 2023 Earth observations assessment report: Agriculture & forestry. Product of the Subcommittee on U.S. Earth Observation Committee on Environment, 17 pp., https://usgeo.gov/eoa/uploads/EOAMethodologyReport_July_2024_Final.pdf.

Glossary of acronyms

Observing systems, including satellites and sensors, and data products:

AIS – Automatic Identification System

AVHRR – Advanced Very High Resolution Radiometer

AVHRR GIMMS-3g – Advanced Very High Resolution Radiometer Global Inventory Modeling and Mapping Studies-3rd Generation

CryoSat-2 – Cryospheric Satellite-2

ERA5 – European Centre for Medium-Range Weather Forecasts (ECMWF) Reanalysis, version 5

DMSP SSMI/SSMIS – Defense Meteorological Satellite Program Special Sensor Microwave/Imager and Special Sensor Microwave Imager/Sounder

GMASI – Global Multisensor Automated satellite-based Snow and Ice Mapping System

GNCNm – Global Historical Climatology Network monthly

GPCC – Global Precipitation Climatology Centre

ICESat-2 – Ice, Cloud, and land Elevation Satellite 2

MODIS – Moderate Resolution Imaging Spectroradiometer

MSWEP – Multi-Source Weighted-Ensemble Precipitation

NIC IMS – National Ice Center Interactive Multisensor Snow and Ice Mapping System

OISST – Optimum Interpolation Sea Surface Temperature

PACE – Plankton, Aerosol, Cloud, ocean Ecosystem (satellite)

SMOS – Soil Moisture and Ocean Salinity (satellite)

SSMIS – Special Sensor Microwave Imager/Sounder

VIIRS – Visible Infrared Imaging Radiometer Suite

Organizations and agencies:

A-BON – Arctic Beaver Observation Network

Arctic PASSION project – Pan-Arctic Observing System of Systems: Implementing Observations for Societal Needs

CBMP – Circumpolar Biodiversity Monitoring Program

EU-PolarNet – European Union PolarNetwork

DOI – Department of the Interior

INTAROS – Integrated Arctic Observation System

NASA – National Aeronautics and Space Administration

NOAA – National Oceanic and Atmospheric Administration

NSF – National Science Foundation

USFWS – United States Fish and Wildlife Service

USGS – United States Geological Survey

February 6, 2026

AMAP and the Arctic Report Card: A Collaboration that is 20 Years Strong

https://doi.org/10.25923/mj1c-j447

The Arctic Report Card (ARC) occupies a unique and highly valuable position within the broader, international framework of climate assessment and scientific outreach. Since its inception in 2006, it has provided annual, authoritative updates on the state of the Arctic, a region experiencing some of the most rapid and consequential climate-driven changes on the planet. This steady cadence distinguishes the ARC from other major reporting frameworks, such as the Arctic Monitoring and Assessment Programme (AMAP) comprehensive Arctic assessments or the Intergovernmental Panel on Climate Change (IPCC) global assessment cycles, which are published on multi-year timelines.

AMAP is proud to support the work of the Arctic Report Card, particularly by facilitating the behind-the-scenes peer review process, drawing on an international network of more than 800 specialists. This collaboration exemplifies the strength of multidisciplinary, international partnerships in advancing Arctic science.

The Arctic Report Card's importance lies in its ability to deliver timely, science-based insights that track evolving conditions in near real time. By focusing on key indicators—such as sea ice extent, permafrost stability, ocean temperature, and ecosystem health—it offers a concise yet robust snapshot of trends that have both regional and global implications. This immediacy is critical for informing decision-makers, researchers, Arctic residents, and stakeholders who require up-to-date information to guide policy and adaptation strategies.

Further, the Arctic Report Card increasingly weaves together physical sciences, social sciences, and Indigenous Knowledge, recognizing the leadership and contributions of Indigenous Peoples in advancing understanding of the changes being observed across the Arctic.

Equally significant is its role in science communication and accessibility. The Report Card is designed to be understandable to a broad audience, combining rigorous peer-reviewed science with clear language and compelling visuals. This approach bridges the gap between complex climate data and actionable knowledge, making it an effective tool for outreach and education.

In the constellation of climate reporting, the Arctic Report Card complements the depth of AMAP's periodic assessments and the global perspective of IPCC reports. Together, these products form a layered system of knowledge: annual snapshots for rapid awareness, regional deep dives for detailed understanding, and global syntheses for comprehensive context. This synergy ensures that the accelerating changes in the Arctic remain visible, understood, and integrated into global climate discourse. By providing timely and credible information, the Arctic Report Card strengthens the scientific foundation for evidence-based policy decisions in a region critical to global climate stability.

On behalf of AMAP, we warmly congratulate NOAA and the entire team on the 20th edition of the Arctic Report Card. Over two decades, this initiative has become an indispensable resource for the scientific community and policymakers alike, offering clarity and continuity in a time of unprecedented environmental change. The Arctic Report Card's commitment to scientific integrity, transparency, and

accessibility has set a benchmark for effective climate communication, and we look forward to continued collaboration in advancing knowledge and action for the Arctic and beyond.

Sarah Kalhok Bourque
AMAP Chair

Components and contributions to the annual production of the Arctic Report Card.

December 4, 2025

Authors and Affiliations

L. M. Andreassen, Section for Glaciers, Ice and Snow, Norwegian Water Resources and Energy Directorate, Oslo, Norway

M. B. Armstrong, Sea Grant Knauss Fellowship, Arctic Research Program, Global Ocean Monitoring and Observing Program, NOAA, Silver Spring, MD, USA

T. G. Askjaer, Danish Meteorological Institute, Copenhagen, Denmark

J. J. Assmann, Department of Evolutionary Biology and Environmental Studies, University of Zurich, Zurich, Switzerland

T. J. Ballinger, International Arctic Research Center, University of Alaska Fairbanks, Fairbanks, AK, USA

L. A. K. Barnett, Resource Assessment and Conservation Engineering Division, Alaska Fisheries Science Center, NOAA, Seattle, WA, USA

B. Barst, University of Calgary, Calgary, AB, Canada

A. Bartsch, b.geos GmbH, Korneuburg, Austria

C. Baughman, U.S. Geological Survey, Alaska Science Center, Anchorage, AK, USA

L. T. Berner, Department of Natural Sciences, University of Alaska Southeast, Juneau, AK, USA; School of Informatics, Computing and Cyber Systems, Northern Arizona University, Flagstaff, AZ, USA

U. S. Bhatt, Geophysical Institute, University of Alaska Fairbanks, Fairbanks, AK, USA

S. Bigalke, Department of Geography, Portland State University, Portland, OR, USA

A. Bishop, University of Alaska Anchorage, Anchorage, AK, USA

J. W. Bjerke, Norwegian Institute for Nature Research, FRAM – High North Research Centre for Climate and the Environment, Tromsø, Norway; Tromsø Arctic-Alpine Botanical Garden, The Arctic University Museum of Norway, UiT The Arctic University of Norway, Tromsø, Norway

A. Bliss, Cryospheric Sciences Laboratory, Goddard Space Flight Center, NASA, Greenbelt, MD, USA

B. A. Bluhm, Department of Arctic and Marine Biology, UiT The Arctic University of Norway, Tromsø, Norway

J. E. Box, Geological Survey of Denmark and Greenland, Copenhagen, Denmark

B. Brettschneider, National Weather Service Alaska Region, NOAA, Anchorage, AK, USA

D. Burgess, Geological Survey of Canada, Ottawa, ON, Canada

M. P. Carey, U.S. Geological Survey, Alaska Science Center, Anchorage, AK, USA

L. W. Cooper, Chesapeake Biological Laboratory, University of Maryland Center for Environmental Science, University of Maryland, Solomons, MD, USA

A. Crawford, Department of Environment and Geography, University of Manitoba, Winnipeg, MB, Canada

S. G. Crawford, University of Alaska Fairbanks, Fairbanks, AK, USA

B. Decharme, Centre National de Recherches Météorologiques, Météo-France, Toulouse, France

C. Derksen, Climate Research Division, Environment and Climate Change Canada, Toronto, ON, Canada

D. Divine, Norwegian Polar Institute, Fram Centre, Tromsø, Norway

M. L. Druckenmiller, National Snow and Ice Data Center, Cooperative Institute for Research in Environmental Sciences, University of Colorado Boulder, Boulder, CO, USA

A. Elias Chereque, Department of Physics, University of Toronto, Toronto, ON, Canada

H. E. Epstein, Department of Environmental Sciences, University of Virginia, Charlottesville, VA, USA

T. Evinger, Department of Environmental Toxicology, University of California Davis, Davis, CA, USA

S. Farrell, Department of Geographical Sciences, University of Maryland, College Park, MD, USA

R. S. Fausto, Geological Survey of Denmark and Greenland, Copenhagen, Denmark

B. C. Forbes, Arctic Centre, University of Lapland, Rovaniemi, Finland

K. E. Frey, Graduate School of Geography, Clark University, Worcester, MA, USA

R. Fried, University of Alaska Anchorage, Anchorage, AK, USA

G. V. Frost, Alaska Biological Research, Inc., Fairbanks, AK, USA

C. Garcia, Arctic Research Program, Global Ocean Monitoring and Observing Program, NOAA, Silver Spring, MD, USA

A. R. Gastaldi, University of Alaska Fairbanks, Fairbanks, AK, USA

S. Gerland, Norwegian Polar Institute, Fram Centre, Tromsø, Norway

O. M. Gologergen, University of Alaska Anchorage, Anchorage, AK, USA

S. Gonzalez, Climate and Oceanography, Institute of Marine Research, Bergen, Norway; Bjerknes Centre for Climate Research, Bergen, Norway

E. Graham, Geophysical Institute, University of Alaska Fairbanks, Fairbanks, AK, USA

J. M. Grebmeier, Chesapeake Biological Laboratory, University of Maryland Center for Environmental Science, University of Maryland, Solomons, MD, USA

E. Hanna, Department of Geography and Lincoln Climate Research Group, University of Lincoln, Lincoln, UK

S. Hendricks, Alfred Wegener Institute, Helmholtz Centre for Polar and Marine Research, Bremerhaven, Germany

K. Hill, National Park Service, Arctic Network, Fairbanks, AK, USA

R. B. Ingvaldsen, Institute of Marine Research, Bergen, Norway; Department of Arctic and Marine Biology, UiT The Arctic University of Norway, Tromsø, Norway

L. Kaleschke, Alfred Wegener Institute, Helmholtz Centre for Polar and Marine Research, Bremerhaven, Germany

S. -J. Kim, Korea Polar Research Institute, Incheon, Republic of Korea

J. C. Koch, U.S. Geological Survey, Alaska Science Center, Anchorage, AK, USA

J. Kohler, Norwegian Polar Institute, Tromsø, Norway

Z. M. Labe, Climate Central, Princeton, NJ, USA

H. -M. Ladd, Aleut Community of St. Paul Island Tribal Government, St. Paul Island, AK, USA

R. Lader, International Arctic Research Center, University of Alaska Fairbanks, Fairbanks, AK, USA

M. J. Lara, Department of Plant Biology, University of Illinois, Urbana, IL, USA; Department of Geography, University of Illinois, Urbana, IL, USA

B. D. Loomis, Goddard Space Flight Center, NASA, Greenbelt, MD, USA

E. López-Blanco, Department of Ecoscience and Arctic Research Centre, Aarhus University, Roskilde, Denmark

B. Luks, Institute of Geophysics, Polish Academy of Sciences, Warsaw, Poland

K. Luojus, Arctic Research Centre, Finnish Meteorological Institute, Helsinki, Finland

M. J. Macander, Alaska Biological Research, Inc., Fairbanks, AK, USA

R. Í. Magnússon, Plant Ecology and Nature Conservation Group, Wageningen University & Research, Wageningen, Netherlands

K. D. Mankoff, Goddard Institute for Space Studies, NASA, New York, NY, USA; Autonomic Integra, New York, NY, USA

B. C. Medley, Goddard Space Flight Center, NASA, Greenbelt, MD, USA

W. N. Meier, National Snow and Ice Data Center, Cooperative Institute for Research in Environmental Sciences, University of Colorado Boulder, Boulder, CO, USA

D. Melovidov, Aleut Community of St. Paul Island Tribal Government, St. Paul Island, AK, USA

P. M. Montesano, Goddard Space Flight Center, NASA, Greenbelt, MD, USA; ADNET Systems, Inc., Bethesda, MD, USA

T. A. Moon, National Snow and Ice Data Center, Cooperative Institute for Research in Environmental Sciences, University of Colorado Boulder, Boulder, CO, USA

T. L. Mote, Department of Geography, University of Georgia, Athens, GA, USA

H. Motrøen Gjelten, Norwegian Meteorological Institute, Oslo, Norway

L. R. Mudryk, Climate Research Division, Environment and Climate Change Canada, Toronto, ON, Canada

C. S. R. Neigh, Goddard Space Flight Center, NASA, Greenbelt, MD, USA

J. A. O'Donnell, National Park Service, Arctic Network, Anchorage, AK, USA

K. M. Orndahl, School of Informatics, Computing and Cyber Systems, Northern Arizona University, Flagstaff, AZ, USA

I. Ortiz, Cooperative Institute for Climate, Ocean, and Ecosystem Studies, University of Washington, Seattle, WA, USA

J. E. Overland, Pacific Marine Environmental Laboratory, NOAA, Seattle, WA, USA

V. M. Padula, Aleut Community of St. Paul Island Tribal Government, St. Paul Island, AK, USA

F. Pálsson, Institute of Earth Sciences, University of Iceland, Reykjavík, Iceland

D. Perovich, Thayer School of Engineering, Dartmouth College, Hanover, NH, USA

A. Petty, Earth System Science Interdisciplinary Center, University of Maryland, College Park, MD, USA

G. K. Phoenix, School of Biosciences, University of Sheffield, Sheffield, UK

K. Poinar, University at Buffalo, Buffalo, NY, USA

I. V. Polyakov, International Arctic Research Center and College of Natural Science and Mathematics, University of Alaska Fairbanks, Fairbanks, AK, USA

B. A. Poulin, Department of Environmental Toxicology, University of California Davis, Davis, CA, USA

A. Pruitt, Department of Environmental Toxicology, University of California Davis, Davis, CA, USA

K. Rand, Lynker, Leesburg, VA, USA; Resource Ecology and Fisheries Management, Alaska Fisheries Science Center, NOAA, Seattle, WA, USA

R. Ricker, NORCE Norwegian Research Centre, Tromsø, Norway

B. Robson, Aleut Community of St. Paul Island Tribal Government, St. Paul Island, AK, USA

G. Schaepman-Strub, Department of Evolutionary Biology and Environmental Studies, University of Zurich, Zurich, Switzerland

M. C. Serreze, National Snow and Ice Data Center, Cooperative Institute for Research in Environmental Sciences, University of Colorado Boulder, Boulder, CO, USA

H. Shapiro, UIC Science, Utqiaġvik, AK, USA

B. E. Smith, University of Washington, Seattle, WA, USA

A. Spear, Resource Assessment and Conservation Engineering Division, Alaska Fisheries Science Center, NOAA, Seattle, WA, USA

S. Starkweather, Cooperative Institute for Research in Environmental Sciences, University of Colorado Boulder, Boulder, CO, USA; Physical Sciences Laboratory, NOAA, Boulder, CO, USA

L. V. Stock, Cryospheric Sciences Laboratory, Goddard Space Flight Center, NASA, Greenbelt, MD, USA

R. L. Thoman, Alaska Center for Climate Assessment and Preparedness, University of Alaska Fairbanks, Fairbanks, AK, USA; International Arctic Research Center, University of Alaska Fairbanks, Fairbanks, AK, USA

C. Thompson, National Park Service, Arctic Network, Fairbanks, AK, USA

L. Thomson, Queen's University, Kingston, ON, Canada

J. T. Thorson, Resource Ecology and Fisheries Management, Alaska Fisheries Science Center, NOAA, Seattle, WA, USA

T. Thorsteinsson, Icelandic Meteorological Office, Reykjavík, Iceland

X. Tian-Kunze, Alfred Wegener Institute, Helmholtz Centre for Polar and Marine Research, Bremerhaven, Germany

M. -L. Timmermans, Department of Earth and Planetary Sciences, Yale University, New Haven, CT, USA

H. Tømmervik, Norwegian Institute for Nature Research, FRAM – High North Research Centre for Climate and the Environment, Tromsø, Norway

C. Waigl, International Arctic Research Center, University of Alaska Fairbanks, Fairbanks AK, USA

D. A. Walker, Institute of Arctic Biology, University of Alaska Fairbanks, Fairbanks, AK, USA

J. E. Walsh, International Arctic Research Center, University of Alaska Fairbanks, Fairbanks, AK, USA

M. Wang, Cooperative Institute for Climate, Ocean, and Ecosystem Studies, University of Washington, Seattle, WA, USA; Pacific Marine Environmental Laboratory, NOAA, Seattle, WA, USA

M. Webster, Polar Science Center, Applied Physics Laboratory, University of Washington, Seattle, WA, USA

S. P. Wise, Economic and Social Science Research Program, Alaska Fisheries Science Center, NOAA, Seattle, WA, USA

G. Wolken, University of Alaska Fairbanks, Fairbanks, AK, USA; Alaska Division of Geological and Geophysical Surveys, Fairbanks, AK, USA

B. Wouters, Department of Geoscience and Remote Sensing, Delft University of Technology, Delft, The Netherlands

D. Yang, Environmental Sciences Division, Oak Ridge National Laboratory, Oak Ridge, TN, USA

Q. Zhou, Goddard Space Flight Center, NASA, Greenbelt, MD, USA; Science Systems and Applications, Inc., Lanham, MD, USA